ZooKeys 680: 1–11 (2017)
doi: 10.3897/zookeys.680.12727
http://zookeys.pensoft.net

RESEARCH ARTICLE

A peer-reviewed open-access journal
ZooKeys
Launched to accelerate biodiversity research

Search for mesophotic octocorals (Cnidaria, Anthozoa) and their phylogeny: I. A new sclerite-free genus from Eilat, northern Red Sea

Yehuda Benayahu[1], Catherine S. McFadden[2], Erez Shoham[1]

1 *School of Zoology, George S. Wise Faculty of Life Sciences, Tel Aviv University, Ramat Aviv, 69978, Israel*
2 *Department of Biology, Harvey Mudd College, Claremont, CA 91711-5990, USA*

Corresponding author: *Yehuda Benayahu* (yehudab@tauex.tau.ac.il)

Academic editor: *B.W. Hoeksema* | Received 15 March 2017 | Accepted 12 May 2017 | Published 14 June 2017

http://zoobank.org/578016B2-623B-4A75-8429-4D122E0D3279

Citation: Benayahu Y, McFadden CS, Shoham E (2017) Search for mesophotic octocorals (Cnidaria, Anthozoa) and their phylogeny: I. A new sclerite-free genus from Eilat, northern Red Sea. ZooKeys 680: 1–11. https://doi.org/10.3897/zookeys.680.12727

Abstract

This communication describes a new octocoral, *Altumia delicata* **gen. n. & sp. n.** (Octocorallia: Clavulariidae), from mesophotic reefs of Eilat (northern Gulf of Aqaba, Red Sea). This species lives on dead antipatharian colonies and on artificial substrates. It has been recorded from deeper than 60 m down to 140 m and is thus considered to be a lower mesophotic octocoral. It has no sclerites and features no symbiotic zooxanthellae. The new genus is compared to other known sclerite-free octocorals. Molecular phylogenetic analyses place it in a clade with members of families Clavulariidae and Acanthoaxiidae, and for now we assign it to the former, based on colony morphology. The polyphyletic family Clavulariidae is, however, in need of a thorough revision once the morphological distinctions among its phylogenetically distinct clades are better understood.

Keywords

Octocorallia, new genus, taxonomy, mesophotic coral ecosystem, Eilat, Red Sea

Introduction

Sclerites are microscopic, calcitic skeletal elements embedded in the tissues of certain groups of invertebrates, such as holothurians, tunicates and octocorals. Amongst the latter, they are considered to be one of the most prominent characteristic features and their form and anatomical arrangement are of major taxonomic importance (Fabricius and Alderslade 2001). Octocoral sclerites may vary greatly in morphology and size among different parts within a colony as well as among distinct taxa. They also differ in density and spatial orientation in the coenenchyme, and therefore in the degree to which they provide mechanical support and protection to colonies. In some taxa (e.g. gorgonians belonging to the subordinal group Scleraxonia) dense aggregations of fused sclerites form rigid axes that support very large, arborescent colonies (Fabricius and Alderslade 2001). In other taxa (e.g. some Nephtheidae) there is no skeletal axis and relatively few sclerites can be found in the coenenchyme, but bundles of large sclerites nonetheless support and protect individual polyps. Rarely, octocoral species may lack sclerites entirely.

Octocorals that completely lack sclerites or other calcitic skeletal elements have been described previously within seven octocoral families. These include the Acanthoaxiidae: *Acanthoaxis wirtzi* Ofwegen & McFadden, 2010; Acrossotidae: *Acrossota amboinensis* (Burchardt, 1902) (see also Alderslade and McFadden 2007); Alcyoniidae: *Malacacanthus capensis* (Hickson, 1900) (see also Williams 1987, 1992); Clavulariidae: *Clavularia celebense* Hickson, 1894, *C. reptans* Hickson, 1894, *C. pregnans* Thomson & Henderson, 1906, and *Phenganax parrini* Alderslade & McFadden, 2011; Cornulariidae: *Cervera* spp. López-Gonzáles et al., 1995, *Cornularia cornucopiae* (Pallas, 1766) (see also López-González al. 1995) and *C. pabloi* McFadden & Ofwegen, 2012; Dendrobrachiidae: *Dendrobrachia* spp. (Opresko & Bayer, 1991); and Xeniidae: *Anthelia gracilis* (May, 1898); *Cespitularia coerulea* May, 1898; *C. taeniata* May, 1899; *C. wisharti* Hickson, 1931; *C. hypotentaculata* Roxas, 1933 and *C. quadriserta* Roxas, 1933; *Efflatounaria totoni* Gohar, 1939; *Heteroxenia ghardaqensis* Gohar, 1940; *Xenia quinqueserta* May, 1898; *X. tumbatuana* May, 1898; *Xenia hicksoni* Ashworth, 1899; *X. sansibariana* May, 1899; *X. kükenthali* Roxas, 1933; *X. fimbriata* Utinomi, 1955; *X. novaecaledoniae* Verseveldt, 1974 and *X. mucosa* Verseveldt & Tursch, 1979. So far, the families Acanthoaxiidae, Acrossotidae, Cornulariidae and Dendrobrachiidae include only sclerite-free species; it should, however, be noted that some of the original type-material of the Cornulariidae should be re-examined in order to confirm the status of their sclerites (see also López-González and Garcia-Gomez 1995).

The majority of species in the families Alcyoniidae, Clavulariidae and Xeniidae have sclerites, however species without sclerites represent unusual exceptions. The families Alcyoniidae and Clavulariidae are highly polyphyletic (McFadden and Ofwegen 2012, 2013), and the few species that lack sclerites belong to unique clades that are not closely related to other members of those families. The depth of collection has been indicated for some of the above sclerite-free species, but none specifically refer to

mesophotic coral ecosystems (MCEs). Thus, these octocorals are principally shallow-reef inhabitants (<30 m depth), except for *Dendrobrachia* spp., which are deep-water inhabitants. A recent remote-operated vehicle survey (ROV) conducted in Eilat (Gulf of Aqaba, northern Red Sea) at mesophotic depths (see also Benayahu et al. 2017) revealed a sclerite-free octocoral, whose morphological features and phylogenetic affinities justify the establishment of a new genus, described below.

Materials and methods

Samples were collected by ROV (ECA H800) operated at a depth range of 50-190 m, by Sam Rothberg R/V of the Interuniversity Institute for Marine Sciences in Eilat (IUI). *In situ* photography was carried out by a low-light black and white camera VS300 (Eca Robotics) and 1CAM Alpha HD camera (SubCimaging). Samples were obtained by the ROV arm; fragments were removed on board and preserved in 100% ethanol for molecular work. The original samples were placed in 70% ethanol for taxonomic identification, and deposited at the Steinhardt Museum of Natural History, Israel National Center for Biodiversity Studies (ZMTAU).

Molecular phylogenetic analyses

DNA was extracted from EtOH-preserved samples, and two mitochondrial gene regions (*mtMutS*, *igr1* + *COI*) were sequenced using previously published primers and protocols (Alderslade and McFadden 2007) (GenBank accession nos. KY979504, KY979505). Attempts to sequence the nuclear 28S rDNA gene failed. *mtMutS* (699 bp) and *COI* (coding region only, 560 bp) were aligned with the comprehensive, 130-taxon dataset of McFadden and Ofwegen (2012), which includes representatives of all other sclerite-free octocoral taxa for which molecular data are available: *Acanthoaxis wirtzi*, *Acrossota amboinensis*, *Cervera atlantica* (Johnson, 1861), *Cornularia cornucopiae* and *C. pabloi*, *Malacacanthus capensis*, *Phenganax parrini*, *Xenia hicksoni*, and an undescribed species of *Xenia* from Indonesia (*Xenia* sp. 3, see: McFadden et al. 2014). Phylogenetic analyses followed the procedure of McFadden and Ofwegen (2012) using a combined dataset with different models of evolution applied to two separate data partitions, mitochondrial genes (*mtMutS* + *COI*; TVM+I+G) and 28S rDNA (GTR+I+G). Bayesian analyses were run using MrBayes v.3.2 (Ronquist et al. 2012) with a GTR+I+G model applied to both data partitions separately. Analyses were run for 4 million generations (until standard deviation of split partitions <0.01) with a burn-in of 25% and default Metropolis coupling parameters. Pairwise genetic distance values (Kimura 2-parameter) between species were estimated using MEGA v. 5.10 (Tamura et al. 2011). Alignment and tree files are available in TreeBase (http://purl.org/phylo/treebase/phylows/study/TB2:S20950).

Results

Systematic section

Family Clavulariidae Hickson, 1894
Sub-family Clavulariinae Roxas, 1933

***Altumia* gen. n.**
http://zoobank.org/03DD2AAA-D26D-4E41-A6B8-A6DB1CAEF749

Diagnosis. Clavulariinae with a thin and soft encrusting base, sometimes resembling a short stolon. Polyps erect when expanded, separate from each other; the stolon may feature a few polyps, occasionally only one. Polyps fully retractile into base of the colony, forming low truncated dome-shaped mounds. No sclerites in any part of the colony. Colonies lack symbiotic algae (zooxanthellae). Type species: *Altumia delicata* sp. n. by original designation and monotypy.

Etymology. The generic name is derived from the Latin 'altum', deep, referring to the habitat of the new genus at MCE depths and beyond. Gender female.

Molecular results. Maximum likelihood and Bayesian analyses yielded identical tree topologies that both support the phylogenetic placement of *Altumia* n. gen. as the sister taxon to *Acanthoaxis wirtzi* (Acanthoaxiidae), within a larger well-supported clade that also includes the Clavulariidae genera *Carijoa* F. Müller, 1867 and *Cryptophyton* Williams, 2000 (Figure 1). Pairwise genetic distances (Kimura 2-parameter) between *Altumia* n. gen. and *Acanthoaxis* (*mtMutS*: 9.4%, *COI*: 2.9%) are comparable to values among different genera and some family-level clades of octocorals (McFadden et al. 2011).

***Altumia delicata* sp. n.**
http://zoobank.org/4D9A82B8-F305-43E1-A5A4-3F9DB672781A
Figures 2–3

Holotype. ZMTAU CO 37427, Israel, Gulf of Aqaba, Eilat, 29°30'38.31"N, 34°55'59.30"E, 132 m, 30 May 2016, collected by ROV, coll. M. Weis; paratype: ZMTAU CO 37495, Israel, Gulf of Aqaba, Eilat, 29°30'37.29"N, 34°55'59.28"E, 118 m, 8 March 2017, collected by ROV, coll. M. Weis

Diagnosis. The ethanol-preserved holotype is comprised of thin patches of short stolon-like crusts growing over the dead branch of a black coral (Antipatharia) (Figure 2A), almost invisible to the naked eye. The milky-white, thin (<0.5 mm) crusts are a few mm long (Figure 2B), very soft, almost slime-like. Polyps completely retracted and practically invisible in the preserved colonies. No sclerites observed in any part of the colony.

When alive, the delicate, semi-transparent expanded polyps are distinct and are up to 20 mm long, featuring eight pinnate tentacles (Figure 3A). The ROV photographs indicate that the colonies commonly grow on dead black corals; the latter may reach a

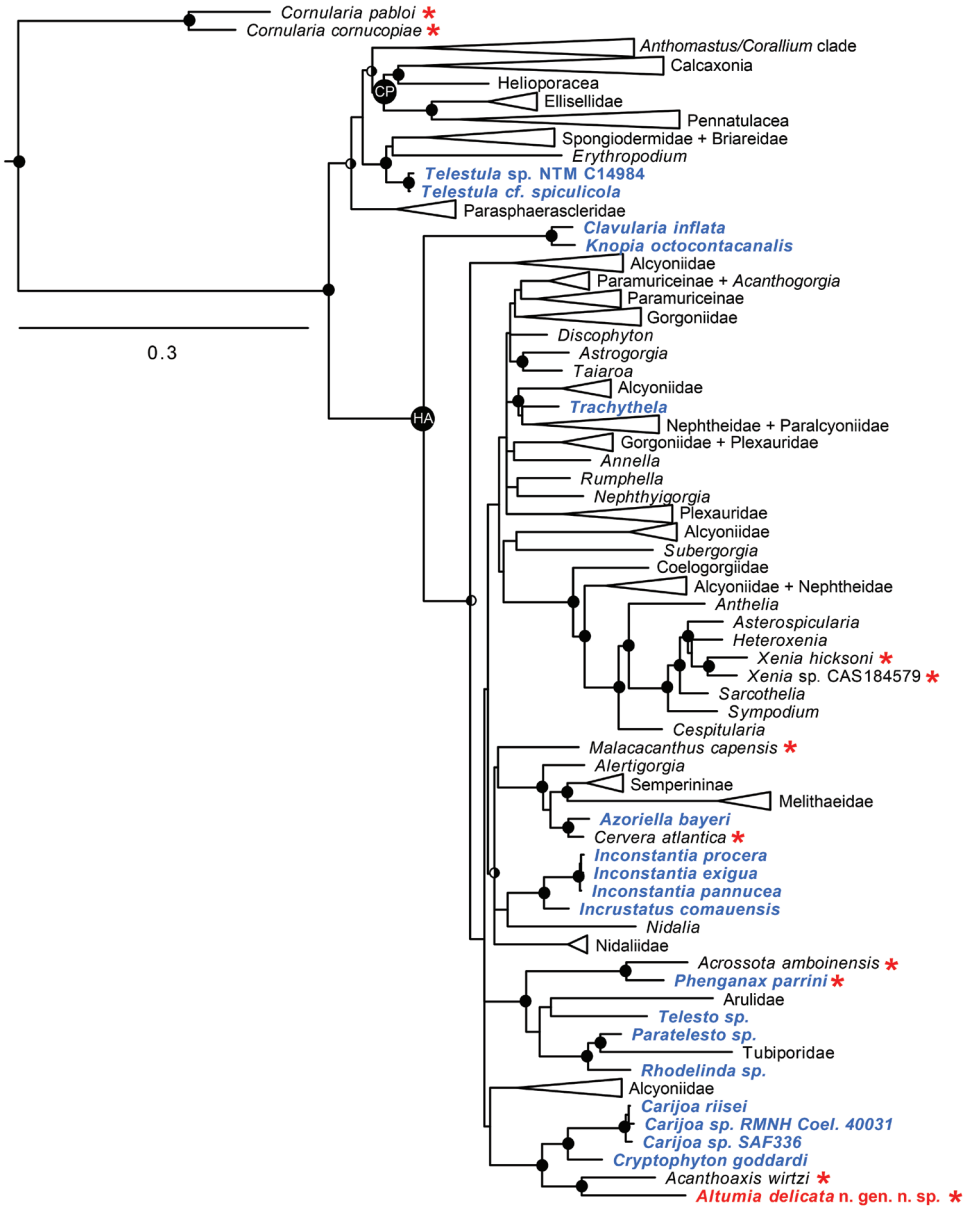

Figure 1. Phylogenetic relationships among species of octocorals that lack sclerites (red asterisks) and members of family Clavulariidae (blue labels), including *Altumia delicata* gen n. sp. n. (red label). Solid circles at nodes indicate strong support from both maximum-likelihood (bootstrap value >70%) and Bayesian (posterior probability >0.90) analyses; split circles indicate strong support from one analysis only (left half solid: supported by ML; right half solid: supported by Bayesian analysis). Strongly supported clades that include no clavulariid or sclerite-free species have been collapsed. Hexacorallian outgroup taxa used to root tree are not shown. For a comprehensive list of taxa and sequences included in the analyses see McFadden and Ofwegen (2012).

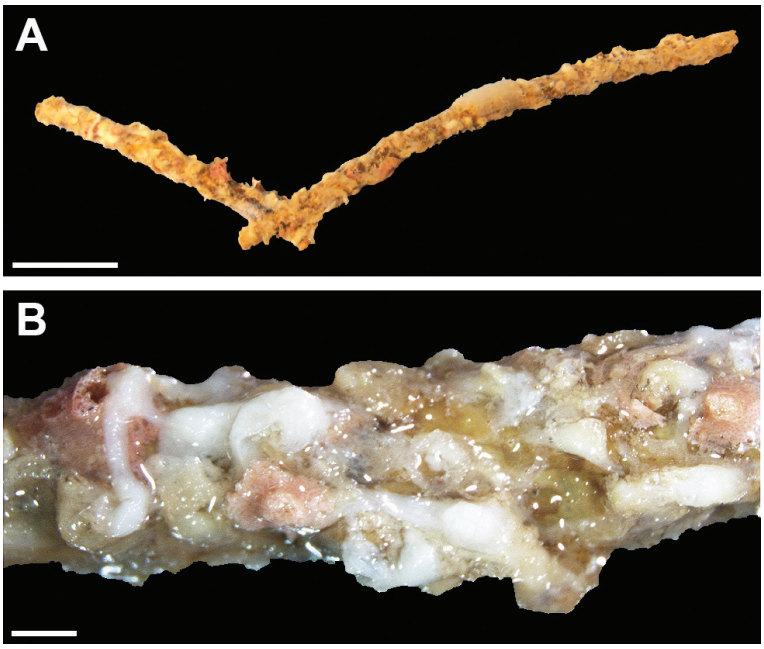

Figure 2. *Altumia delicata* gen. n. sp. n. holotype ZMTAU CO 37427. **A** Colony growing over a branch of a black coral **B** close up of holotype. Scale 10 mm at **A**, 1 mm at **B**.

large size (~45 cm in length) and can be predominantly fouled by *A. delicata* (Figure 3B). Interestingly, debris, such as PVC net found at a depth of 100 m, was found to be colonized by this octocoral (Figure 3C).

Intraspecific variability. There are no differences between the holotype and the paratype except for the size of the colonies.

Etymology. The species name is formed from the Latin 'delicata', delicate, referring to the fine texture of the colonies and their polyps. Gender female.

Discussion

Assignment of *Altumia* gen. n. to family Clavulariidae is complicated by the recognition that this family is highly polyphyletic, comprising at least seven distinct clades distributed across the Octocorallia (McFadden and Ofwegen 2012). Among other species that lack sclerites, *Altumia delicata* n. gen. n. sp. is most similar morphologically to *Cervera atlantica*, an azooxanthellate, stoloniferous species formally classified in the family Cornulariidae (López-González and Garcia-Gomez 1995). *Cervera* is, however, far removed phylogenetically from *Cornularia*, a genus that is characterized by a theca-like peridermal envelope that surrounds the polyp, a unique morphological feature not found in *Cervera* or any other octocoral. Phylogenetically, *Cornularia* occupies a unique, basal position within Octocorallia. In contrast, *Cervera* belongs to the large

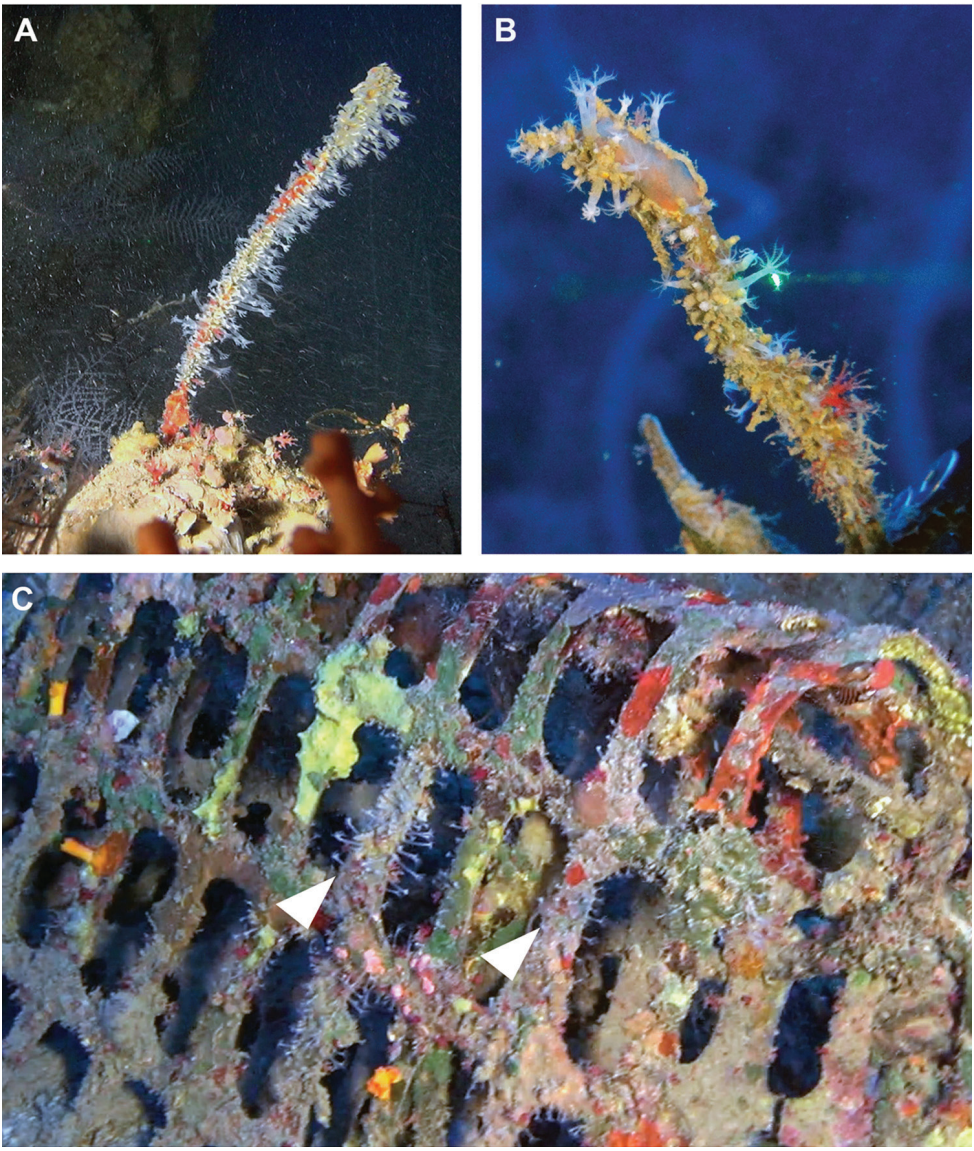

Figure 3. *Altumia delicata* gen. n. sp. n. live colonies. **A, B** colonies growing over branch of black coral with expanded polyps **C** colonies growing on PVC net (arrow heads).

Holaxonia-Alcyoniina clade, where it is a close sister taxon of *Azoriella*, a genus of Clavulariidae (Figure 1). These morphological and phylogenetic differences suggest that *Cervera* should not be classified in Cornulariidae, but instead in Clavulariidae. *Cervera* and *Altumia* gen. n. are also morphologically similar to another clavulariid, *Phenganax parrini*, although that sclerite-free species has zooxanthellae.

Despite its morphological similarity to *Cervera* and *Phenganax*, the molecular phylogenetic analyses suggest that *Altumia* gen. n. is not closely related to either of those

genera (Figure 1). Instead it falls within a clade comprising two other genera of Clavulariidae, *Carijoa* and *Cryptophyton*, as well as *Acanthoaxis wirtzi*, the sole member of family Acanthoaxiidae. *Altumia* gen. n. is, however, morphologically distinct from each of those genera. *Carijoa* and *Cryptophyton* both have sclerites; *Carijoa* is further distinguished by a growth form in which secondary polyps arise from primary, axial polyps, while *Cryptophyton* has a membranous growth form. Like *Altumia* gen. n., *Acanthoaxis wirtzi* lacks sclerites, but it has an axis of gorgonin with a hollow, cross-chambered core and spines, which are unique morphological features that define the monotypic family Acanthoaxiidae. Because of its morphological similarity to other Clavulariidae and its phylogenetic position within a clade that includes members of that family, we have assigned *Altumia* gen. n. to Clavulariidae. As discussed by McFadden and Ofwegen (2012), the polyphyletic family Clavulariidae will require extensive revision once the morphological distinctions among its phylogenetically distinct, component clades are better understood.

At present there is only scant information on MCE octocorals (Shoham and Benayahu 2017 and references therein), and no study has referred to any octocoral similar to *Altumia delicata*. Undoubtedly, the discovery of *A. delicata* highlights the need for an in-depth study of MCE octocoral diversity. The photographic records from the ROV indicate a continuous distribution of this species from 69 to 140 m depth and, therefore, it can be concluded that it inhabits lower MCEs (> 60 m, see Loya et al. 2016). However, its possible occurrence at deeper sites should be further explored. For instance, Kahng et al. (2014) noted that it is still unclear whether MCEs host specialized coral communities, or are merely marginal extensions of their shallower counterparts.

Conclusion

The current study highlights the possibility that MCEs may host octocorals also found below the deepest fringes of these MCEs; and that specifically, deep-water octocorals may populate the zone alongside those of the lower MCEs, contributing to the biodiversity there. Consequently, questions related to the genetic/demographic connectivity between MCEs and shallower reefs (Loya et al. 2016) are potentially relevant to understanding the connectivity between MCEs and deeper communities.

Acknowledgements

We thank the Interuniversity Institute for Marine Sciences in Eilat (IUI) for the use of the Sam Rothberg R/V and the professional assistance of its crew members. We are indebted to EcoOcean staff members for operating the ROV. The reviewers are acknowledged for their important comments which improved the manuscript. We acknowledge M. Weis and R. Liberman for help in the field work, A. Gonzalez for

laboratory assistance, A. Shlagman for curatorial skills, V. Wexler for digital editing and N. Paz for editorial assistance. This research was supported by the TASCMAR project (Tools and Strategies to access original bioactive compounds from cultivated marine invertebrates and associated symbionts) that has received funding from the *European Union's Horizon 2020 research and innovation programme* under grant agreement No 634674; and by the Israel Cohen Chair in Environmental Zoology to YB. Collection of animals complied with a permit issued by the Israel Nature and National Parks Protection Authority.

References

Alderslade P, McFadden CS (2007) Pinnule-less polyps: a new genus and new species of Indo-Pacific Clavulariidae and validation of the soft coral genus *Acrossota* and the family Acrossotidae (Coelenterata: Octocorallia). Zootaxa 1400: 27–44. https://doi.org/10.11646/zootaxa.1400.1.2

Alderslade P, McFadden CS (2011) A new sclerite-free genus and species of Clavulariidae (Coelenterata: Octocorallia). Zootaxa 3104: 64–68.

Ashworth JH (1899) The structure of *Xenia hicksoni* nov. sp. with some observations on *Heteroxenia elizabethae* Kölliker. Quarterly Journal of Microscopic Sciences (N.S.) 42(3): 245–304.

Benayahu Y, McFadden CS, Shoham E, Ofwegen LP van (2017) Search for mesophotic octocorals (Cnidaria, Anthozoa) and their phylogeny: II. A new zooxanthellate species from Eilat, northern Red Sea. ZooKeys 676: 1–12. https://doi.org/10.3897/zookeys.676.12751

Burchardt E (1902) Alcyonaceen von Thursday Island (Torres-Strasse) und von Amboina, II. Jenaische Denkschriften für Medizinisch-naturwissenschaftliche Gessellschaft zu Jena 8: 655–682.

Fabricius K, Alderslade P (2001) Soft corals and sea fans: a comprehensive guide to the tropical shallow water genera of the central-west Pacific, the Indian Ocean and the Red Sea. Australian Institute of Marine Science (AIMS), 264 pp.

Gohar HAF (1939) On a new xeniid genus *Efflatounaria*. Annals and Magazine of Natural History 3: 32–35. https://doi.org/10.1080/00222933908526896

Gohar HAF (1940) Studies on the Xeniidae of the Red Sea. Their ecology, physiology, taxonomy and phylogeny. Publications of the Marine Biological Station, Al Ghardaqa, Egypt 2: 27–118.

Hickson SJ (1894) A revision of the genera of the Alcyonaria Stolonifera, with a description of one new genus and several new species. The Transactions of the Zoological Society of London 13: 325–347. https://doi.org/10.1111/j.1096-3642.1894.tb00052.x

Hickson SJ (1900) Alcyonaria of the Maldives. Pt 1. Willy's Zoological Results Vol. ii, pt. 1, 473 pp.

Hickson SJ (1931) The alcyonarian family Xeniidae, with a revision of the genera and species. Great Barrier Reef Expedition 1928–29, Scientific Reports 4: 137–179.

Kahng SE, Copus JM, Wagner D (2014) Recent advances in the ecology of mesophotic coral ecosystems (MCEs). Current Opinion in Environmental Sustainability 7: 72–81. https://doi.org/10.1016/j.cosust.2013.11.019

López-González PJ, Ocaña O, García-Gómez JC, Núñez J (1995) North-eastern Atlantic and Mediterranean species of Cornulariidae Dana, 1846 (Anthozoa: Stolonifera) with the description of a new genus. Zoologische Mededelingen 69: 261–272.

Loya Y, Eyal G, Treibitz T, Lesser MP, Appeldoorn R (2016) Theme section on mesophotic coral ecosystems: advances in knowledge and future perspectives. Coral Reefs 35: 1–9. https://doi.org/10.1007/s00338-016-1410-7

May W (1898) Die von Dr. Stuhlmann im Jahre 1889 gesammelten ostafrikanischen Alcyonaceen des Hamburger Museums. Mitteilungen des naturhistorischen Musems Hamburg 15(2): 3–38.

May W (1899) Beiträge zur Systematik und Chorologie der Alcyonaceen. Jenaische Zeitschrift Naturwissenschaften 33: 1–180.

McFadden CS, Benayahu Y, Pante E, Thoma JN, Nevarez PA, France SC (2011) Limitations of mitochondrial gene barcoding in Octocorallia. Molecular Ecology Resources 11: 19–31. https://doi.org/10.1111/j.1755-0998.2010.02875.x

McFadden CS, Ofwegen LP van (2012) Stoloniferous octocorals (Anthozoa, Octocorallia) from South Africa, with descriptions of a new family of Alcyonacea, a new genus of Clavulariidae, and a new species of *Cornularia* (Cornulariidae). Invertebrate Systematics 26: 331–356. https://doi.org/10.1071/IS12035

McFadden CS, Ofwegen LP van (2013) Molecular phylogenetic evidence supports a new family of octocorals and a new genus of Alcyoniidae (Octocorallia: Alcyonacea). ZooKeys 346: 59–83. https://doi.org/10.3897/zookeys.346.6270

McFadden CS, Reynolds AM, Janes MP (2014) DNA barcoding of xeniid soft corals (Octocorallia: Alcyonacea: Xeniidae) from Indonesia: species richness and phylogenetic relationships. Systematics & Biodiversity 12: 247–257. https://doi.org/10.1080/14772000.2014.902866

Müller F (1867) Uber *Balanus armatus* und einen Bastard dieser Art und des *Balanus improvisus* var. *assimilis* Darw. Archiv für Naturgeschichte 33: 329–356.

Ofwegen LP van, McFadden CS (2010) A new family of Octocorals (Anthozoa: Octocorallia) from Cameroon waters. Journal of Natural History 44: 23–29. https://doi.org/10.1080/00222930903359669

Opresko DM, Bayer FM (1991) Rediscovery of the enigmatic coelenterate *Dendrobranchia* (Octocorallia; Gorgonacea), with descriptions of two new species. Transactions the Royal Society of South Australia 115: 1–19.

Pallas PS (1766) Elenchus Zoophytorum: Petrus van Cleef, Hagae Comitrum, i-xvi, 1–451.

Ronquist F, Teslenko M, van der Mark P, Ayres D, Darling A, Höhna S, Larget B, Liu L, Suchard MA, Huelsenbeck JP (2012) MrBayes 3.2: Efficient Bayesian phylogenetic inference and model choice across a large model space. Systematic Biology 61: 539–542. https://doi.org/10.1093/sysbio/sys029

Roxas HA (1933) Philippine Alcyonaria, the Families Cornulariidae and Xeniidae. The Philippine Journal of Science 50: 49–108.

Shoham E, Benayahu Y (2017) Higher species richness of octocorals in the upper mesophotic zone in Eilat (Gulf of Aqaba) compared to shallower reef zones. Coral Reefs 36: 71–81. https://doi.org/10.1007/s00338-016-1528-7

Tamura K, Peterson D, Peterson N, Stecher G, Nei M, Kumar S (2011) MEGA5: Molecular evolutionary genetics analysis using maximum likelihood, evolutionary distance, and maximum parsimony methods. Molecular Biology and Evolution 28: 2731–2739. https://doi.org/10.1093/molbev/msr121

Thomson JA, WD Henderson (1906) The marine fauna of Zanzibar and British East Africa, from collections made by Cyril Crossland in the years 1901 and 1902. Proceedings of the Zoological Society of London 76: 393–443. https://doi.org/10.1111/j.1469-7998.1906.tb08441.x

Utinomi H (1955) Two new species of *Xenia* from Kusimoto (Coelenterata, Alcyonaria). Publications of the Seto Marine Biological Laboratory 4: 105–109. https://doi.org/10.5134/174522

Verseveldt J (1974) Octocorallia from New Caledonia. Zoologische Mededelingen 48: 96–122.

Verseveldt J, Tursch A (1979) Octocorallia from the Bismarck Sea (Part I). Zoologische Mededelingen 54: 133–148.

Williams GC (1987) The aberrant and monotypic soft coral genus *Malacacanthus* Thomson, 1910 (Octocorallia: Alcyoniidae) endemic to southern Africa. Journal of Natural History 21: 1337–1346. https://doi.org/10.1080/00222938700770841

Williams GC (1992) The Alcyonacea of southern Africa. Stoloniferous octocorals and soft corals (Coelenterata, Anthozoa). Annals of the South African Museum 100: 249–358.

Williams GC (2000) A new genus and species of stoloniferous octocoral (Anthozoa: Clavulariidae) from the Pacific coast of North America. Zoologische Mededelingen 73: 333–343.

ZooKeys 680: 13–31 (2017)
doi: 10.3897/zookeys.680.12048
http://zookeys.pensoft.net

RESEARCH ARTICLE

A peer-reviewed open-access journal
ZooKeys
Launched to accelerate biodiversity research

A new species of *Microcharon* from marine interstitial waters, Shizuoka, Japan (Isopoda, Lepidocharontidae)

Jeongho Kim[1], Wonchoel Lee[1], Ivana Karanovic[1,2]

1 *Department of Life Science, Hanyang University, Seoul, Korea* **2** *Institute for Marine and Antarctic Studies, University of Tasmania, Hobart, Tasmania, 7001, Australia*

Corresponding author: *Ivana Karanovic* (ivana.karanovic@utas.edu.au)

Academic editor: *S. Brix* | Received 1 February 2017 | Accepted 18 April 2017 | Published 14 June 2017

http://zoobank.org/3E41270A-A8CA-40FE-AD10-210200232F5D

Citation: Kim J, Lee W, Karanovic I (2017) A new species of *Microcharon* from marine interstitial waters, Shizuoka, Japan (Isopoda, Lepidocharontidae). ZooKeys 680: 13–31. https://doi.org/10.3897/zookeys.680.12048

Abstract

A new species of *Microcharon* Karaman, 1934 (Asellota: Lepidocharontidae) is described from Miho-Uchihama beach, Shizuoka, Japan. *Microcharon tanakai* **sp. n.** differs from its congeners by having nine simple, five penicillate setae on antennal article 6; one simple distal seta on article 1 of the mandibular palp and having the apical lobe of male pleopod 1 convex, rounded, armed with seven setae. A key to Asian species of the genus and 16S rRNA of the new species are provided.

Keywords

interstitial, isopoda,Japan, morphology, taxonomy

Introduction

Members of the genus *Microcharon* Karaman, 1934, are free-living interstitial isopods. Being highly adapted to the narrow spaces of the interstitial environment, the species possesses an elongated body without visual organs or pigmentation (Coineau 1994, 2000; Wilson and Wägele 1994). When Karaman (1934) described *Microcharon*, it was included in the family Microparasellidae Karaman, 1934. However, following a recent revision (Galassi et al. 2016), the genus is currently a member of the family Lepidocharontidae. Besides *Microcharon*, Lepidocharontidae also includes *Lepidocharon* Galassi & Bruce, 2016 and *Janinella* Albuquerque, Boulanouar & Coineau, 2014. The most

prominent diagnostic character of *Microcharon* is the shapes of pereonites 1-7. Pereonites are cylindrical and each is rectangularly shaped in dorsal view whereas, *Lepidocharon* and *Janinella* have trapezoidal pereonites (Galassi et al. 2016).

The genus *Microcharon* is one of the best studied groups of the family Lepidocharontidae and 69 species have been described from all over the world (Boyko et al. 2008). The majority of species are known from Europe, especially from the Mediterranean region (Coineau 1994; Boyko et al. 2008; Galassi et al. 2016). On the other hand, only the following three Asian species have been recorded so far: *M. halophilus* Birstein & Ljovuschkin, 1965; *M. kirghisicus* Jankowskaya, 1964; and *M. raffaellae* Pesce, 1979. They are known from Turkmenistan, Kyrgyzstan, and Iran respectively (Coineau 1994; Boyko et al. 2008; Galassi et al. 2016). Diversity of *Microcharon* in East Asia remains particularly unknown. Only Shimomura et al. (2006) briefly noted a single species of *Microcharon* collected together with an ingolfiellidean amphipod from marine interstitial of Okinawa archipelago.

During a survey of the interstitial fauna of Miho-Uchihama beach (Shizuoka, Japan), a small number of psammolittoral isopods were collected together with other marine interstitial fauna such as, harpacticoid copepods, nematodes and ostracods. The isopod specimens had a typical *Microcharon* body plan, but a unique combination of morphological characters which lends support to the establishment of the new species described herein. Beside its description an identification key to the four Asian species of this genus currently recorded. In addition, a partial sequence of 16S rRNA gene was obtained and this may be useful for the future phylogenetic study studies of *Microcharon* and the family Lepidocharontidae.

Materials and methods

Specimen collection and identification

Seven female and two male specimens were collected from coarse sand from Miho-Uchihama beach, Shizuoka City, Shizuoka Prefecture, Japan on 7 February 2015 (Fig. 1). Coarse sand samples were washed five times in a bucket with fresh water. The top layer of water was strained through nets of 40 μm mesh size and material was immediately preserved in 99% ethanol. Sorting from sediment sample and dissection of specimens were done under an Olympus SZX 12 dissecting microscope. Dissected appendages were mounted onto glass slides in lactophenol. Line drawings were prepared using a Zeiss Axioskop 50 compound microscope equipped with a camera lucida. All studied material was deposited at the invertebrate collection of the National Institute of Biological Resources (NIBR), Korea. Two female and one male were transferred to isoamyl acetate for 20 minutes and dried in a critical-point dryer Hitachi E-1010. Dried specimens were mounted onto a SEM stub and coated with gold using a sputter coater to a thickness of 15-30 nm. Coated specimens were examined and photographed with a Hitachi S-3400 scanning electron microscope at Chungang University

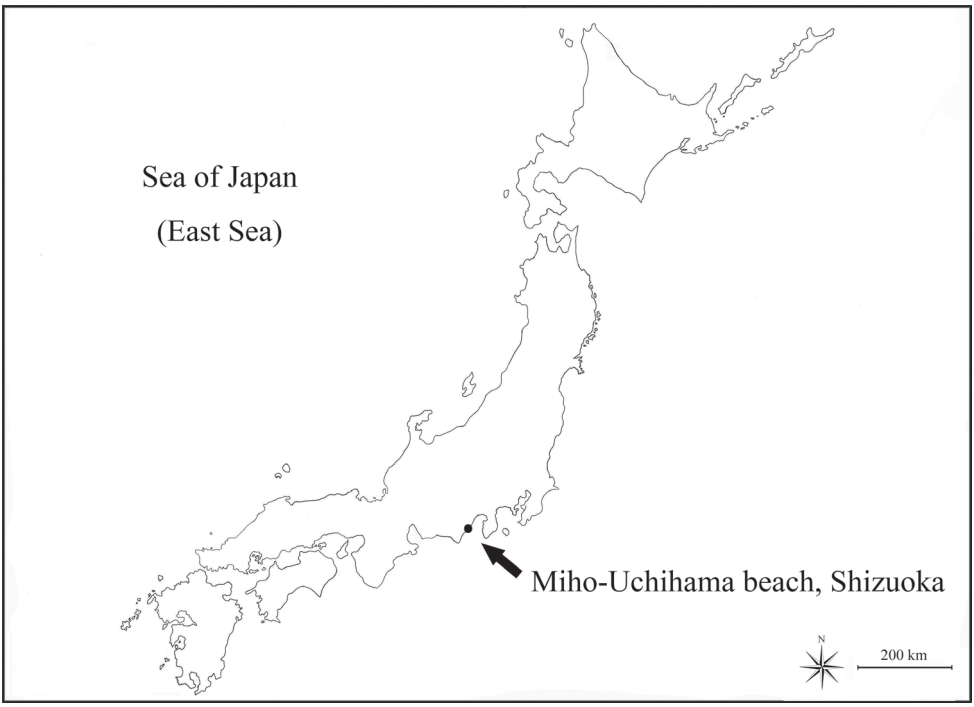

Figure 1. Sampling site. The arrow indicating the type locality of *Microcharon tanakai* sp. n. (Miho-Uchihama beach, Shizuoka, Japan).

(Seoul). Measurements were done following the method of Riehl and Brandt (2010). All measurements were taken from the dorsal view of line drawings using the distance measurement tools of Adobe Acrobat Professional. The ratios of appendages were given in distal to proximal order, excluding setae. The body ratios were given in anteromedial to posteromedial point order excluding appendages. Whole body length was measured from biggest female specimen. Terminology is largely based on Galassi et al. (2016).

DNA extraction and amplification

Two females from the type locality sample were identified without dissection under an Olympus SZX 12 dissecting microscope. Before amplification, specimens were transferred into distilled water for 20 minutes to remove ethanol and then macerated with a small glass rod. Whole specimens were used to isolate genomic DNA with the aid of the LaboPassTM Kit (COSMO Co. Ltd., Korea) following the manufacturer's protocols. 16S rRNA was amplified with polymerase chain reaction (PCR) using PCR premix (BIONEER.Co) in TaKaRa PCR thermal cycler (TaKaRa Bio Inc., Otsu, Shiga, Japan). The primers used were 16sar-L (5`-CWAAYCATAAAGAYATTGGNAC-3`) and 16sar-H (5`-ACTTCAGERTGNCCAAARAAYCA-3`) (Palumbi et al. 1991).

The amplification protocol consisted of the initial denaturation at 94°C for 2 min and 35 cycles each consisting of denaturation at 94°C for 50 sec, annealing at 50°C for 50 sec, extension at 72°C for 1 min 20 sec; the final extension was at 72°C for 7 min. Successful amplifications were confirmed by electrophoresis on 1% agarose gel. The PCR products were purified for sequencing reactions, using the Labopass PCR Purification Kit (COSMO Co. Ltd., Korea) following the guidelines provided with the kit. DNA was sequenced on an ABI automatic capillary sequencer (Macrogen, Seoul, Korea) using the same set of primers. All obtained sequences were visualized using Finch TV version1.4.0 (http://www.geospiza.com/Products/finchtv.shtml). Each sequence was checked for the quality of signal and sites with possible low resolution, and corrected by comparing forward and reverse strands.

Systematics

Suborder Asellota Latreille, 1802
Family Lepidocharontidae Galassi & Bruce, 2016

Genus *Microcharon* Karaman, 1934

Type species. *Microcharon stygius* (Karaman, 1933)

Genus diagnosis (modified from Galassi et al. 2016). Body cylindrical; rostrum weakly developed or absent; antennula 5 or 6 articles; antennal flagellum longer than podomere, pereonites rectangular in dorsal view, with subparallel lateral margins; free pleonite as wide as preonite 7; pereopodal coxal plate hardly discernible, incorporated to sternite body wall; distolateral lobe of male pleopod 1 with folded hyaline lamella running parallel to lateral margin; female operculum as long as pleotelson, with two or four apical setae; well-developed uropods with slender endopod and exopod.

***Microcharon tanakai* sp. n.**
http://zoobank.org/638F2AF3-DF77-4293-8077-8E3ECC810F82
Figures 2–10

Type locality. Interstitial water of coarse sand, Miho-Uchihama beach, Shizuoka city, Shizuoka Prefecture, Japan, 35°01'83"N, 138°51'71"E (Fig. 1).

Material examined. Holotype: adult female, (NIBRIV0000787789) completely dissected and mounted in lactophenol on four slides; paratype 1 female (NIBRIV0000787790) dissected on three slides, paratype 2 female (NIBRIV0000787791) dissected on one slide; adult male pleotelson dissected on three slides; 2 females and 1 male used for SEM.

Diagnosis. Antennular article 6 smallest, with one aesthetasc, one penicillate, three simple setae distally; article 1 of mandibular palp with one distal simple seta;

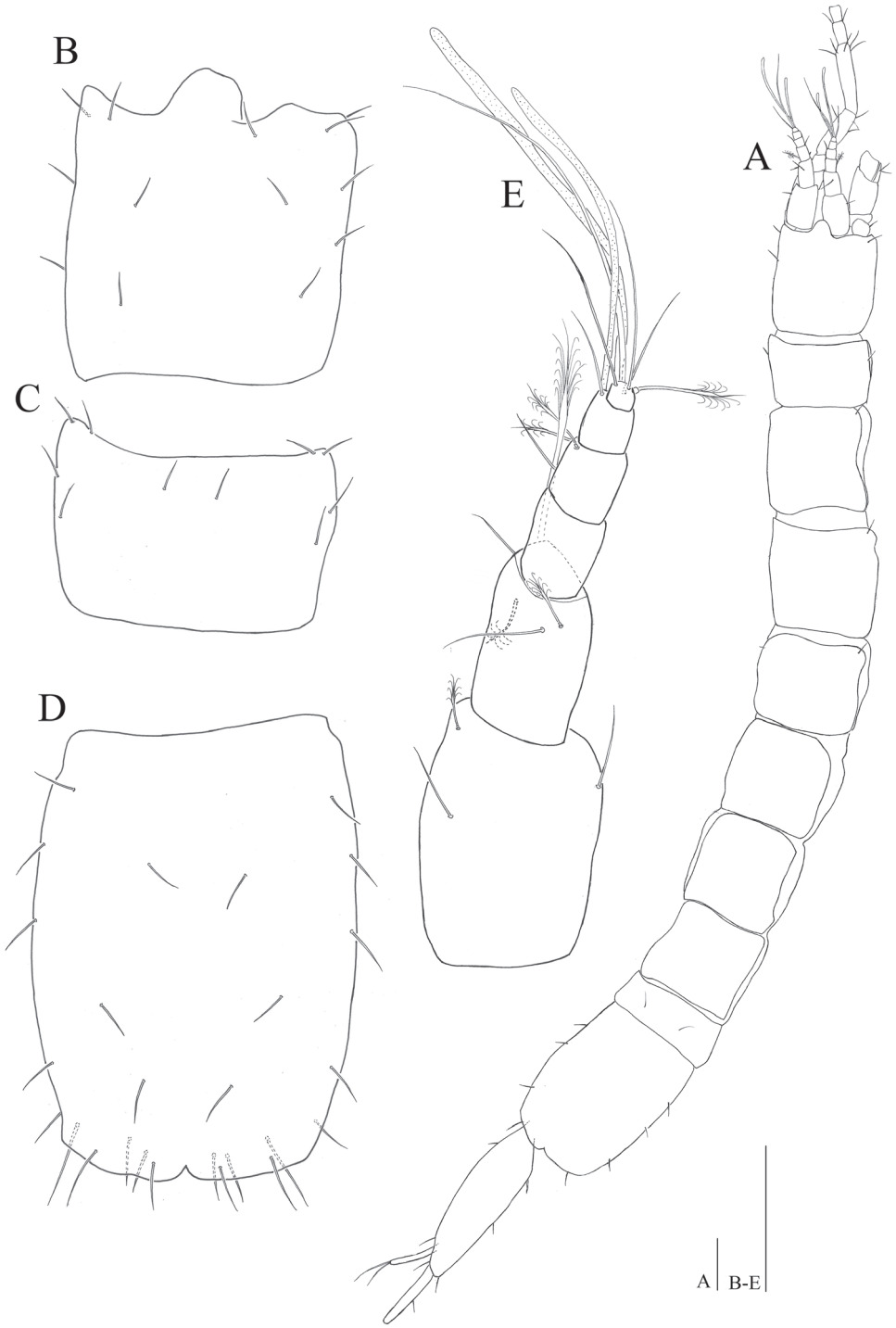

Figure 2. *Microcharon tanakai* sp. n., holotype, female. **A** habitus, dorsal **B** cephalon, dorsal **C** pereonite 1, dorsal **D** pleotelson, dorsal **E** antennula, dorsal. Scale bars 100 μm.

lateral lobe of maxillula with eleven robust setae; distal apex of male pleopod 1 convex, round, with three apical, four subapical setae; protopod of male pleopod 2.9 times longer than wide; protopod of uropod 3.1 times longer than wide, with fifteen setae.

Description of the female holotype. *Body* (Fig. 2A): elongate, slender in whole appearance, total length, 1.95 mm, measured from anteromedial point of cephalon to posteromedial point of pleotelson, body approximately 8.5 times longer than wide, maximum body width in pereonite 3, 0.92 times of maximum width of pleotelson; color of preserved specimens transparent, whole surface of body with many ornamentation looking like lines.

Cephalon (Fig. 2B): 1.12 times longer than wide and 0.12 times of whole body; anterior margin with weak rostrum; lateral margins straight, with four pairs of simple setae, three pairs of simple setae along dorsomedial surface.

Pereon (Fig. 2A, C): 0.68 times of whole body length, medial margin of tergite convex, pereonites with lateral margin, straight, pereonite 1, 0.62 times longer than wide, four simple setae along lateral margin, two setae on dorsal surface; pereonite 2, 1.12 times longer than wide, with four pairs of setae along lateral margin, two setae on anteromedial edge; pereonite 3, 1.06 times longer than wide, with four pairs of setae along lateral margin, two pairs of setae along dorsal surface; pereonite 4, 1.02 times longer than wide, with nine setae on both lateral and dorsal surface; pereonite 5, 0.99 times longer than wide, with six setae on both lateral and dorsal margin; pereonite 6, 1.13 times longer than wide, with eight simple setae on dorsal margin; pereonite 7, 1.02 times longer than wide, with two setae on both anterolateral corner and three pairs of setae along dorsal surface.

Pleonite 1 (Fig. 2A): as wide as pereonite 7, 0.38 times longer than wide, with two simple setae on dorsomedial margin.

Pleotelson (Fig. 2D): 1.33 times longer than wide, wider than preceding pereonites, with several setae, becoming slightly narrow from basal part to distal end, weak cleft on middle of posterior rim.

Antennula (Fig. 2E): 6 articles; article 1 robust, 1.5 times longer than wide, with three setae: two distomedial simple, one penicillate short setae distolaterally; article 2, smaller than 1, distoventral projection, 1.8 times longer than wide, with two simple, three penicillate setae, one of them elongate, stout, reaching distal tip of antennula; article 3, naked, 1.5 times longer than wide; article 4 with one proximolateral simple seta, two penicillate setae distolaterally; article 5, 1.2 times longer than wide with one simple seta, one aesthetasc distomedially; article 6, smallest 0.6 times of article 5, with one aesthetasc, one penicillate, three simple setae on distal end.

Antenna (Fig. 3A, B): six podomeres, twelve flagellar articles; article 1 globular in dorsal view, with one lateral simple seta; article 2 semicircular, naked; article 3, 1.8 times longer than wide, with one distomedial simple seta, scale thick, robust, with two simple setae laterally (Fig. 8A); article 4, as long as wide, with two simple setae distolaterally; article 5, 3.02 times longer than wide, with three distoventral simple setae, one simple, one penicillate setae distodorsally; article 6, longest, 5.3 times longer than wide, with two simple, five penicillate setae on lateral margin, seven simple setae on

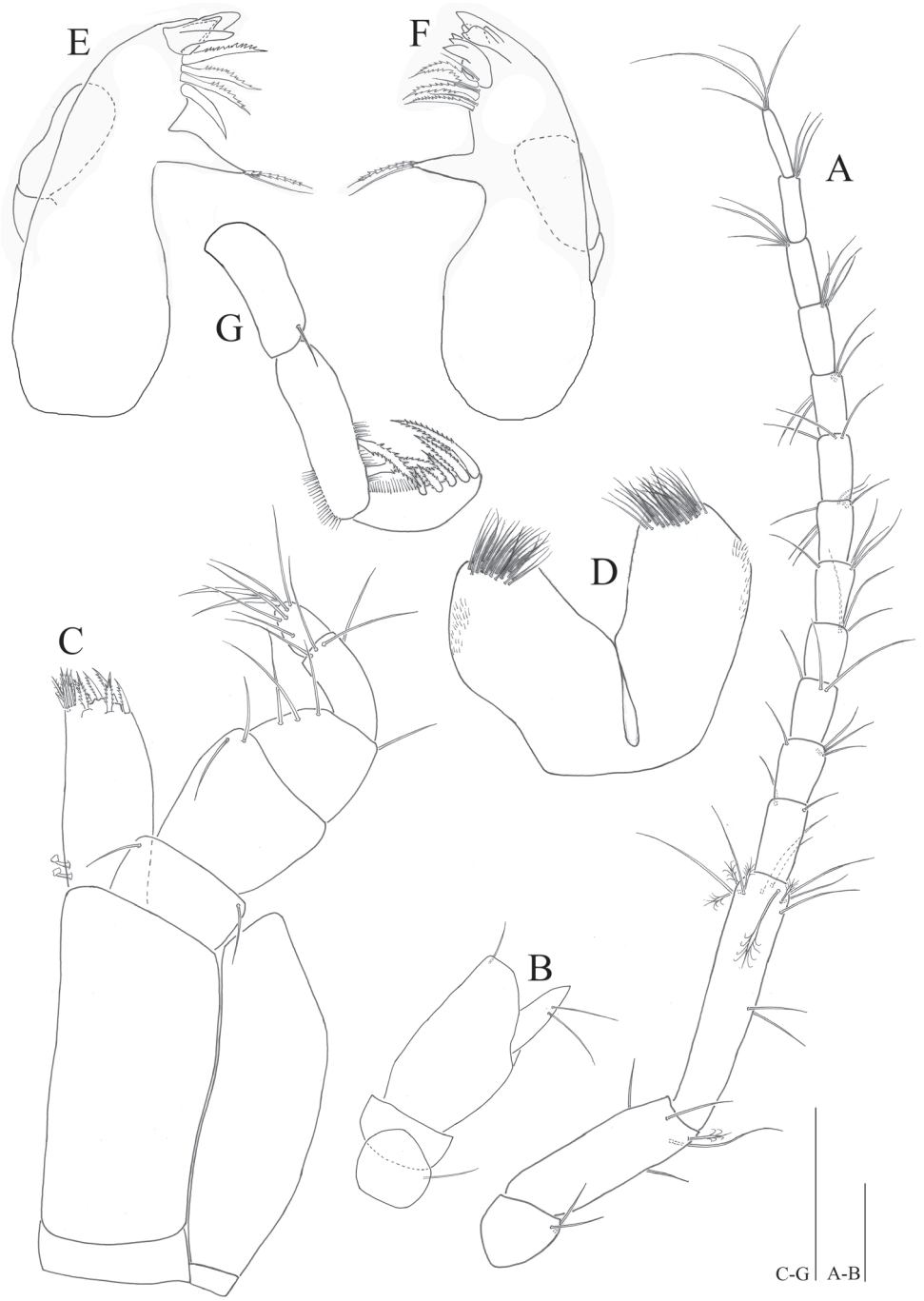

Figure 3. *Microcharon tanakai* sp. n., holotype, female. **A** antennal articles 4-6 with flagellum, dorsal **B** antennal articles 1-3, dorsal **C** maxilliped dorsal **D** paragnaths dorsal **E** left mandible, dorsal **F** right mandible, dorsal **G** mandibular palp, ventral. **A–B** scale bars 100μm, **C–G** scale bars 50 μm.

distal margin; flagellar articles from 2 to 8 subequal in length, armature of each articles as follows: article 1 with two simple setae distally, article 2 with four simple setae distally, article 3 with three simple setae distally, article 4 with three simple setae distally, article 5 with four simple setae distally, article 6 with six simple setae distally, article 7 with three simple setae distally, article 8 with four simple setae distally, article 9 with four simple setae distally, article 10 with four simple setae distally, article 11 with three simple setae distally, article 12 with four simple setae distally

Mandible (Figs 3E–G, 8B): body robust, curved inwardly; *pars incisiva* of both mandibles with four cusps; right mandible (Fig. 3F), *lacinia mobilis*, with five cusps, tapering proximally three pinnate, three simple setae located below *lacinia mobilis*; *pars molaris* of both mandibles with one simple, one pinnate distal setae, slightly longer than *pars molaris*, almost same length as seta on palp; left mandible (Fig. 3E), *pars incisiva* with four cusps, *lacinia mobilis* missing, with three pinnate and one naked robust setae located below *pars incisiva*; palp (Fig. 3G) with three articles, inserted on cuticular projection; article 1 with one simple seta distally (Fig. 8B), article 2 longest, with two pinnate and several hair-like setae on distal margin, article 3 curved outwardly, with five pinnate and with several hair-like setae on lateral margin.

Paragnaths (Fig. 3D): deeply incised, with two lobes, each distal part of lobes covered with numerous setae.

Maxillula (Fig. 4D): lateral lobe with eleven strong robust setae on distal edge, some denticulate, some setulose, two spinular rows along outer margin; mesial lobe nearly half as long and wide as outer endite, with three short simple and several hair-like setae on distal end.

Maxilla (Fig. 4C): lateral rami slightly shorter than median one, with four pectinate setae on distal end respectively; mesial ramus coalescent with basis, much thicker than others with eight strong setae distally and one of them pectinate.

Maxilliped (Fig. 3C): epipodite wide, apically pointed, distal tip reaching distal part of first palp article; basis 2.1 times longer than wide; palp with 5 articles; article 1, 0.5 times longer than wide, with two simple setae on both distal corners; article 2, 1.7 times longer than article 1, with two simple setae on distomedial corner; article 3 tapering distally, with three simple setae along medial margin, one seta on distolateral corner; article 4 curved inwardly, with four simple setae distally; article 5 with five simple setae, 2 claws distally; endite 2.4 times longer than wide, with five apical pinnate setae, numerous spinules on distomedial corner.

Pereopods 1–4 (Figs 4A, B, 5A, B): inserted on pereon anterolaterally (Fig. 8C); coxal plate minute, hardly discernible (Fig. 8D); anteromedial margin of basis protruded, with one small seta on distal corner, pereopod 1 and 4 with two penicillate, one simple setae (vs pereopod 2, with one penicillate, one simple setae; pereopod 3 with one penicillate, two simple setae); ischium, pereopod 1 and 2 with two simple setae on both anteroposterior margin (vs pereopod 3 with two simple, one penicillate setae; pereopod 4 with three simple setae); merus, shortest article, broaden distally, distinctly shorter than ischium, pereopod 2-4 with four simple setae on both side of distal corner (vs pereopod 1 with five simple setae); carpus, longer than ischium, pereopods

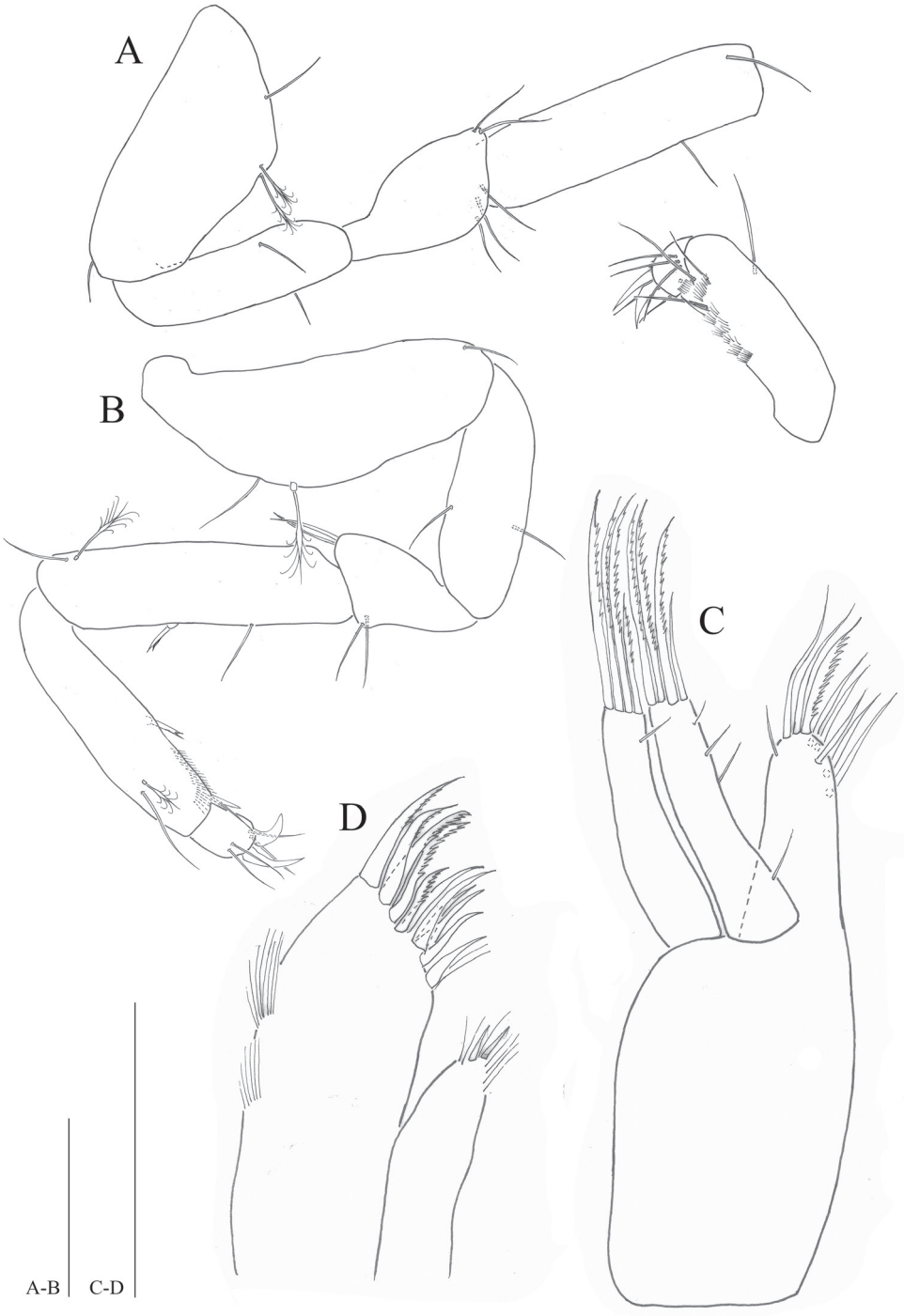

Figure 4. *Microcharon tanakai* sp. n., holotype, female. **A** pereopod 1, lateral **B** pereopod 2, lateral **C** Maxilla, ventral **D** Maxillula, ventral. Scale bars 50μm.

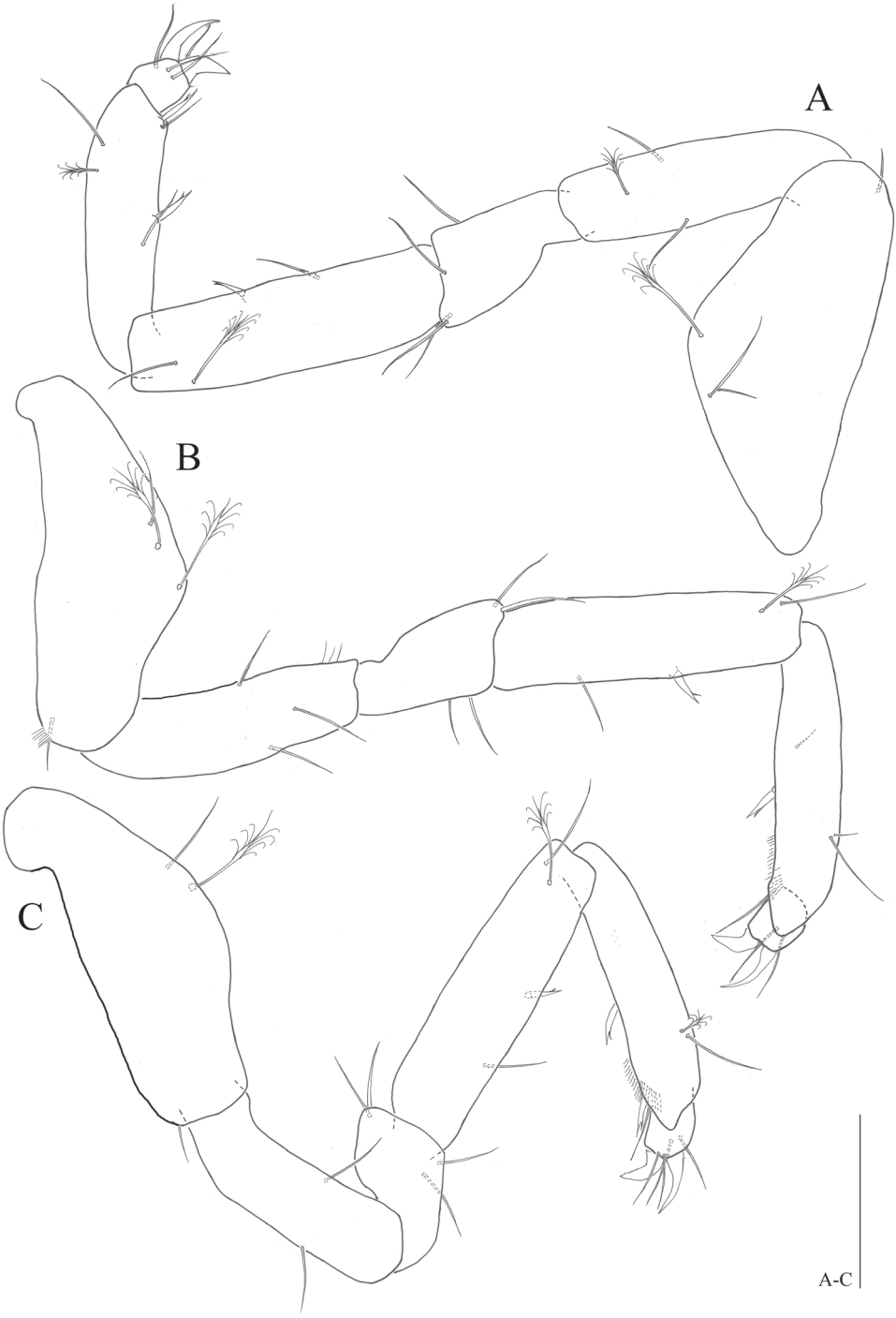

Figure 5. *Microcharon tanakai* sp. n., holotype, female. **A** pereopod 3, lateral **B** pereopod 4, lateral **C** pereopod 5, lateral. Scale bars 50μm.

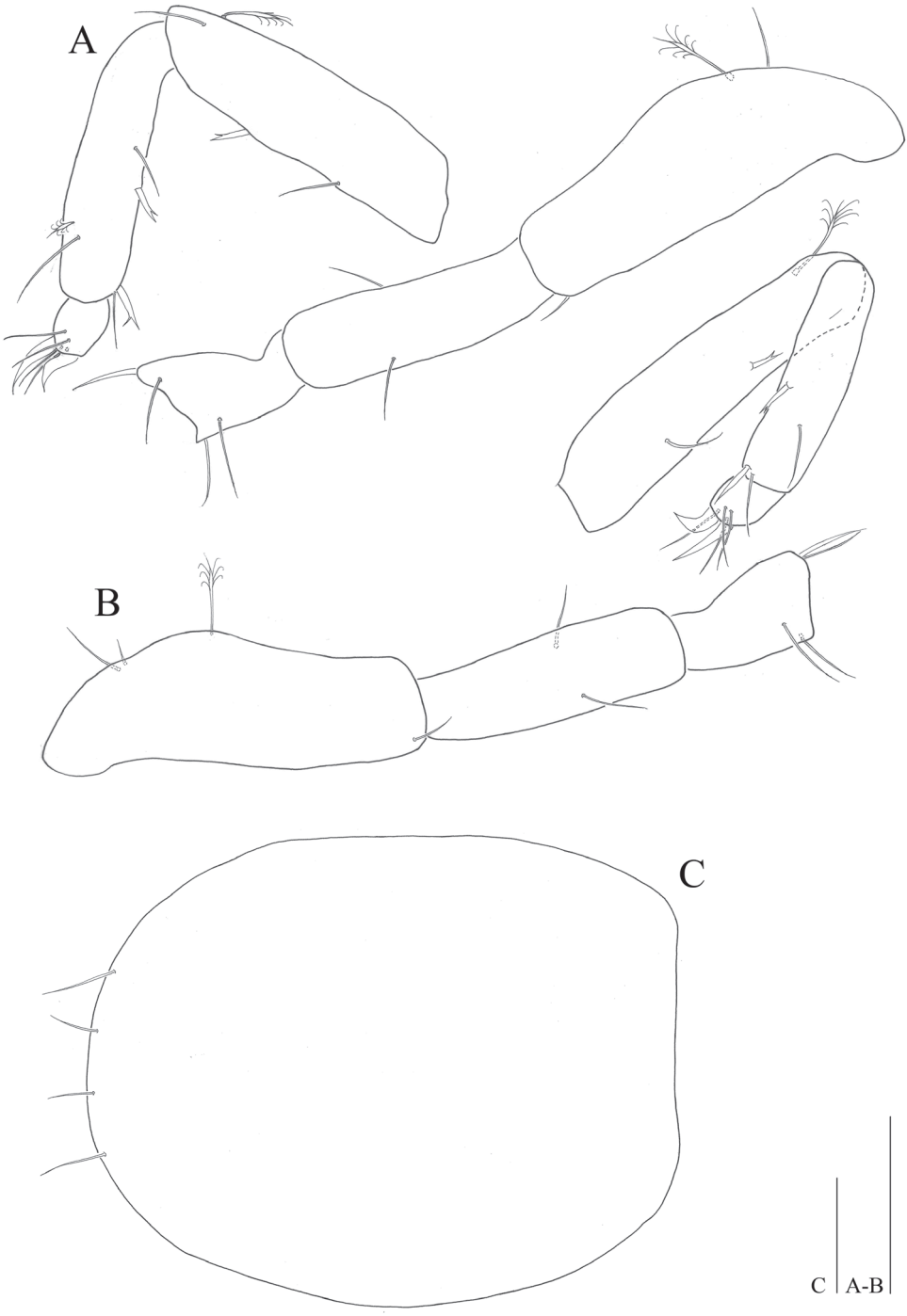

Figure 6. *Microcharon tanakai* sp. n., holotype, female. **A** pereopod 6, lateral **B** pereopod 7, lateral **C** operculum, dorsal. Scale bars 50μm.

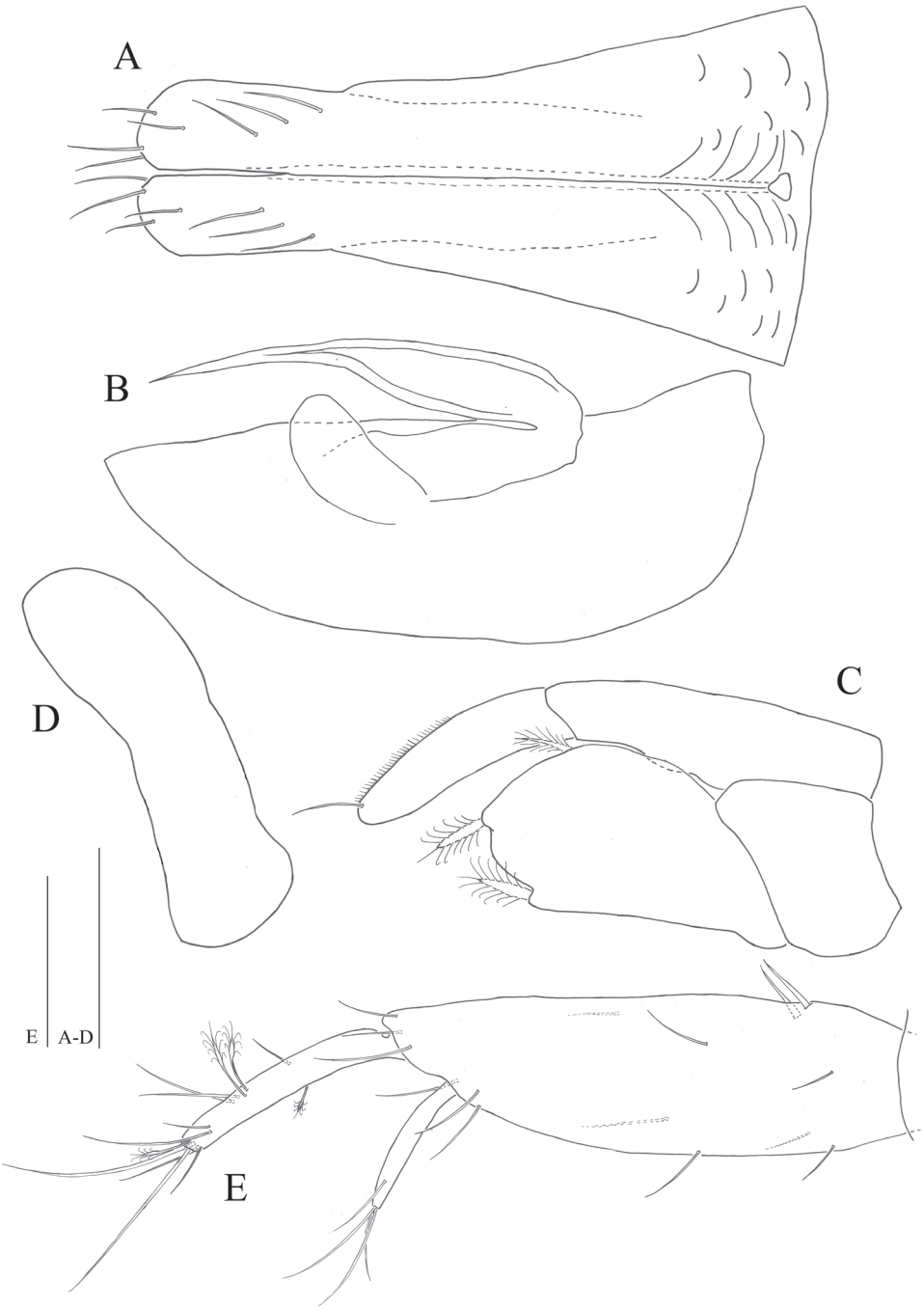

Figure 7. *Microcharon tanakai* sp. n., male. **A** pleopod 1, dorsal **B** pleopod 2, dorsal **C** pleopod 3, dorsal **D** pleopod 4, dorsal **E** female right uropod, dorsal. Scale bars 50μm.

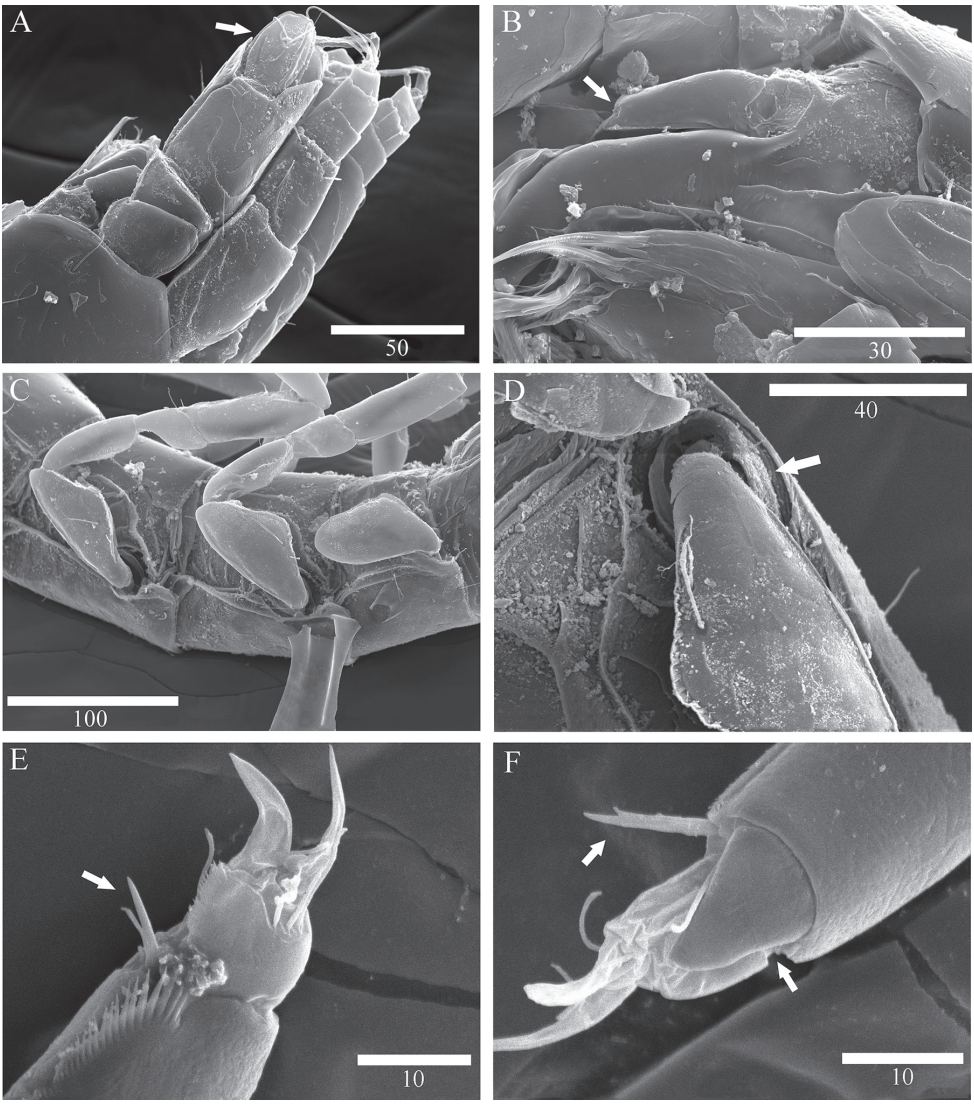

Figure 8. Scanning electron microscope images of *Microcharon tanakai* sp. n., **A** female antennal scale, lateral, **B** female mandibular palp, lateral **C** female pereopod 1-3, lateral, **D** female coxal plate of perepod 2, ventral **E** female bifurcate seta of pereopod 4, lateral, **F** female articular plate of pereopod 5, lateral. Scale bar unit μm.

2-4 with one bifid, two simple, one penicillate setae (Fig. 8E, F), (vs pereopod 1 with two simple setae); propodus, slightly shorter than carpus, pereopod 1 with four simple setae (vs pereopod 2 with two bifid, two simple, one penicillate setae; pereopod 3 with two bifid, three simple, one penicillate setae; pereopod 4 with one bifid, four simple setae); pereopod 4 with distal sclerite covering proximal part of dactylus, dactylus with

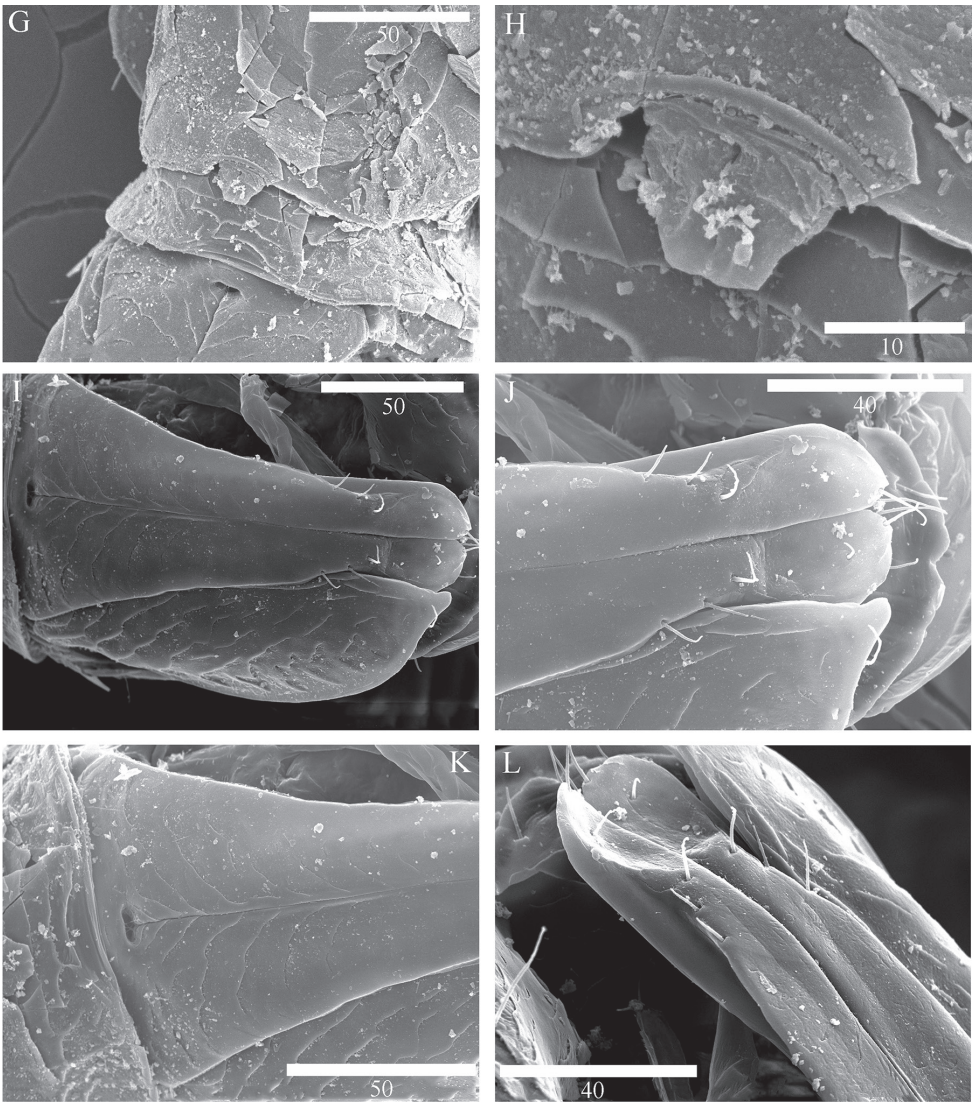

Figure 9. Scanning electron microscope images of *Microcharon tanakai* sp. n., **G** pereonite 7 and free pleonite, ventral, paratype male **H** penial papillae, ventral, **I** pleopod 1, dorsal, **J** distal part of male pleopod 1, dorsal **K** proximal part of male pleopod 1, dorsal **L** distolateral view of male pleopod 1. Scale bar unit μm.

two claws (Fig. 8E), two pairs of setae on both dorsal and ventral margin (vs pereopod 1 with three simple, two simple setae on both dorsoventral margin respectively).

Pereopods 5–7 (Figs 5C, 6A, B): inserted on pereon posterolaterally, subequal in whole appearance with preceding ones, with small differences in chaetotaxy; coxal plate minute, hardly discernable; basis, with one small seta on distal corner, pereopod 5 with one simple, one penicillate, setae on anteromedial margin (vs pereopod 7 with two simple, one penicillate setae); ischium, with two simple setae on both anteroposterior

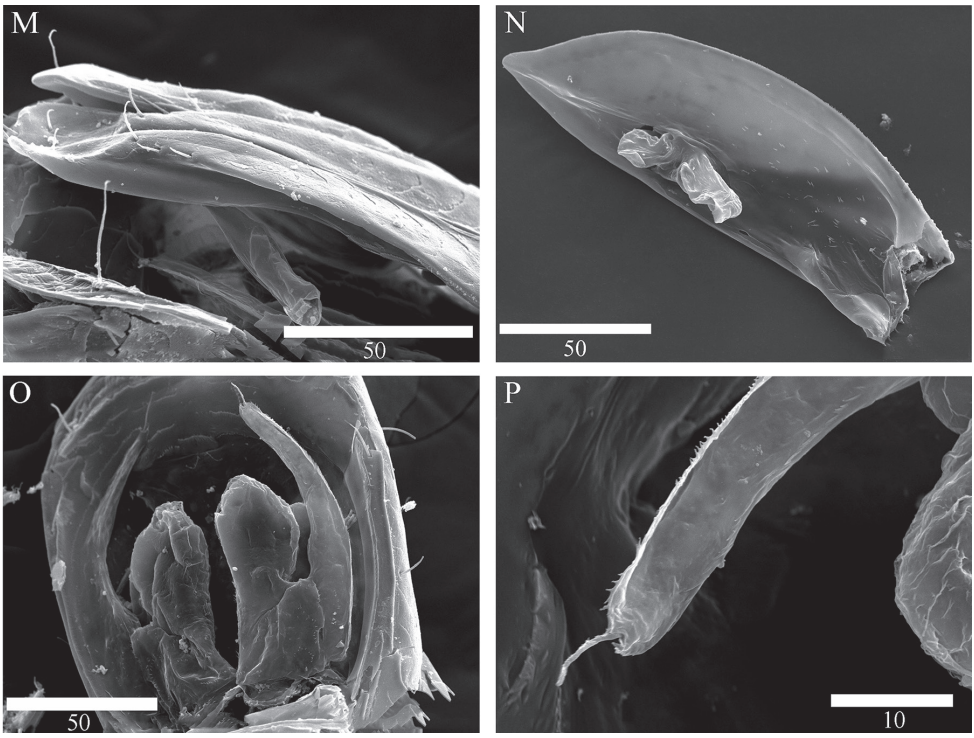

Figure 10. Scanning electron microscope images of *Microcharon tanakai* sp. n., **M** lateral view of male pleopod 1 **N** protopod of male pleopod 2, ventral **O** pleopod 3, dorsal, female **J** distal tip of pleopod 3 exopod. Scale bar unit μm.

margin; merus, with four simple setae on both side of distal corner; carpus, with one bifid, two simple, one penicillate setae (vs pereopod 7 with one bifid, one simple, one penicillate setae); propodus, pereopod 5 with two bifid, two simple, one penicillate setae (vs pereopod 6 with two bifid, thre simple, one penicillate setae; pereopod 7 with two bifid, two simple setae), with sclerite on distal margin, covering proximal part of dactylus (Fig. 8F); dactylus with two claws, two pairs of setae on both dorsal, ventral margins.

Female operculum (Fig. 6C): 1.2 times longer than wide, with no ornamentation on dorsal surface, with four setae on distal margin.

Uropods (Fig. 7E): protopod robust, slightly longer than pleotelson, length 3.1 times longer than wide, with thirteen simple and two robust setae proximomedially; endopod 0.5 times longer than protopod, 1.7 times longer than exopod, with nine simple and four penicillate setae; exopod 0.6 times longer than endopod, with four simple setae distally.

Description of male. *Penial papillae* (Fig. 9G, H): located at posteromedial margin of pereonite 7 in ventral view, coalescent, proximal margin round, tapering distally, but distal margin straight, with proximomedial opening channel.

Pleopod 1 (Figs 7A, 9I–L, 10M): elongate, total length almost reaching posterior margin of pleotelson, composed of two coalescent halves, proximal part enlarged, gradually tapering at its distal part, approximately 1.9 times longer than maximum

wide (measured at widest section of proximal part); separated in half by medial sperm tube running from triangular opening on proximal part of medial groove, distolateral edge of hyaline lamella straight, without ornamentations; parallel to lateral margin of pleopod, in lateral view distal end of lobes convex, rounded at distal apex, each with three simple setae distally, four subapical setae on ventral margin.

Pleopod 2 (Figs 7B, 10N): protopod elongate, robust, 2.9 times longer than wide; appendix masculina, curved, tapering distally, tip nearly reaching to protopod apex, with no armature; exopod rounded apically, broad.

Pleopod 3 (Figs 7C, 10O, P): no sexual dimorphism, endopod two-articulated, second article suboval, with ornamentation like turtle shell shape, and with one apical, one mesial, one lateral plumose setae; exopod two-articulated, clearly longer than endopod, reaching far beyond tip of endopod, with one simple seta distally.

Pleopod 4 (Fig. 7D): rudimentary, uniramous, no ornamentation, distal margin rounded.

Etymology. The species is named in honor of the collector, Dr. Hayato Tanaka, to express our appreciation for his support in this study.

Key to Asian species of *Microcharon*

1	Endopod of pleopod 3 with three plumose setae; article 1 of mandibular palp with one single seta distally	***M. tanakai* sp. n.**
–	Endopod of pleopod 3 naked; article 1 of mandibular palp naked	**2**
2	Antennula consist of 6 articles	***M. halophilus***
–	Antennula consist of 5 articles	**3**
3	Female operculum with 4 distal simple setae; distal part of male pleopod 1, rounded	***M. raffaellae***
–	Female operculum with 2 distal simple setae; distal part of male pleopod 1, straight	***M. kirghisicus***

DNA amplification

Partial 16S rRNA sequence was obtained only from a single female. The final length of trimmed sequence was 493 base pairs (GenBank accession number KY498031) and BLAST (Altschul et al. 1990) analysis of the GenBank data base revealed that the obtained sequence was isopod in origin and was not contaminated. *Chelator rugosus* (GenBank accession number KJ578668.1, Desmosomatidae) was the most similar sequence to *M. tanakai* resulted by Megablast optimization with the 74% identity, 1e-36 E-value, 92% of query cover, 165 of total and max score. On the other hand, when Blastn optimization was chosen, *Betamorpha fusiformis* (GenBank accession number EF116503.1, Munnopsidae) was the most similar sequence to that of our new species with 73% identity, 4e-67 E-value, 100% of query cover, and 266 of total and max score.

Discussion

Microcharon tanakai sp. n. is identified as a member of the genus *Microcharon* based on the combination of the following characters: 1) body slender, elongate and all somites subequal in width, 2) pereopods 1-4 inserted anterolaterally, pereopods 5-7 inserted posterolaterally 3) coxal plates indiscernible in dorsal view, 4) pleotelson longer than wide, longer than any pereonite, 5) antennal article three with scale laterally 6) antennal flagellum longer than podomeres 7) maxillipedal palps composed of five articles, which are broader than the endite, 8) pereopod 1 leg-like, 9) uropods with long, broad protopod, both endopod and expod shorter than protopod in all other marine species of *Microcharon* and exopod inserted subapically (Wilson and Wägele 1994; Albuquerque et al. 2014; Galassi et al. 2016). The new species can be clearly distinguished from the three Asian species. Like *M. halophilus* described from the Kaptar-Khana cave, Turkmenistan (Birstein and Ljovuschkin 1965), it shows six articles of antennula. However, their differences include: a weak rostrum on the anterior margin of cephalon in the new species; larger length/width ratio of article 6 of the antennula (1.7 vs 1); setal formula of the antennula (article 1 with two simple, one penicillate setae vs one simple seta); the presence of one simple distal seta on the article 1 of the mandibular palp; only a simple setae along the medial margin (vs with combination of bifid, simple setae) on the carpus and propodus of pereopod; the female operculum with four setae distally (vs two distal setae in *M. halophilus*); and the endopod of the pleopod 3 with three penicillate setae (vs naked in *M. halophilus*). The other Asian species, *M. kirghisicus* and *M. raffaellae* described from Kyrgyzstan (Jankowskaya 1964) and Iran (Pesce 1979) can be easily distinguished from *M. tanakai* by the number of articles on the antennula (5 vs 6); both the carpus and propodus of the pereopod with only one simple seta along the medial margin and a difference in the setal formula of the endopod of pleopod 3 (naked vs with three penicillate setae).

We were able to amplify 16S rRNA partial sequence of *M. tanakai*. To date, 228 16S rRNA sequences of the suborder Janiroidea G.O. Sars, 1897 have been deposited on GenBank belonging to the following 7 families: Desmosomatidae G.O. Sars, 1897, Macrostylidae Hansen, 1916, Joeropsididae Nordenstam, 1933, Janiridae G.O. Sars, 1897, Munnopsidae Lilljeborg, 1864, Haploniscidae Hansen, 1916 and Acanthaspidiidae Menzies, 1962. Although this molecular marker has not been commonly used for barcoding (Hebert et al. 2003; Costa et al. 2007), the 16S rDNA has been proven a valid marker for distinguishing morphologically similar species of families Serolidae Dana, 1852, Chaetiliidae Dana, 1849 and Munnopsidae Lilljeborg, 1864 (Held 2000; Held and Wägele 2005; Raupach et al. 2007).

Acknowledgements

This study was supported by the BK21 Plus Program (Future-oriented innovative brain raising type, 22A20130012806) funded by the Ministry of Education (MOE, Korea). This study was also supported by a grant (NIBR201601201) of National Research

Foundation of Korea (NRF) and National Institute of Biological Resource (NIBR) funded by the Ministry of Environment (MOE), Republic of Korea. We would like to express our great appreciation to Dr. Nicole Coineau for her kind help and invaluable comments for the improvement of this paper.

References

Albuquerque EF, Boulanouar M, Coineau N (2014) First record of *Janinella* nom. n. (Crustacea: Isopoda: Microparasellidae) in the South Atlantic: revision of the genus and description of a new Brazilian species. Journal of Natural History 48(29–39): 1817–1823. https://doi.org/10.1080/00222933.2013.877996

Altschul SF, Gish W, Miller W, Myers EW, Lipman DJ (1990) Basic local alignment search tool. Journal of Molecular Biology 215: 403–410. https://doi.org/10.1016/S0022-2836(05)80360-2

Birstein J A, Ljovuschkin SI (1965) Subterranean Paraselloidea (Crustacea, Isopoda) in USSR. Zoologicheskii Zhurnal 44: 997–1013.

Boyko CB, Bruce NL, Merrin KL, Ota Y, Poore GCB, Taiti S, Schotte M, Wilson GDF (2008 onwards) (Eds) World marine, Freshwater and Terrestrial isopod crustaceans database. http://www.marinespecies.org/isopoda [on 2017-03-28]

Coineau N (1994) Evolutionary biogeography of the Microparasellid isopod *Microcharon* (Crustacea) in the Mediterranean Basin. Hydrobiologia 287: 77–93. https://doi.org/10.1007/BF00006898

Coineau N (2000) Adaptations to interstitial groundwater life. In: Wilkens H, Culver DC, Humphreys WF (Eds) Subterranean ecosystems, ecosystems of the world 30. Elsevier, 189–210.

Costa FO, deWaard JR, Bouthillier J, Ratnasingham S, Dooh RT, Hajibabaei M, Hebert PDN (2007) Biological identification through DNA barcodes: the case of the Crustacea. Canadian Journal of Fisheries and Aquatic Sciences, 64: 272–295. https://doi.org/10.1139/f07-008

Galassi DMP, Bruce NL, Fiasca B, Dole-Oliver MJ (2016) A new family Lepidocharontidae with description of *Lepidocharon* gen. n., from the Great Barrier Reef, Australia, and redefinition of the Microparasellidae (Isopoda, Asellota). Zookeys 594: 11–50. https://doi.org/10.3897/zookeys.504.8049

Hebert PDN, Cywinska A, Ball SL, deWaard JR (2003) Biological identifications through DNA barcodes. Proceedings of the Royal Society of London B 270: 313–321. https://doi.org/10.1098/rspb.2002.2218

Held C (2000) Phylogeny and Biogeography of Serolid Isopods (Crustacea, Isopoda, Serolidae) and the Use of Ribosomal Expansion Segments in Molecular Systematics. Molecular Phylogenetics and Evolution 15(2): 165–178. https://doi.org/10.1006/mpev.1999.0739

Held C, Wägele JW (2005) Cryptic speciation in the giant Antarctic isopod *Glyptonotus antarcticus* (Isopoda: Valvifera: Chaetiliidae). Scientia Marina: 69(2) 175–181. https://doi.org/10.3989/scimar.2005.69s2175

Jankowskaya AJ (1964) Relict Crustacean of coastal bottom waters of the lake Issyk Kul (North Tien-Shan). Zoologicheskii Zhurnal 43(7): 975–986.

Karaman S (1934) Beitrage zur Kenntnis des Isopoden-Familie Microparasellidae. Mitteilungen über Hohlen- und Karstforschung 1934: 42–44.

Palumbi SR, Martin A, McMillan WO, Stice L, Grabowski G (1991) The simple fool's guide to PCR, Version 2.0. http://palumbi.stanford.edu/SimpleFoolsMaster.pdf

Pesce GL (1979) The first Microparasellid from subterranean water of Iran, *Microcharon raffaellae* n. sp. (Crustaca, Isopoda). Vie et Milieu, 28–29, fasc. 2 série C 237–245.

Riehl T, Brandt A (2010) Descriptions of two new species in the genus *Macrostylis* Sars, 1864 (Isopoda, Asellota, Macrostylidae) from the Weddell Sea (Southern Ocean), with a synonymisation of the genus *Desmostylis* Brandt, 1992 with *Macrostylis*. ZooKeys 57: 9–49. https://doi.org/10.3897/zookeys.57.310

Raupach MJ, Malyutina M, Brandt A, Wägele JW (2007) Molecular data reveal a highly diverse species flock within the munnopsoid deep-sea isopod *Betamorpha fusiformis* (Barnard, 1920) (Crustacea: Isopoda: Asellota) in the Southern Ocean. Deep-Sea Research II 54: 1820–1830. https://doi.org/10.1016/j.dsr2.2007.07.009

Shimomura M, Ohtsuka S, Tomikawa K (2006) *Ingolfiella inermis* n. sp., a New Interstitial Ingolfiellid Amphipod from Okinawa, Southern Japan (Peracarida, Amphipoda). Crustaceana 79(9): 1097–1105. https://doi.org/10.1163/156854006778859614

Wilson GDF, Wägele JW (1994) A systematic review of the family Janiridae (Crustacea: Isopoda: Asellota). Invertebrate Taxonomy 8: 683–747. https://doi.org/10.1071/IT9940683

ZooKeys 680: 33–56 (2017)
doi: 10.3897/zookeys.680.13213
http://zookeys.pensoft.net

RESEARCH ARTICLE

A peer-reviewed open-access journal
ZooKeys
Launched to accelerate biodiversity research

Two new Oribatid mites from Costa Rica, *Mixacarus turialbaiensis* sp. n. and *Paulianacarus costaricensis* sp. n. (Acari, Oribatida, Lohmanniidae)

Nestor Fernandez[1,2], Pieter Theron[2], Sergio Leiva[3], Louwrens Tiedt[4]

1 *National Council of Scientific and Technological Research, Argentina (CONICET). Subtropical Biological Institute (IBS). Evolutionary Genetic Laboratory FCEQyN, Misiones National University. Felix de Azara 1552, 6º, (3300) Posadas Misiones Argentina* **2** *Research Unit for Environmental Sciences and Management, North-West University, Potchefstroom Campus, 2520, South Africa* **3** *Fellowship, National Institute Agricultural Technology (INTA). Experimental Rural Agency, Aimogasta. La Rioja, Argentina* **4** *Laboratory for Electron Microscopy, North-West University, Potchefstroom Campus, 2520, South Africa*

Corresponding author: *Nestor Fernandez* (nestorfernand51@yahoo.fr)

Academic editor: *V. Pesic* | Received 11 April 2017 | Accepted 3 June 2017 | Published 14 June 2017

http://zoobank.org/238D1394-D08F-4906-A869-5BAF5CB70D64

Citation: Fernandez N, Theron P, Leiva S, Tiedt L (2017) Two new Oribatid mites from Costa Rica, *Mixacarus turialbaiensis* sp. n. and *Paulianacarus costaricensis* sp. n. (Acari, Oribatida, Lohmanniidae). ZooKeys 680: 33–56. https://doi.org/10.3897/zookeys.680.13213

Abstract

In this paper we describe two new species belonging to the family Lohmanniidae: *Mixacarus turialbaiensis* **sp. n.** and *Paulianacarus costaricensis* **sp. n.** from Costa Rica.

Keywords

Acari, Oribatida, Lohmanniidae, Costa Rica, *Mixacarus turialbaiensis* sp. n., *Paulianacarus costaricensis* sp. n.

Introduction

Approximately three years ago, the authors commenced the study of materials housed at the Museum d'Histoire Naturelles de Genève (MHNG), which was collected from the Turrialba forest in Costa Rica. In this initial paper, we describe two new species belonging to genera *Mixacarus* and *Paulianacarus* of the family Lohmanniidae. The taxonomy of the first species, *Mixacarus turialbaiensis* sp. n., was problematic as taxonomically important characters of related species were not adequately described in most prior studies. For the second species, *Paulianacarus costaricensis* sp. n., the situation is similar, but with seemingly misinterpreted original descriptions an aggravating factor.

Material and methods

Specimens studied by means of light microscopy were macerated in lactic acid, and observed in the same medium using the open-mount technique (cavity slide and cover slip) as described by Grandjean (1949), Krantz and Walter (2009). Drawings were made using a Zeizz GFL (Germany) compound microscope equipped with a drawing tube. Specimens preserved in ethanol, studied under Scanning Electron Microscope (SEM), were carefully rinsed by sucking them several times into a Pasteur pipette, after which they were transferred to buffered glutaraldehyde (2,5%) in Sörensen phosphate buffer: pH 7,4; 0,1 m for two hours. After postfixation for 2hr. in buffered 2% OsO4 solution and being rinsed in buffer solution; all specimens were dehydrated in a series of graded ethanol and dried in a critical point apparatus. After mounting on Al-stubs with double sided sticky tape, specimens were gold coated in a sputter apparatus (Alberti and Fernandez 1988, 1990a, 1990b; Alberti et al. 1991, 1997, 2007; Fernandez et al. 1991). For SEM observations, a FEI-Quanta Feg 250 Scanning Electron Microscope; with 10 Kv and working distant (WD) variable was used.

Measurements taken: total length (tip of rostrum to posterior edge of notogaster); width (widest part of notogaster) in micrometers (μm). Setal formulae of the legs include the number of solenidia (in parentheses); tarsal setal formulae include the famulus (ε).

Morphological terminology and abbreviations

Morphological terms and abbreviations used are those developed by Grandjean (1928–1974) (cf. Travé and Vachon, 1975; Norton and Behan-Pelletier (in Krantzand Walter 2009);); Norton and Behan-Pelletier (2009); Fernandez et al. (2013a–c).

Institutions

MHNG (Muséum d'Histoire Naturelles, Genève, Switzerland).

New taxa descriptions

Family Lohmanniidae Berlese, 1916
Genus *Mixacarus* Balogh, 1958

***Mixacarus turialbaiensis* sp. n.**
http://zoobank.org/BE1D6634-752A-4E97-8E51-128B3E96F96E
Figs 1–28; Table 1

Etymology. The specific epithet is dedicated to the Turrialba forest of Costa Rica, where the specimens were collected.

Type material. Holotype. Label details: "CCR 0978 Tu 11 Costa Rica Turrialba forêt naturelle du catie alt. 560 m. Triage d'humus cote est surface nid d'*Atta* au pied de *Castilla elastica* 1.IX. 1978. LEG P.WERNER 10.140744, alt. 120 m" conserved in 70% ethanol, deposited in MHNG.

Paratypes. same data, 2 ♀♀ deposited in MHNG; preserved in 70% ethanol.

Diagnosis (adult female). Setae *ro* inserted anteriorly on transversal cuticular ridge; *le*, *in* setae erect; setae *ro*, *le*, *in* more or less similar length. Several ribbon-like bands near *ro*, *le*, *exa*, *exp* setae; sensillus pectinate (6–9 pectines); clearly visible superior cornea of naso (*CSO)*.

Sixteen pairs of setae: c_1, c_2, c_3, d_1, d_2, d_3, e_1, e_2, f_1, f_2, h_1, h_2, h_3, p_1, p_2, p_3; eight transversal bands: *S2, S3, S4; S5, S6, S7, S8, S9*. Bands *S2, S6, S8, S9* cross medial notogastral plane transversally; *S3, S4, S5, S7* not crossing medial notogastral plane. Five pairs of lyrifissures: *ia, ip, ips, im, ih.*

Adoral setae: or_1 spoon-shaped, largest; or_2 elongate, tip beak-shaped; or_3 large, rounded apex. Epimeral setal formula 3–1–3–(3–4), epimere IV with either three or four pairs of setae; genital plate undivided, rounded elevated central zone bearing nine or ten pairs of setae; six or seven pairs of simple setae aligned paraxially,

Description (female). *Measurements*. 525 (485–560) × 233 (224–245) (ten specimens measured).

Shape. Oval (Figures 1, 9, 10, 12).

Colour. Yellow to light brown; slightly shiny when observed in reflected light.

Cerotegument. Almost nonexistent; or disappeared during extensive period of conservation in ethanol.

Integument. Smooth: prodorsum, notogaster, ventral region (Figures 1, 12); depressed areas of variable size with polyhedral microsculpture (Figure 7): *sb* (ribbon-like prodorsal bands) (Figure 1); lateral prodorsal zone (Figures 5, 6); zone of *l.d* (Figures 8, 13, 14); notogastral band *S2, S3, S4, S5, S6, S7, S8, S9* (Figures 1, 2, 9, 11, 12, 19); notogastral marginal zone (Figures 12, 19); subcapitular zone around setae *h*, m_1, m_2, *a* (Figure 20); epimeral zone (Figures 16, 17, 21, 23); anogenital zone (Figure 18); ventral zone external to anogenital zone (Figures 16, 18); legs (Figures 24–28).

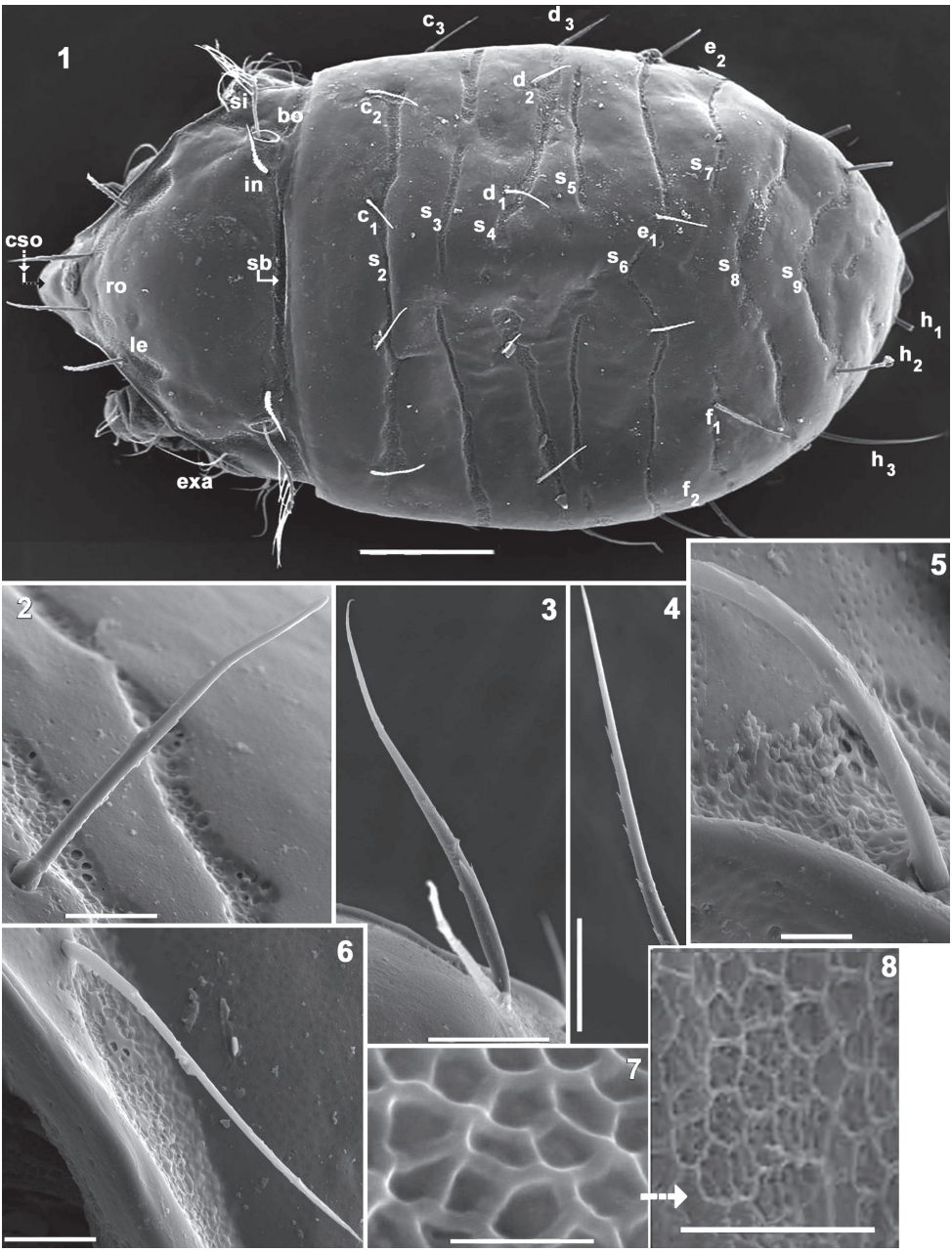

Figures 1–8. *Mixacarus turialbaiensis* sp. n. Adult with cerotegumental layer. SEM. **1** dorsal view **2** notogastral setae d_3 **3** *ro* setae **4** *in* setae **5** *exa* setae **6** *exp* setae **7** detail of cuticular microsculpture **8** polyhedral microsculpture from porose area. Abbreviations: See Material and methods. Scale bars: **1** = 100 μm; **2** = 20 μm; **3** = 10 μm; **4** = 20 μm; **5** = 5 μm; **6** = 10 μm; **7** = 2 μm; **8** = 5 μm.

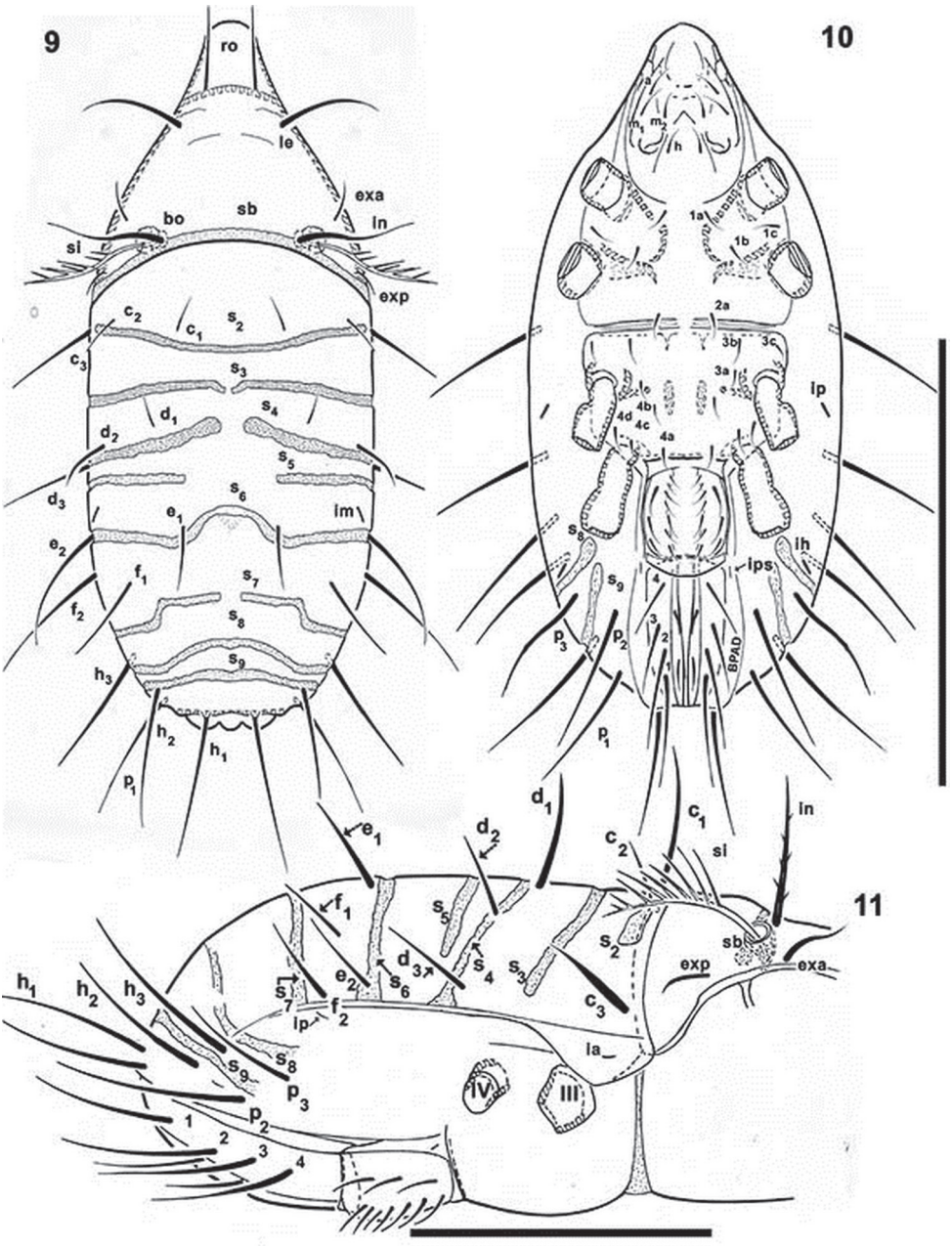

Figures 9–11. *Mixacarus turialbaiensis* sp. n. Adult, optical microscopy. **9** dorsal view **10** ventral view **11** lateral view. Abbreviations: See Material and methods. Scale bars: 9, 10 = 300 μm; 11 = 200 μm.

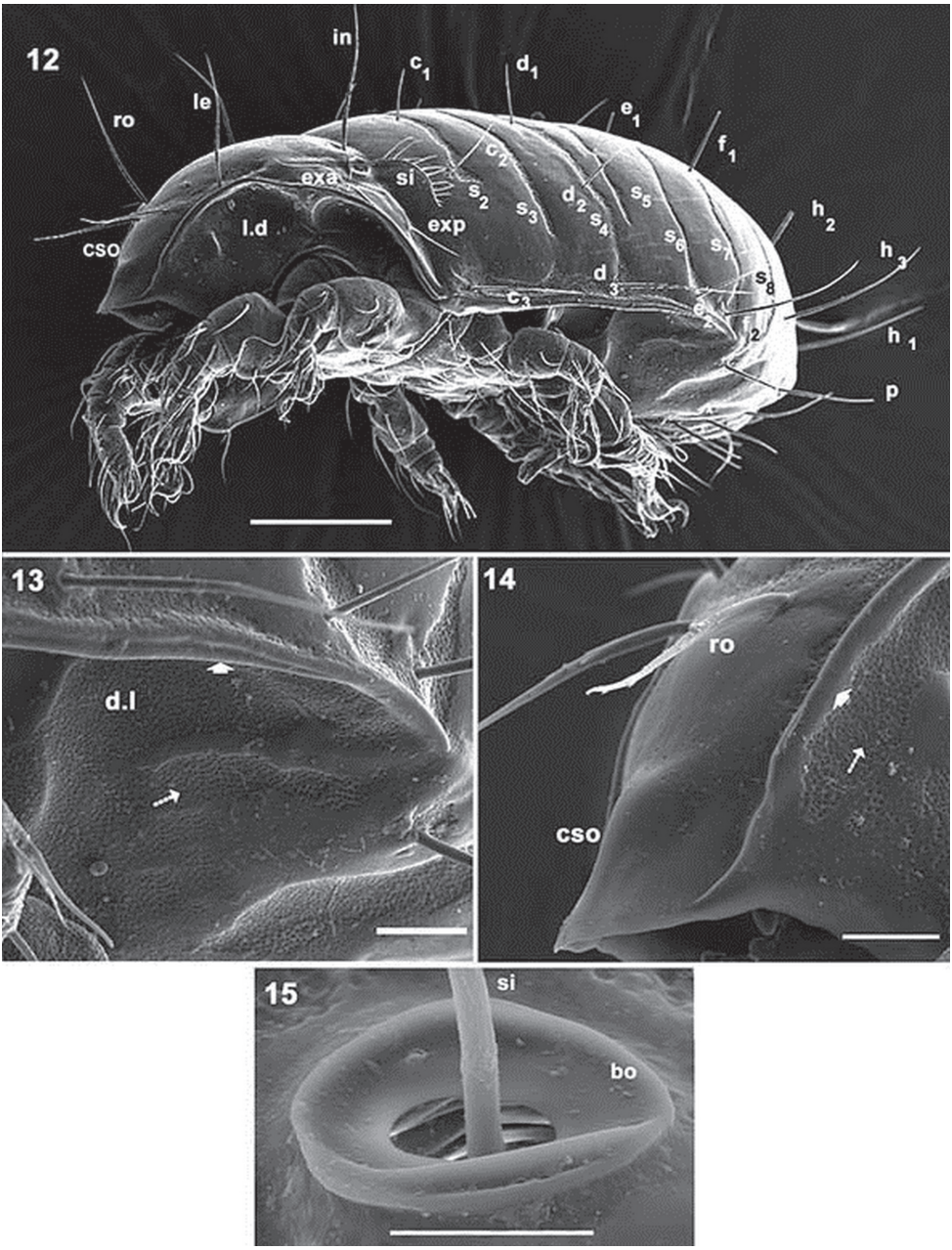

Figures 12–15. *Mixacarus turialbaiensis* sp. n. Adult with cerotegumental layer. SEM. **12** lateral view **13** microsculpture lateral zone **14** anterior prodorsal zone **15** bothridial zone. Abbreviations: See Material and methods. Scale bars: **12 =** 100 μm; **13 =** 20 μm., **14** μm = 20 μm; **15** = 10 μm.

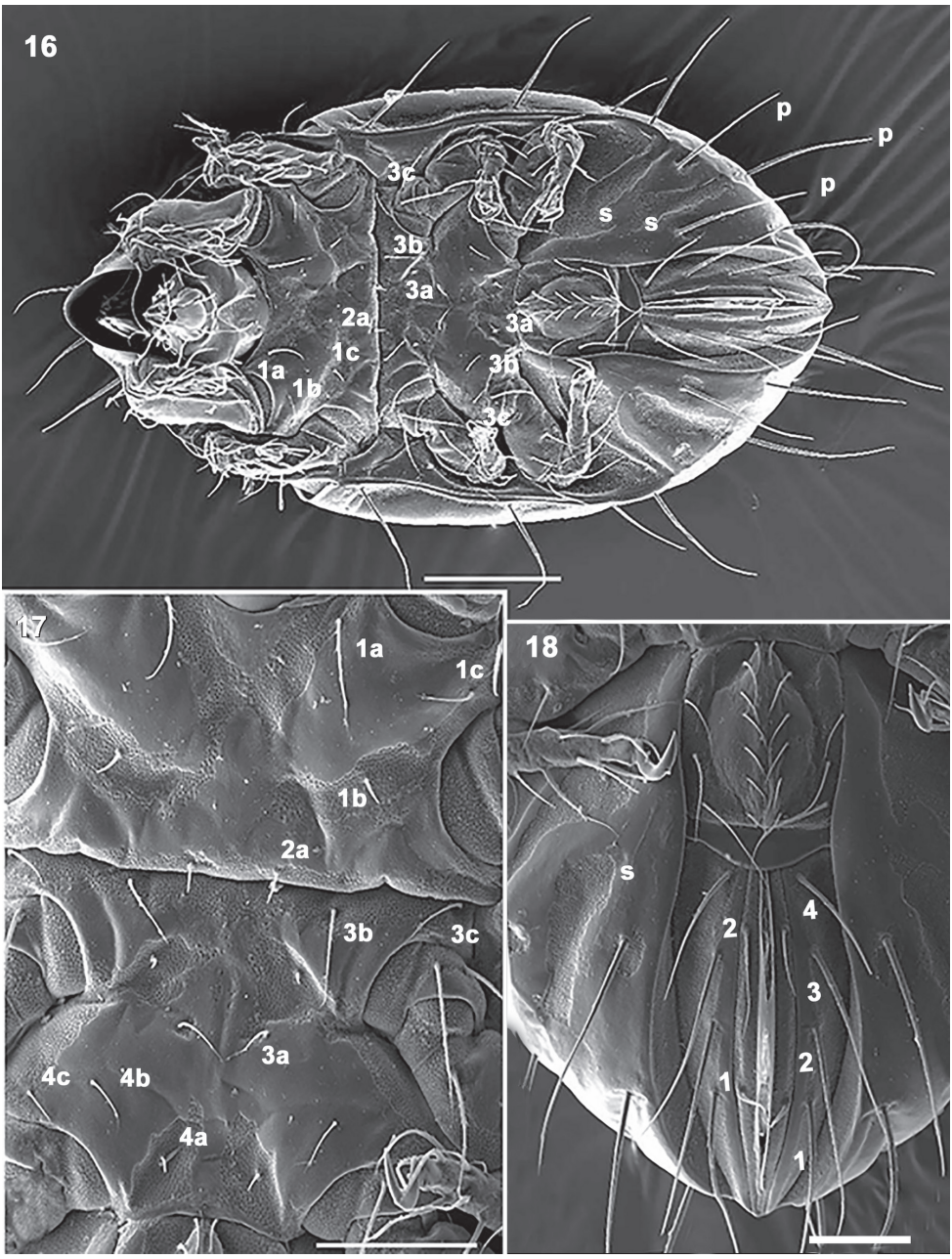

Figures 16–18. *Mixacarus turialbaiensis* sp. n. Adult with cerotegumental layer. SEM. **16** ventral zone **17** Epimeral zone **18** anogenital region. Abbreviations: See Material and methods. Scale bars: **16**=100 μm; **17, 18**= 50 μm.

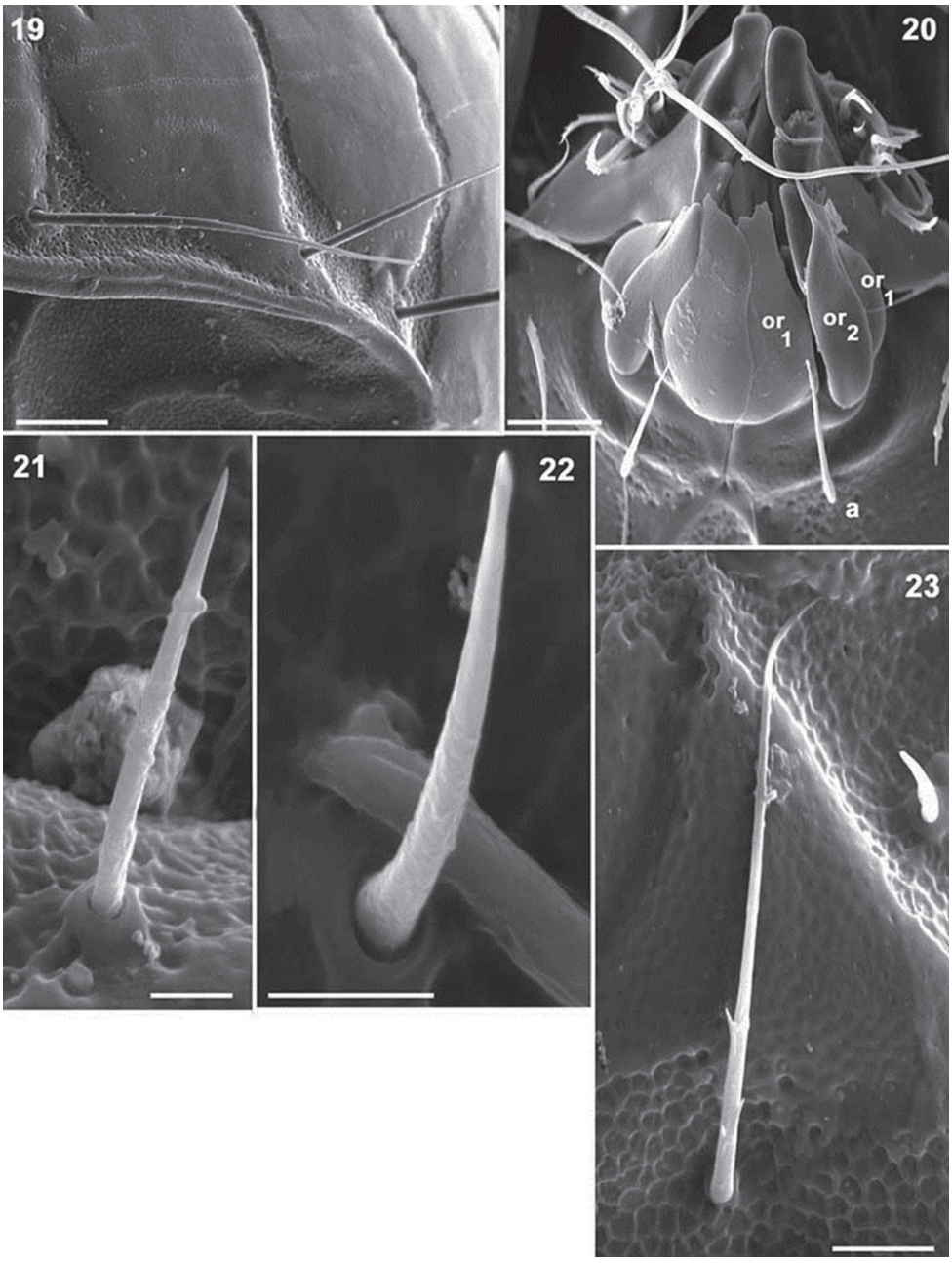

Figures 19–23. *Mixacarus turialbaiensis* sp. n. Adult with cerotegumental layer. SEM. **19** lateral notogastral zone **20** adoral setae **21** epimeral zone, *2a* setae **22** epimeral zone, *3a* setae **23** epimeral zone, *3b* setae. Abbreviations: See Material and methods. Scale bars: **19** = 20 μm**; 20** = 10 μm; **21, 22** = 2 μm; **23** = 5 μm.

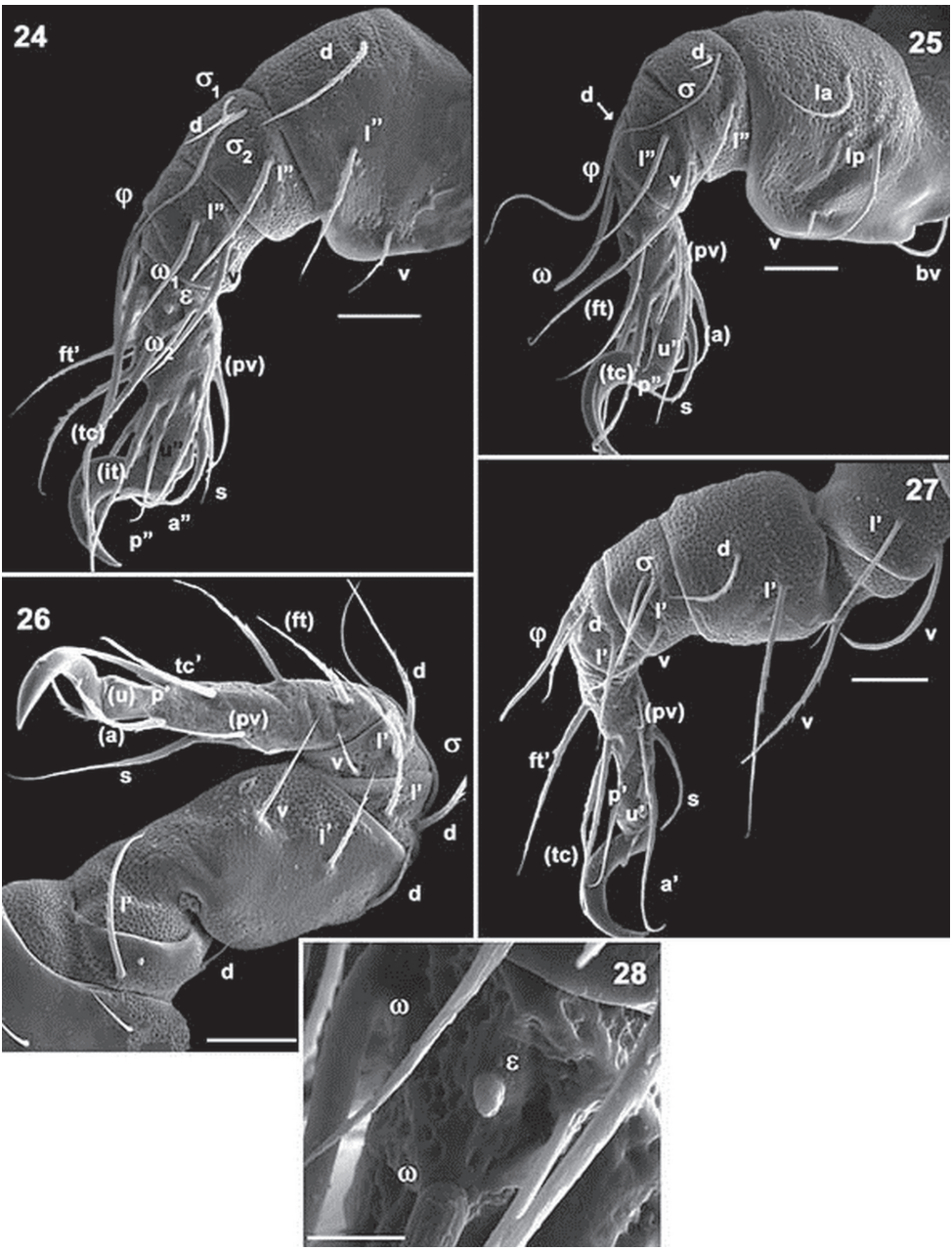

Figures 24–28. *Mixacarus turialbaiensis* sp. n. Adult with cerotegumental layer. SEM. **24** leg I antiaxial view **25** leg II antiaxial view **26** leg IV antiaxial view **27** leg III antiaxial view **28** tarsus I, famulus zone. Abbreviations: See Material and methods. Scale bar: **23** = 50 μm; **24** = 20 μm; **25** = 20 μm; **26** = 20 μm; **27** = 20 μm; **28** = 5 μm.

Setation (legs not included). Two types: *simple, smooth*: genital, anal (Figures 1, 2, 18); *simple, barbed*: prodorsum, notogaster, epimeral, subcapitular (Figures 3, 4, 5, 14, 21, 23). Barbs are small, difficult to observe.

Prodorsum. Shape: triangular, rounded apex in dorsal view (Figures 1, 9); triangular in lateral view (Figures 12, 14). Rostrum broadly rounded (Figures 1, 9); elevated chitinous ridge present on either side of prodorsal area, externally to *exa*, *exp*, *le* setae, derived from margins of leg depressions (Figures 12, 14); *ro* setae inserted anteriorly on transversal cuticular ridge, generally directing forward (Figures 1, 9, 12); *le*, *in* setae erect (Figure 12); setae *ro*, *le*, *in* more or less similar length. Several ribbon-like bands near *ro*, *le*, *exa*, *exp* setae, extending laterally to elevated lateral ridge (Figures 5, 6, 12, 13). *Bo* rounded, slightly elevated from the cuticular surface (Figure 15), laterally tilted (Figures 1, 9, 12). Sensillus pectinate (6–9 pectines) (Figures 9, 11, 12). Postbothridial transverse band *sb* clearly discernible, situated posterior to *bo* and *in* setae (Figures 1, 9, 11). On anterior zone near apex, in front of *ro* setal insertion and between cuticular elevations of *l.d*, *CSO* clearly visible (Figures 1, 12, 14).

Notogaster. Sixteen pairs of primary notogastral setae: c_1, c_2, c_3, d_1, d_2, d_3, e_1, e_2, f_1, f_2, h_1, h_2, h_3, p_1, p_2, p_3 clearly discernible (Figures 1, 9, 11, 12). Nine transversal bands: *S2, S3, S4, S5, S6, S7, S8, S9* (Figures 1, 9, 11 ,12); *S2* crossing transverse medial notogastral plane, exceeding slightly beyond c_2 setae, terminating near c_3 in a large rectilinear tip (Figures 11, 12); *S3* situated behind *c* setal alignment and in front of *d* setal alignment, not crossing medial notogastral plane; laterally stopping above c_3, d_3 setal insertion level (Figures 11, 12); S4 observed anterior to *d* setal alignment, not crossing medial notogastral plane, running obliquely, exceeding d_1 setal insertion level, terminating in rounded end (Figures 1, 9); S4 extending to unsclerotized lateral longitudinal line (Figures 11, 12); S5 thin (Figures 1, 9), not crossing medial notogastral plane, laterally terminating before d_3 setal insertion level (Figures 11, 12); S6 situated behind e_1, crossing medial notogastral plane (Figures 1, 9), laterally reaching unsclerotized lateral longitudinal line (Figures 1, 9, 11, 12); S7 situated behind f_1 setal insertion, not crossing medial notogastral plane, extending to unsclerotized lateral longitudinal line (Figures 1, 9, 11, 12); S8, S9 crossing medial notogastral plane and unsclerotized lateral longitudinal line (Figure 11).

Five pairs of lyrifissures present: *ia*, *ip* situated below the unsclerotized lateral longitudinal line (see Lateral region); *ips* situated on the adanal fold band (BPDA) (Figures 9, 10, 11); *im* near e_2 setae and *ih* behind h_3.

Lateral region. Prodorsal margin present on either side of cavities housing legs I-IV when retracted. Anterior notogastral zone presenting conspicuous tectum and clearly defined unsclerotized lateral longitudinal line, terminating almost posterior to level of *ip* lyrifissure and delimiting unpaired dorsal notaspis and pleuraspis (paired narrow lateral zones) (Figure 11). In posterior notogastral zone, when unsclerotized line does not exist, notaspis and pleuraspis not delimited (Figure 11). Each pleuraspis presenting an anterior rounded lobe between legs II and III, where lyrifissure *ia* is observed. Posteriorly, at level of d_3 and e_2 setae, well delimited edges form canopies over cavities in which legs III and IV are housed when retracted, with a protruding angle between them.

Table 1. *Mixacarus turrialbai* sp. n.: setae and solenidia.

	Femur	Genu	Tibia	Tarsus	Claw
Leg I					
setae	*l",d,v*	*l",d*	*l",v*	*(p),(u),(a),σ,(it),(tc),(ft),(pv),e*	1
solenidia		σ, σ	φ	ω_1 , ω_2	
Leg II					
setae	*la,lp,vb,v*	*d,l",*	*d,l",v*	*(p),(u),(a),σ,(tc),(ft),(pv)*	1
solenidia		σ	φ	ω	
Leg III					
setae	*l',v*	*d,l',v*	*d,l',v*	*(p),(u),(a),σ,(tc),(ft),(pv)*	1
solenidia		σ	φ		
Leg IV					
setae	*d,l',v*	*d,l'*	*d,l'v*	*(p),(u),(a),σ,(tc),(ft),(pv)*	1
solenidia		σ			

Ventral region. Anterior zone of subcapitulum more or less triangular, posterior zone ovoid. Four pairs of subcapitular setae (Figure 10) *h*, m_1, m_2, *a*. Characteristic adoral setae: or_1 largest, spoon shaped; or_2 elongate, terminating in beak-shape; or_3 large, rounded apex (Figure 20).

Coxisternal region divided into two parts by ventrosejugal groove (Figures 10, 16, 17). Apodemes short and clearly visible; epimeral setal formulae 3-1-3-(3-4), epimere IV with three or four pairs of setae; all setae similarly shaped, but vary in length (Figures 21, 22, 23). Genital plate undivided, elevated central zone rounded with ten pairs of setae, sometimes with only nine pairs; (Figures 10, 16, 18); six or seven simple setae aligned paraxially, and three antiaxially. Preanal plate more or less triangular, rounded central zone.

Anal and adanal plates with four pairs of adanal and two pairs anal setae (Figures 16, 18). Band BPAD clearly visible in specimens immersed in lactic acid for lengthy period; lyrifissure *ips* present near margin of this band (Figure 10).

Legs. Two types of femora can be distinguished. Femora of legs I and II displaying large ventral blade (Figures 24, 25), femora of legs III and IV lacking ventral blade (Figures 26, 27).

Setal formulae I (0–3–2–2–16–1) (2–1–2); II (0–4–2–3–13–1) (1–1–1); III (2–3–2–2–13–1) (1–1–0); IV (2–3–2-3–13–1(1–0–0). See Table 1.

Genus *Paulianacarus* Balogh, 1960

***Paulianacarus costaricensis* sp. n.**
http://zoobank.org/662FF0B7-A77E-441D-90D2-2720B07FA833
Figs 29–55; Table 2

Etymology. The specific epithet is dedicated to Costa Rica *costaricensis* (Latin = from Costa Rica), the country where the specimens were collected.

Type material. Holotype. Label details: "♀ CR 0978 Tu 18a. Costa Rica Turrialba forêt naturelle du catie alt. 560 m. Racines d'epiphytes sur branche tombe 1 mois avant. 24. IX. 1978 LEG P.WERNER". MHNG, preserved in 70% ethanol. **Paratypes:** same data and locality 2 ♀♀. MHNG, preserved in 70% ethanol.

Diagnosis. *Prodorsum.* Triangular to slightly polyhedral; rostrum rectilinear; *ro* setae inserted far from rostrum; *si* pectinate (5-8 pectines). *Notogaster*. Sixteen pairs of setae: c_1, c_2, c_3, d_1, d_2, d_3, e_1, e_2, f_1, f_2, h_1, h_2, h_3, p_1, p_2, p_3. Cuticular surface with nine elevated transversal thickenings; 1-5 complete, crossing medial notogastral plane; 6-9 not crossing medial notogastral plane; elevated transversal thickening, nine transverse bands present; 3, 4, 7 smooth, others with promontories.

Description (Adult female). *Measurements.* Length 960 (1100–890) ×535 (526–540) (three specimens).

Shape. Elongate ovoid (Figures 29, 30, 31, 32).

Colour. Dark to light brown; slightly shiny when observed in reflected light.

Cerotegument. Nonexistent.

Integument. Complex microsculpture. Rounded promontories (Figures 29, 30, 38, 40, 41); elevated transversal thickening (*tr.e.t*) (Figures 29, 30, 31, 33); polyhedral microsculpture (0.7–0.8) (Figures 42, 43, 44, 45, 46 indicated by arrow) in depressed areas (Figure 46, under large magnification), this type of microsculpture observed on cuticular structures on various areas of body and legs (Figures 42, 43, 44, 45 indicated by u), principally on transverse bands.

Setation (legs not included). Two types: *simple, smooth*: prodorsum: *le*, *ro* length 163 (140–180); *exp, exa* length 153 (140–160); notogaster: 167 (140–180); epimeral (40–53); genital 53 (40–52); aggenital 59.5 (45–72); anal 74 (63–81); adanal 119 (100–136); subcapitular (*h*, *m*) 51.5 (50–54); *a* 39.5 (36–41) (Figures 49, 50); *simple barbate*: *in* setae 142 (130–150) (Figures 38, 41).

Prodorsum. Triangular to slightly polyhedral in dorsal view (Figures 30, 31); triangular in lateral view (Figures 29, 34).

Rostrum rectilinear (Figures 33–35). Prodorsal margin dentate (Figures 34, 39). Depression housing legs *l.d* (for legs I and II) (Figure 36) clearly observed as laterally situated concave arc-shaped zone; *ro* setae inserted far from rostrum, in some instances situated slightly anterior to *tr.l.t* (transversal elevated thickening) (Figures 29, 30, 31); margins of *l.d* formed by elevated cuticular thickening (indicated by arrows ¿ Figures 33, 34). Medial prodorsal zone, situated between *sb* (transverse postbothridial band), transversal linear thickening (*tr.l.t*) and setae *exp*, *exa*, *le*, with prominent elevated round promontories (Figure 33); smooth polyhedral area situated between *l.d* elevated margins, *tr.l.t* and rostrum; with an interior rectangular zone (Figures 33, 34 indicated by s); *le* setal insertion anterior to *tr.l.t* (Figure 33), situated near *l.d* elevated margin (Figure 33, indicated by arrows ¿); *bo* cup-shaped, dorsally open (Figures 36, 38); *si* pectinate, with 5–8 large pectines (Figures 33, 38, 41); *in* setae inserted at level of *bo*, situated internally to *bo* and in front of *sb* (Figures 30, 31); *exa* and *exp* well visible, situated marginally on a smooth area (Figure 43); *sb* clearly discernible, situated behind *in* setal insertions (Figures 30, 31).

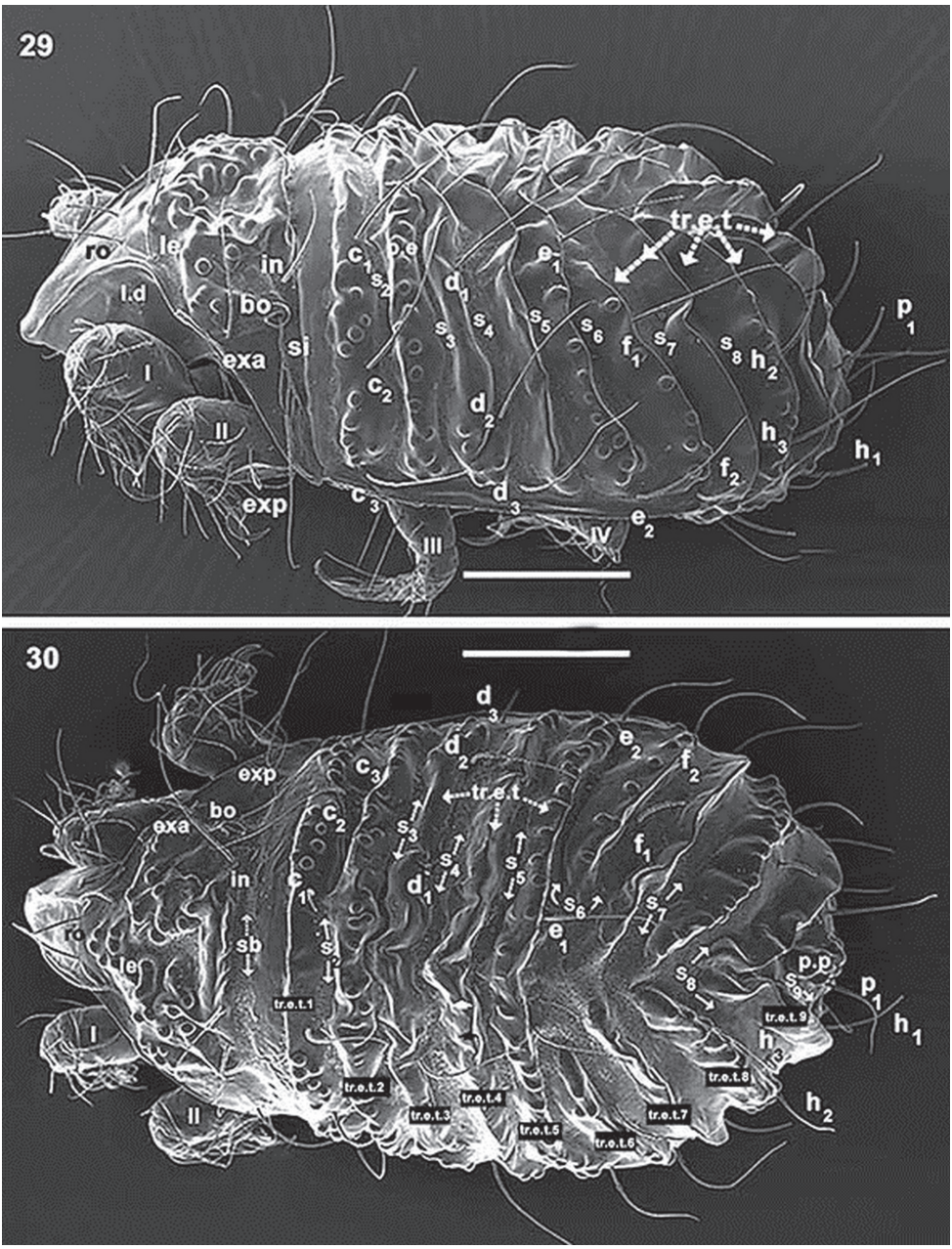

Figures 29–30. *Paulianacarus costaricensis* sp. n. Adult with cerotegumental layer. SEM. **29** lateral inclined view **30** dorsal with slight lateral tilt. Abbreviations: See Material and methods. Scale bars: **29, 30** = 200 μm.

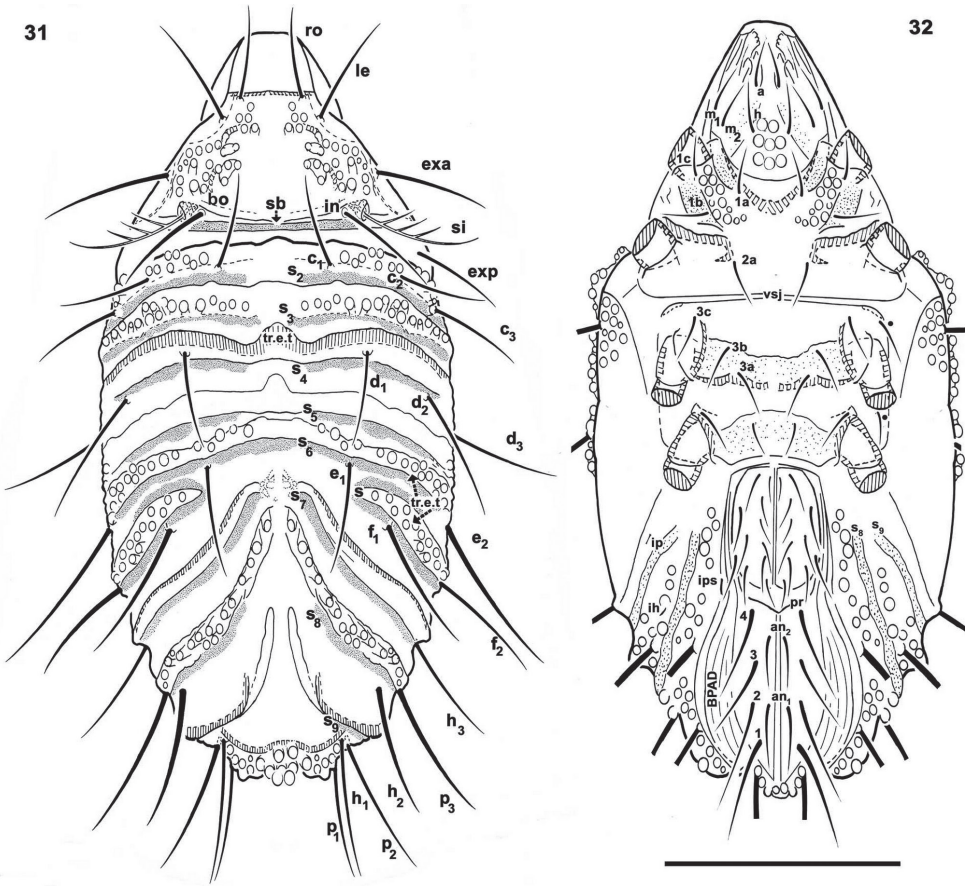

Figures 31–32. *Paulianacarus costaricensis* sp. n. Adult, optical microscopy**. 31** dorsal view **32** ventral view. Abbreviations: See Material and methods. Scale bar: **31**, **32** = 400 μm.

Frontal view. Rostrum rectilinear, situated in medial zone between *l.d* elevated cuticular thickening (Figures 33, 34, indicated by arrows ¿); prodorsal border at first concave and becoming convex towards the posterior; in boundary zone between concave and convex, a series of dentate projections (Figures 34, 39). Anterior subcapitular zone (Figures 32, 34, 35), adoral setae clearly visible: or_3 sigmoid; or_2 very complex, leaf-shaped in ventral view (Figure 35), in lateral view (Figure 46) resembling a bird's head and beak; or_1 very complex, resembling a leaf with edges eaten by a caterpillar (Figures 35, 46).

Notogaster. Sixteen pairs of notogastral setae: c_1, c_2, c_3, d_1, d_2, d_3, e_1, e_2, f_1, f_2, h_1, h_2, h_3, p_1, p_2, p_3, clearly discernible and directing backward (Figures 29, 30, 31).

Cuticular surface with elevated transversal thickenings (*tr.e.t*); *tr.e.t.1* with rounded promontories, situated in front of *c* setal alignment, externally to c_1 setae; smooth zone

between c_1 setal pair (Figure 29). Transverse bands: S2 clearly visible (Figures 29, 30, 31), situated behind *c* setal alignment. Thickenings *tr.e.t.2* and *tr.e.t.3* between *c* and *d* setal alignment; *tr.e.t.2* with rounded promontories, close to *c* alignment; *tr.e.t.3* smoothly surfaced, close to *d* setal alignment; longitudinal furrow running between d_1 setal insertions. Transverse band S3 observed between *tr.e.t.2* and *tr.e.t.3* (Figures 29, 30, 31). S4 situated posterior to *d* setal alignment. Transverse thickenings *tr.e.t.4* and *tr.e.t.5* between *d* and *e* setal alignment; *tr.e.t.4* smooth, with deep central furrow (Figure 30, indicated by¿) running along *tr.e.t4*; *tr.e.t5* with rounded promontories. S5 situated between *tr.e.t4* and *tr.e.t5*. U-shaped S6, with rounded promontories, observed between *e* and *f* setal alignment, situated on either side of *tr.e.t.6*. Posterior to *f* setal alignment, in oblique position, with central zone not corssing longitudinal medial plane, smooth *tr.e.t. 7*. S7 situated behind *tr.e.t.7*; *tr.e.t8* in oblique position, not crossing medial longitudinal plane, surface with rounded promontories. S8 behind *tr.e.t8*; *tr.e.t.9* in oblique position, not crossing medial longitudinal plane, smooth; S9 situated behind *tr.e.t.* A series of more or less triangular posterior promontories (*p.p*) observed in posterior medial zone (Figures 29, 30, 31). Only lyrifissure *ia* discernible anteriorly on frontal lobe of pleuraspis.

Lateral region. Bothridium (*bo*): margin elevated, ovoid, clearly visible (Figures 36, 38); *sb* depressed zone situated close to and behind *bo* and *in* (Figures 30, 31, 38); polyhedral microsculpture (Figure 45); small depressed marginal zone situated above longitudinal unsclerotized line (Figure 37). Rounded promontories easily visible (Figures 36, 38, 40). Prodorsal margin presenting conspicuous depression *l.d* (Figure 36), housing legs I–IV during leg folding. Polyhedral lobe with lyrifissure *ia* and rounded promontories (Figure 37) on anterior zone of pleuraspis. Conspicuous tectum on anterior notogastral zone. Unsclerotized longitudinal line easily discernible, exceeding level of f_2 setal insertions and clearly delimiting notaspis and pleuraspis (Figure 36).

Ventral region. Four pairs of subcapitular setae (Figure 49); setae *h*, m_2 and *a* clearly visible (more or less similar length); setae m_1 situated marginally and hardly discernible (Figures 32, 37, 49). Infracapitulum: complex microsculpture. Triangular microsculpture with rounded promontories in central zone between setae *h*, surrounded by smooth zone. Several areas with polyhedral microsculpture (Figure 49, indicated by ¿).

Epimeral zone: only epimere I with rounded promontories, easily observed in insertion zones of setae *1a, 1b, 1c* (Figure 47). Other epimeres smooth; epimeral setae variable on epimeres 3, 4 with formulae: 3–1–[3 (2)]–[4 (3)] (Figure 32 indicated by l). All setae similarly shaped (Figure 47). Genital plate undivided with nine to ten pairs of setae (Figures 32, 49); six or seven aligned paraxially and three or four antiaxially. Preanal plate typically shaped, characteristic of the genus (Figures 47–48). Anal plate fused with adanal, delimiting single plate with six pairs of setae (Figures 47, 48). BPAD clearly visible after lengthy soaking in lactic acid (Figure 32); lyrifissures *ia, ip, ih*, *ip* observed (Figures 32, 37).

Legs. Setal formulae I (0–4–3–3–16–1) (2–1–2); II (0–6–3–5–13–1 (1–1–1); III (2–2–3–3–13–1 (1–1–0); IV (2–3–3–2–13–1(1–0–0). See Table 2 and Figures 52–55.

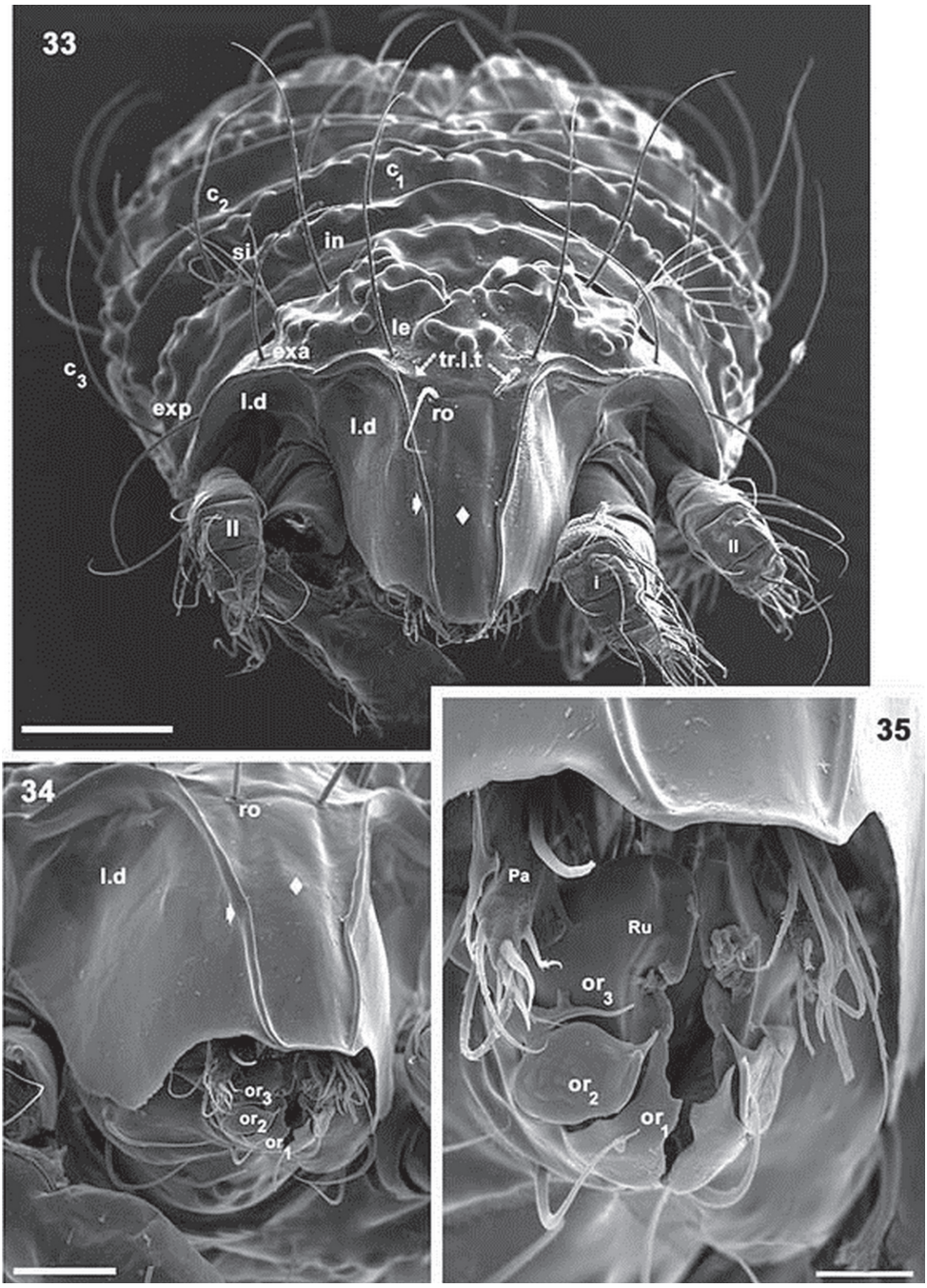

Figures 33–35. *Paulianacarus costaricensis* sp. n. Adult with cerotegumental layer. SEM. **33** frontal view **34** prodorsum, laterally inclined **35** apical zone, infracapitulum. Abbreviations: See Material and methods. Scale bars: **33** = 100 μm; **34** = 50 μm; **35** = 20 μm.

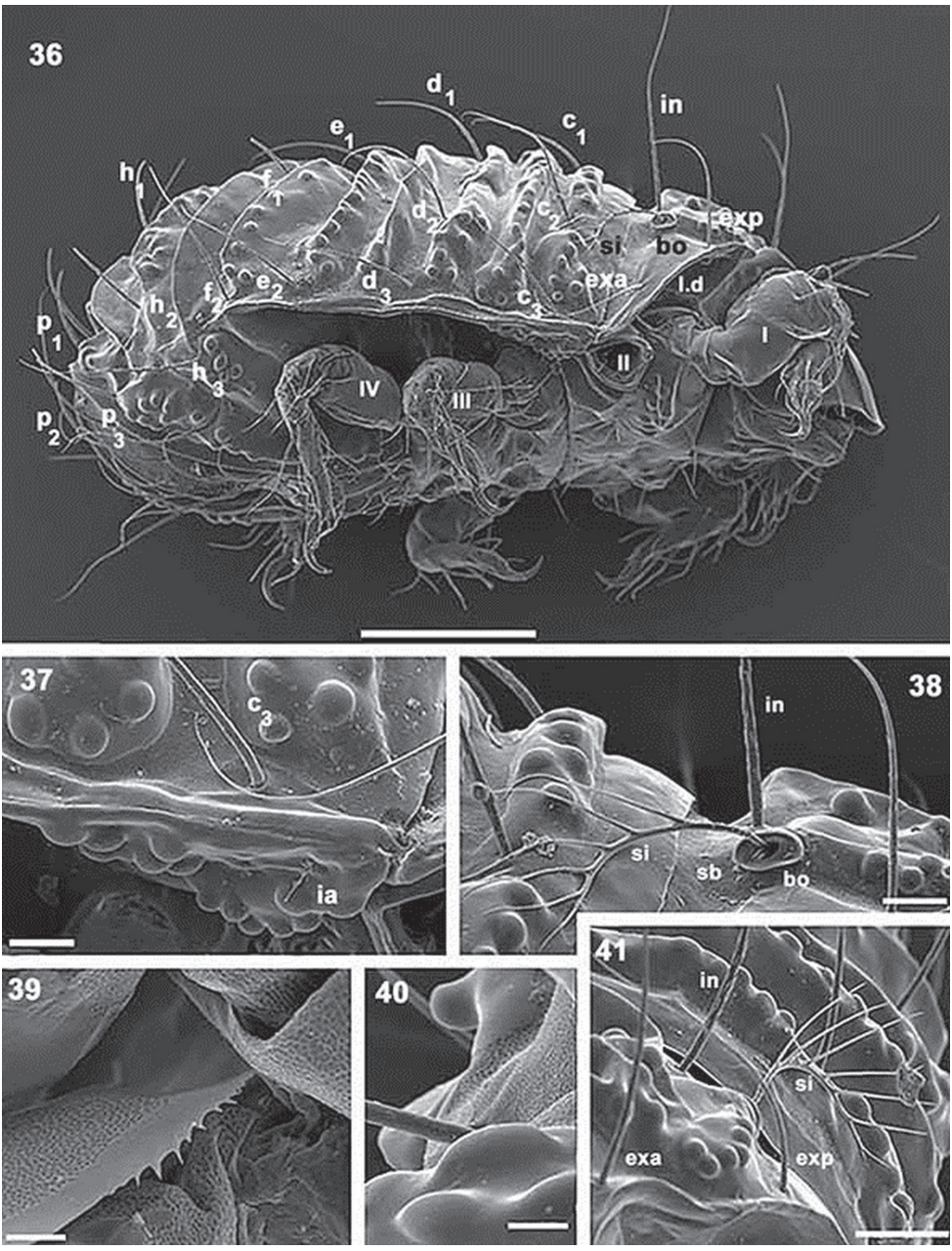

Figures 36–41. *Paulianacarus costaricensis* sp. n. Adult with cerotegumental layer. SEM. **36** lateral view **37** anterior lateral notogastral zone **38** bothridial zone **39** prodorsal marginal zone **40** promontories **41** lateral view, sensillus zone. Abbreviations: See Material and methods. Scale bars: **36** = 200 μm; **37** = 20 μm; **38** = 50 μm; **39** = 10 μm; **40** = 10 μm; **41** = 50 μm.

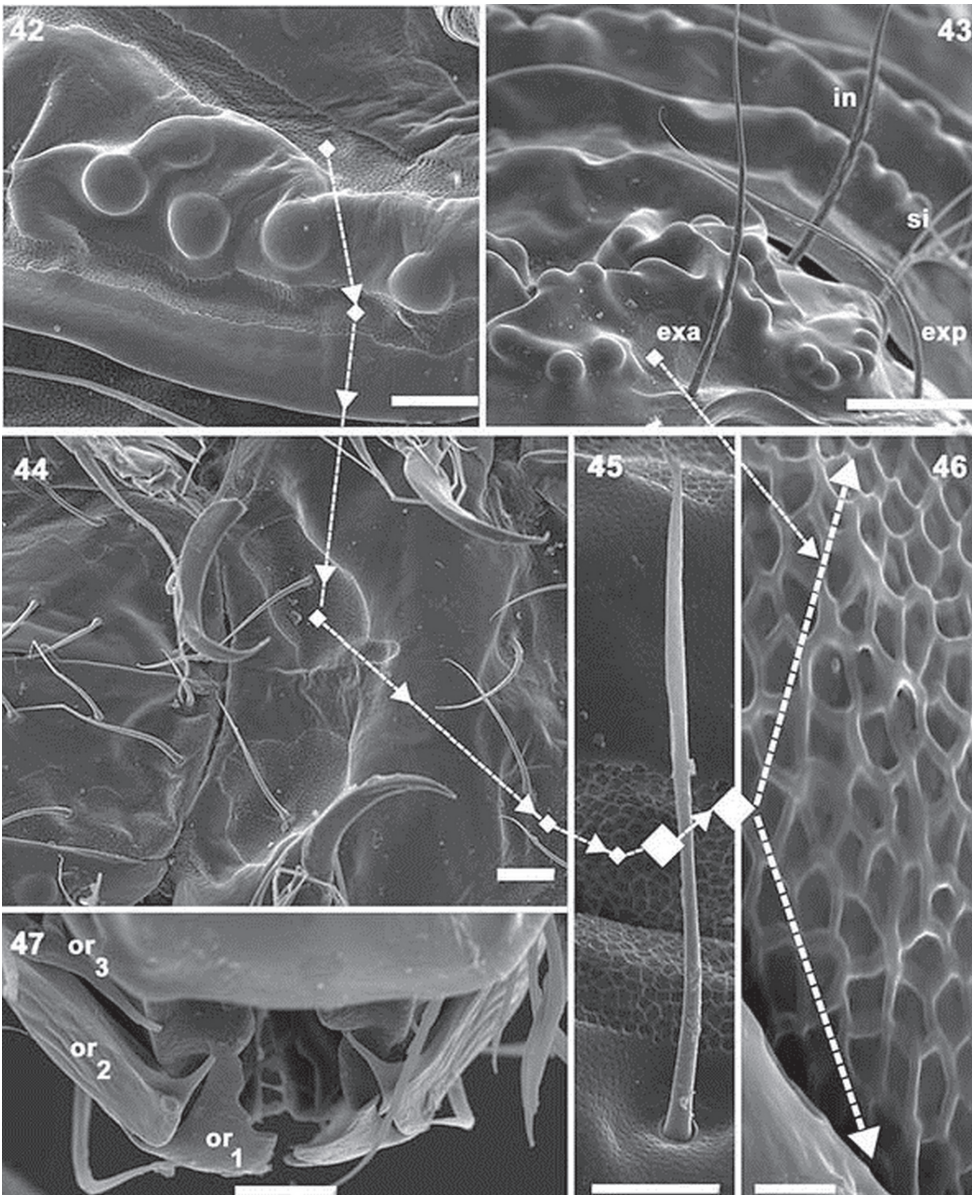

Figures 42–47. *Paulianacarus costaricensis* sp. n. Adult with cerotegumental layer. SEM. **42** lateral view, notogastral promontories **43** Frontal prodorsum detail promontories **44** epimeral posterior zone **45** notogastral setae and microsculpture, "porose area" **46** depressed area microsculpture, notogastral zone **47** adoral setae, frontal view. Abbreviations: See Material and methods. Scale bars: **42** = 20 μm; **43** = 50 μm; **44** = 20 μm; **45** = 10 μm; **46** = 2 μm; **47** = 10 μm.

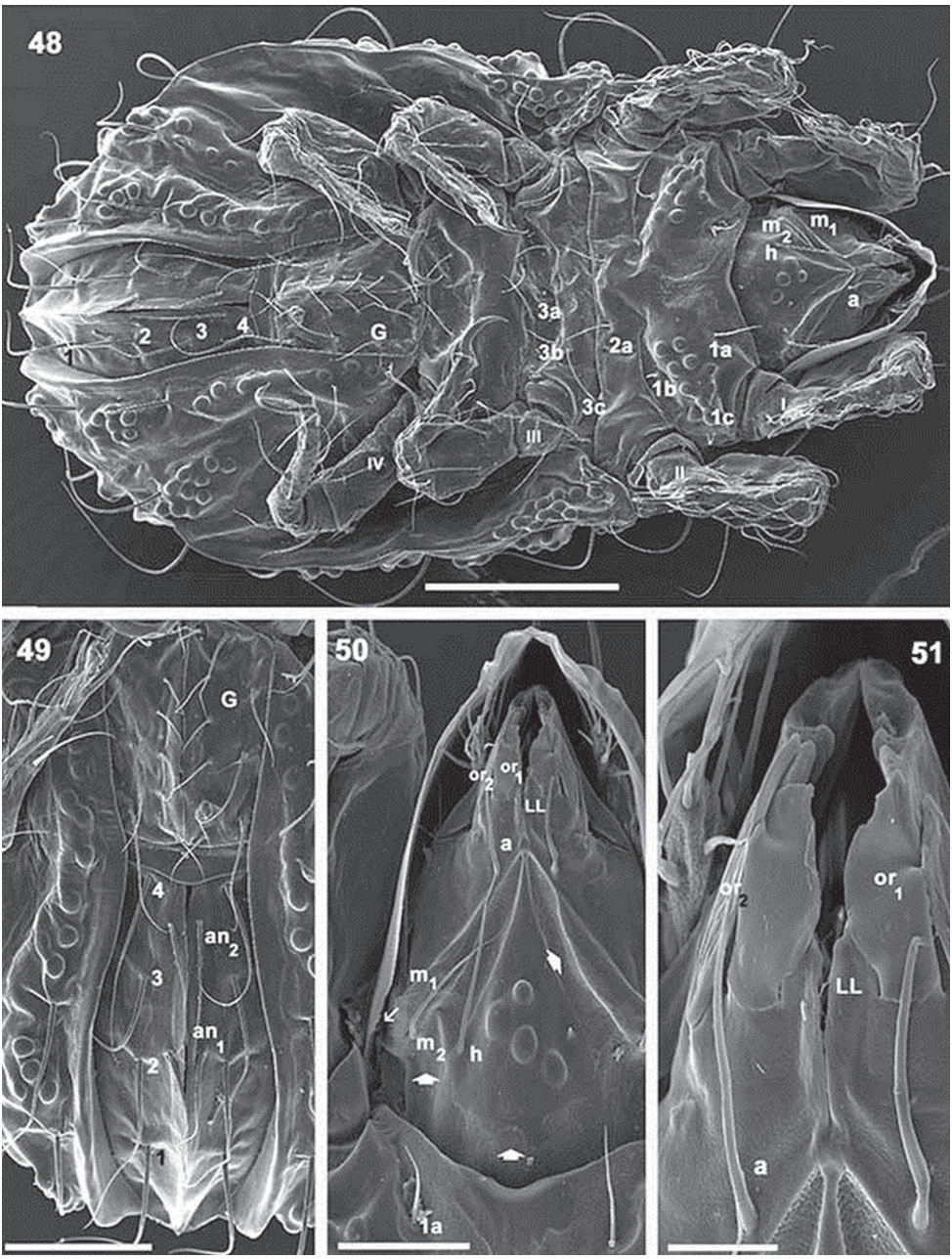

Figures 48–51. *Paulianacarus costaricensis* sp. n. Adult with cerotegumental layer. SEM. **48** ventral view **49** anogenital region **50** infracapitulum **51** apical infracapitular zone. Abbreviations: See Material and methods. Scale bars: **48** = 200 μm; **49** = 100 μm; **50** = 50μm; **51** = 20μm.

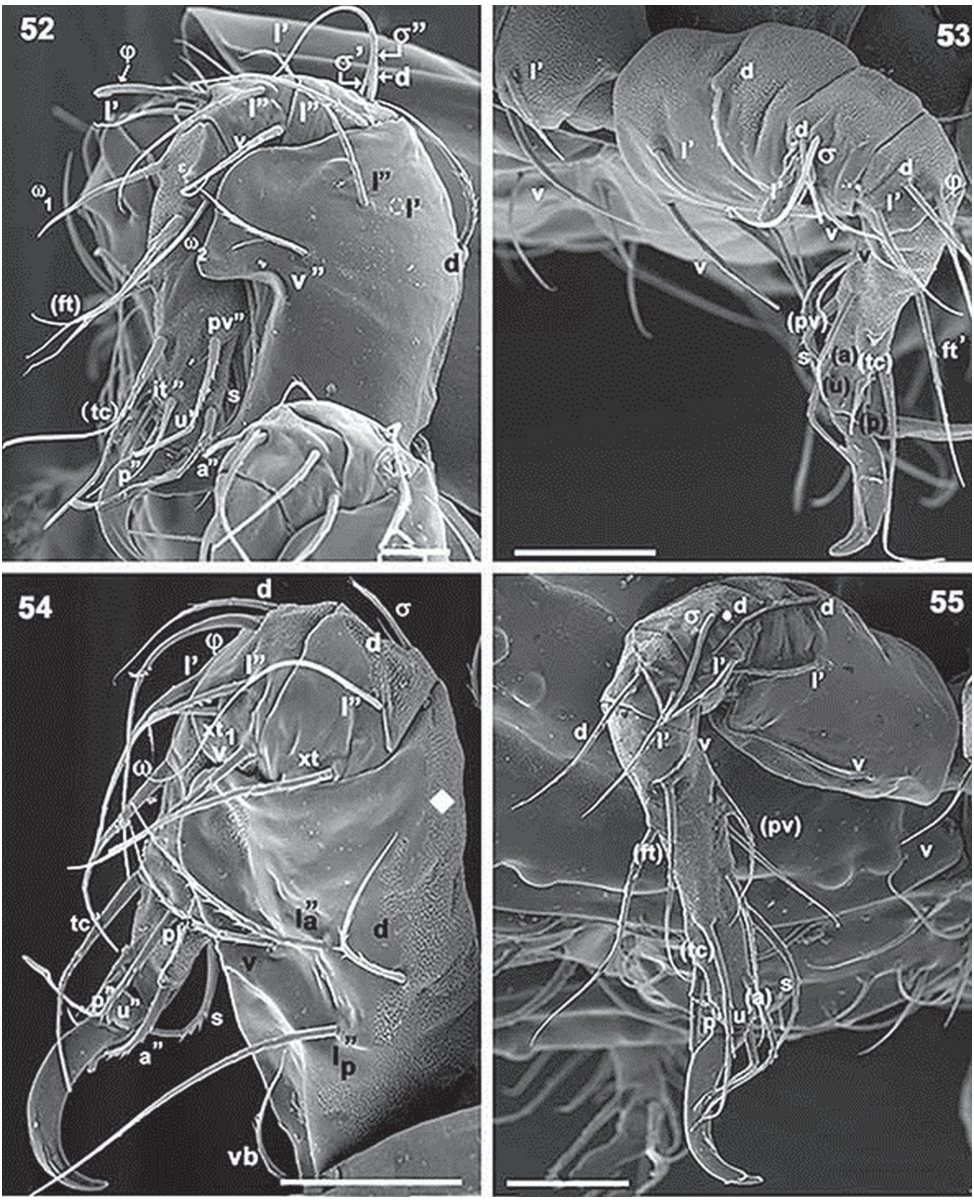

Figures 52–55. *Paulianacarus costaricensis* sp. n. Adult with cerotegumental layer. SEM. **52** leg I, antiaxial **53** leg III, antiaxial **54** leg II, antiaxial **55** leg IV, antiaxial. Abbreviations: See Material and methods. Scale bars: **52** = 20 μm; **53** = 50 μm; **54** = 50 μm; **55** = 50 μm.

Remarks. Polyhedral microsculpture observed in several areas. Porous areas are very difficult to observe, as in most cases they are situated in the same zone as the microsculpture. On legs this microsculpture is present on all segments.

Table 2. *Paulianacarus costaricensis* sp. n.: setae and solenidia.

	Femur	Genu	Tibia	Tarsus	Claw
Leg I					
setae	*(l),d,v"*	*(l),d*	*(l),v*	*(p),(u),(a),σ,(it),(tc),(ft),(pv), ε*	1
solenidia		σ', σ"	φ	ω_1 , ω_2	
Leg II					
setae	*d,la"lp",l',vb, v*	*d,l",xt*	*d,(l),v,xt*	*(p),(u),(a),σ,(tc),(ft),(pv)*	1
solenidia		σ	φ	ω	
Leg III					
setae	*l',v*	*d,l',v*	*d,l',v*	*(p),(u),(a),σ,(tc),(ft),(pv)*	1
solenidia		σ	φ		
Leg IV					
setae	*d,l',v*	*d l',v*	*d,l'*	*(p),(u),(a),σ,(tc),(ft),(pv)*	1
solenidia		σ			

Discussion

The genus *Mixacarus* was proposed by Balogh (1958); but later Balogh and Balogh (1987) proposed another new genus, *Phyllolohmannia*. Currently *Mixacarus* is divided into two sub-genera, *Mixacarus* and *Phyllolohmannia*, and includes 22 species (Subias 2017).

A comparison between *Mixacarus turialbaiensis* sp. n. and *Mixacarus exilis* Aoki 1970 is quite complex, as some aspects of the initial description is detailed and others are deficient, for example: lateral observations are ignored and for the ventral region, drawings are referred to, but in a preceding paper by Wallwork 1962. Other problematic aspects include the absence of any reference to the porose areas of *M. exilis*. Making use of different study methods and technology, the authors were able to observe structures evidently not previously observed, such as the particular microsculpture in depressed areas (Figure 7), and transversal bands on notogaster (Figures 2, 5, 6, 13, 14, 16, 17, 19, 21, 23). Porose areas (Figure 8) were discernible on transversal notogastral band in the zone of this microsculpture.

Mixacarus turialbaiensis sp. n. is close to *Mixacarus exilis* Aoki 1970, but is differentiated by the depressed areas with particular microsculpture; all prodorsal setae have similar characteristics and length; ribbon-like bands on prodorsum distributed very differently; notogastral setae slightly barbate; nine transversal bands; epimeres with large number of depressed areas; variable chaetotaxy in genital and epimeral zone.

Paulianacarus was proposed by Balogh (1960) from Madagascar. Subias (2004) considered *Millotacarus* to be a subgenus of *Paulianacarus*. At present there are 15 species allocated to *Paulianacarus* and *Millotacarus*. The taxonomy of these genera are complex, and considering one a subgenus of the other is complicated by the lack of a detailed comparative study of type materials. Several authors have expressed their opinions (Mahunka 1985; Coetzee 2001; Chen et al. 2012, Fernandez et al. 2014), and these considerations highlight the incongruences in the descriptions, indicating that some do

not consider that these are different genera, or do not consider one to be a subgenus of the other, while other researchers accept both subgenera. An analysis of these opinions is not repeated here in order to avoid redundancy. The only way to solve the problem is the study and comparison of type material, which was not possible in this instance.

The new species *Paulianacarus costaricensis* sp. n. was described using optical and SEM microscopy. These techniques allowed us to understand some of the complex structures also observed in *Paulianacarus rugosus* Balogh, 1961, a species close to the newly described species.

P. costaricensis displays the following characters: elevated transversal thickening (*tr.e.t*) with transverse bands: 1) some cross the transverse medial notogastral plane, others do not; 2) some are rectilinear, others oblique; 3) some present superficial rounded protuberances, others are smooth; 4) smooth thickenings either with complete furrow running the entire length, or partial furrow; 5) *tr.e.t* are associated with transversal furrows (*S*); 6) transversal furrows are related to one or both sides of the elevated transversal thickenings. Variable number and disposition of genital and epimeral setae, difficulty in observing lyrifissures. These are only some of the characteristics of this species, but they emphasize the need for detailed studies.

P. rugosus Balogh 1961 is close to *P. costaricensis*, but is differentiated by the presence of prodorsal transversal band; barbate *in* setae; elevated transversal thickening, transverse medial notogastral plane *tr.e.t* 1, 2, 3, 4, 5; *tr.e.t* 6, 7, 8, 9 not crossing medial notogastral plane; elevated transversal thickening with rounded protuberances: *tr.e.t* 1, 2 ,5, 6, 8, 9; with smooth surface: *tr.e.t* 3, 4, 7; epimeral chaetotaxy: (3–1–[3 (2)]–[4 (3)]); porose area rounded, very difficult to observe as it is situated in polyhedral microsculpture zone; genital setae variable with 9–10 pairs, of which 6–7 are aligned paraxially and 3-4 antiaxially.

Acknowledgements

Our gratitude is expressed towards Peter Schwendinger of NHNG, Switzerland, for valuable assistance in obtaining study material. This work is based on research supported in part by the National Research Foundation of South Africa (UID) 85288. Any opinion, findings and conclusions or recommendations expressed in the material are those of the authors and therefore the NRF does not accept any liability in regard thereto.

References

Alberti G, Fernandez NA (1988) Fine structure of a secondarily developed eye in the fresh water moss mite, *Hydrozetes lemnae* (Coggi 1899) (Acari: Oribatida). Protoplasma 146: 106–117. https://doi.org/10.1007/BF01405919

Alberti G, Fernandez N (1990a) Aspects concerning the structure and function of the lenticulus and clear spot of certain oribatids (Acari: Oribatida). Acarologia 31: 65–72.

Alberti G, Fernandez NA (1990b) Fine structure and function of the lenticulus and clear spot of Oribatids (Acari: Oribatida). In: Andre HM, Lions J-Cl (Eds) L'ontogènese et le concept de stase chez les arthropodes. Agar, Wavere, 343–354.

Alberti G, Fernandez N, Coineau Y (2007) Fine structure of spermiogenesis, spermatozoa and spermatophore of *Saxidromus delamarei* (Saxidromidae, Actinotrichida, Acari). Arthropod Structure Development 36: 221–231. https://doi.org/10.1016/j.asd.2006.11.002

Alberti G, Fernandez N, Kümmel G (1991) Spermatophores and spermatozoa of oribatid mites (Acari: Oribatida). Part II.Functional and systematical considerations. Acarologia 32: 435–449.

Alberti G, Norton R, Adis J, Fernandez N, Franklin E, Kratzmann M, Moreno A, Ribeiro E, Weigmann G, Woas S (1997) Porose integumental organs of oribatid mites (Acari: Oribatida). Zoologica 48: 33–114.

Aoki J-I (1970) The oribatid mites of the island of Tsushima. Bulletin of the National Science Museum Tokyo, Japan 13(3): 395–442

Aoki J-I (1987) Three species of oribatid mites from Kune-Jima island, Southwest Japan. Proceedings of the Japanese Society of Systematic Zoology 36: 25–28.

Balogh J (1960) Oribates (Acari) nouveaux de Madagascar (X serie). Mémoires Institut Scientifique Madagascar Série A. 14: 7–37.

Balogh J (1961) The scientific results of the first Hungarian Zoological expedition to East Africa 4. Acarina: Oribatida. Annales Historico Naturales Musei Nationalis Hungarici 53: 517–524.

Balogh J (1962) Some new Lohmanniids from Peru (Acari: Oribatei). Opuscula Zoogica (Budapest) 4(2-4): 59–61.

Balogh J, Balogh P (1987) A new outline of the Family Lohmanniidae Berlese,1916 (Acari, Oribatei). Acta Zoologica Hungarica 33(3-4): 327–398.

Chen Y, Liang W, Yang M (2012) First record of the genus *Paulianacarus* Balogh from China, with description of a new species (Acari,Oribatida, Lohmanniidae). Acta Zootaxonomica Sinica 37(1): 97–100.

Coetzee L (2001) New species of the family Lohmanniidae(Acari, Oribatida) from South Africa. Navorsinge van die Nasionale Museum Bloemfontein 17(3): 53–67.

Evans GO (1992) Principles of acarology. Wallingford (UK): C.A.B International, Cambridge, 563 pp.

Fernandez NA, Alberti G, Kümmel G (1991) Ultrastructure of the spermatophores and spermatozoa of some Oribatid mites (Acari: Oribatida) Part I. Fine structure and histochemistry. Acarologia. 32(3): 261–286.

Fernandez N, Theron P, Rollard C (2013a) The family Carabodidae (Acari: Oribatida) I. Description of a new genus, *Bovicarabodes* with three new species, and the redescription of *Hardybodes mirabilis* Balogh. International Journal of Acarology 39(1): 26–57. http://dx.doi.org/10.1080/01647954.2012.741144

Fernandez N, Theron P, Rollard C (2013b) Revision of the family Carabodidae (Acari: Oribatida) IV. *Aftibodes anjavidilavai* n.gen., n.sp., *Rugocepheus joffrevillei* sp.n, and redefinition of the genus *Rugocepheus* Mahunka, 2009. International Journal of Acarology 39(6): 462–480. https://doi.org/10.1080/01647954.2013.822928

Fernandez N, Theron P & Rollard C (2013c) The family Carabodidae (Acari: Oribatida) V. The genus *Congocepheus* (second part), with a redescription of *Congocepheus involutus* Mahunka 1997, and descriptions of *Congocepheus gabonensis* and *Congocepheus extactastesi* sp. nov. Zoosystema 35(4): 551–579. https://doi.org/10.5252/z2013n4a8

Fernandez N, Theron P, Rollard C, Castillo E (2014) Oribatid mites from deep soils of Hòn Chông limestone hills, Vietnam: the family Lohmanniidae (Acari: Oribatida), with the descriptions of *Bedoslohmannia anneae* n. gen., n. sp., and *Paulianacarus vietnamese* n. sp. Zoosystema 36(4): 771–787. https://doi.org/10.5252/z2014n4a5

Grandjean F (1949) Observation et conservation des très petits Arthropodes. Bulletin de Muséum d'Histoire Naturelles, Paris, 21(2): 363–370.

Krantz G, Walter D (2009) A manual of acarology. 3rd ed. Texas Tech University Press, Lubbock (TX), 807 pp.

Norton R, Behan-Pelletier V (2009) Suborder Oribatida. In: Krantz GW, Walter DE (Eds) A manual of acarology. 3rd ed. Texas Tech University Press, Lubbock (TX), 430–564.

Subias S (2004) Listado sistemático, sinonímico y biogeográfico de los Acaros Oribátidos (Acariformes: Oribatida) del mundo (excepto fósiles). Graellsia 60: 3–305. https://doi.org/10.3989/graellsia.2004.v60.iExtra.218

Travé J, Vachon M (1975) François Grandjean 1882–1975 (Notice biographique et bibliographique). Acarologia 17(1): 1–19.

Wallwork JA (1962) Some Oribatei from Ghana X.The family Lohmanniidae. Acarologia I, 4(3): 457–487.

ZooKeys 680: 57–72 (2017)
doi: 10.3897/zookeys.680.12835
http://zookeys.pensoft.net

RESEARCH ARTICLE

A peer-reviewed open-access journal
ZooKeys
Launched to accelerate biodiversity research

A new, morphologically cryptic bush-cricket discovered on the basis of its song in the Carpathian Mountains (Insecta, Orthoptera, Tettigoniidae)

Ionuţ Ştefan Iorgu[1], Elena Iulia Iorgu[1], Gergely Szövényi[2], Kirill Márk Orci[3]

1 *"Grigore Antipa" National Museum of Natural History, Kiseleff blvd. 1, Bucharest, Romania* **2** *Department of Systematic Zoology & Ecology, Eötvös Loránd University, Pázmány P. sétány 1/c, H–1117, Budapest, Hungary* **3** *MTA-ELTE-MTM Ecology Research Group of the Hungarian Academy of Sciences, Eötvös Loránd University and Hungarian Natural History Museum, Pázmány P. sétány 1/c, H–1117, Budapest, Hungary*

Corresponding author: *Ionuţ Ştefan Iorgu* (ionut.iorgu@antipa.ro)

Academic editor: *F. Montealegre-Z* | Received 21 March 2017 | Accepted 4 May 2017 | Published 14 June 2017

http://zoobank.org/61BD7A32-BE30-46A5-B1DD-6DAD729989A7

Citation: Iorgu IŞ, Iorgu EI, Szövényi G, Orci KM (2017) A new, morphologically cryptic bush-cricket discovered on the basis of its song in the Carpathian Mountains (Insecta, Orthoptera, Tettigoniidae). ZooKeys 680: 57–72. https://doi.org/10.3897/zookeys.680.12835

Abstract

A new, morphologically cryptic species of phaneropterine bush-crickets is described from the grasslands of the Romanian Eastern Carpathians. Despite the morphological and acoustic similarities with the recently described *Isophya nagyi* Szövényi, Puskás & Orci, *I. bucovinensis* **sp. n.** is characterized by a peculiar male calling song, with faster syllable repetition rate (160–220 syllables per minute, at 22–27°C) and less complex syllable structure (composed of only two elements instead of three observable in *I. nagyi*). The morphological description of the new species is supplemented with an oscillographic and spectrographic analysis of the male calling song and male–female pair-forming acoustic duet. An acoustic signal-based identification key is provided for all the presently known species of the *Isophya camptoxypha* species group, including the new species.

Keywords

Bioacoustics, Carpathians, *Isophya*, new species, taxonomy

Introduction

The glaciers of the Quaternary ice ages shaped distribution patterns in biodiversity and are considered as one of the primary forces of population divergence and speciation (Stewart et al. 2010; Homburg et al. 2013). The Carpathians proved to be one of the main glacial refugia for the re-colonization of northern regions of Europe in Late Glacial and Postglacial periods (Mráz and Ronikier 2016, Varga 2011). During the Last Glacial Maximum, this mountain range was mostly unglaciated, providing suitable conditions for many species of temperate fauna and flora to survive (Zasadni and Kłapyta 2014). Also, the Carpathians are an important center of biodiversity that developed a characteristic biota with a high proportion of endemic taxa, due mainly to the isolation from other mountain ranges and to its archipelago-like structure, forming a series of habitat islands (Mráz and Ronikier 2016). The Eastern and Southern Carpathians proved to be biodiversity hotspots within the Carpathian Mountains, being the richest areas in endemics regarding several groups of vascular plants and invertebrates, such as arachnids, mollusks and insects (Kenyeres et al. 2009, Bálint et al. 2011, Theissinger et al. 2013, Gajdoš et al. 2014, Cameron et al. 2016, Hurdu et al. 2016, Mraz et al. 2016). Most of these endemics are organisms with low-dispersal abilities, species likely to show stronger genetic differentiation patterns due to the absence of gene flow (Homburg et al. 2013). This appears to be also the case for the flightless bush-crickets of the *Isophya camptoxypha* species-group, which could be an interesting model to explore speciation driven by climate changes in high mountainous landscapes. These species are slowly moving brachypterous insects, occurring in cold and mesic meadows from montane to subalpine altitudes, always preferring broadleaved dicotyledonous plants: *Veratrum* sp., *Rubus* sp., *Rumex* sp., *Urtica* sp., *Aconitum* sp., *Vaccinium* sp., *Gentiana* sp. etc. (Orci et al. 2010b, Iorgu 2012, Szövényi et al. 2012).

Although the species-level identification of specimens in this species-group is difficult due to morphological uniformity, the oscillographic structure of male calling songs shows clear differences between species (Heller et al. 2004, Orci et al. 2005, Orci et al. 2010a, Iorgu 2012, Iorgu et al. 2017). In these bush-crickets, one of the main functions of acoustic signaling is to transmit information between males and females during their pair-forming behavior. Typically, males stridulate spontaneously and females decide which male to approach or to respond to acoustically (Heller 1990). In the latter case, the singing interaction of male and female forms a duet. Female song preferences and male song pattern is believed to be a significant ethological component of the species-specific mate recognition system of these insects (Orci 2007, Orci et al. 2010a, Iorgu 2012, Szövényi et al. 2012). Therefore, analyzing the acoustic signals of these bush-crickets may reveal previously unrecognized, morphologically cryptic species when studying formerly unexamined populations. Here we describe a new *Isophya* species recognized by studying its male calling song. A characterization of the basic features of its distinctive male calling song and male–female acoustic duet are presented, and a male calling song based identification key for the *Isophya camptoxypha* species-group is provided.

Materials and methods

Specimen collection

During the first visit in Călimani Mountains in the summer of 2012, several *Isophya* specimens were collected by visual examination of the subalpine vegetation in meadows below Pietrosul Peak (1800–1900 m asl) and at lower altitudes, near the village Gura Haitii (900–1000 m asl). These specimens turned out to be very different from all other known *Isophya* species regarding the pattern of male calling song and are described here as a new, cryptic species: *Isophya bucovinensis* sp. n. Later, we discovered this insect at other highland locations in the northern and western areas of the large volcanic caldera of Călimani Mountains and also in Suhard Mountains, in the southwestern and western parts of Bucovina region.

Morphology

The description of examined morphometric characters follows Orci et al. 2005. Measurements were taken with a digital caliper for the following morphometric variables in males: width of head, length of pronotum, frontal width of pronotum, caudal width of pronotum, length of left tegmen, width of left tegmen, length of cercus, length of hind femur.

Photos were taken with a Canon EOS 6D DSLR camera, Canon EF 180 mm f3.5L 1:1 and Canon MP–E 65 mm f2.8 5:1 macro lenses. Scanning Electron Microscope photos were taken of the stridulatory files and male cerci.

Acoustic examination and terminology

The calling song of eleven males and the "mate searching" duet of four males and five females were recorded and analyzed. Recordings were taken with an Edirol R–09HR digital recorder (microphone frequency response 20–40000 Hz, sampling rate of 96000 Hz, 24–bit amplitude resolution). The sound analyses were run using the software Audacity 2.1.2.

The acoustic terminology follows Ragge and Reynolds (1998) and Heller et al. (2004): *calling song* – spontaneous song produced by an isolated male; *syllable* – the song produced by one opening–closing movement cycle of the tegminae; *impulse* – a simple, undivided transient train of sound waves (the highly-damped sound impulse arising as the impact of one tooth of the stridulatory file); *click* – an isolated, distinct impulse. As the calling songs of *Isophya* species are amplitude modulated signals similarly to the stridulation of most phaneropterine (Heller et al. 2015), we measured several oscillographic characters which may be useful when comparing the song of the new species with the songs of other *Isophya* species: duration of syllable (DS), duration of "B"–element (DB), duration of "C"–element (DC), number of impulses

in "B"–element (NIB), number of impulses in "C"–element (NIC), silent interval between "B"– and "C"–elements (IntBC), silent interval between successive syllables (IntS), the longest impulse series in a syllable (LIS). The delay of female response was measured from the beginning of "C"–element in male syllable to the beginning of female reply (F). The detailed terminology of the measured male song characters in *I. bucovinensis* sp. n. reflects our hypothesis about the homology of these signal elements with syllable-elements of *Isophya nagyi* (see Szövényi et al. 2012), which seems to be the closest relative of *I. bucovinensis* sp. n. The first element of the syllables produced by *Isophya nagyi* is missing in the syllables of *I. bucovinensis* sp. n., therefore in the latter species the first syllable element is referred to as "B", and the second one is termed "C".

Taxonomy

***Isophya bucovinensis* sp. n.**
http://zoobank.org/797AC7E6-0702-4510-AC0C-4C0E454EF81C
Fig. 1A, B

Type locality. Romania, Eastern Carpathian Mountains, Călimani Mountains.

Type material. Holotype: male. Original label: "Romania, Suceava County, Călimani Mountains, 12 Apostoli Peak, 47.221233°N, 25.213896°E, alt. 1730 m asl, 2015.07.27, leg. I. Ș. Iorgu", coll. "Grigore Antipa" National Museum of Natural History, Bucharest, Romania. **Paratypes:** 1 ♂ 1 ♀, labeled: "Romania, Suceava County, Gura Haitii, 47.226236°N, 25.300690°E, alt. 990 m asl, 2012.06.21, leg. I. Ș. Iorgu"; 2 ♂♂ 2 ♀♀, labeled: "Romania, Suceava County, Călimani Mountains, meadow below Pietrosul Peak, 47.130767°N, 25.191679°E, alt. 1800 m asl, 2012.07.20, leg. I. Ș. Iorgu"; 1 ♂ 1 ♀, labeled: "Romania, Suceava County, Suhard Mountains, Omu Peak, 47.507519°N, 25.090278°E, alt. 1860 m asl, 2013.07.21, leg. I. Ș. Iorgu"; 2 ♂♂ 2 ♀♀, labeled: "Romania, Suceava County, Călimani Mountains, 12 Apostoli Peak, 47.221233°N, 25.213896°E, alt. 1730 m asl, 2015.07.27, leg. I. Ș. Iorgu"; 2 ♀♀, labeled: "Romania, Suceava County, Călimani Mountains, 12 Apostoli Peak, 47.222835°N, 25.212571°E, alt. 1730 m asl, 2016.09.03, leg. I. Ș. Iorgu", all in coll. "Grigore Antipa" National Museum of Natural History, Bucharest, Romania; 3 ♂♂ 3 ♀♀, labeled: "Romania, Suceava County, Călimani Mountains, 12 Apostoli Peak, 47.221233°N, 25.213896°E, alt. 1730 m asl, 2015.07.27, leg. I. Ș. Iorgu", coll. Hungarian Natural History Museum, Budapest, Hungary.

Audio recordings: 1 ♂, Gura Haitii, 2012.06.21 (air temperature 25°C); 1 ♂, meadow below Pietrosul Peak, Călimani Mts., 2012.07.20 (22°C); 2 ♂♂ 3 ♀♀, meadow below Pietrosul Peak, Călimani Mts., 2012.07.20 (27°C); 3 ♂♂, Omu Peak, Suhard Mts., 2013.07.21 (25°C); 4 ♂♂ 2 ♀♀, 12 Apostoli Peak, Călimani Mts., 2015.07.27 (24°C).

Other material. *Isophya bucovinensis* sp. n.: 1 ♂ 1 ♀, Romania, Suceava County, Călimani Mountains, 47.208928°N, 25.200489°E, alt. 1640 m asl, 2015.07.27, leg. I.

Figure 1. *Isophya bucovinensis* sp. n.: **A** female habitus **B** male habitus **C** habitat in Călimani Mountains, at 12 Apostoli Peak (1730 m asl) on 27 July 2015.

Ş. Iorgu; 2 ♂♂ 3 ♀♀, Romania, Suceava County, Călimani Mountains, 47.202448°N, 25.197817°E, alt. 1620 m asl, 2015.07.28, leg. I. Ş. Iorgu; 1 ♂ 4 ♀♀, Romania, Suceava County, Călimani Mountains, 47.134651°N, 25.178858°E, alt. 1680 m asl, 2016.08.07, leg. I. Ş. Iorgu. *Isophya nagyi*: 10 ♂♂ 2 ♀♀ (audio recorded at 21.2–24°C), Romania, Suceava County, Călimani Mountains, 47.137°N, 25.256°E, alt. 1340 m asl and 47.141°N, 25.267°E, alt. 1580 m asl, 2011.07.27, leg. K. M. Orci, G. Puskás & G. Szövényi.

Diagnosis. Fastigium verticis approximately half as wide as scapus, male elytra short and narrow, slightly shorter than or as long as pronotum, reaching anterior part of second abdominal tergite. Length of cubital vein 3/4 of the width of pronotum

posterior margin, forming an obtuse angle of nearly 110° at the right margin of left tegmen. The stridulatory file is 2.2–2.5 mm long and contains 105–130 pegs. Male cerci slender, 2.4–2.7 mm long, gradually and moderately incurved in distal 1/4, tapering in an apical denticle. Ovipositor short, upcurved, 8.3–9.2 mm long. Male calling song consists of a long sequence of two-component syllables (Fig. 3A, B) repeated at a rate of 160–220 per minute (at 22–27°C air temperature). Each syllable lasts for 237–385 ms and is formed of two parts: a longer group of 46–79 impulses (156–286 ms) shortly followed by a higher amplitude group of 2–7 clicks (3–28 ms) (Fig. 3C, D). Females reply right after the male syllable, with a latency of 48–66 ms (Fig. 4C). All these sounds are produced by closing the tegmina.

Morphologically, *Isophya bucovinensis* sp. n. belongs to the *Isophya camptoxypha* species group. Within this complex, *I. bucovinensis* sp. n. and *I. nagyi* differ from all the other species in the relatively high number of pegs observable in the male stridulatory file. Furthermore, *Isophya bucovinensis* sp. n. can be easily distinguished from *I. nagyi* by examining the number of impulse groups within a syllable (three in *I. nagyi* vs. two in *I. bucovinensis* sp. n.) and the syllable repetition rate during continuous singing: 60–80 syllables/minute in *I. nagyi* (21–24°C) and 160–220 in *I. bucovinensis* sp. n. (22–27°C) (Fig. 4).

Description. ***Male*** (Fig. 2A, C, H, J, K; Table 1). Fastigium verticis half as wide as scapus, slightly tapering frontward. Head width 3.1–3.7 mm, 1.3 times the maximum pronotum width. The pronotum is 3.9–5 mm long, with lateral carinae nearly parallel in prozona, broken at traverse sulcus, widen and divergent in metazona. Saddle–shaped from a lateral view, the paranota with concave dorsal margin; anterior and ventral borders straight, posterior edge moderately convex. Tegmina short and narrow, slightly shorter than or as long as pronotum, reaching the second abdominal tergite. Venation reticulate, Cu2 vein swollen, its length 3/4 of pronotum posterior margin. The angle between cubital veins of approximately 70–80°, speculum large and quadrangular. At the distal end of Cu2, the right margin of left tegmen forms an obtuse angle of nearly 110°. Stridulatory file arcuate, 2.2–2.5 mm long, with 105–130 teeth. Hind femur without ventral spines, 3.5–4 times long as pronotum. Epiproct almost twice as wide as long. Cerci covered by fine hairs, slender, 2.4–2.7 mm long, gradually narrowing towards tip, slightly curved in apical fourth. Terminal denticle strong, located in middle of cercus apex. Subgenital plate moderately elongated, narrowed apically with triangular apical incision and more or less acute lobes on its caudal margin.

Coloration green, densely punctuated with fine, dark green and brown spots. Some specimens with two dorsal, parallel, bilateral stripes from pronotum to end of abdomen, red, orange, or yellow colored. Antennae greenish, reddish or brownish, compound eyes bicolored: upper part brown or red and lower part green. Disc of pronotum green, bordered by a yellowish or whitish band, from behind the eye to the posterolateral angle of wing, complemented by a reddish brown stripe in metazona. Tegmina brown or dark red, with green margins and greenish or yellowish white costal margin, as continuation of pronotum band. Legs usually green, brownish or reddish. Cerci brown or reddish brown.

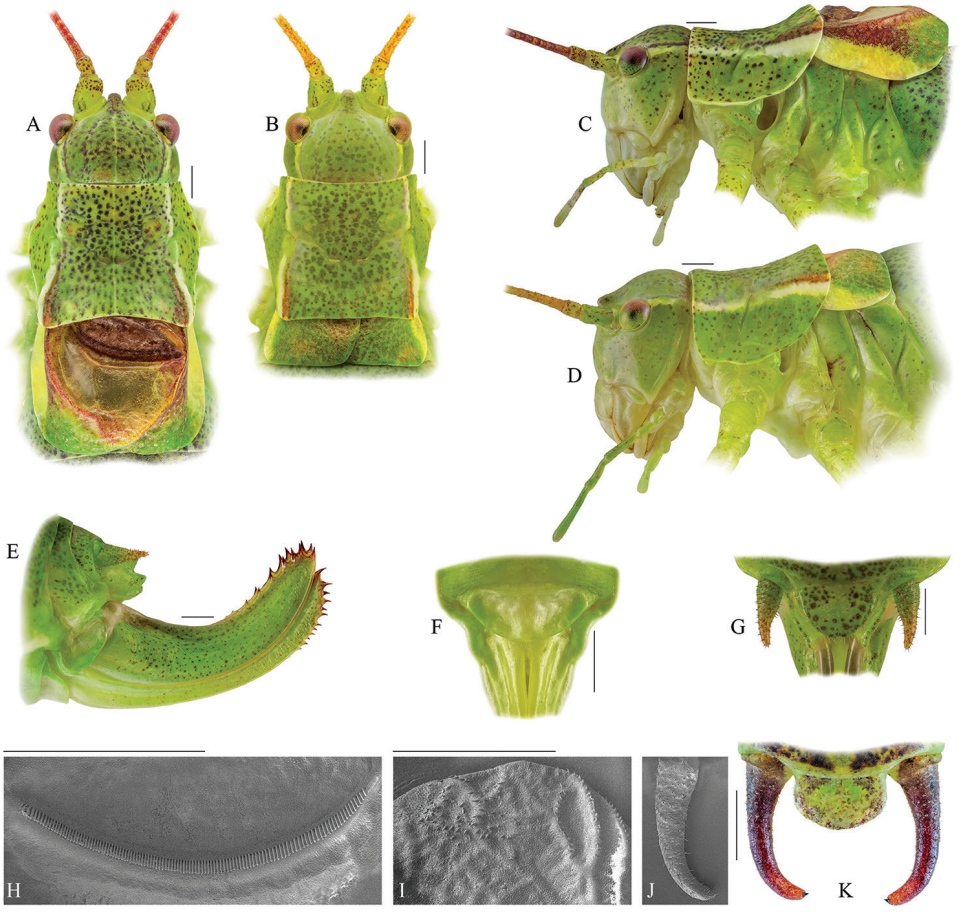

Figure 2. Photographs of the typical eidonomy of *Isophya bucovinensis* sp. n. male (**A, C, H, J, K**) and female (**B, D, E, F, G, I**). **A, B** head, pronotum and tegmina in dorsal view **C D** head, pronotum and tegmina in lateral view **E** ovipositor in lateral view **F** female subgenital plate **G** female cerci in dorsal view **H** male stridulatory file (SEM) **I** female stridulatory bristles (SEM) **J** male cercus (SEM) **K** male cerci in dorsal view. Scale bars 1 mm.

Female (Fig. 2B, D, E, F, G, I). Head roughly as in male. Pronotum disc marginally widening in its posterior part, with lateral carinae straight in prozona. Paranota similar to these of male. Tegmina with dense reticulate venation, approximately 1/4–1/3 the length of pronotum, reaching the first abdominal tergite, with more or less rounded margins. Right tegmen with two dorsal fields of stridulatory bristles on cubital veins. Epiproct semicircular. Cercus short, hairy, conical. Subgenital plate rounded, narrow. Ovipositor relatively short, upcurved, 8.3–9.2 mm long, with 8–9 spines on dorsal margin and 7–9 spines on ventral margin, gonangulum ellipsoid.

Body coloration similar to that of male. Tegmina green with brownish inner and whitish or yellowish lateral edges. Ovipositor green with dark brown spines.

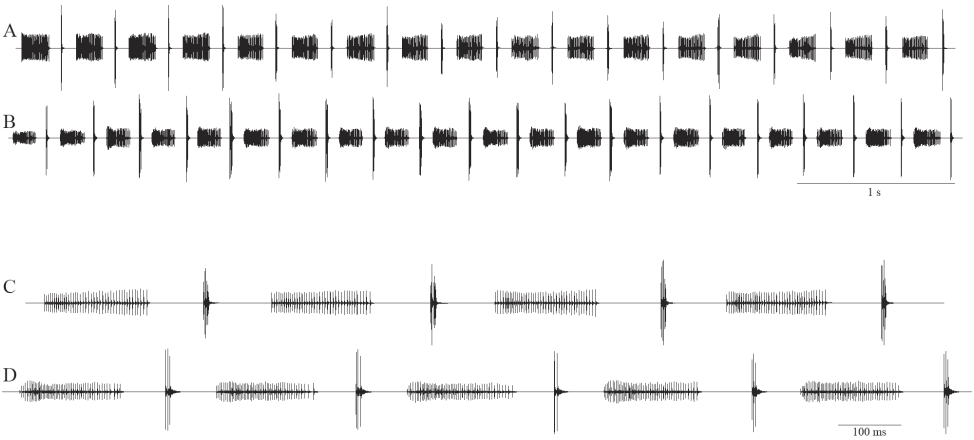

Figure 3. Oscillographic representation of the calling songs (**A, B**) of two males of *Isophya bucovinensis* sp. n. and detailed syllables (**C, D**). **A, C** Călimani Mountains, 12 Apostoli peak, 1730 m asl (air temperature 24°C) **B, D** Suhard Mountains, Omu peak, 1860 m asl (air temperature 25°C).

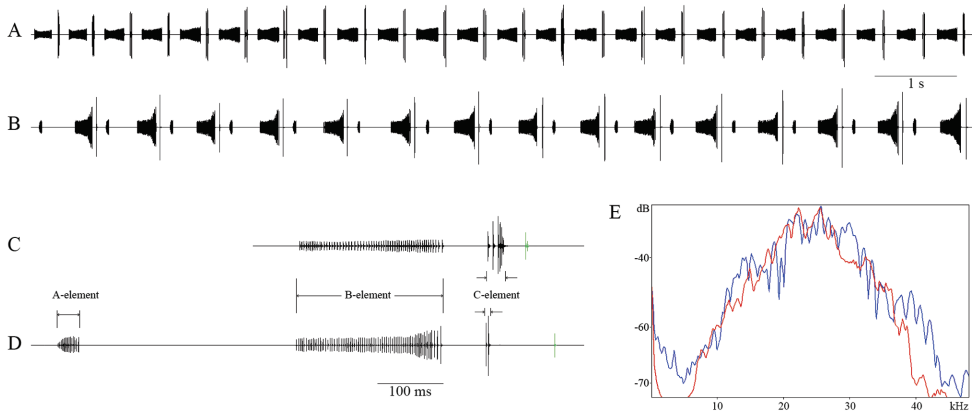

Figure 4. Acoustic signals analysis in two close–related species: **A, B** oscillographic pattern of male calling song **C, D** a detailed syllable and the female response (marked with green) **E** spectrum (function: Hanning window, size: 512). **A, C, E** red line *Isophya bucovinensis* sp. n. **B, D, E** blue line *Isophya nagyi*.

Bioacoustics (Figs 3, 4; Table 2). Males stridulate in the evening and at night. Typically, the song consists of series of 8–35 syllables; uninterrupted series of more than 200 syllables were also recorded. Syllable repetition rate is 160–220 syllables/minute at 22–27°C. *Isophya bucovinensis* sp. n. produces a single syllable type, lasting for 237–385 ms (mean ± SD: 311.6 ± 57.85 ms, n = 11 males) and formed of two elements: the main part ("B") is a longer group of 46–79 impulses (mean ± SD: 60.1 ± 11.54), 156–286 ms (mean ± SD: 215.2 ± 52.7 ms) long, shortly followed by the terminal "C" part, a higher amplitude group of 2–7 impulses (mean ± SD: 4.4 ± 1.64), 3–28 ms (mean ± SD: 16.45 ± 7.39 ms) long. The same impulse interval was measured in both "B" and "C" groups,

Table 1. Morphometric characters measured in males of *Isophya bucovinensis* sp. n. (N = 10) and *I. nagyi* (N = 20) (values in millimeters).

Morphometric parameters	*Isophya bucovinensis* sp. n.			*Isophya nagyi*		
	Min	Max	Mean ± SD	Min	Max	Mean ± SD
Width of head	3.1	3.7	3.37 ± 0.213	3.4	3.8	3.64 ± 0.105
Length of pronotum	3.8	4.3	4.02 ± 0.198	3.3	4.3	3.84 ± 0.261
Frontal width of pronotum	3.2	3.4	3.32 ± 0.083	3	3.6	3.19 ± 0.159
Caudal width of pronotum	3.9	5.0	4.41 ± 0.442	4.4	5.2	4.6 ± 0.201
Length of left tegmina	3.4	4.8	3.88 ± 0.449	4	4.8	4.44 ± 0.211
Width of left tegmina	3.1	4.2	3.7 ± 0.361	3.8	4.4	4.1 ± 0.16
Length of hind femur	13.5	15.9	14.7 ± 0.718	14.3	16.8	15.58 ± 0.747
Length of cercus	2.4	2.7	2.5 ± 0.103	2.2	2.8	2.54 ± 0.131

Table 2. Descriptive statistics for oscillographic parameters of the male calling song and for female response delay in *Isophya bucovinensis* sp. n. and *I. nagyi* (duration values in milliseconds). Number of specimens for which measurements were made: *I. bucovinensis* 11 males, 5 females; *I. nagyi* 10 males, 2 females.

Calling song parameters	*Isophya bucovinensis* sp. n.			*Isophya nagyi*		
	Min	Max	Mean ± SD	Min	Max	Mean ± SD
Duration of syllable (DS)	237	385	311.6 ± 57.85	489.6	934.3	727.33 ± 148.27
Duration of "B"–element (DB)	156	286	215.2 ± 52.7	129.5	217.8	188.96 ± 32.03
Number of impulses in "B"–element (NIB)	46	79	60.1 ± 11.54	38.7	79	56.83 ± 12.77
Silent interval between "B"– and "C"–elements (IntBC)	59	94	76.85 ± 10.56	54.2	91.5	69.43 ± 12.36
Duration of "C"–element (DC)	3	28	16.45 ± 7.39	1	5.4	3.59 ± 1.62
Number of impulses in "C"–element (NIC)	2	7	4.4 ± 1.64	1	4	2.6 ± 0.96
Silent interval between successive syllables (IntS)	76	125	94.2 ± 17	121.2	227.9	160.24 ± 34.24
Female response delay (F)	48	66	58.7 ± 4.77	71	127	112.2

2–4 ms. The two parts are separated by a short silent interval of 59–94 ms (mean ± SD: 76.85 ± 10.56 ms). The following syllable begins 76–125 ms (mean ± SD: 94.2 ± 17 ms) later (Fig. 3). All sounds are produced when the male closes the tegmina. Apart from the described typical syllable structure, some males produce syllables without the "C" element at the beginning of syllable series. The calling song's dominant frequency components are between 10–35 kHz, highest peak at approximately 25 kHz (Fig. 4E).

Females find males by phonotaxis and emit simple clicks if the male song is attractive for them. In the resulting male–female acoustic duet, the female replies only after the male syllables ("C"–part), with a latency of 48–66 ms (mean ± SD: 58.7 ± 4.77 ms, n = 200 replies from 5 females) (Fig. 4C).

Etymology. The specific name is derived from the historical region of Bucovina, "Land of the beech forests".

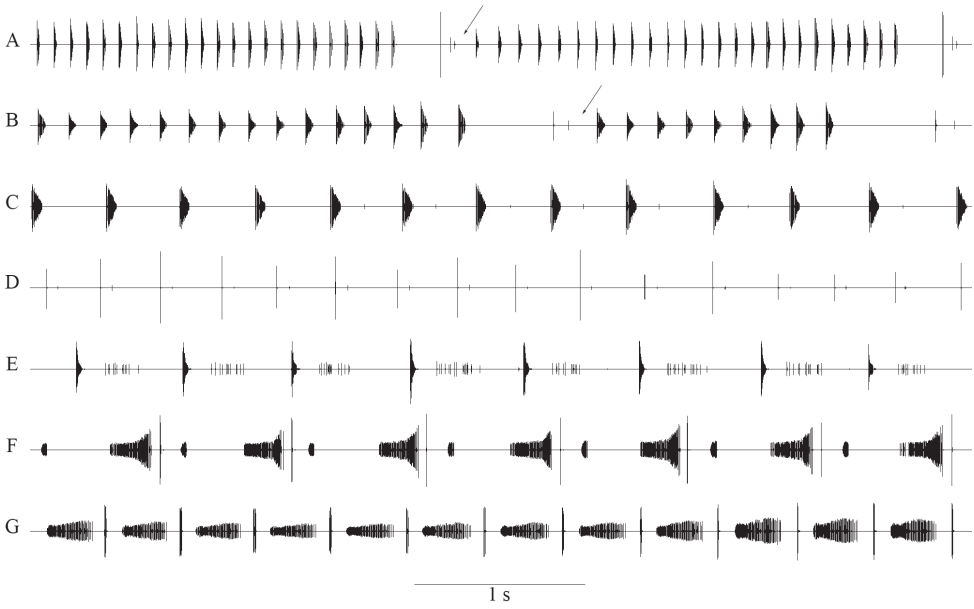

Figure 5. Oscillograms showing the typical pattern of male calling songs in each species of the *Isophya camptoxypha* species-group: **A** *I. posthumoidalis* (25°C, Bieszczady Mountains, Poland) **B** *I. dochia* (24.8°C, Gurghiu Mountains, Romania) **C** *I. camptoxypha* (25°C, Bieszczady Mountains, Poland) **D** *I. sicula* (24.8°C, Harghita-Ciceu Mountains, Romania) **E** *I. ciucasi* (25°C, Ciucaș Mountains, Romania) **F** *I. nagyi* (22.5°C, Călimani Mountains, Romania) **G** *I. bucovinensis* sp. n. (25°C, Suhard Mountains, Romania). Time scale (shown at the bottom) is the same for all oscillograms in the figure. The arrows indicate the characteristic interval separating syllable groups.

Distribution and natural history. The new species populates mesophytic montane meadows in the south–western part of Bucovina, within the altitudinal range of 900–1900 m (Fig. 1C). The insects were collected from broad leaves of various dicotyledonous plants: *Veratrum* sp., *Rumex* sp., *Rubus* sp., *Aconitum* sp., *Vaccinium* sp., *Urtica* sp., *Gentiana* sp., *Hypericum* sp. etc. The distribution of this bush-cricket includes highlands from northern and western Călimani Mountains, the northern part of Suhard Mountains (Eastern Carpathians) (Fig. 6) and most likely occurs also in Dorna depression and the central and southern parts of Suhard Mountains.

Conservation status. *Isophya bucovinensis* sp. n. is known only from Călimani and Suhard Mountains. It could be considered as *Endangered B1ab(iii, v)+2ab(iii, v)* following IUCN's Red List categories and criteria version 3.1 (known EOO=234 km^2 and AOO=28 km^2; the constant degradation of species' habitat is the result of mechanized mowing in June and July, and overgrazing, especially in Suhard highlands) (IUCN 2012).

Discussion. In this study, we report the discovery and give the description of a new bush-cricket species recognized based on its distinctive calling song. The basic pattern of its song is not unique within the genus *Isophya*: a series of evenly repeated syllables,

each consisting of two elements: a longer impulse series followed by a short impulse group (see e. g. Heller 1988, Chobanov et al. 2013). However, species producing this male song pattern can be found in several different, morphology-based species-groups (Warchałowska-Śliwa et al. 2008, Chobanov et al. 2013). One of these species-groups is the *Isophya camptoxypha* complex. Six morphologically closely-related species inhabiting the Carpathians were recently placed within this group: *I. camptoxypha* Fieber, *I. ciucasi* Iorgu & Iorgu, *I. nagyi*, *I. sicula* Orci, Szövényi & Nagy, *I. posthumoidalis* Bazyluk and *Isophya dochia* Iorgu (Szövényi et al. 2012, Iorgu 2012). Because of its similar morphology, *I. bucovinensis* sp. n. also belongs to this group.

Since the species of the *Isophya camptoxypha* species-group are all very similar to each other regarding the morphology, we believe that a male calling song based identification key will be helpful to identify specimens from populations of unknown species identity.

Identification key for the presently recognized species of *I. camptoxypha* species group, based on male song characters:

1 Male calling song consists of syllable groups separated from each other by a characteristic interval. Syllable groups are composed of two syllable types ("A" and "B"), each group being a series of "A" syllables followed by one "B" syllable containing conspicuous, high amplitude clicks (Fig. 5A, B).....**2**

– Male calling song is a series of syllables, no regular syllable groups are observable, syllables show the same basic structure (i.e. the song is composed of one syllable type) (Fig. 5C–G).....**3**

2 "A" syllables are shorter than 25 ms, the conspicuous click(s) follow(s) a silent interval of 300–450 ms (Fig. 5A).....***I. posthumoidalis***

– "A" syllables have a duration of 30–60 ms, the high amplitude click(s) between the syllable groups follow(s) a 550–950 ms long silent interval (Fig. 5B) ....***I. dochia***

3 The longest impulse series in the syllables (LIS) is shorter than 80 ms.....**4**

– LIS is longer than 100 ms.....**5**

4 LIS falls between 25–60 ms, consisting of more than 10 impulses (Fig. 5C)... .....***I. camptoxypha***

– LIS is shorter than 25 ms, consisting of 1–3 impulse(s) (Fig. 5D).... ***I. sicula***

5 Syllables consisting of two impulse groups.....**6**

– Syllables consisting of three impulse groups (Fig. 5F) .....***I. nagyi***

6 Interval after LIS is longer than 300 ms (Fig. 5E) .....***I. ciucasi***

– Interval after LIS is shorter than 150 ms (Fig. 5G)..... ***I. bucovinensis* sp. n.**

The duration values given in the above key are based on male songs recorded at an ambient air temperature between 20–25°C. To identify specimens, a song recording should be made in that range of air temperature. The key is most reliable when mean values based on at least 5–10 measurements per specimen are used in all quantitative characters.

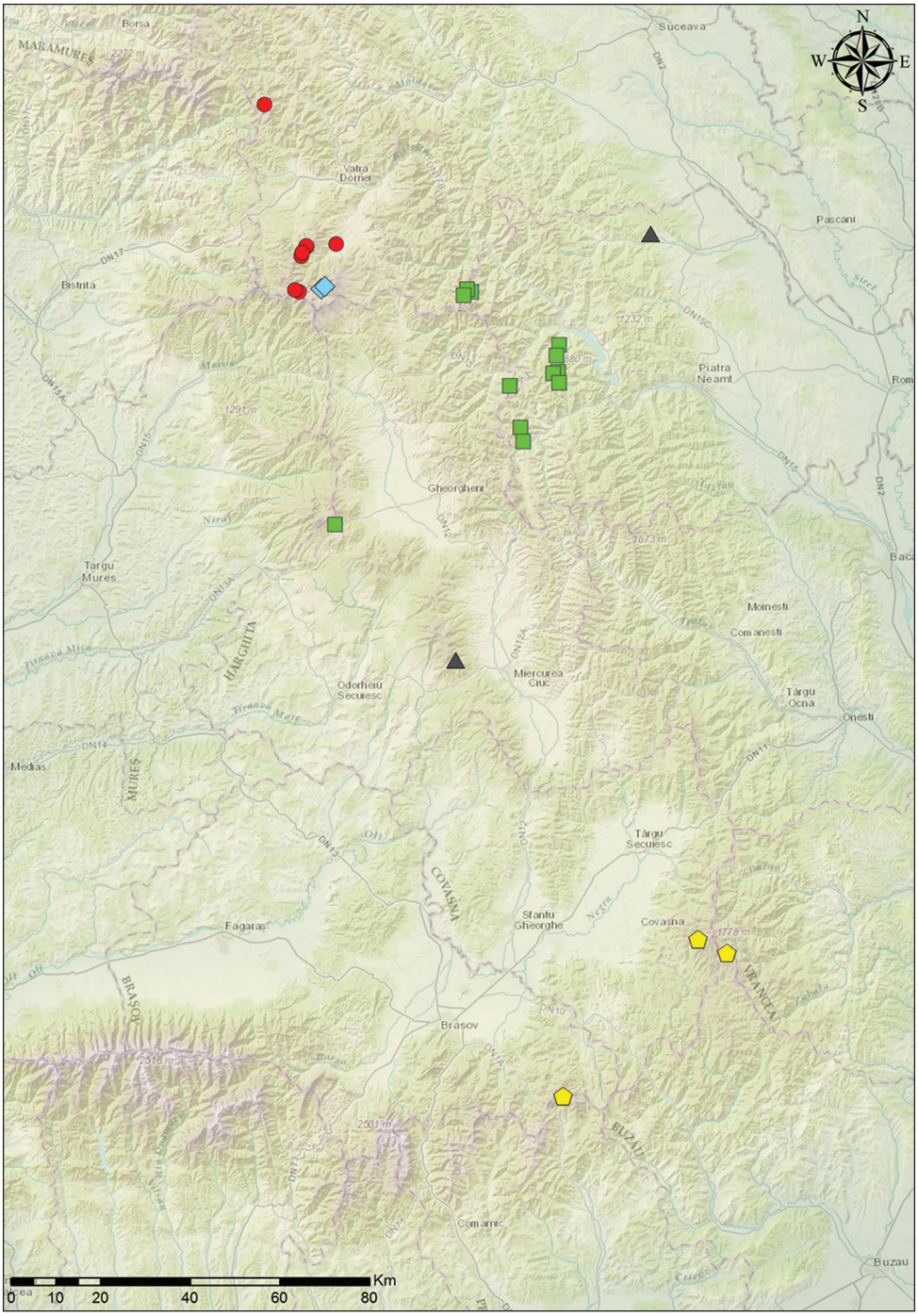

Figure 6. Geographic distribution of the Eastern Carpathian endemic *Isophya* species: red dots – *I. bucovinensis* sp. n., yellow pentagons – *I. ciucasi*, green squares – *I. dochia*, blue diamonds – *I. nagyi*, black triangles – *I. sicula*.

The easiest way to identify male specimens of *Isophya bucovinensis* sp. n. is to examine both the male stridulatory file and the pattern of male calling song. Within the *I. camptoxypha* species group, only two species have male stridulatory files containing more than 100 stridulatory pegs: *I. nagyi* and *I. bucovinensis* sp. n. Interestingly, except for the different number of syllabic elements and syllable repetition rates, the syllables produced by males of *Isophya bucovinensis* sp. n. and *I. nagyi* show remarkable similarities in oscillographic structure (Fig. 4). The longest impulse series of their syllables (element "B") are almost identical (156–286 ms, 46–79 impulses in *I. bucovinensis* sp. n. and 129–217 ms, 38–79 impulses in *I. nagyi*), and also the high amplitude, short impulse group (element "C") after the long impulse series is rather similar in the two species (3–28 ms, 2–7 impulses in *I. bucovinensis* sp. n. and 1–6 ms, 1–4 impulses in *I. nagyi*). Because of these similarities in song and due to the high level of morphological similarity, we hypothesize that the two species are likely to be a pair of young sister species. This premise should be examined during subsequent studies relying on molecular genetic analysis. Spectral properties of the male calling songs are similar in these two species, most likely due to the comparable dimensions of male stridulatory apparatus (Fig. 4E).

In *Isophya bucovinensis* sp. n., the delay of female response is much shorter (48–66 ms) than that in *I. nagyi* (71–127 ms) (Fig. 4C, D). Since female reply delay proved to be a critical parameter for males to recognize female response as a conspecific signal in a number of phaneropterine bush-crickets (Heller & von Helversen, 1986), the detected difference in response delay is likely to make the responses of *I. bucovinensis* sp. n. females ineffective for communicating with *I. nagyi* males and vice versa. Also, another impediment for heterospecific communication in these two species is that the responses of *I. nagyi* females would overlap with a dense impulse series of the male's next syllable if she would try to duet with a male *I. bucovinensis* sp. n.; the detection of the female signal is less likely if the male's own signal masks it. Therefore, in addition to the clear difference of male songs, the divergence of female response delay also suggests that the two taxa are best treated as specifically distinct. However, several interesting questions arise regarding the male–female communication of these two species. Presently, it is uncertain which feature of the male signal serves as a marker to start the timing of female response. Females of duetting Phaneropterinae bush-crickets usually use a conspicuous motif of the male song as a response timing marker (Heller and von Helversen 1986, Heller 1990, Dobler et al. 1994). Clearly detectable features of the male song in *I. bucovinensis* sp. n. are the beginning and end of "B" and "C" elements. Among these, we consider the beginning of "C" element to be most likely the female response timing marker (this is why we measured female response delay from that male song feature). However, it is only a presumption and a future laboratory test with playback experiments applying modified male syllables will be needed to answer this question.

The *Isophya camptoxypha* species-group shows a surprisingly high rate of endemism in the Eastern Carpathians. Five of its recently described species have very small distribution areas (Fig. 6) : *I. ciucasi* populates montane meadows in the southern part of

the Eastern Carpathians: in Ciucaș and Vrancea Mountains, *I. dochia* is known to occur in Ceahlău, Bistriței and Gurghiu Mountains, *I. sicula* is distributed in Harghita-Mădăraș and Stânișoarei Mountains, *I. nagyi* occurs in small areas in the southern part of Călimani volcanic caldera and *I. bucovinensis* sp. n. is known from the northern and western parts of Călimani, reaching Suhard mountains in north. The ancestors of these species presumably penetrated from the distribution center of this genus in Balkan–Asia Minor along the western part of Southern Carpathians and Apuseni Mountains dispersal routes (Kenyeres et al. 2009), and speciated during their expansion by isolation of the populations in the mountain chains of Eastern Carpathians.

Acknowledgments

This study was supported by a grant from the Romanian National Authority for Scientific Research and Innovation CNCS – UEFISCDI, project number PN–II–RU–TE–2014–4–2093, awarded to IȘI. The work of KMO and GSz was supported by a grant from the Hungarian National Research Fund (OTKA/NKFI K81929). We want to thank T. Sahlean for preparing the distribution map. The authors acknowledge Călimani National Park Administration for the excellent working conditions and L. Moscaliuc, A. Derscariu, T. Sahlean, V. Gavril, G. Chișamera, L. Fusu, M. Dascălu, O. Popovici and M. Mitroiu for their company on field expeditions. We thank K.-G. Heller and H. Braun for their helpful comments on the manuscript.

References

Bálint M, Ujvárosi L, Theissinger K, Lehrian S, Mészáros N, Pauls S (2011) The Carpathians as a major diversity hotspot in Europe. In: Zachos F, Habel J (Eds) Biodiversity Hotspots. Springer, Heidelberg, Germany, 189–205. http://link.springer.com/chapter/10.1007%2F978-3-642-20992-5_11

Cameron RAD, Pokryszko BM, Gheoca V, Horsák M (2016) At the Central European–Balkan transition: forest land snail faunas of the Banat contrasted with those of the Carpathian chain. Biological Journal of the Linnean Society 119: 560–570. https://doi.org/10.1111/bij.12498

Chobanov DP, Grzywacz B, Iorgu IȘ, Çiplak B, Ilieva MB, Warchałowska-Śliwa E (2013) Review of the Balkan *Isophya* (Orthoptera: Phaneropteridae) with particular emphasis on the *Isophya modesta* group and remarks on the systematics of the genus based on morphological and acoustic data. Zootaxa 3658(1): 1–81. https://doi.org/10.11646/zootaxa.3658.1.1

Dobler S, Heller K-G, von Helversen O (1994) Song pattern recognition and an auditory time window in the female bushcricket *Ancistrura nigrovittata* (Orthoptera: Phaneropteridae). Journal of Comparative Physiology A 175(1): 67–74. https://doi.org/10.1007/BF00217437

Gajdoš P, Moscaliuc LA, Rozwałka R, Hirna A, Majkus Z, Gubányi A, Heltai MG, Svatoň J (2014) Red list of spiders (Araneae) of the Carpathian Mts. In: Kadlečík J (Ed.) Carpathian Red List of forest habitats and species, Carpathian list of invasive alien species (draft). Banská Bystrica: State Nature Conservancy of the Slovak Republic, 186–199.

Heller K-G, von Helversen D (1986) Acoustic communication in phaneropterid bushcrickets: species-specific delay of female stridulatory response and matching male sensory time window. Behavioral Ecology and Sociobiology 18(3): 189–198. https://doi.org/10.1007/BF00290822

Heller K-G (1988) Bioakustik der europaeischen Laubheuschrecken. Josef Margraf, Weikersheim, 358 pp.

Heller K-G (1990) Evolution of song pattern in East Mediterranean Phaneropterinae. In: Bailey WJ, Rentz DCF (Eds) The Tettigoniidae: Biology, Systematics, Evolution. Crawford House Press, Bathurst, 130–151. https://doi.org/10.1007/978-3-662-02592-5_8

Heller K-G, Orci KM, Grein G, Ingrisch S (2004) The *Isophya* species of Central and Western Europe (Orthoptera: Tettigonioidea: Phaneropteridae). Tijdschrift voor Entomologie 147: 237–258. https://doi.org/10.1163/22119434-900000153

Heller K-G, Hemp C, Ingrisch S, Liu C (2015) Acoustic communication in Phaneropterinae (Tettigonioidea) – a global review with some new data. Journal of Orthoptera Research 24(1): 7–18. https://doi.org/10.1665/034.024.0103

Homburg K, Drees C, Gossner MM, Rakosy L, Vrezec A, Assmann T (2013) Multiple Glacial Refugia of the Low-Dispersal Ground Beetle *Carabus irregularis*: Molecular Data Support Predictions of Species Distribution Models. PLoS ONE 8(4): e61185. https://doi.org/10.1371/journal.pone.0061185

Hurdu B-I, Escalante T, Puşcaş M, Novikoff A, Bartha L, Zimmermann N (2016) Exploring the different facets of plant endemism in the South-Eastern Carpathians: a manifold approach for the determination of biotic elements, centres and areas of endemism. Biological Journal of the Linnean Society 119: 649–672. https://doi.org/10.1111/bij.12902

Iorgu IŞ (2012) Acoustic analysis reveals a new cryptic bush-cricket in the Carpathian Mountains (Orthoptera, Phaneropteridae). ZooKeys 254: 1–22. https://doi.org/10.3897/zookeys.254.3892

Iorgu IŞ, Krištín A, Szövényi G, Kaňuch P, Jarčuška B, Sahlean CT, Iorgu EI, Orci KM (2017) Distinctive male–female acoustic duetting supports the specific status of *Isophya fatrensis*, a West-Carpathian endemic bush-cricket (Insecta: Orthoptera: Tettigoniidae: Phaneropterinae). Bioacoustics (online first). http://dx.doi.org/10.1080/09524622.2016.1272005

IUCN (2012) IUCN Red List Categories and Criteria: Version 3.1, 2nd Edition. Gland, Switzerland and Cambridge, UK, iv + 32 pp.

Kenyeres Z, Rácz IA, Varga Z (2009) Endemism hot spots, core areas and disjunctions in European Orthoptera. Acta zoologica cracoviensia 52B(1–2): 189–211. http://db.isez.pan.krakow.pl/AZC/pdf/azc_i/52B(1-2)/52B(1-2)_16.pdf

Mráz P, Ronikier M (2016) Biogeography of the Carpathians: evolutionary and spatial facets of biodiversity. Biological Journal of the Linnean Society 119: 528–559. https://doi.org/10.1111/bij.12918

Mráz P, Barabas D, Lengyelová L, Turis P, Schmotzer A, Janišová M, Ronikier M (2016) Vascular plant endemism in the Western Carpathians: spatial patterns, environmental correlates and taxon traits. Biological Journal of the Linnean Society 119: 630–648. https://doi.org/10.1111/bij.12792

Orci KM (2007) Female preferences for male song characters in the Bush-cricket *Isophya camptoxypha* (Orthoptera, Tettigonioidea, Phaneropteridae). Journal of Insect Behavior 20(5): 503–513. http://link.springer.com/article/10.1007/s10905-007-9096-x

Orci KM, Nagy B, Szövényi G, Racz IA, Varga Z (2005) A comparative study on the song and morphology of *Isophya stysi* and *I. modestior* (Orthoptera, Tettigoniidae). Zoologischer Anzeiger 244(1): 31–42. https://doi.org/10.1016/j.jcz.2004.11.002

Orci KM, Szövényi G, Nagy B (2010a) A characterization of the pair forming acoustic signals of *Isophya harzi* (Orthoptera, Tettigonioidea, Phaneropteridae). Acta Zoologica Academiae Scientiarum Hungaricae 56(1): 43–53. http://actazool.nhmus.hu/56/1/azh56_1_Orci.pdf

Orci KM, Szövényi G, Nagy B (2010b) *Isophya sicula* sp. n. (Orthoptera: Tettigonioidea), a new, morphologically cryptic bush-cricket species from the Eastern Carpathians (Romania) recognized from its peculiar male calling song. Zootaxa 2627: 57–68. http://www.mapress.com/zootaxa/2010/f/zt02627p068.pdf

Ragge DR, Reynolds WJ (1998) The songs of the grasshoppers and crickets of Western Europe. Harley Books, Colchester, Essex, 591 pp.

Szövényi G, Puskás G, Orci KM (2012) *Isophya nagyi*, a new phaneropterid bush-cricket (Orthoptera: Tettigonioidea) from the Eastern Carpathians (Căliman Mountains, North Romania). Zootaxa 3521: 67–79. http://www.mapress.com/zootaxa/2012/f/zt03521p079.pdf

Stewart JR, Lister AM, Barnes I, Dalen L (2010) Refugia revisited: individualistic responses of species in space and time. Proceedings of the Royal Society B 277: 661–671. https://doi.org/10.1098/rspb.2009.1272

Theissinger K, Bálint M, Feldheim KA, Haase P, Johannesen J, Laube I, Pauls SU (2013) Glacial survival and post-glacial recolonization of an arctic–alpine freshwater insect (*Arcynopteryx dichroa*, Plecoptera, Perlodidae) in Europe. Journal of Biogeography 40: 236–248. https://doi.org/10.1111/j.1365-2699.2012.02793.x

Varga Z (2011) Extra-Mediterranean refugia, post-glacial vegetation history and area dynamics in Eastern Central Europe. In: Zachos FE, Habel JE (Eds) Biodiversity hotspots distribution and protection of conservation priority areas. Part 2. Springer Verlag, Berlin, 57–87.

Warchałowska-Śliwa E, Chobanov DP, Grzywacz B, Maryańska-Nadachowska A (2008) Taxonomy of the genus *Isophya* (Orthoptera, Phaneropteridae, Barbitistinae): comparison of karyological and morphological data. Folia biologica (Kraków) 56 (3–4): 227–241. https://doi.org/10.3409/fb.56_3-4.227-241

Zasadni J, Kłapyta P (2014) The Tatra Mountains during the last glacial maximum. Journal of Maps 10: 440–456. https://doi.org/10.1080/17445647.2014.885854

ZooKeys 680: 73–104 (2017)
doi: 10.3897/zookeys.680.11162
http://zookeys.pensoft.net

RESEARCH ARTICLE

A peer-reviewed open-access journal
ZooKeys
Launched to accelerate biodiversity research

An elusive Neotropical giant, *Hondurantemna chespiritoi* gen. n. & sp. n. (Antemninae, Mantidae): a new lineage of mantises exhibiting an ontogenetic change in cryptic strategy

Henrique M. Rodrigues[1,2], Julio Rivera[3,4], Neil Reid[5,6], Gavin J. Svenson[1,2]

1 *Department of Invertebrate Zoology, Cleveland Museum of Natural History, 1 Wade Oval Drive, Cleveland, Ohio, USA* **2** *Department of Biology, Case Western Reserve University, 10900 Euclid Avenue, Cleveland, Ohio, USA* **3** *Universidad San Ignacio de Loyola, Peru* **4** *Museo de Entomología Klaus Raven Büller, Universidad Nacional Agraria La Molina, Lima, Peru* **5** *School of Biological Sciences, Queen's University Belfast, MBC, 97 Lisburn Road, Belfast, BT9 7BL, Northern Ireland, UK* **6** *Operation Wallacea Ltd., Wallace House, Old Bolingbroke, Lincolnshire, PE23 4EX, England, UK*

Corresponding author: *Henrique M. Rodrigues* (hmrbio@gmail.com)

Academic editor: *D. Evangelista* | Received 12 November 2016 | Accepted 5 May 2017 | Published 14 June 2017

http://zoobank.org/A59AF4C7-2C30-40CC-B7DD-ACADA007A005

Citation: Rodrigues HR, Rivera J, Reid N, Svenson GJ (2017) An elusive Neotropical giant, *Hondurantemna chespiritoi* gen. n. & sp. n. (Antemninae, Mantidae): a new lineage of mantises exhibiting an ontogenetic change in cryptic strategy. ZooKeys 680: 73–104. https://doi.org/10.3897/zookeys.680.11162

Abstract

We present the description of a new genus and new species of praying mantis, *Hondurantemna chespiritoi* **gen. n. & sp. n.** This species of cryptic mantis, collected in National parks in Mexico and Honduras, remained unknown despite its considerable body size. Based on a phylogenetic analysis with molecular data and traditional morphological analysis, we place this new genus within Antemninae, a monotypic Mantidae subfamily. We update the subfamily concept for Antemninae and provide a key to the two genera. We describe the external morphology of immatures and adults of the new species as well as the genital complexes of both sexes and the ootheca of *Antemna rapax*. The observed morphological changes between immature and adult females suggests that the selection for an alternate strategy for crypsis is a response to size increase of the abdomen during development. Immatures exploit a stick/branch habitat based on their morphological appearance while adult females appear as a leaf to disguise the profile of the body.

Resumen

Se presenta la descripción de un nuevo género y una nueva especie de mantis religiosa, *Hondurantemna chespiritoi* **gen. n. & sp. n**. Esta nueva especie de mantis críptica, colectada en ciertos parques nacionales de México y Honduras, había permanecido hasta ahora desconocida para la ciencia a pesar de su gran tamaño corporal. Utilizando un análisis filogenético con datos moleculares y junto con análisis tradicional de morfología, se logró clasificar a este nuevo género dentro de la subfamilia monotípica Antemninae que pertenece a la familia Mantidae. Como resultado se actualiza el concepto taxonómico de Antemninae y se presenta una clave para identificar los dos géneros atribuidos a esta subfamilia. Se describe la morfología externa de los juveniles y adultos de la nueva especie, así como el complejo genital de ambos sexos y la ooteca de *Antemna rapax*. La diferencia morfológica observada entre juveniles y adultos sugiere que existen fuerzas selectivas divergentes, posiblemente en respuesta al aumento del tamaño del abdomen durante el desarrollo, para así mantener su camuflaje a lo largo de su ciclo de vida. Sobre la base de su apariencia general, los juveniles utilizarían una estrategia críptica asemejando ramas, mientras que las hembras adultas asemejan hojas verdes para ocultar el contorno corporal.

Keywords

Mantodea, Praying mantis, Dictyoptera, crypsis

Palabras clave

Mantodea, mantis religiosa, Dictyoptera, crypsis

Introduction

The taxonomy of Mantodea has been revised several times during the 20th century, leading to unstable family and subfamily arrangements (Giglio-Tos 1927, Beier 1964, Terra 1995). Ehrmann and Roy (Ehrmann 2002) proposed the most recent classification of the order, which greatly improved the classification proposed by Beier (1964), although some problems remained. Svenson and Whiting (2004, 2009) conducted molecular phylogenetic analyses and found evidence that around half of the families and subfamilies were not monophyletic, concluding that patterns of convergent morphology mislead taxonomists into creating artificial groups. Their findings indicated the need of revisionary work at almost all levels of Mantodea systematics to better understand the diversity and create a natural classification. In phylogenetic studies, most Neotropical mantises are recovered in two major clades (Yager and Svenson 2008, Svenson and Whiting 2009). The first clade is comprised of the primitively deaf species, the Acanthopoidea (recently revised by Rivera and Svenson 2016), diverging early in the evolution of the group while the second clade diverged much later and includes almost all Neotropical species within Mantidae (Svenson and Whiting 2009). Finally, Rivera (2010b) reviewed the state of the systematics of Neotropical genera and highlighted several groups that needed revision, including all Mantidae subfamilies, calling for increased studies on the diversity and taxonomy of the group.

Two enigmatic praying mantis specimens, one male and one female, were discovered in collections from the United States and France. Shared characteristics of the two speci-

mens suggested they were conspecific, but they were incompatible with the descriptions of known Neotropical genera. Additional material collected in Honduras, including two adult females and nymphs of both sexes, confirmed the conspecificity of the specimens and provided the opportunity to study some morphological variation. Initial examination of other Neotropical taxa allied our unknown specimens with *Antemna rapax* Stål, 1877, the only representative of Antemninae. In both species, mid- and hindlegs present a posteroventral sub-apical lobe on the femora; males have a medial ocellar process; and the shape of the forewing of the females is similar, with an enlarged costal area, which is unusual for Neotropical species. No other Neotropical genus included with the Acanthopoidea *sensu* Rivera and Svenson (2016), Vatinae *sensu* Svenson et al. (2016), Stagmomantinae - Stagmatopterinae - Choeradodinae *sensu* Ehrmann and Roy (Ehrmann 2002) demonstrated enough similarity to suggest close relation. However, the high level of morphological convergence in the order (Svenson and Whiting 2009) prevented a definitive placement of the new lineage in the absence of a phylogenetic analysis. The description of immatures of this new species also presents an opportunity to shed new light on an often-neglected aspect of praying mantis natural history: ontogenetic changes in morphological traits associated with camouflage and mimicry.

Ontogenetic studies on Mantodea are uncommon and most species are described based on adult specimens, while nymphs remain unknown or undescribed, with a few exceptions. Heitzmann-Fontenelle (1969) revised *Cardioptera* Burmeister, 1838 and described the nymphal stages of two species of the genus while Terra (1980) studied the development of raptorial forelegs in four species of Neotropical mantises. Avendaño and Sarmiento (2011) did the most complete work by characterizing morphological changes during the post-embryonic development of *Callibia diana* Stål, 1877 while collecting data to characterize allometric growth. However, these works dealt with cases where the morphology of immatures and adults were similar enough that matching life stages was not difficult. Wieland (2013) reviewed Mantodea post-embryonic development of different body parts and recent studies have revealed a number of cases across Mantodea where nymphal strategy and appearance differ from adults. For instance, nymphs of *Acontista* Saussure & Zehntner, 1894 (Acontistidae) have been reported to resemble ants both in overall shape and in behavior, a strategy not seen in adults (Salazar 2003). The Amazonian *Mantillica nigricans* Westwood, 1889 (Thespidae, Bantiinae) was recently reported to also exhibit ant-mimicry, a strategy observed in nymphs of both sexes as well as adult females, but not in adult males (Agudelo and Rafael 2014). Immature males of the lichen-mimic *Pseudopogonogaster kanjaris* Rivera & Yagui, 2011 (Thespidae, Pseudopogonogastrinae) exhibit cuticular, lichen-like lobes on the abdominal terga similar to those observed in adult females, but in the adult stage these become reduced and tucked under the well-developed wings (Rivera et al. 2011).

Morphological sexual dimorphism, frequently present in Mantodea species (Hurd 1999), can be reflected during development as considerable changes occurring between instars. In cases of moderate to extreme dimorphism, males, females and nymphs have been described as separate genera due to discrepant morphologies, e.g. *Antemna* Stål, 1877, *Phyllomantis* Saussure, 1892 and *Neacromantis* Beier, 1931 (Rehn 1935), *Pseudopogonogaster*

Beier, 1942 and *Calopteromantis* Terra, 1982 (Rivera et al. 2011), and *Pachymantis* Saussure, 1871 and *Triaenocorypha* Wood-Mason, 1890 (Svenson et al. 2015). Careful study including adults and immatures can prevent life stages being described as separate taxa or resolve instances where that happened. Studies tracking changes during post-embryonic development not only add descriptive knowledge (e.g. Heitzmann-Fontenelle 1969, Avendaño and Sarmiento 2011) they can also reveal different life strategies between immatures and adults (e.g. Salazar 2003) and shifts between male and female ecologies.

Herein, we leverage a molecular based phylogeny paired with traditional comparative morphology to place our unknown taxon among other Neotropical praying mantises. We 1) place our unknown taxon in a newly created genus allied with *Antemna* within Antemninae; 2) provide a diagnosis for the new genus and an extensive description of the new species, high-resolution images and morphological illustrations; and 3) describe morphological changes occurring through post-embryonic development with comments on the ecological significance and present the distribution for the new species.

Methods

Specimens examined and depository

We examined twenty specimens of the new taxon, one male genitalia and one ootheca of *Antemna rapax*. Specimens are accessioned in four collections: the Muséum National d'Histoire Naturelle (MNHN) Paris, France, the California Academy of Sciences (CAS) San Francisco, USA, the Academy of Natural Sciences of Drexel University (ANSP) and the Cleveland Museum of Natural History (CLEV) Cleveland, USA.

Morphology

We examined specimens using a Leica M80 stereomicroscope and measured them with a Leica M165C stereomicroscope fitted with an IC80 HD coaxial video camera and the live measurement mode of the Leica Application Suite (LAS). Measurements are given in millimeters and include: body length (measured from the frons to the apex of the abdomen); prozona length (measured from the anterior end of the prothorax to the sulcus above the supracoxal dilation); metazona length (measured from the sulcus above the supracoxal dilation to the posterior end of the prothorax); prothorax width (measured at the level of the supracoxal dilation); forewing length (measured from the point where the forewing articulates with the thorax to the tip); hindwing length (measured from the point where the hindwing articulates with the thorax to the tip); forecoxa length (measured from the articulation with the prothorax to the articulation with the trochanter); forecoxa width (measured at the widest point of the coxa); forefemur length (measured from the articulation with the trochanter to the articulation with the tibia); forefemur width (measured at the widest point of the femur); foretibia length (measured from

the articulation with the femur to the articulation with the tarsus); mesofemur length (measured from the articulation with the trochanter to the articulation with the tibia); metafemur length (measured from the articulation with the trochanter to the articulation with the tibia). We calculated ratios useful for species identification (Svenson 2014, Rodrigues and Cancello 2016) for the new species: metazona length/prozona length; pronotum length/width; pronotum length/forecoxa length; forefemur length/width. We give spine count for forelegs according to the spination formula proposed by Rivera (2010a) and modified by Brannoch and Svenson (2016), e.g. F= 3DS/10AvS/4PvS; T=12AvS/15PvS where F is forefemur, T is foretibia, DS is discoidal spines, AvS is anteroventral spines and PvS is posteroventral spines. All spines are numbered from the base of the segment to the apex. We extracted male and female genital complexes from the abdomen and treated them in a heated weak KOH solution for 5 minutes to dissolve soft tissues (Rodrigues and Cancello 2016). Treated genital structures were either placed inside vials filled with glycerin and pinned with the specimen or placed with the specimen inside an ethanol-filled vial. Nomenclature of genital structures follows Klass (1997, 1998). Morphological features of the adult female and nymphs that are identical in the males were omitted from the description to avoid redundancy.

Digital imaging

We took high resolution photos with a Passport Storm© system (Visionary Digital™, 2012), which included a Stackshot z-stepper, a Canon 5D SLR, macro lenses (50mm, 100mm and MP-E 65mm), three Speedlight 580EX II flash units with initial image processing done on Adobe Lightroom 3.6. Z-stepper was controlled using Zerene stacker 1.04, and images stacked with P-Max protocol. Photos were edited using Adobe Photoshop CC to correct for background noise and to add scale bars. We created illustrations with Adobe Illustrator CC based on high-resolution photos of the structures. We constructed plates with Adobe Illustrator CC.

Phylogenetic analysis

We conducted phylogenetic analyses to test the position of our new taxon using molecular data. The ingroup sample included taxa within Antemninae, Stagmatopterinae, Stagmomantinae, and Vatinae (Table 1), which provided coverage across the four major lineages of Neotropical Mantidae. Representative outgroup taxa were included to test the position of our new taxon relative to Acanthopoidea (Rivera and Svenson 2016) and African and Asian taxa recovered in close relation to our ingroup (Svenson and Whiting 2009). Representatives of Chaeteessidae and Mantoididae were included to root the phylogeny based on their consistent recovery as the two earliest branches of Mantodea (Svenson and Whiting 2009, Wieland 2013, Svenson et al. 2015). We assembled a molecular dataset from previously published works (Svenson and Whiting

Table 1. List of species used in the phylogenetic analyses with their families and subfamilies given.

Species	Family	Subfamily	MN Code	GenBank accession number – COI	GenBank accession number – H2A	GenBank accession number – H3	GenBank accession number – ND4
Mantoida sp.	Mantoididae	-	MN180	FJ802822.1	-	FJ806771.1	FJ802586.1
Chaeteessa sp.	Chaeteessidae	-	MN482	KR360623.1	-	KR360691.1	-
Acanthops falcataria	Acanthopidae	Acanthopinae	MN112	EF383861.1	-	EF384117.1	FJ802526.1
Macromantis nicaraguae	Mantidae	Photininae	MN144	EF383873.1	-	EF384129.1	FJ802554.1
Cardioptera squalodon	Mantidae	Photininae	MN178	EF383889.1	-	EF384145.1	FJ802584.1
Epaphrodita musarum	Acanthopidae*	Epaphroditinae	MN435	KY783773	-	KY783805	KY783826
Hymenopus coronatus	Hymenopodidae	Hymenopodinae	MN010	EF383800.1	KR360626.1	AY491334.1	FJ802425.1
Choeradodis rhombicollis	Mantidae	Choeradodinae	MN016	EF383805.1	-	AY491340.1	FJ802431.1
Rhombodera basalis	Mantidae	Mantinae	MN344	FJ802913.1	-	FJ806867.1	FJ802738.1
Vates pectinicornis	Mantidae	Vatinae	MN014	EF383803.1		AY491338.1	FJ802429.1
Vates sp.	Mantidae	Vatinae	MN760	-	-	KY783825	-
Zoolea orba	Mantidae	Vatinae	MN351	KT732082.1	-	KT732101.1	-
Oxyopsis 1	Mantidae	Stagmatopterinae	MN294	FJ802868.1	-	FJ806822.1	FJ802689.1
Oxyopsis 2	Mantidae	Stagmatopterinae	MN734	KY783777	-	KY783808	KY783828
Oxyopsis 3	Mantidae	Stagmatopterinae	MN739	KY783780	-	KY783811	KY783829
Oxyopsis 4	Mantidae	Stagmatopterinae	MN743	KY783784	-	KY783815	KY783832
Oxyopsis 5	Mantidae	Stagmatopterinae	MN749	-	-	-	KY783841
Parastagmatoptera sottilei 1	Mantidae	Stagmatopterinae	MN740	KY783781	-	KY783812	-
Parastagmatoptera sottilei 2	Mantidae	Stagmatopterinae	MN742	KY783783	KY783797	KY783814	KY783831
Parastagmatoptera flavoguttata 1	Mantidae	Stagmatopterinae	MN741	KY783782	KY783796	KY783813	KY783830
Parastagmatoptera flavoguttata 2	Mantidae	Stagmatopterinae	MN751	KY783788	KY783801	KY783819	KY783836
Parastagmatoptera vitreola 1	Mantidae	Stagmatopterinae	MN731	KY783775	KY783794	KY783806	-
Parastagmatoptera vitreola 2	Mantidae	Stagmatopterinae	MN735	KY783778	-	KY783809	-
Stagmatoptera hyaloptera	Mantidae	Stagmatopterinae	MN733	KY783776	-	KY783807	KY783827
Stagmatoptera septentrionalis	Mantidae	Stagmatopterinae	MN029	FJ802763.1	-	AY491353.1	FJ802444.1

Species	Family	Subfamily	MN Code	GenBank accession number – COI	GenBank accession number – H2A	GenBank accession number – H3	GenBank accession number – ND4
Stagmatoptera supplicaria 1	Mantidae	Stagmatopterinae	MN117	EF383863.1	-	EF384119.1	FJ802531.1
Stagmatoptera supplicaria 2	Mantidae	Stagmatopterinae	MN736	KY783779	KY783795	KY783810	-
Stagmatoptera supplicaria 3	Mantidae	Stagmatopterinae	MN748	KY783787	KY783800	KY783818	KY783835
Stagmomantis 1	Mantidae	Stagmomantinae	MN747	-	KY783804	KY783824	-
Stagmomantis 2	Mantidae	Stagmomantinae	MN744	KY783785	KY783798	KY783816	KY783833
Stagmomantis 3	Mantidae	Stagmomantinae	MN745	KY783786	KY783799	KY783817	KY783834
Stagmomantis 4	Mantidae	Stagmomantinae	MN730	KY783774	KY783793	-	-
Stagmomantis 5	Mantidae	Stagmomantinae	MN753	KY783789	KY783802	KY783820	KY783837
Antemna rapax	Mantidae	Antemninae	MN147	EF383875.1	-	EF384132.1	FJ802557.1
Hondurantemna chespiritoi gen. n. & sp. n. 1	Mantidae	Antemninae	MN757	KY783790	-	KY783821	KY783838
Hondurantemna chespiritoi gen. n. & sp. n. 2	Mantidae	Antemninae	MN758	KY783791	-	KY783822	KY783839
Hondurantemna chespiritoi gen. n. & sp. n. 3	Mantidae	Antemninae	MN759	KY783792	KY783803	KY783823	KY783840

*Follow the classification of Terra, 1995 although the correct placement of the genus is currently unknown.

2004, 2009, Svenson et al. 2016) and newly generated sequence data (see Table 1 for GenBank accession numbers). The molecular dataset included four genes: the mitochondrial cytochrome oxidase I (COI) and NADH dehydrogenase subunit 4 (ND4) and the nuclear Histone subunits 2 and 3 (H2A and H3). Lab protocols for extraction, amplification, and sequencing followed published procedures (Svenson and Whiting 2004, 2009, Svenson et al. 2015). New sequence data was imported, verified, and aligned along with published data using Geneious alignment on Geneious v7.1.4. The resulting alignment included 3512 characters. We determined the best fit models for each gene using the Akaike Information Criterion implemented in MEGA v.7 (Kumar et al. 2015): GTR+Γ+I for COI, T92+Γ for ND4, HKY+Γ for H2A and T92+I for H3. We conducted four independent mixed model Bayesian inference (BI) using MrBayes ver. 3.2.5 (Altekar et al. 2004, Ronquist et al. 2012). For all BI, each run was started from a random tree. All sampled generations (every 1000) prior to stationarity were discarded (burn-in). The trees sampled from the stationary distribution were summarized as a 50% majority rule consensus tree to find posterior probabilities (PP) (Huelsenbeck and Imennov 2002, Huelsenbeck et al. 2002). We also performed partitioned maximum likelihood (ML) analysis using RAxML v8 (Stamatakis 2014). Nucleotide substitution parameters were estimated independently from each data partition. One thousand nonparametric bootstrap (BS) pseudoreplicates were performed under a GTR model with CAT approximation of Gamma-distributed among-site rate heterogeneity. Every fifth BS tree was used as a starting tree for more thorough optimization of the real data under GTR+Gamma. FigTree v1.4.2 (Rambaut 2012) was used to visualize topologies and produce figures for both ML and Bayesian analyses.

Results

Phylogeny

The results of BI and ML analyses were largely congruent and generally well supported (Fig. 1). The partitioned ML analysis recovered a topology (likelihood score: -22681.630120) with a moderate BS value (83) resolving our new taxon as sister to *Antemna* within a clade including one *Stagmomantis* Saussure, 1869 taxon (Fig. 1). However, BS values within (*Stagmomantis* 1 + *Antemna* + the new taxon) indicate taxon relationships within the clade and with other *Stagmomantis* taxa may be unstable. The BI (harmonic mean: -22653.69) also recovered our new taxon as sister to *Antemna* with high PP, with the remainder of the topology in almost complete congruence with the ML topology. PP for nodes within the (*Stagmomantis* 1 + *Antemna* + the new taxon) clade firmly place the new taxon within this lineage (Fig. 1). We recovered *Stagmomantis* 1 as sister to the new genus plus *Antemna* in both analyses rather than sister to other *Stagmomantis* taxa, indicating a paraphyletic *Stagmomantis*.

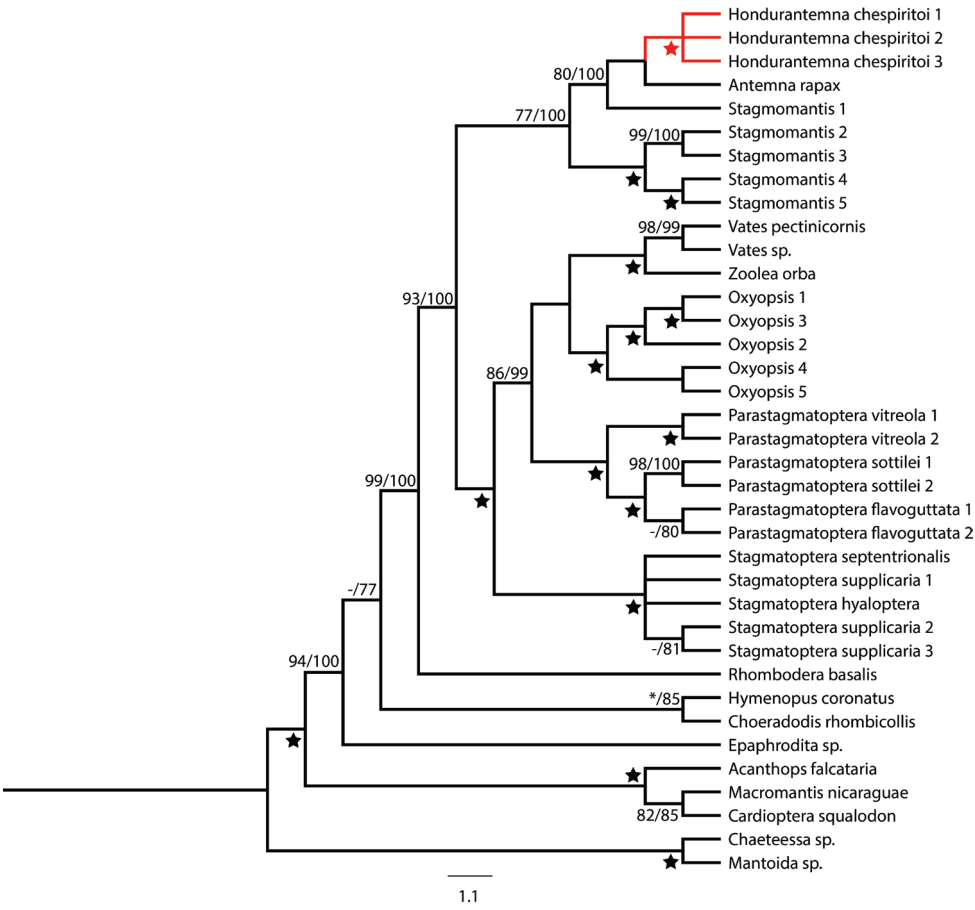

Figure 1. Bayesian Inference (BI) tree with bootstrap values from the Maximum-likelihood and posterior probabilities values higher than 70 shown. Star represent clades with maximum support in both analyses, dash represents support lower than 70 in one of the analyses and asterisk represents a clade recovered only in the BI analysis. *Hondurantemna chespiritoi* n.gen. n. sp. is highlighted in red.

Systematics

The phylogenetic analyses recovered the new taxon as closely related to *Antemna rapax* (Fig. 1). This result corroborates our initial hypothesis based on morphological observations and supports inclusion of the new taxon within Antemninae. Terra (1995) created the subfamily Antemninae to accommodate only the type-genus *Antemna*. With the description of a new genus within Antemninae, we update the concept of the subfamily to reflect its new composition. We also present the first photos of the male genitalia of *Antemna rapax* (see below) (Figs 20, 21).

Antemninae Terra, 1995

Type-genus. *Antemna* Stål, 1877.

Diagnosis. Males have a medial ocellar process that originates posteriorly to the ocelli but anterior to the postfrontal sulcus. The dorsal margin of the forefemora at least partially produced, forming a lamellar projection. Forefemora with four discoidal spines. Meso- and metathoracic legs bearing a posteroventral sub-apical lobe originating from an expansion of the keel running along the margin of the femur. Abdomen of the females swollen, almost as wide as long.

Key to Antemninae genera

1 Five posteroventral forefemoral spines. Dorsal expansion of forefemur extending to femoral apex (Fig. 7). Forewing of females with a spot on the center of the discoidal area. Apofisi falloide of male genitalia with the anterior apex recurved dorsally (Fig. 12). Processo ventrale of the right phallomere longer than wide (Fig. 13) .....***Hondurantemna* gen. n.**

– Four posteroventral forefemoral spines. Dorsal expansion of forefemur ending abruptly before femoral apex (Fig. 19). Forewing of females with a spot on the border of the discoidal and costal areas. Apofisi falloide of male genitalia with the anterior apex not recurved dorsally (Fig. 20). Processo ventrale of the right phallomere wider than long (Fig. 21) .....***Antemna***

***Hondurantemna* gen. n.**
http://zoobank.org/4B298C0B-9D51-44ED-9E12-860116CA0E24
Figs 2–18

Type species. *Hondurantemna chespiritoi* sp. n. by monotypy

Diagnosis. Rounded compound eyes, nymphs and adult males have a medial ocellar process, subadult and adult females without the process. Forelegs with five posteroventral spines and four discoidal spines. Mid- and hindlegs with a single small lobe near the apex of the femur. Male's forewings are hyaline with green crossveins, forewings of females with a spot close to the center of the discoidal area.

Etymology. The generic epithet combines the words Honduras, country were the majority of specimens we studied were collected, and *Antemna*, in reference to the morphological similarities of both Antemninae genera.

***Hondurantemna chespiritoi* sp. n.**
http://zoobank.org/08043DE8-6E08-4930-BC22-288FA7C6386B

Type-specimens. Holotype. 1 ♂ Mexico, Chiapas, Municipio de La Trinitaria, Lagunas de Monte Bello National Park, bellow Dos Lagos on rd. to Santa Elena, 1219m,

14.x.1981, D.E. & P.M. Breedlove (CAS). **Allotype**. 1 ♀ Honduras, Cortes 18km O. San Pedro Sula, Cra. El Merendon, 1650m, vii.1995, T. Porion A. Grange (MNHN). **Paratypes**. *Adults*: 1♀ Honduras, Cortez, San Pedro Sula, Cusuco National Park, Base Camp, 15.4964 -88.2119, 27.vii.2015, N. Reid col. GD0073, MN758; 1♀ Honduras, Cortez, San Pedro Sula, Cusuco National Park, Base Camp, 15.4964 -88.2119, 31.vii.2015, N. Reid col. GD0072. *Immatures*: 1♀ Honduras, Cortez, San Pedro Sula, Cusuco National Park, Santo Tomas, 15.5611 -88.2974, 21.vii.2015, N. Reid col.; 1♂ Honduras, Cortez, San Pedro Sula, Capuca, 15.5031 -88.2222, 17.vi.2015, N. Reid col.; 1♂ 6♀ Honduras, Cortez, San Pedro Sula, Cusuco National Park, Base Camp, low vegetation, 15.4964 -88.2119, 09.vi.2015, N. Reid col.; 1♂ Honduras, Cortez, San Pedro Sula, Cusuco National Park, Base Camp, low vegetation, 15.4964 -88.2119, 09.vi.2015, N. Reid col., MN757; 2♀ Honduras, Cortez, San Pedro Sula, Cusuco National Park, Base Camp, 15.4964 -88.2119, 17.vi.2015, N. Reid col.; 1♀Honduras, Cortez, San Pedro Sula, Cusuco National Park, Base Camp, 15.4964 -88.2119, 17.vi.2015, N. Reid col., MN759; 1♀ Honduras, Cortez, San Pedro Sula, Cusuco National Park, Base Camp, 15.4964 -88.2119, 26.vii.2015, N. Reid col.; 2♀ Honduras, Cortez, San Pedro Sula, Cusuco National Park, Base Camp, 15.4964 -88.2119, vi–vii.2015, N. Reid col. (all paratypes are accessioned at CLEV).

Description. ***Male***: Medium sized. General coloration light brown with dark brown spots (Fig. 2A, B). Body length: 34.2; prozona length: 2.9; metazona length: 5.9; prothorax width: 3.8; forewing length: 21.9; hindwing length: 18.1; forecoxa length: 7.2; forecoxa width: 1.9; forefemur length: 8.8; forefemur width: 2.4; foretibia length: 5.0; mesofemur length: 12.0; midleg metatarsus length: 1.8; metafemur length: 15.3; hindleg metatarsus length: 2.5; metazona length/prozona length: 2.0; pronotum length/width: 2.3; pronotum length/forecoxa length: 1.2; forefemur length/width: 3.6.

Head (Fig. 3A): Rounded eyes. Vertex with dark brown spots, straight, on the same level as the imaginary line connecting the dorsal margin of compound eyes, and separated from the ocelli by two lateral keels and a central depression, the latter bearing the medial ocellar process with a rounded apex. Juxtaocular bulges not developed, on the same level as the vertex. Ocelli medium sized, arranged in the shape of a "V", with the two lateral ocelli further away from each other due to the central depression. Scape and pedicel light brown, flagellomeres of antennae filiform, dark brown. One small tubercle between the eye and the antennal socket. Lower frons subpentagonal, almost as high as wide, bearing two small tubercles, upper margin arcuate, sinuous, the apex straight. Clypeus with a vertical central keel on the lower half. Maxillary palps with black spots on the medial surface, progressively larger towards the apical segments. Labial palps black on the medial surface of all segments.

Thorax (Fig. 4A): General shape cruciform, with the supracoxal dilation pronounced and rounded, metazona two times longer than the prozona. Margins of the prozona convergent anteriorly, ciliated, posteriorly slightly expanded, produced as flat projections, herein called shelves. Margins of the metazona also slightly produced in shelves, ciliated, with small tubercles, almost all of which are black, the anterior part of the metazona with symmetrical depressions on the dorsal surface. Cervix framed by lateral and intercervical sclerites, two ventral sclerites present; the intercervical sclerites

Figure 2. Dorsal and ventral habitus of *Hondurantemna chespiritoi* gen. n. sp. n., **A** dorsal habitus of the male **B** ventral habitus of the male **C** dorsal habitus of the female **D** ventral habitus of the female. Scale bar = 10mm.

with a pronounced torus intercervicalis, the first ventral cervical sclerite constricted in the middle (Fig. 5). Metathoracic hearing organ with deep groove, without knobs (DNK type) (see Yager and Svenson, 2008).

Prothoracic legs: Forecoxae (Fig. 6A) triangular in cross-section, light brown except for the dorsal apical lobe, which is dark brown; posteroventral margin with dispersed tubercles, anteroventral margin with small tubercles bearing slender setae, dorsal margin bearing five large spines and smaller spines between them, the former dark brown on the posterior surface and black on the anterior surface and around the base; ante-

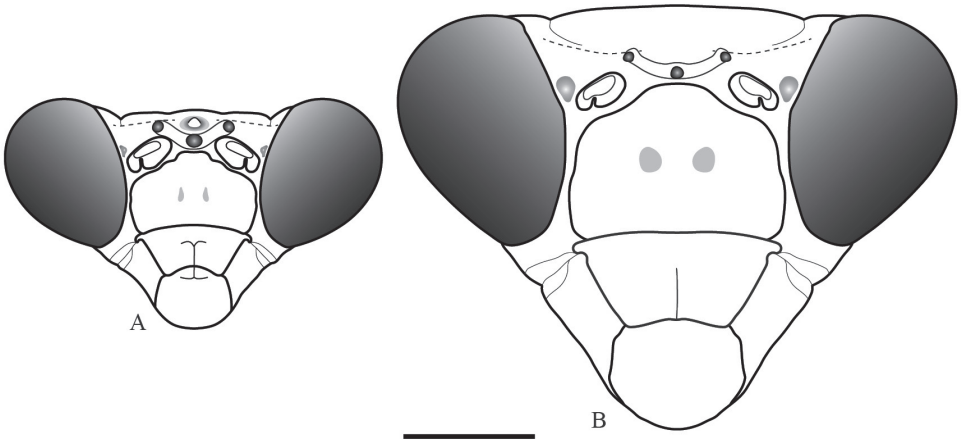

Figure 3. Frontal view of the head of *Hondurantemna chespiritoi* gen. n. sp. n. **A** male **B** female. Scale bar = 2mm.

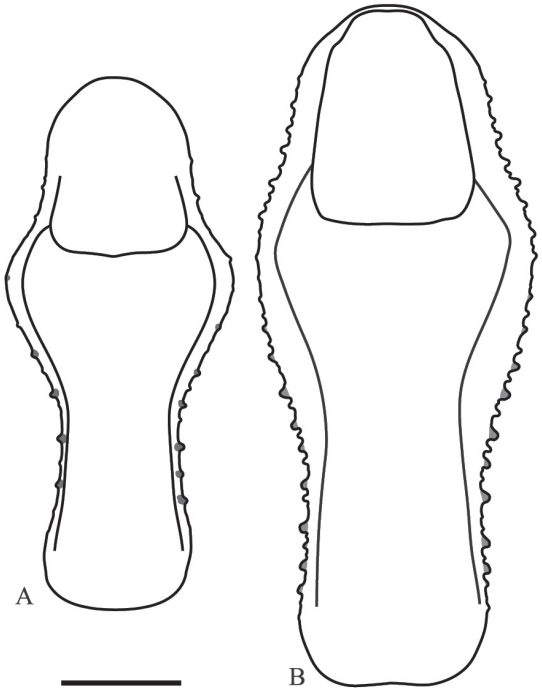

Figure 4. Dorsal view of the prothorax of *Hondurantemna chespiritoi* gen. n. sp. n. **A** male **B** female. Scale bar = 5mm.

rior apical lobes divergent. Forefemora (Fig. 7A) light brown with three dark brown spots on the dorsal area of the anterior surface, dorsal margin regularly convex, slightly compressed anteroposteriorly; F=4DS/15AvS/5PvS; crenulation between posteroven-

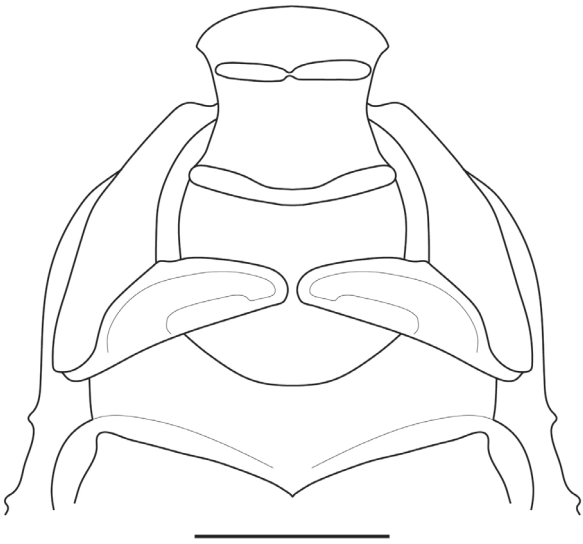

Figure 5. Ventral view of the cervical region of male *Hondurantemna chespiritoi* gen. n. sp. n. Scale bar = 1mm.

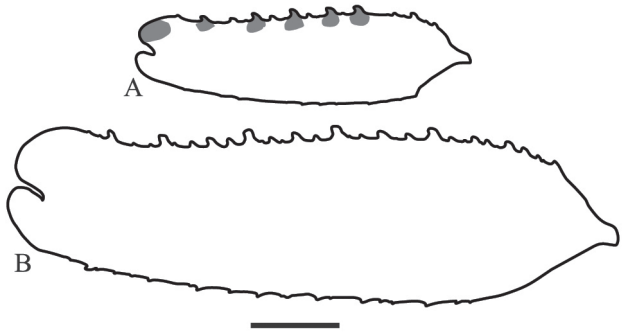

Figure 6. Anterior view of the forecoxa of *Hondurantemna chespiritoi* gen. n. sp. n. **A** male **B** female. Scale bar = 2mm.

tral spines II, III and IV; all discoidal spines black on the anterior surface, the first spine with a dark spot on its base; all the large anteroventral spines black on the inner surface with a dark spot on their bases, a dark spot on the anterior surface above the first two spines; genicular spine developed on both sides of the femora; spur sulcus located in the proximal quarter of the femora; femoral brush extending from the 13th anteroventral spine to beyond the most distal. Foretibiae (Fig. 8A) light brown; T= 12–13AvS/12–13PvS. Foretarsi light brown, with an anterior-basal dark brown spot on the first tarsomere and dark brown anterior-apical spots on tarsomeres I–III.

Wings: Forewings reaching the apex of the abdomen, costal area with a sinuous margin, reticulate veins, opaque green; discoidal area mostly hyaline, with an anterior area smoky green and all the veins and crossveins opaque green. Hindwings shorter

Figure 7. Anterior view of the forefemur of *Hondurantemna chespiritoi* gen. n. sp. n. **A** male **B** female. Scale bar = 2mm.

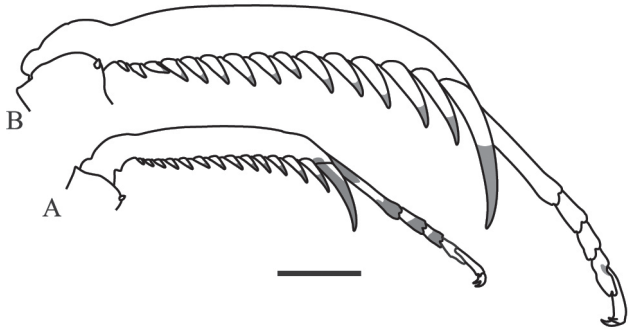

Figure 8. Anterior view of the foretibia of *Hondurantemna chespiritoi* gen. n. sp. n. **A** male **B** female. Scale bar = 2mm.

than the forewings, not reaching the apex of the abdomen; hyaline with brown-red veins and crossveins (Fig. 2A, B).

Meso- and metathoracic legs: Coxa with two strong keels, one anterodorsal and the other posterodorsal. Trochanter with a notch on apical ventral margin, bearing a spine on the articulation with the femora (Fig. 9). Femora smooth except for one keel that runs along the posteroventral margin and originates one single subapical lobe (Fig. 10A); one genicular spine present on the anterior surface. Tibiae smooth, circular in cross-section with two genicular spines. Tarsi with metatarsomeres shorter than other tarsomeres together.

Abdomen: With black spots on the sides of tergites II–V and VII–IX, and a black stripe on tergites VI–VII. Slightly dorsoventrally compressed, with apical lobes on sternites IV–VI, more developed on segments V and VI, the lobes flat against the body (Fig. 11). Supra-anal plate triangular, wider than long, posterior margin arcuate. Cerci elongated but not reaching the apex of subgenital plate, the latter almost as wide as long, flat between styli.

Figure 9. Anterior view of the mesotrochanter and mesofemur of an adult male, arrow showing the spine on the articulation between the trochanter and the femur. Scale bar = 1mm.

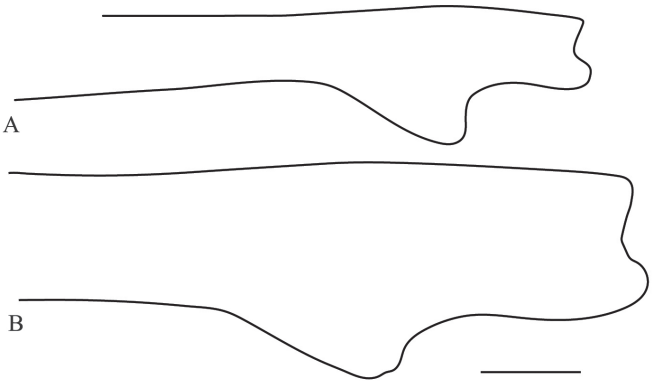

Figure 10. Apex of the hindfemur of *Hondurantemna chespiritoi* gen. n. sp. n. **A** male **B** female. Scale bar = 1mm.

Genitalia: Left phallomere – Sclerite L4B roughly rectangular, longer than wide, left margin projected anteriorly; apofisi falloide (afa) with the anterior part bearing small spines and extremely elongate, projecting dorso-posteriorly, posterior part also elongated, curved towards the left, tapering distally and bearing small spines at the apex; lobo membranoso (loa) elongate, without projections, glabrous; processo apical (paa) elongate, slightly flattened, curved 30° to the left, apex curved anteriorly; sclerite L4A roughly circular, without projections other than the processo distal (pda); pda elongate, curved to the right, uniformly broad, tapering at the distal third, ending in a strongly sclerotized spine (Fig. 12). Right phallomere – roughly triangular, rounded posterior apex; right arm elongate, slender, without projections; anterior process elongate and slender; apodema anterior (aa) oval and slender; processo ventrale (pva) elongate, smooth, apex rounded and well sclerotized; piastra ventrale (pia) elongate, well sclerotized, with "U" shaped striations (Fig. 13).

Female: Medium to large sized. General coloration light green without any spots (Fig. 2C, 2D). Body length: 52.9–53.9; prozona length: 5.1–5.5; metazona length: 10.8–11.2; prothorax width: 6.7–7.0; forewing length: 29.4–31.6; hindwing length: 31.6–31.9; forecoxa length: 12.7–14.0; forecoxa width: 3.0–3.9; forefemur length: 15.6–16.0; forefemur width: 4.3–4.6; foretibia length: 8.5–8.9; mesofemur length: 12.0–12.4; metafemur: length 15.3–15.8; metazona length/prozona length: 2.0–2.1;

Figure 11. Close up of the ventral side of the abdomen of an adult male of *Hondurantemna chespiritoi* gen. n. sp. n., arrows indicate the ventral lobes. Scale bar = 2mm.

pronotum length/width: 2.4–2.5 pronotum length/forecoxa length: 1.2–1.3; forefemur length/width: 3.4–3.6.

Head (Fig. 3B): Vertex straight or slightly sinuous, raised above imaginary line connecting dorsal margins of the eyes, juxtaocular bulges slightly developed. Ocelli small, arranged in the shape of an arc. Scape, pedicel and first half of the flagellomeres of the antennae green, the second half of the flagellomeres dark brown. Lower frons bearing two small central tubercles, except in one of the specimens. Maxillary palps green, the last segment with black spot on the medial surface.

Thorax (Fig. 4B): Supracoxal dilation pronounced and rounded. Margins of the prozona convergent, ciliated with small tubercles, produced in shelves. The posterior third of the metazona with a central keel. The first ventral cervical sclerite in one of the specimens constricted in the middle, in the other two specimens not constricted.

Prothoracic legs: Forecoxae (Fig. 6B) green, dorsal margin bearing six to eight large spines, dark brown on the anterior surface and around the base, apical lobes parallel. Forefemora (Fig. 7B) green, dorsal margin bearing small tubercles, regularly convex, slightly compressed anteroposteriorly; F=4DS/15AvS/5PvS; posteroventral spines with crenulation present after the second spine; the first discoidal spine black on the anterior surface, the other three dark brown; the first anteroventral spine and all the large anteroventral spines dark brown on the anterior surface, the large spines may

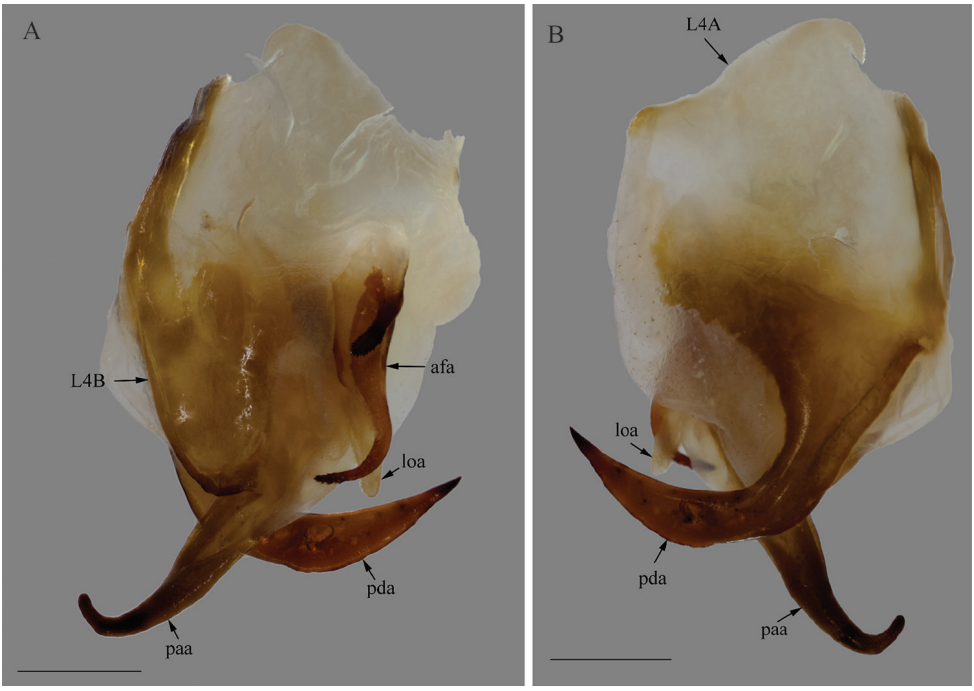

Figure 12. Left phallomere complex of the male genitalia of *Hondurantemna chespiritoi* gen. n. sp. n., afa (apofisi falloide), loa (lobo membranoso), paa (processo apicale), pda (processo distale). **A** dorsal view **B**- ventral view. Scale bar = 1mm.

present a dark spot on their base. Foretibiae (Fig. 8B) green; T= 14AvS/13–14PvS. Foretarsi green, without dark spots.

Wings: Forewings opaque green, costal area almost as wide as the discoidal area, the apex constricted, making the tegmina follow the abdomen contour, with 7–10 branches of the sub-costa vein, crossveins with a reticulate appearance; spot in the center of the discoidal area, composed of an anterior small crescent-shaped brown portion and a posterior round white portion; anal area smoky green. Hindwings as long as the tegmina, reaching the apex of the abdomen, apex of the discoidal area well developed, opaque green, the remainder of the hindwing hyaline (Fig. 2C, D).

Meso- and metathoracic legs: Femora with three keels, one runs along the posteroventral margin and originates one single subapical lobe (Fig. 10B), the second runs along the dorsoposterior margin and the third, less marked, runs along the dorsoanterior margin. Tibiae with two rows of aligned setae. Metatarsi with the metatarsomeres equal or slightly smaller than the other tarsomeres together.

Abdomen: Without black spots. Slightly dorsoventrally compressed, without apical lobes on sternites. Cerci elongated, cercomeres cylindrical, except the last one, which is conical.

Genitalia: Gonoplacs (gl) simple, bearing setae along the dorsal margin and the base, apex bearing a ventral projection. Gonapophysis IX (gp) mostly membranous,

Figure 13. Right phallomere of the male genitalia of *Hondurantemna chespiritoi* gen. n. sp. n., aa (apodema anterior), pia (piastra ventrale), pva (processo ventrale). **A** dorsal view **B** ventral view. Scale bar = 1mm.

with two sclerotized ribbons, one elongate and tapering towards the apex of gp, the other shorter and occupying a medial projection of gp, this projection being rounded; gl and gp of almost the same length. Gonapophysis VIII (ga) bearing setae on the base, on the ventral surface and on the apex, a dorsal groove spanning the two basal thirds, ending in a pointed projection, the apex enlarged ventrally. Basivalvula (bv) with the lateral surface smooth, bearing a central depression, the medial surface rugose, with two projections, one central directed medially, the other more posterior, directed to the base of the ga. Interbasivalvula (ib) well sclerotized, rugose and shaped like a sectioned rhombus. Laterosternal shelves (ls) weakly sclerotized, roughly rhomboid, with short rounded posterior projections (Fig. 14).

Nymphs (unless specified, description applies to male and female nymphs of all instars): General coloration varies from entirely light brown to light brown mottled with dark brown.

Head: Vertex higher than imaginary line connecting dorsal margin of the compound eyes, without lateral keels and a central depression but with the medial ocellar process. In female nymphs, the process becomes increasingly smaller during development, being absent on the instar before the final molt (Fig. 15). Juxtaocular bulges

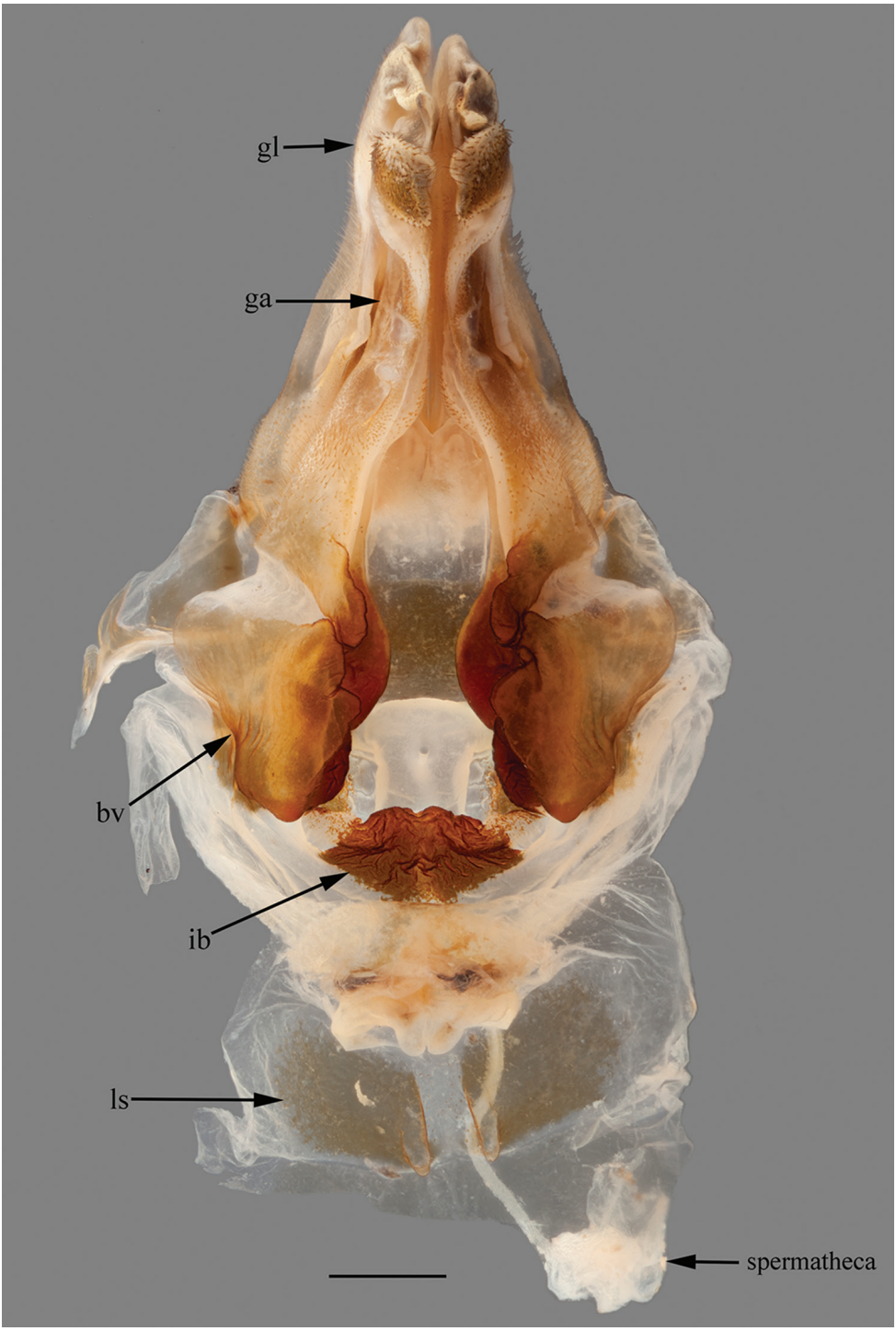

Figure 14. Female genital complex of *Hondurantemna chespiritoi* gen. n. sp. n., bv (basivalvula), ga (gonapophysis VIII), gp (gonoplacs), ib (interbasivalvula), ls (laterosternal shelf). Scale bar = 1mm.

Figure 15. Dorsolateral view of the head of female nymphs of *Hondurantemna chespiritoi* gen. n. sp. n. Black arrows point the medial ocellar process that degenerates during ontogenetic development, grey arrow points the region where the process stood. **A** early instar nymph **B** mid instar nymph **C** late instar nymph. Scale bars = 1mm.

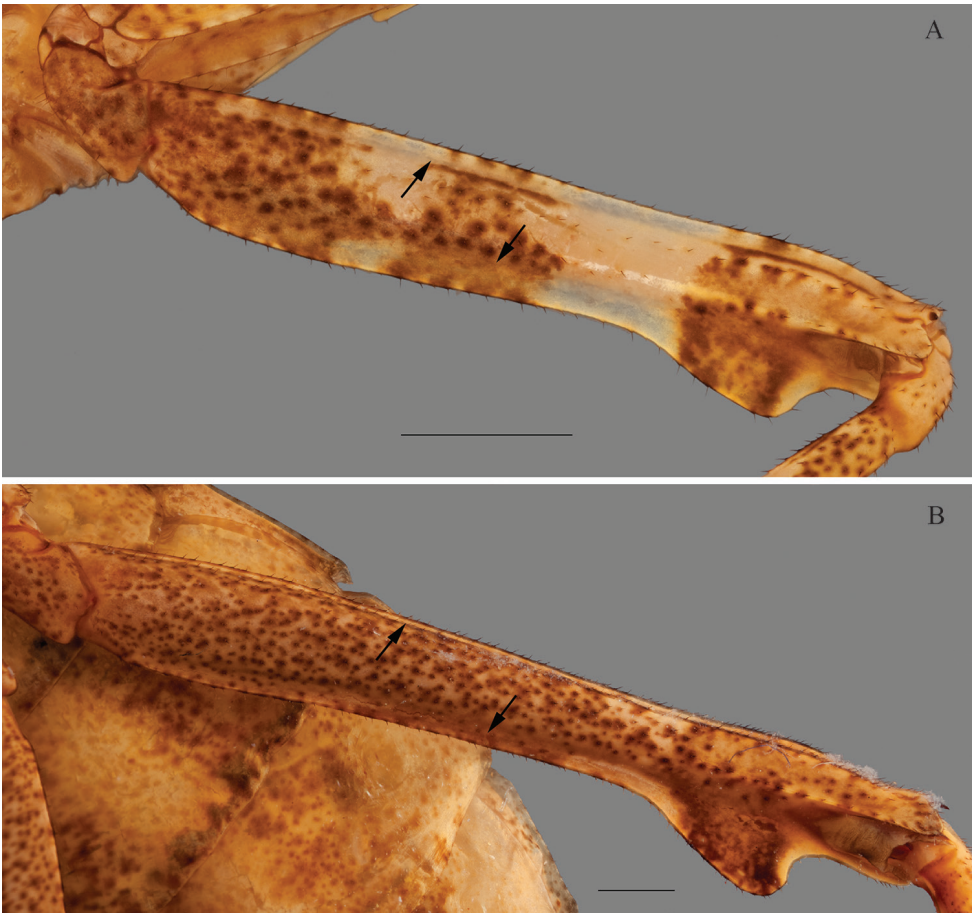

Figure 16. Anteroventral view of the femur of female nymphs of *Hondurantemna chespiritoi* gen. n. sp. n. with arrows showing the end of the expansion of the carina. **A** early instar nymph **B** late instar nymph. Scale bars = 1mm.

Figure 17. Lateral view of the abdomen of a male nymph of *Hondurantemna chespiritoi* gen. n. sp. n., arrows indicate the ventral lobes. Scale bar = 1mm.

slightly developed. Ocelli small, underdeveloped. Lower frons mottled dark brown to completely light brown, with the upper margin not sinuous, tubercles light brown. Clypeus with a transversal keel on the middle, light brown or with the upper half mottled dark brown and the lower half light brown. Maxillary palps with segments I and II black on the medial surface, IV light brown to light brown with a dark brown spot, segment V light brown to completely dark brown. Labial palps segments black on the medial surface or completely dark brown.

Thorax: The first ventral cervical sclerite may be split in two. Metathoracic hearing organ underdeveloped.

Prothoracic legs: Forecoxae light brown except for the lower apical lobe, which is dark brown. Dorsal margin bearing five to six large spines. Forefemora varying, light brown with three dark brown spots on the dorsal area of the anterior surface to dark brown with light brown spots; F=4DS/15AvS/5PvS; males without crenulation between posteroventral spines, females with crenulation; discoidal spines black on the anterior surface, the first spine presenting a dark spot on its base; the first anteroventral spine black, a dark spot on the anterior surface above the first two to four spines; femoral brush extending from the 12th anteroventral spine to the last, a dark spot may be present under the femoral brush. T=13–14AvS/12–14PvS. Foretarsi with an anterior-basal dark brown spot on the first tarsomere and dark brown anterior-apical spots on all tarsomeres.

Meso- and metathoracic legs: Femora with three keels, one runs along the posteroventral margin and originates one single subapical lobe, the second runs along the dorsoposterior margin and the third, less marked, runs along the dorsoanterior margin, the keels on the youngest female nymphs are expanded into shelves (Fig. 16A). Metatarsi with the metatarsomeres equal or slightly smaller than the other tarsomeres together.

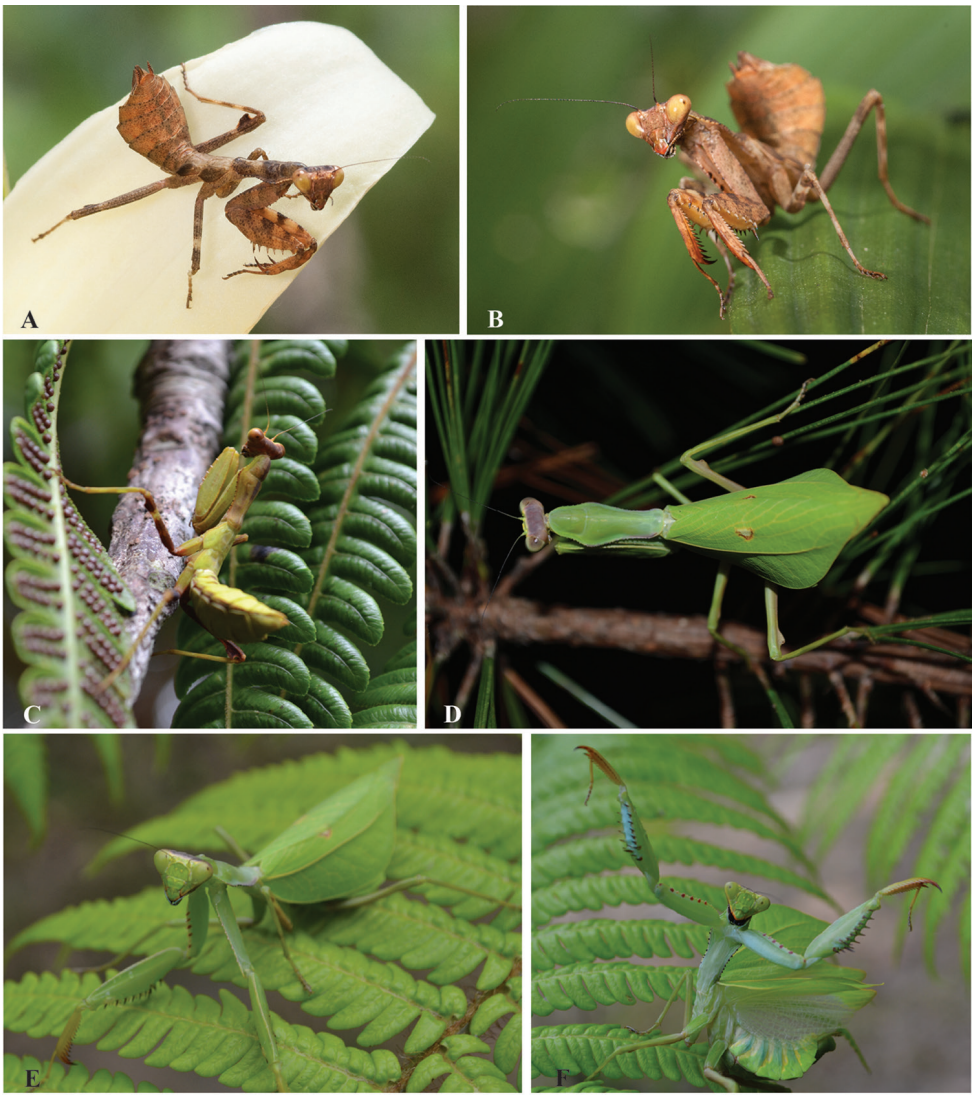

Figure 18. Living specimens of *Hondurantemna chespiritoi*. **A–C** nymph females **D–F** adult females. Female in F is showing deimatic display. Credits: **A–B** by Andrew Snyder, **C–F** by Ethan Staats.

Abdomen: Without black spots or bands on the tergites. Not dorsoventrally compressed, on males apical lobes present on sternites IV–VI, lobe on segment V more developed, the lobes pointing down instead of being held against the body (Fig. 17), on females, lobes absent. Supra-anal plate triangular, almost as long as wide, posterior margin arcuate. Cerci short, styli developed on males, absent on females.

Distribution and habitat. The Lagunas de Montebello National Park, Mexico, from which the holotype was collected, is ca. 6,500 hectares located on the high plains of Chiapas, with an altitude between 1,200 and 1,800 meters above sea level (UNESCO: Lagunas de Monte-

bello http://www.unesco.org/mabdb/br/brdir/directory/biores.asp?mode=gen&code=MEX+37). The predominant vegetation is Central American pine-oak forest over a highly rugged terrain. The Sierra del Merendón, from which the allotype and paratypes were collected, is a mountain range extending from northwest Honduras into southeast Guatemala bordered by the Lempa and Motagua River valleys. The size of the region and its typographical complexity supports four principal forest ecotypes; 1) tropical lowland dry forest, 2) tropical moist forest, 3) montane cloud forest (above 1,200m) and 4) the Bosque Enano or 'dwarf forest' occurring at the highest elevations (above 2,000m). The Parque Nacional Cusuco, surrounding Montaña San Ildefonso (also known as Cerro Jilinco), from which the paratypes were collected, is located within the Sierra del Merendón, and is a protected area of 23,440 hectares (Slater et al. 2011). The vegetation is mostly montane secondary broadleaved forest interspersed with pines, which dominate steeper slopes with palms or bamboo thickets along elevated ridges and tree ferns at lower altitudes (NR, pers. comm.). All nymph specimens were collected in small clearings on low vegetation, usually in the early morning when individuals were found commonly at the apex of herbaceous plants ca. 1-2m tall often hanging upside-down on the underside of a leaf or branch.

Etymology. A name in the genitive case, this species is named after "Chespirito", the screen name of famous late Mexican TV comedian Roberto Gomez Bolaños. Chespirito created and portrayed several characters cherished across Latin America, including "El Chavo del Ocho" and "El Chapulín Colorado", the latter a sort of superhero whose outfit was inspired by grasshoppers or "chapulines".

Antemna rapax Stal, 1877

Figs 19–22

Description. *Genitalia*: Left phallomere – Sclerite L4B roughly oval, much longer than wide, left margin projected anteriorly; afa with the anterior part smooth and short, posterior part elongated, curved towards the right, clubbed and bearing spines at the apex; loa elongate, without projections, glabrous; paa elongate, slightly flattened, curved 30° to the left, apex curved anteriorly; sclerite L4A elongate, without projections other than the pda; pda elongate, curved to the right, uniformly broad, tapering at the apex, ending in a sclerotized spine (Fig. 20). Right phallomere – roughly triangular, rounded posterior apex; right arm elongate, broad, without projections; anterior process elongate and slender; aa oval and slender; pva short, smooth, apex blunt and well sclerotized; pia short, well sclerotized (Fig. 21).

Egg case: somewhat barrel-like, laterally compressed, posteroventral end encircling substrate to which it is attached, ventral surface away from, and forming an angle with the substrate. External wall russet brown in color and rough in appearance. External coating in the form of a whitish layer of frothy material. The coating extends over the emergence area and adjacent dorsal surface of egg case. Exhibiting 40–44 egg chambers whose boundaries are clearly visible as sigmoidal markings along the dorsolateral surface the egg case (external coating might conceal this feature in some specimens), and

Figure 19. Posterior view of the forefemur of a male *Antemna rapax*. Scale bar = 5mm.

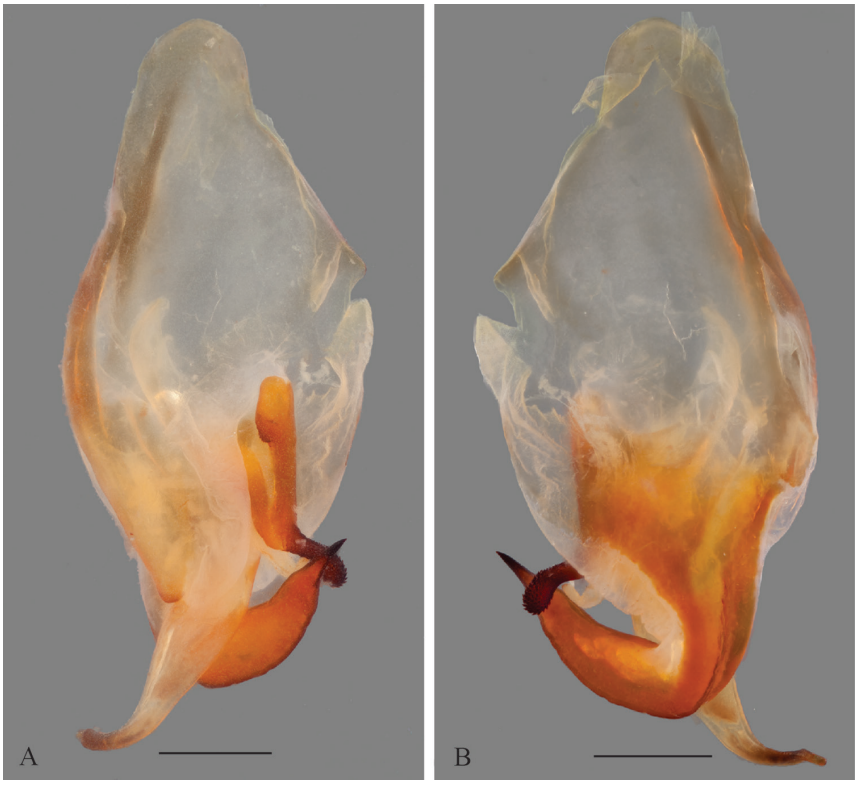

Figure 20. Left phallomere complex of the male genitalia of *Antemna rapax*. **A** dorsal view **B** ventral view. Scale bar = 1mm.

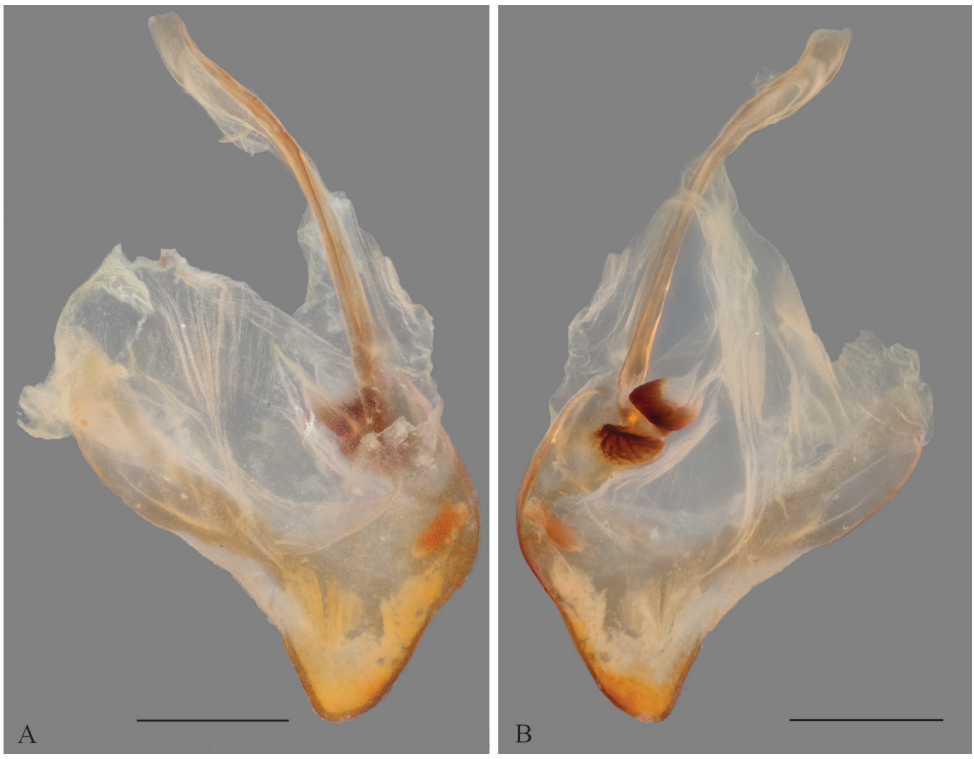

Figure 21. Right phallomere of the male genitalia of *Antemna rapax*. **A** dorsal view **B** ventral view. Scale bar = 1mm.

Figure 22. Lateral habitus of the egg case of *Antemna rapax*. Scale bar = 10mm.

with as many emergence openings as egg cambers, aligned to form two parallel rows along the dorsal margin. Some emergence openings can be seen on a long, relatively straight, and upwardly projected, distal process (Fig. 22). Approximated measurements: length: 35; width: 15; distal process: 22.

Examined material. Male genitalia: Costa Rica, Puntarenas, P. N. Piedras Blancas, Esquinas Lodge (NW – Golfito), 15.v.1996, D. Brzoska, GSMC005332, GD0097 (CLEV). Ootheca: *Antemna rapax*, ANSP.

Discussion

Our molecular phylogenetic analyses confirmed our morphology based hypothesis of a unique taxon, *Hondurantemna chespiritoi*, being placed within the subfamily Antemninae. Our analysis also recovered Antemninae and Stagmomantinae as closely related, with the latter recovered as paraphyletic. This result suggests that current classification does not represent natural lineages, a pattern that repeats across various major lineages within Mantodea (Svenson and Whiting 2009, Svenson et al. 2015, Rivera and Svenson 2016). Our results being incongruent with current classification is due to either: 1) Antemninae is a lineage within Stagmomantinae, or 2) *Stagmomantis* does not represent a monophyletic genus and Stagmomantinae is likely in need of revision. Given the highly complex taxonomic history, and poorly understood relationships within *Stagmomantis* (Maxwell 2014), it is likely that the genus in its current composition is not monophyletic. We recovered a nymphal specimen, listed as *Stagmomantis* 1, as sister to (*Antemna* + *Hondurantemna*) (Fig. 1). *Stagmomantis* 1 was collected in the Dominican Republic and this specimen is likely *Stagmomantis domingensis* (Palisot de Beauvois, 1805), a species placed in a monospecific genus, *Isomantis* Giglio-Tos, 1917, which Terra (1995) synonymized with *Stagmomantis*. The position of *Stagmomantis* 1 in this analysis indicates that it is not a true *Stagmomantis*, adding support to Giglio-Tos' (1917) *Isomantis*. However, a larger taxon and gene sampling within Stagmomantinae is necessary to better understand the organization within Stagmomantinae and its affinities with other lineages.

There are two non-exclusive explanations for differing morphologies in immatures and adults. Adaptive responses to changes in habitat and resource (i.e. prey) use during postembryonic development, e.g. *Acontista* (Salazar 2003) or different selective pressures on adult males and females leading to sexual dimorphism (Slatkin 1984, Shine 1989, Svenson et al. 2016). Praying mantis females are thought to be under selective pressure for increased fitness leading to a more cryptic life style, while males are selected for increased mobility and mate location (Edmunds 1976, Hurd 1999). As the development of immatures progresses, morphological differences between males and females become more accentuated, with nymphs resembling only one of the sexes, e.g. *Pseudopogonogaster* (Rivera et al. 2011).

Nymphs of both sexes and adult males of *Hondurantemna chespiritoi* exhibit cryptic features to resemble small twigs. These include brown coloration, presence of a medial ocellar process (Figs 3A and 15A), mid- and hindlegs bearing lobes (Figs 9, 10, 16), and the presence of abdominal, sternal lobes on males (Figs 11 and 17). All of these characters can have a masquerading effect by disrupting the body outline, making difficult location of individuals in their natural environment (Edmunds and Brunner 1999). In females, as immatures reach adulthood, the medial ocellar process becomes increasingly small and eventually is lost (Fig. 15), the size of the leg lobes relative to the leg decreases (Fig. 16),

coloration changes from brown to green (Fig. 18), and the abdomen swells. This latter feature is particularly pronounced, as the abdomen becomes increasingly enlarged during postembryonic development due to the production of large egg masses (Roy 1999). The enlarged abdomen would be prohibitive to a twig-like cryptic strategy in females, as body outline becomes too distinct and conspicuous. We hypothesize that different selective pressures on females forced their departure from the twig strategy employed as a nymph and drove the reduction of twig-like characters and the evolution of enlarged, leaf-like forewings that could conceal the large abdomen. Their predominately green coloration would additionally enhance the cryptic effect by blending within strongly green vegetation. These features would help adult females resemble leaves as their central cryptic strategy, unlike adult males, which retain the same cryptic strategy of nymphs.

The ontogenetic changes of *Hondurantemna chespiritoi* brings to question the identity of nymphs described by Agudelo et al. (2002). The authors described first instar nymphs, which they assigned to Antemninae based on the morphological similarity of the nymphs with adults of *Antemna rapax*. Those nymphs, despite their general similarity to *A. rapax*, lacked the medial ocellar process and femoral lobes on the mid- and hindlegs, characteristic of *A. rapax*. The authors noted those characters could develop during posterior development, but chose not to assign the nymphs to a genus until early instar nymphs of *A. rapax* or the adult of the nymphs they described became known. The changes during ontogenetic development of *Hondurantemna* described here are comparable to the changes expected if those nymphs are *A. rapax*. However, the *Antemna* ootheca described here is distinct from the description and images provided by Agudelo et al. (2002). Additional material and studies are necessary to confirm the placement of those nymphs within Neotropical Mantodea.

Conclusion

Hondurantemna chespiritoi is exemplary of large, undiscovered insect diversity yet to be documented. Although *H. chespiritoi* has fascinating post-embryonic changes that indicate distinct selective pressures acting on both sexes, the pattern may be more common than we realize, considering the lack of information on nymphal biology. This study shows the importance of describing all life stages and both sexes whenever possible, to prevent misidentification of conspecific specimens and bring to light the natural history of the species.

Acknowledgements

We thank Mr Roger Roy and Dr Philippe Grandcolas from the Muséum National d'Histoire Naturelle and Dr Brian Fisher and Dr Norm Penny from the California Academy of Sciences for the loan of the material. Dr. Jason Weintraub for allowing

JR to access the *Antemna rapax* ootheca and Rick Wherley for imaging it. Operation Wallacea Ltd organized the field expedition to Honduras. Permits for collections in El Parque Nacional Cusuco and export permits were provided by the Instituto Nacional de Conservación y Desarrollo Forestal facilitated by Roberto Downing. We thank Dr Merlijn Jocque, Royal Belgian Institute of Natural Sciences, Aquatic & Terrestrial Ecology (ATECO), Belgium, for support in acquiring immature and adult specimens used to describe the post-embryonic development and to carry out the molecular analyses. We also thank Dr Nicole Gunter and Marlene Harmon for their help with the DNA extraction and PCR, and to Andrew Snyder and Ethan Staats for kindly allowing us to reproduce their photograph of living specimens taken at Cusuco National Park, Honduras. HMR thanks CNPq for the funding through the Brazilian program "Ciências sem Fronteiras", process number 2007002014-6. This project was supported, in part, by the National Science Foundation under the grant DEB-1216309 to GJS. Any opinions, findings and conclusions or recommendations expressed in this material are those of the authors and do not necessarily reflect the views of the National Science Foundation or the Cleveland Museum of Natural History. No conflict of interests exist.

References

Agudelo AA, Chica LM, Morales JE (2002) Observaciones sobre ejemplares eclosionados de una ooteca de Antemninae Terra, 1995. Un Nuevo registro para Colombia (Mantodea: Vatidae: Antemninae). Boletín Científico del Centro de Museos de la Universidad de Caldas 6: 95–102.

Agudelo AA, Rafael JA (2014) Genus *Mantillica* Westwood, 1889: rediscovery and review of the Amazonian "ant-mantis" (Mantodea: Thespidae: Oligonicinae). Entomological Science 17: 400–408. https://doi.org/10.1111/ens.12072

Altekar G, Dwarkadas S, Huelsenbeck JP, Ronquist F (2004) Parallel metropolis-coupled Markov chain Monte Carlo for Bayesian phylogenetic inference. Bioinformatics 20: 407–415. https://doi.org/10.1093/bioinformatics/btg427

Avendaño J, Sarmiento CE (2011) Allometry and ontogeny in *Callibia diana* Stål (Mantodea: Acanthopidae). Neotropical Entomology 40 (4): 462–469. https://doi.org/10.1590/S1519-566X2011000400009

Beier M (1931) Neue und seltene Mantodeen aus dem Zoologischen Staatsinstitut und Zoologischen Museum in Hamburg. Mitteilungen aus dem Zoologischen Staatsinstitut und Zoologischen Museum in Hamburg 45: 1–21.

Beier M (1942) Neue und seltene Mantodeen aus deutschen Museen. Annalen des Naturhistorischen Museums in Wien 52: 126–154.

Beier M (1964) Blattopteroidea, Mantodea. In: Bronns HG (Ed.) Klassen und Ordnungen des Tierreichs. Fünfter Band: Arthropoda. III. Abteilung: Insecta, 6 Buch, 5 Lieferung. Geest & Portig, Leipzig, 849–970.

Brannoch SK, Svenson GJ (2016) A new genus and species (*Cornucollis* gen. n. *masoalensis* sp. n.) of praying mantis from northern Madagascar (Mantodea, Iridopterygidae, Tropidomantinae). Zookeys 556: 65–81. https://doi.org/10.3897/zookeys.556.6906

Burmeister CHC (1838) Mantodea. In: Handbuch der Entomologie. Berlin. v. 2, pt. 2, 517–552.

Edmunds M (1976) The defensive behaviour of Ghanaian praying mantids with a discussion of territoriality. Zoological Journal of the Linnean Society 58: 1–37. https://doi.org/10.1111/j.1096-3642.1976.tb00818.x

Edmunds M, Brunner D (1999) Ethology of defenses against predators. In: Prete FR, Wells H, Wells PH, Hurd LE (Eds) The Praying Mantids. The Johns Hopkins University Press, Baltimore, 276–299.

Ehrmann R (2002) Mantodea: Gottesanbeterinnen der Welt. Natur und Tier – Verlag GmbH, Münster, 519 pp.

Giglio-Tos E (1917) Mantidi esotici. Generi e specie nuove. Bullettino della Società Entomologica Italiana, 48: 43–108.

Giglio-Tos E (1927) Mantidae. In: Das Tierreich. Walter de Gruyter & Co., Berlin und Leipzig, XL+1–707.

Heitzmann-Fontenelle TJ (1969) Revisão dos Mantodea do gênero *Cardioptera* Burmeister (Orthoptera, Mantidae, Vatinae). Studia Entomologica 12(1-4): 245–272.

Huelsenbeck JP, Imennov NS (2002) Geographic origin of human mitochondrial DNA: Accomodating phylogenetic uncertainty and model comparison. Systematic Biology, 51(1): 155–165. https://doi.org/10.1080/106351502753475934

Huelsenbeck JP, Larget B, Miller RE, Ronquist F (2002) Potencial applications and pitfalls of Bayesian inference phylogeny. Systematic Biology 51(5): 673–688. https://doi.org/10.1080/10635150290102366

Hurd LE (1999) Ecology of praying mantids. In: Prete FR, Wells H, Wells PH, Hurd LE (Eds) The Praying Mantids. The Johns Hopkins University Press, Baltimore, 43–60.

Klass KD (1997) The external male genitalia and the phylogeny of Blattaria and Mantodea. Bonner Zoologische Monographien 42: 1–341.

Klass KD (1998) The ovipositor of Dictyoptera (Insecta): homology and ground-plan of the main elements. Zoologischer Anzeiger, 236(2-3): 69–101.

Kumar S, Stecher G, Tamura K (2015) MEGA7: Molecular Evolutionary Genetics Analysis version 7.0 for bigger datasets. Molecular Biology and Evolution. https://doi.org/10.1093/molbev/msw054

Maxwell MR (2014) A synoptic review of the genus *Stagmomantis* (Mantodea: Mantidae). Zootaxa 3765: 501–525. https://doi.org/10.11646/zootaxa.3765.6.1

Palisot de Beauvois AMFJ (1805) Insectes recueillis en Afrique et en Amérique, dans les royaumes d'Oware et de Benin, à Saint-Domingue et dans les États-Unis, pendant les années 1786-1797. Paris, Levrault, Schoell et Cie, 276 pp.

Rambaut A (2012) FigTree v1.4.2. http://tree.bio.ed.ac.uk/software/figtree/

Rehn JAG (1935) The Orthoptera of Costa Rica, Part I: Mantidae. Proceedings of the Academy of Natural Sciences of Philadelphia 87: 167–272.

Rivera J (2010a) *Chromatophotina*, a remarkable new genus of praying mantid from the Neotropical Region and its two new species (Mantodea: Mantidae: Photinainae). Zootaxa 2415: 22–32.

Rivera J (2010b) A historical review of praying mantis taxonomy and systematics in the Neotropical Region: State of knowledge and recent advances (Insecta: Mantodea). Zootaxa, 2638: 44–64.

Rivera J, Svenson GJ (2016) The Neotropical 'polymorphic earless praying mantises' – Part I: molecular phylogeny and revised higher-level systematics (Insecta: Mantodea, Acanthopoidea). Systematic Entomology 41(3): 607–649. https://doi.org/10.1111/syen.12178

Rivera J, Yagui H, Ehrmann R (2011) Mantids in the mist – Taxonomy of the Andean genus *Pseudopogonogaster* Beier, 1942, a cloud forest specialist, with notes on its biogeography and ecology (Mantodea: Thespidae: Miopteryginae). Insect Systematics and Evolution 42: 313–335. https://doi.org/10.1163/187631211X595056

Rodrigues HM, Cancello EM (2016) Taxonomic revision of *Stagmatoptera* Burmeister, 1838 (Mantodea, Mantidae, Stagmatopterinae). Zootaxa 4183(1): 1–78. https://doi.org/10.11646/Zootaxa.4183.1.1

Ronquist F, Teslenko M, van der Mark P, Ayres DL, Darling A, Höhna S, Larget B, Liu L, Suchard MA, Huelsenbeck JP (2012) Mr.Bayes 3.2: Efficient Bayesian Phylogenetic Inference and Model Choice across a Large Model Space. Systematic Biology 61(3):539–542. https://doi.org/10.1093/sysbio/sys029

Roy R (1999) Morphology and Taxonomy. In: Prete FR, Wells H, Wells PH, Hurd LE (Eds) The Praying Mantids. The Johns Hopkins University Press, Baltimore, 19–40.

Salazar JA (2003) On some mimetic resemblances of *Acontista multicolor* Saussure, 1870 in Colombia (Insecta: Mantodea). Lambillionea 53: 649–654.

Saussure H (1869) Essai d'un système des Mantides. Mittheilungen der Schweizerischen Gesellschaft 3(2): 49–73.

Saussure H (1871) Mélanges orthoptérologiques (troisième fascicule). Mémoires de la Société de Physyque et d'Histoire Naturelle de Genève 21: 1–215.

Saussure H (1892) Orthoptera Centrali-Americana — Famille des Mantidis. Societas Entomologica 7(16): 121–124.

Saussure H, Zehntner L (1894) Familie Mantidae. In: Biologia Centrali-Americana. — Insecta, Orthoptera, Mantidae, 1123–197.

Shine R (1989) Ecological causes for the evolution of sexual dimorphism: A review of the evidence. The Quarterly Review of Biology 64(4): 419–461. https://doi.org/10.1086/416458

Slater K, Burdekin O, Long P (2011) Cusuco National Park — 2011 status report. 17pp. http://opwall.com/wp-content/uploads/2011-Cusuco-Status-Report.pdf

Slatkin M (1984) Ecological causes of sexual dimorphism. Evolution 38(3): 622–630. https://doi.org/10.2307/2408711

Stamatakis A (2014) RAxML version 8: a tool for phylogenetic analysis and post-analysis of large phylogenies. Bioinformatics 30: 1312–1313. https://doi.org/10.1093/bioinformatics/btu033

Stål C (1877) Systema Mantodeorum. Essai d'une systématisation nouvelle des Mantodées. Bihang till Kongl. Svenska vetenskaps-akademiens handlingar 4(10): 1–91.

Svenson GJ (2014) Revision of the Neotropical bark mantis genus *Liturgusa* Saussure, 1869 (Insecta, Mantodea, Liturgusini). Zookeys 390: 1–214. https://doi.org/10.3897/Zookeys.390.6661

Svenson GJ, Brannoch SK, Rodrigues HM, O'Hanlon J, Wieland F (2016) Selection for predation, not female fecundity, explains sexual size dimorphism in the orchid mantises. Scientific Reports 6, 37753. https://doi.org/10.1038/srep37753

Svenson GJ, Hardy NB, Cahill Wightman HM, Wieland F (2015) Of flowers and twigs: phylogenetic revision of the plant-mimicking praying mantises (Mantodea: Empusidae and Hymenopodidae) with a new suprageneric classification. Systematic Entomology, 40 (4): 789–834. https://doi.org/10.1111/syen.12134

Svenson GJ, Medellin C, Sarmiento CE (2016) Re-evolution of a morphological precursor of crypsis investment in the newly revised horned praying mantises (Insecta, Mantodea, Vatinae). Systematic Entomology 41: 216–255. https://doi.org/10.1111/syen.12151

Svenson GJ, Whiting MF (2004) Phylogeny of Mantodea based on molecular data: evolution of a charismatic predator. Systematic Entomology 29(3): 359–370. https://doi.org/10.1111/j.0307-6970.2004.00240.x

Svenson GJ, Whiting MF (2009) Reconstructing the origins of praying mantises (Dictyoptera, Mantodea): the roles of Gondwanan vicariance and morphological convergence. Cladistics 25(5): 468–514. https://doi.org/10.1111/j.1096-0031.2009.00263.x

Terra PS (1980) Ontogênese da perna raptória em "louva-a-deus" (Mantodea): Um estudo comparativo de alometria. Revista Brasileira de Entomologia 24(2): 117–122.

Terra PS (1982) Novos gêneros e novas espécies de louva-a-deus da América do Sul (Mantodea, Mantidae). Revista Brasileira de Zoologia 26(3/4): 327–332.

Terra PS (1995) Revisão sistemática dos gêneros de louva-a-deus da região Neotropical (Mantodea). Revista Brasileira de Entomologia 39(1): 13–94

Westwood JO (1889) Revisio Insectorum – Familiae Mantidarum, speciebus novis aut minus cognitis descriptis et delineatis. London, Gurney and Jackson, 53+IV pp + XIV pl.

Wieland F (2013) The phylogenetic system of Mantodea (Insecta: Dictyoptera). Species, Phylogeny and Evolution 3: 3–222.

Wood-Mason J (1890) Description of *Triaenocorypha dohertii*, the type of a new genus and species of Mantodea. The Annals and Magazine of Natural History, including Zoology, Botany and Geology, 6th series, 5: 439–440.

Yager DD, Svenson GJ (2008) Patterns of praying mantis auditory system evolution based on morphological, molecular, neurophysiological and behavioural data. Biological Journal of the Linnean Society 94: 541–568. https://doi.org/10.1111/j.1095-8312.2008.00996.x

ZooKeys 680: 105–150 (2017)
doi: 10.3897/zookeys.680.12135
http://zookeys.pensoft.net

RESEARCH ARTICLE

A peer-reviewed open-access journal
ZooKeys
Launched to accelerate biodiversity research

Demosponge diversity from North Sulawesi, with the description of six new species

Barbara Calcinai[1], Azzurra Bastari[1], Giorgio Bavestrello[2], Marco Bertolino[2], Santiago Bueno Horcajadas[3], Maurizio Pansini[2], Daisy M. Makapedua[4], Carlo Cerrano[1]

1 *Dipartimento di Scienze della Vita e dell'Ambiente, Università Politecnica delle Marche, Via Brecce Bianche, 60131, Ancona, UO Conisma, Italy* **2** *Dipartimento di Scienze della Terra, dell'Ambiente e della Vita, Università degli Studi di Genova, Corso Europa, 26, 16132, Genova, UO Conisma, Italy* **3** *Pharma Mar S.A.U. Av. de los Reyes, 1, 28770 Colmenar Viejo, Community of Madrid, Spain* **4** *University of Sam Ratulangi, Jl. Kampus Unsrat 95115, Manado, Indonesia*

Corresponding author: *Barbara Calcinai* (b.calcinai@univpm.it)

Academic editor: *M. Pfannkuchen* | Received 6 February 2017 | Accepted 28 April 2017 | Published 20 June 2017

http://zoobank.org/657770F9-FCFA-4D72-BB08-AFAF7371B1BA

Citation: Calcinai B, Bastari A, Bavestrello G, Bertolino M, Horcajadas SB, Pansini M, Makapedua DM, Cerrano C (2017) Demosponge diversity from North Sulawesi, with the description of six new species. ZooKeys 680: 105–150. https://doi.org/10.3897/zookeys.680.12135

Abstract

Sponges are key components of the benthic assemblages and play an important functional role in many ecosystems, especially in coral reefs. The Indonesian coral reefs, located within the so-called "coral triangle", are among the richest in the world. However, the knowledge of the diversity of sponges and several other marine taxa is far from being complete in the area. In spite of this great biodiversity, most of the information on Indonesian sponges is scattered in old and fragmented literature and comprehensive data about their diversity are still lacking. In this paper, we report the presence of 94 species recorded during different research campaigns mainly from the Marine Park of Bunaken, North Sulawesi. Six species are new for science and seven represent new records for the area. Several others are very poorly known species, sometimes recorded for the second time after their description. For most species, besides field data and detailed descriptions, pictures *in vivo* are included. Moreover, two new symbiotic sponge associations are described.

This work aims to increase the basic knowledge of Indonesian sponge diversity as a prerequisite for monitoring and conservation of this valuable taxon.

Keywords
associations, diversity, Indonesia, new species, Porifera

Introduction

Baseline knowledge on species and assemblages is indispensable for monitoring the more and more frequent changes in biodiversity (Bell and Smith 2004). Sponges are often a key component of the benthic fauna for their abundance, dominance, wide pattern of interactions they develop (e.g. Cerrano et al. 2006, Wulff 2006, Wulff 2012, Bell 2008), longevity (Hogg et al. 2010) and role in the functioning of several ecosystems (Scheffers et al. 2010, de Goeij et al. 2013). Unfortunately, also due to the lack of taxonomic expertise, sponges are usually not considered in monitoring surveys and conservation programs (Bell and Smith 2004, Bell 2008).

The Indonesian archipelago, with its large number of islands (more than 17,000), hosts various and diversified habitats supporting high levels of diversity and endemism in marine life; this exceptional biodiversity is also the result of its geographic location and geological history (Tomascik et al. 1997). However, the impressive diversity of several marine taxa, such as sponges, corals, molluscs, ascidians etc., is still poorly known (Tomascik et al. 1997).

The knowledge on Indonesian sponges is mainly based on old expedition reports (such as Snellius II and Siboga expeditions) and on fragmented, recent studies including a few genera revisions (Hofman and van Soest 1995, de Voogd and van Soest 2002, Sim-Smith and Kelly 2011, Becking 2013) and new species descriptions (Azzini et al. 2008, de Weerdt and van Soest 2001, de Voogd 2003, de Voogd 2004, Calcinai et al. 2005a, Calcinai et al. 2006, Calcinai et al. 2007, de Voogd and van Soest 2007, de Voogd et al. 2008, Calcinai et al. 2013, Muricy 2011); for a more complete list, see also van Soest (1990). A few other papers concerning sponge ecology, distribution and symbiosis (Bavestrello et al. 2002, Bell and Smith 2004, Calcinai et al. 2004, Cerrano et al. 2006, de Voogd and Cleary 2008, de Voogd et al. 2009, Powell et al. 2014, Rossi et al. 2015) have been published.

In this paper, a list of 94 sponge species collected during several research expeditions conducted in this area is reported, and six new species are described from the North Sulawesi peninsula. Moreover, two new symbiotic associations are documented.

The aim of this study is to improve the knowledge on sponge diversity and distribution of North Sulawesi, a prerequisite for any study of monitoring and conservation of tropical coral reef assemblages.

Materials and methods

The Bunaken Park is located in the northwest part of Sulawesi Island, Indonesia, in the coral triangle. It covers a total surface area of more than 89,000 hectares and includes five principal islands (Bunaken, Manado Tua, Mantehage, Nain and Siladen) (Fig. 1). Reefs can show different degrees of conservation (Fava et al. 2009) due to different

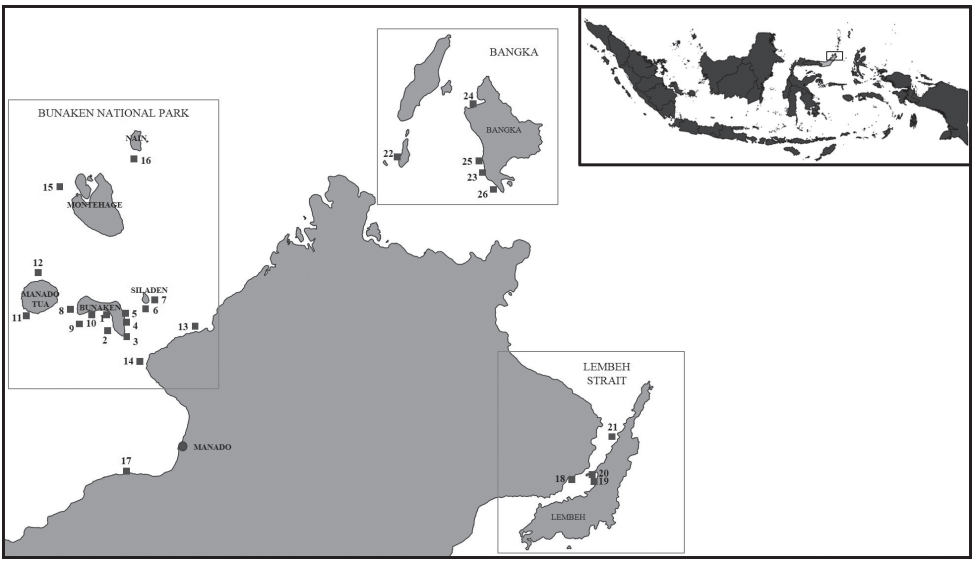

Figure 1. Locality map of North Sulawesi area showing the sponge collection sites. Black squares are the sampling sites. Key: **1** Liang **2** Lekuan II **3** Depan Kampung **4** Pangalisan **5** Timur **6** Siladen Jetty **7** Siladen Barat **8** Raymond's Point **9** Fukui **10** Aluang Banua **11** Bualo **12** Tanjung Kopi **13** Tiwoho **14** Tanjung Pisok **15** Barracuda Point **16** Nain **17** Mapia Resort **18** Police Pier **19** Lembeh **20** Pintu Kolada **21** Angel's window **22** Gangga Jetty **23** Bangka 2 **24** Bangka2 **25** Busa Bora **26** Yellow Coco.

anthropogenic impacts. The Lembeh Strait is a long, narrow, calm, and sheltered channel between the eastern coast of Sulawesi and the island of Lembeh that protects Bitung's natural harbour. Bangka Island is an island of 4,778 hectares situated north of Manado, on the northeast tip of Sulawesi. Around the island, there are phanerogam meadows and mangrove forests as well as a reef with different steepness degrees (Calcinai et al. 2016).

The studied collection is the result of several expeditions performed in different years (August 1999, March 2000, May 2001, May 2002, September 2003, June 2004, January 2005) in the framework of bilateral agreements between Italy and Indonesia, focused on the exchange of researchers between the Italian Universities of Genoa and Polytechnic of Marche and the University of Sam Ratulangi (Manado, North Sulawesi). In May 2005, a further expedition in collaboration with the biopharmaceutical company Pharma Mar (http://www.pharmamar.com) was organised. In 2011, an expedition at Bangka Island in the frame of a joint project between Sam Ratulangi University and the Polytechnic University of Marche allowed to characterise the diversity of Porifera inside two small mangrove forests. Table 1 shows a list of all species and their distributions. In the Suppl. material 1, we included underwater photos of the species.

Spicule preparations, for optical and scanning electron microscopy (SEM), were made according to Rützler (1974). Spicule dimensions were obtained by measuring 30 spicules per type. Maximal, minimal, and average sizes, ± standard deviation (length and width) are given. The skeletal architecture, under light and scanning electron microscope (SEM), was studied on hand-cut sections of sponge portions, following Hooper (2000). The SEM analysis was conducted using a Philips XL 20 SEM.

Table 1. List of the families and species of sponges collected during several research expeditions in the North Sulawesi peninsula, with sampling sites and depth ranges. Numbers in bold (1–26) match the sampling sites showed in Fig. 1. The samples, here indicated in bold, are showed in Suppl. material 1, Figure 11. The asterisk (*) marks the species considered as new records for the Indonesian area.

Family	Specie	Samples	Figure	Notes	1	2	3	4	5	6	7	8	9	10	11	12	13	14	15	16	17	18	19	20	21	22	23	24	25	26	Depth (m)
Plakinidae	*Plakortis lita* de Laubenfels, 1954	**PH33**, BU88	Figs 1–1	Short description and discussion in Chianese et al. 2012	-	√	-	√	-	-	-	-	-	-	-	-	-	-	-	-	-	-	-	-	-	-	-	-	-	-	20–24
Suberitidae	*Aaptos lobata* sp. n.	BU82, BU580, **PH1, PH27,** INDO079, INDO278, INDO339, INDO336	Fig. 2	This work	-	√	-	-	√	-	-	-	-	√	√	√	-	√	-	-	-	-	-	-	-	-	-	-	-	-	16.5–20
Halichondriidae	*Amorphinopsis excavans* Carter, 1887	MA1, **MA20**	Figs 11–2		-	-	-	-	-	-	-	-	-	-	-	-	-	-	-	-	-	-	-	-	-	-	√	√	-	-	0–1
Halichondriidae	*Ciocalypta tyleri* Bowerbank, 1873	**MA5**	Figs 11–3		-	-	-	-	-	-	-	-	-	-	-	-	-	-	-	-	-	-	-	-	-	-	√	-	-	-	0–1
Halichondriidae	*Topsentia halichondrioides* (Dendy, 1905)	**MA18**	Figs 11–4		-	-	-	-	-	-	-	-	-	-	-	-	-	-	-	-	-	-	-	-	-	-	-	√	-	-	0–1
Tethyidae	*Tethytimea tylota* (Hentschel, 1912)	BU98, BU289, BU533, BU545, **BU562**	Fig. 3	This work	-	√	-	-	-	-	√	-	-	√	-	-	-	-	-	-	-	-	-	-	-	-	-	-	-	-	5–20
Clionaidae	*Cliona albimarginata* Calcinai, Bavestrello & Cerrano, 2005	BU50, BU237		See picture in Calcinai et al. 2005a	-	-	-	-	-	-	-	-	-	-	-	-	-	-	√	-	-	-	-	-	-	-	-	-	-	-	7–25
Clionaidae	*Cliona favus* Calcinai, Bavestrello & Cerrano, 2005	BU11, BU54, BU473		See picture in Calcinai et al. 2005a	-	-	-	-	-	-	-	-	√	-	-	-	-	-	√	-	-	-	-	-	-	-	-	-	-	-	5–10

Family	Specie	Samples	Figure	Notes	1	2	3	4	5	6	7	8	9	10	11	12	13	14	15	16	17	18	19	20	21	22	23	24	25	26	Depth (m)
Clionaidae	*Cliona liangae* Calcinai, Bavestrello & Cerrano, 2005	MG1 bis		See picture in Calcinai et al. 2005a	√	-	-	-	-	-	-	-	-	-	-	-	-	-	-	-	-	-	-	-	-	-	-	-	-	Tidal zone
Clionaidae	*Cliona jullieni* Topsent, 1891	BU18, BU52, **BU58**, BU61, BU62, BU121, BU268	Fig. 11–5		-	√	-	-	-	-	-	√	√	-	-	-	-	√	√	-	-	-	-	-	-	-	-	-	-	3–17
Clionaidae	*Cliona mucronata* Sollas, 1878	**BU16bis,** BU79, BU501,	Fig. 11–6	*In situ* photo not available	-	√	-	-	-	-	-	-	√	-	-	-	-	√	-	-	-	-	-	-	-	-	-	-	-	5–21
Clionaidae	*Cliona orientalis* Thiele, 1900	BU73, **BU319**, BU119	Fig. 11–7		-	-	√	-	-	-	-	-	-	√	-	-	-	-	-	-	-	-	-	-	-	-	-	-	-	5–25
Clionaidae	*Cliona schmidtii* (Ridley, 1881)	BU56, **BU58**, BU75, BU83bis, BU255, BU264, BU322	Fig. 11–8		-	√	√	-	-	-	√	-	-	-	-	-	-	-	√	-	-	-	-	-	-	-	-	-	-	10–21
Clionaidae	*Cliona utricularis* Bavestrello & Cerrano, 2005	**BU13**, BU31, BU60, BU115, BU136, BU145, BU474, BU482, BU500, BU505	Fig. 11–9	*In situ* photo not available	√	-	-	-	√	-	-	√	-	-	-	-	-	√	√	-	-	√	-	-	-	-	-	-	-	5–16
Clionaidae	*Cliothosa aurivilli* (Lindgren, 1897)	MG1, **BU72**	Fig. 11–10	*In situ* photo not available	-	-	√	√	-	-	-	-	-	-	-	-	-	-	-	-	-	-	-	-	-	-	-	-	-	-	0–1

Family	Specie	Samples	Figure	Notes	1	2	3	4	5	6	7	8	9	10	11	12	13	14	15	16	17	18	19	20	21	22	23	24	25	26	Depth (m)
Clionaidae	*Cliothosa hancocki* (Topsent, 1888)	**BU17**, BU120	Fig. 1–11	*In situ* photo not available	-	-	-	-	-	-	-	√	√	-	-	-	-	-	-	-	-	-	-	-	-	-	-	-	5
Clionaidae	*Pione carpenteri* (Hancock, 1867)	**BU74**	Fig. 1–12	*In situ* photo not available	-	√	-	-	-	-	-	-	-	-	-	-	-	-	-	-	-	-	-	-	-	-	-	-	9
Clionaidae	*Spheciospongia solida* (Ridley & Dendy, 1886)	BU45, BU228, BU576, **PH24**	Fig. 1–13		-	-	√	√	-	-	-	-	-	√	-	-	-	-	-	-	-	√	-	-	-	-	-	-	-	10–25
Clionaidae	*Spheciospongia vagabunda* (Ridley, 1884)	BU44, **BU64**, BU296	Fig. 1–14	*In situ* photo not available	-	-	√	-	-	-	-	-	-	-	-	-	-	√	-	-	-	-	-	-	-	-	-	-	-	5–20
Spirastrellidae	*Spirastrella pachyspira* Lévi, 1958 *	**BU78**	Fig. 1–2	See Suppl. material 2	-	√	-	-	-	-	-	-	-	-	-	-	-	-	-	-	-	-	-	-	-	-	-	-	-	25
Acarnidae	*Zyzzya fuliginosa* (Carter, 1879)	**BU53**, BU78, BU260, BU265, BU266	Fig. 1–15		-	√	-	-	-	-	-	-	-	-	-	-	-	-	√	-	-	-	-	-	-	-	-	-	-	10–30
Chondropsidae	*Chondropsis subtilis* Calcinai, Bavestrello, Bertolino, Pica, Wagner & Cerrano, 2013	Bugor504	See picture in Calcinai et al. 2013		-	-	-	-	-	√	-	-	-	-	√	-	-	-	-	-	-	-	-	-	-	-	-	-	-	10–15
Crambeidae	*Monanchora enigmatica* (Burton & Rao, 1932)	**PH45**, Bugor410	Fig. 1–16		-	-	-	-	√	√	-	-	-	-	-	-	-	-	-	-	-	-	-	-	-	-	-	-	-	20–27
Desmacididae	*Desmapsamma vervoorti* van Soest, 1998	**BU222**, BU410, BU411, Bugor410, Carramba1, Carramba2, Carramba6, Carramba8, BA4	Fig. 1–17		-	-	-	-	-	√	-	-	-	-	-	-	-	-	-	-	-	-	√	√	-	-	-	-	-	-	1–27

Family	Specie	Samples	Figure	Notes	1	2	3	4	5	6	7	8	9	10	11	12	13	14	15	16	17	18	19	20	21	22	23	24	25	26	Depth (m)
Hymedesmiidae	*Hymedesmia* (*Hymedesmia*) *spinata* Calcinai, Bavestrello, Bertolino, Pica, Wagner & Cerrano, 2013	Bugor513, Bugor311, Bugor309, Bugor-410bis2	See picture in Calcinai et al. 2013		-	-	-	-	-	√	√	-	-	-	-	-	-	-	-	-	-	-	-	-	-	-	-	-	-	23–26
Hymedesmiidae	*Hymedesmia* (*Stylopus*) *perlucida* Calcinai, Bavestrello, Bertolino, Pica, Wagner & Cerrano, 2013	Bugor511	See picture in Calcinai et al., 2013		-	-	-	-	-	-	-	-	-	-	-	-	-	-	-	√	-	-	-	-	-	-	-	-	-	-	17
Isodictyidae	*Coelocarteria agglomerans* Azzini, Calcinai & Pansini, 2007	BU15, BU37, BU38, BU48, BU132, BU219, BU329, BU616, BU644 **PH51**	Fig. 1–18		-	-	-	-	-	√	-	√	-	√	-	-	√	-	-	-	-	-	-	-	√	-	-	-	-	-	20–38
Microcionidae	*Clathria* (*Thalysias*) *cervicornis* (Thiele, 1903)	**PH48**	Fig. 1–19		-	-	-	-	√	-	-	-	-	-	-	-	-	-	-	-	-	-	-	-	-	-	-	-	-	-	20
Microcionidae	*Clathria* (*Thalysias*) *mutabilis* (Topsent, 1897)	**PH19**	Fig. 1–20		-	-	-	-	√	-	-	-	-	-	-	-	-	-	-	-	-	-	-	-	-	-	-	-	-	-	20
Mycalidae	*Mycale* (*Aegogropila*) *furcata* Calcinai, Bavestrello, Bertolino, Pica, Wagner & Cerrano, 2013	Bugor307, Bugor332	See picture in Calcinai et al. 2013		-	-	-	-	-	√	√	-	-	-	-	-	-	-	-	-	-	-	-	-	-	-	-	-	-	-	Depth not stated
Mycalidae	*Mycale* (*Mycale*) *corallina* Calcinai, Cerrano & Bavestrello, 2016	BU485, BU534, BU449	See picture in Calcinai et al. 2006	See Suppl. material 2	-	-	-	-	-	√	-	-	-	-	√	-	-	-	-	-	-	-	-	-	-	-	-	-	-	-	17–20

Family	Specie	Samples	Figure	Notes	1	2	3	4	5	6	7	8	9	10	11	12	13	14	15	16	17	18	19	20	21	22	23	24	25	26	Depth (m)
Podospongiidae	*Podospongia colini* Sim-Smith & Kelly, 2011		Fig. 1–21	Not available data; *in situ* photo not available	-	-	-	-	-	-	-	-	-	-	-	-	-	-	-	-	-	-	-	-	-	-	-	-	-	-	Depth not stated
Tedaniidae	*Tedania* (*Tedania*) *brevispiculata* Thiele, 1903	**MA21**	Fig. 1–22	*In situ* photo not available	-	-	-	-	-	-	-	-	-	-	-	-	-	-	-	-	-	-	-	-	-	-	√	-	-	1
Tedaniidae	*Tedania* (*Tedania*) *coralliophila* Thiele, 1903	**BU582**	Fig. 1–23		-	-	-	-	-	-	-	-	-	√	-	-	-	-	-	-	-	-	-	-	-	-	-	-	-	-	11
Tedaniidae	*Tedania* (*Tedania*) *dirhaphis* Hentschel, 1912	**PH52**	Fig. 1–24		-	-	-	-	-	-	-	-	-	-	-	-	√	-	-	-	-	-	-	-	-	-	-	-	-	-	20
Agelasidae	*Agelas ceylonica* Dendy, 1905	BU1, BU3, **PH54**	Fig. 1–25		-	-	-	-	-	-	-	-	-	√	-	-	√	-	-	-	-	-	-	-	-	-	-	-	-	-	20–30
Agelasidae	*Agelas mauritiana* (Carter, 1883)	BU234, **BU570**	Fig. 1–26		-	-	-	-	-	-	-	-	-	√	-	-	-	-	-	-	-	-	-	-	-	-	-	-	-	-	23–35
Agelasidae	*Agelas nakamurai* Hoshino, 1985	BU583, **PH38**	Fig. 1–27		-	-	-	-	√	-	-	-	-	√	-	-	-	-	-	-	-	-	-	-	-	-	-	-	-	-	12–20
Tetillidae	*Cinachyrella australiensis* (Carter, 1886)	**BU233**, BU308, BU316	Fig. 1–28		-	-	-	-	-	-	-	-	-	√	√	-	-	-	-	-	-	-	-	-	-	-	-	-	-	-	5–13
Tetillidae	*Tetilla ridleyi* Sollas, 1888	**MA17**	Fig. 1–29	*In situ* photo not available	-	-	-	-	-	-	-	-	-	-	-	-	-	-	-	-	-	-	-	-	-	-	√	-	-	-	1
Ancorinidae	*Dercitus* (*Stoeba*) *bangkae* (Calcinai, Bastari, Makapedua, Cerrano, 2016)	**MA16**	Fig. 1–30	*In situ* photo not available	-	-	-	-	-	-	-	-	-	-	-	-	-	-	-	-	-	-	-	-	-	-	√	-	-	-	1
Ancorinidae	*Rhabdastrella distincta* (Thiele, 1900)	**BU560**, **BU575**	Fig. 5, Fig. 6	This work	-	-	-	-	-	-	-	-	-	√	√	-	-	-	-	-	-	-	-	-	-	-	-	-	-	-	Max. depth 30
Ancorinidae	*Rhabdastrella globostellata* (Carter, 1883)	BU288, **BU593**, PH29	Fig. 1–31		-	√	-	-	√	-	-	-	-	-	-	-	-	-	-	-	-	-	-	-	-	-	-	-	-	-	20–23
Ancorinidae	*Stelletta clavosa* Ridley, 1884	**BU543**	Fig. 1–32	See Suppl. material 2	-	√	-	-	-	-	√	√	-	-	-	-	-	-	-	-	-	-	-	-	-	-	-	-	-	-	5–30

Family	Specie	Samples	Figure	Notes	1	2	3	4	5	6	7	8	9	10	11	12	13	14	15	16	17	18	19	20	21	22	23	24	25	26	Depth (m)
Ancorinidae	*Stelletta tethytimeata* sp. n.	BU98, BU289, **BU533**, BU545, BU562	Fig. 4	This work	-	√	-	-	-	-	√	-	-	√	-	-	-	-	-	-	-	-	-	-	-	-	-	-	-	5–20
Geodiidae	*Melophlus sarasinorum* Thiele, 1899	**PH56**	Fig. 1–33	See Suppl. material 2	-	-	-	-	-	-	-	-	-	-	-	-	√	-	-	-	-	-	-	-	-	-	-	-	-	20
Theonellidae	*Theonella cylindrica* Wilson, 1925	**BU568**	Fig. 1–34		-	-	-	-	-	-	-	-	-	√	-	-	-	-	-	-	-	-	-	-	-	-	-	-	-	40
Theonellidae	*Theonella mirabilis* (de Laubenfels, 1954)	**BU585**	Fig. 1–35	See Suppl. material 2	-	-	-	-	-	-	-	-	-	√	-	-	-	-	-	-	-	-	-	-	-	-	-	-	-	11
Theonellidae	*Theonella swinhoei* Gray, 1868	BU96, PH12, **PH60**	Fig. 1–36		-	√	-	-	√	-	-	-	-	-	-	-	√	-	-	-	-	-	-	-	-	-	-	-	-	20–25
Thoosidae	*Thoosa letellieri* Topsent, 1891	MTR	Fig. 15	See Suppl. material 2	-	-	-	√	-	-	-	-	-	-	-	-	-	-	-	-	-	-	-	-	-	-	-	-	-	Depth not stated
Biemnidae	*Biemna fortis* (Topsent, 1897)	**BU143,** MA11	Fig. 1–37	*In situ* photo not available	-	-	-	-	-	-	-	-	-	-	-	-	-	-	-	-	-	-	√	-	-	-	√	-	-	-	1–30
Dictyonellidae	*Acanthella cavernosa* Dendy, 1922	**PH53**	Fig. 1–38		-	-	-	-	-	-	-	-	-	-	-	-	√	-	-	-	-	-	-	-	-	-	-	-	-	-	20
Dictyonellidae	*Phakettia ridley* (Dendy, 1887) *	**BU578**	Fig. 1–39		-	-	-	-	-	-	-	-	-	√	-	-	-	-	-	-	-	-	-	-	-	-	-	-	-	-	20
Scopalinidae	*Stylissa carteri* (Dendy, 1889)	**PH59**	Fig. 1–40		-	-	-	-	-	-	-	-	-	-	-	-	√	-	-	-	-	-	-	-	-	-	-	-	-	-	20
Scopalinidae	*Stylissa massa* (Carter, 1887)	**PH57**	Fig. 1–41		-	-	-	-	-	-	-	-	-	-	-	-	√	-	-	-	-	-	-	-	-	-	-	-	-	-	25
Callyspongiidae	*Callyspongia* (*Cladochalina*) *aerizusa* Desqueyroux-Faúndez, 1984	BU242, **BU577**, PH15	Fig. 1–42		-	-	-	√	-	-	-	-	-	√	-	-	-	-	-	√	-	-	-	-	-	-	-	-	-	-	7–20
Callyspongiidae	*Callyspongia* (*Cladochalina*) *fibrosa* (Ridley & Dendy, 1886)	**PH2**	Fig. 1–43	*In situ* photo not available	-	-	-	-	√	-	-	-	-	-	-	-	-	-	-	-	-	-	-	-	-	-	-	-	-	-	20

Family	Specie	Samples	Figure	Notes	1	2	3	4	5	6	7	8	9	10	11	12	13	14	15	16	17	18	19	20	21	22	23	24	25	26	Depth (m)
Chalinidae	*Chalinula nematifera* (de Laubenfels, 1954)		Fig. 1–44		-	-	-	-	-	-	-	-	-	-	-	-	-	-	-	-	-	-	-	-	-	√	-	-	√	-	
Chalinidae	*Cladocroce burapha* Putchakarn et al. 2004	MA6, MA19a, **MA19c**, MA19e	Fig. 1–45		-	-	-	-	-	-	-	-	-	-	-	-	-	-	-	-	-	-	-	-	-	-	√	-	-	-	0–1
Chalinidae	*Haliclona* (*Reniera*) *fascigera* (Hentschel, 1912)	**PH8**	Fig. 1–46		-	-	-	-	√	-	-	-	-	-	-	-	-	-	-	-	-	-	-	-	-	-	-	-	-	-	20
Chalinidae	*Haliclona* (*Halichoclona*) *centrangulata* (Sollas, 1902)	**MA4**	Fig. 1–47		-	-	-	-	-	-	-	-	-	-	-	-	-	-	-	-	-	-	-	-	-	-	√	-	-	-	0–1
Niphatidae	*Amphimedon anastomosa* sp. n.	PH58	Fig. 7	This work	-	-	-	-	-	-	-	-	-	-	-	-	√	-	-	-	-	-	-	-	-	-	-	-	-	-	20
Niphatidae	*Amphimedon* cf. *sulcata* Fromont, 1983	**BU560**, **BU560-a1**, **BU575**	Fig. 5, Fig. 6		-	-	-	-	-	-	-	-	-	√	√	-	-	-	-	-	-	-	-	-	-	-	-	-	-	-	Max. depth 30
Niphatidae	*Dasychalina fragilis*	**BA8**	Fig. 1–48	Data not available	-	-	-	-	-	-	-	-	-	-	-	-	-	-	-	-	-	-	-	-	-	-	-	-	-	-	Depth not stated
Niphatidae	*Gelliodes fibulata* (Carter, 1881)	**PH20**	Fig. 1–49	*In situ* photo not available	-	-	-	-	√	-	-	-	-	-	-	-	-	-	-	-	-	-	-	-	-	-	-	-	-	-	20
Niphatidae	*Gelliodes hamata* Thiele, 1903	Bugor Onong	See picture in Calcinai et al. 2013		-	-	-	-	-	√	-	-	-	-	-	-	-	-	-	-	-	-	-	-	-	-	-	-	-	-	28
Niphatidae	*Niphates olemda* (de Laubenfels, 1954)	BU581, BU587, **BU591**, BU597, PH7	Fig. 1–50		-	-	-	-	√	-	-	-	-	√	-	-	-	-	-	-	-	-	-	-	-	-	-	-	-	-	8–25
Niphatidae	*Niphates laminaris* sp. n.	PH47	Fig. 8	This work	-	-	-	-	-	-	-	-	-	-	-	-	√	-	-	-	-	-	-	-	-	-	-	-	-	-	20

Family	Specie	Samples	Figure	Notes	1	2	3	4	5	6	7	8	9	10	11	12	13	14	15	16	17	18	19	20	21	22	23	24	25	26	Depth (m)
Petrosiidae	*Acanthostrongylophora ingens* (Thiele, 1899)	BU4, BU35, BU133, BU134, BU297, BU298, BU302, BU320, BU323, BU544, **PH11**, PH16	Fig. 1–51	See Suppl. material 2	-	√	-	-	√	√	-	√	-	√	-	-	-	√	-	-	-	-	-	-	-	-	-	-	-	8–30
Petrosiidae	*Neopetrosia seriata* (Hentschel, 1912)	BU76, BU83, **BU324**, BU508, BU513	Fig. 1–52	*In situ* photo not available	-	√	-	-	-	-	-	√	-	-	-	-	-	-	-	-	-	-	-	-	-	-	-	-	-	30–65
Petrosiidae	*Neopetrosia similis* (Ridley & Dendy, 1886) *	BU122	Fig. 1–53		-	-	-	-	-	-	-	√	-	-	-	-	-	-	-	-	-	-	-	-	-	-	-	-	-	Depth not stated
Petrosiidae	*Petrosia* (*Petrosia*) *hoeksemai* de Voogd & van Soest, 2002	BU518, BU520, **PH14**	Fig. 1–54		-	-	-	√	-	-	-	√	-	-	-	-	-	-	-	-	-	-	-	-	-	-	-	-	-	3–20
Petrosiidae	*Petrosia* (*Petrosia*) *nigricans* Lindgren, 1897	BU1, BU92, BU93, BU232, BU284, BU286, BU299, BU344, BU512, BU517, BU531, **BU571**, BU572, PH10	Fig. 1–55		-	√	-	-	√	-	-	√	-	√	-	-	-	√	-	-	√	-	-	-	-	-	-	-	-	-	4–32

Family	Specie	Samples	Figure	Notes	1	2	3	4	5	6	7	8	9	10	11	12	13	14	15	16	17	18	19	20	21	22	23	24	25	26	Depth (m)
Petrosiidae	*Petrosia* (*Petrosia*) *plana* Wilson, 1925	BU97, BU285, BU509, BU515, **BU565**, BU410	Fig. 1–56		-	√	-	-	-	-	-	√	-	√	-	-	-	-	-	-	-	-	-	-	-	-	-	-	-	-	7–43
Petrosiidae	*Petrosia* (*Petrosia*) *seychellensis* Dendy, 1922 *	**BU595**	Fig. 1–57		-	-	-	-	√	-	-	-	-	-	-	-	-	-	-	-	-	-	-	-	-	-	-	-	-	-	20
Petrosiidae	*Petrosia* (*Strongylophora*) *corticata* (Wilson, 1925)	**BU102**, BU277	Fig. 1–58		-	-	-	-	-	-	-	√	-	-	-	-	-	-	-	-	-	-	-	-	-	-	-	-	-	-	25–30
Petrosiidae	*Petrosia* (*Strongylophora*) *durissima* (Dendy, 1905) *	**PH39**	Fig. 1–59	*In situ* photo not available	-	-	-	√	-	-	-	-	-	-	-	-	-	-	-	-	-	-	-	-	-	-	-	-	-	-	20
Petrosiidae	*Petrosia* (*Strongylophora*) *strongylata* Thiele, 1903	**BU516**	Fig. 1–60	*In situ* photo not available	-	-	-	-	-	-	-	√	-	-	-	-	-	-	-	-	-	-	-	-	-	-	-	-	-	-	Depth not stated
Petrosiidae	*Xestospongia testudinaria* (Lamarck, 1815)	BU250, **BU510**	Fig. 1–61	*In situ* photo not available	-	-	√	-	-	-	-	√	-	-	-	-	-	-	-	-	-	-	-	-	-	-	-	-	-	-	Depth not stated
Phloeodictyidae	*Siphonodictyon maldiviensis* (Calcinai, Cerrano, Sarà & Bavestrello, 2000)	BU16, BU200, BU342	See picture in Calcinai et al., 2007		-	-	-	-	-	√	-	-	-	√	√	-	-	-	-	-	√	-	-	-	-	-	-	-	-	-	1–40
Phloeodictyidae	*Siphonodictyon microterebrans* (Calcinai, Cerrano & Bavestrello, 2007)	BU51, BU125, BU261, BU492, BU493, BU496b	See picture in Calcinai et al., 2007		-	√	-	-	-	√	-	√	-	-	√	-	-	-	√	-	-	-	-	-	-	-	-	-	-	-	5–30
Phloeodictyidae	*Siphonodictyon mucosum* Bergquist, 1965	BU19, **BU20**, BU450, BU484	Fig. 1–62	White arrows	-	-	-	-	-	√	-	-	√	-	√	-	-	-	-	-	-	-	-	-	-	-	-	-	-	-	6–40

Family	Specie	Samples	Figure	Notes	1	2	3	4	5	6	7	8	9	10	11	12	13	14	15	16	17	18	19	20	21	22	23	24	25	26	Depth (m)
Phloeodictyidae	*Oceanapia amboinensis* Topsent, 1897	BU25, BU65, BU147, BU257, BU321	See picture in Bavestrello et al., 2002	The aquiferous system of this species was described in Bavestrello et al., 2002	√	√	√	-	-	-	-	-	-	-	-	-	-	-	-	-	-	-	√	-	-	-	-	-	-	-	0–1
Phloeodictyidae	*Oceanapia fistulosa* (Bowerbank, 1873)	BU6, BU36, BU101, BU103, BU128, BU130, BU274, BU280, BU341, **PH43**, PH50, Bugor514	Fig. 1–63	The aquiferous system of this species was described in Bavestrello et al., 2002	-	-	-	√	-	√	-	√	-	√	-	-	√	-	-	-	√	-	-	-	-	-	-	-	-	-	20–42
Phloeodictyidae	*Oceanapia pedunculata* (Ridley & Dendy, 1886)	BU64bis		Photos not available	-	-	√	-	-	-	-	-	-	-	-	-	-	-	-	-	-	-	-	-	-	-	-	-	-	-	Depth not stated
Phloeodictyidae	*Oceanapia seychellensis* (Dendy, 1922) *	**BU300**, BU290, BU328	Fig. 1–64	*In situ* photo not available	-	-	-	-	-	-	-	√	-	-	-	-	-	√	-	-	-	-	-	-	-	-	-	-	-	-	20–44
Phloeodictyidae	*Oceanapia toxophila* Dendy, 1922 *	BU276, **BU314**	Fig. 1–65	*In situ* photo not available	-	-	-	-	-	-	-	√	-	-	√	-	-	-	-	-	-	-	-	-	-	-	-	-	-	-	13–30
Irciniidae	*Ircinia colossa* sp. n.	BU590, PH44, **BKA 25,** INDO431	Fig. 10	This work	-	-	-	-	√	√	-	-	-	-	-	-	-	-	-	-	-	-	-	-	-	-	-	-	-	√	20–25
Irciniidae	*Psammocinia alba* sp. n.	PH41	Fig. 9	This work	-	-	-	-	√	-	-	-	-	-	-	-	-	-	-	-	-	-	-	-	-	-	-	-	-	-	20
Spongiidae	*Spongia* (*Spongia*) *ceylonensis* Dendy, 1905	**BU589**	Fig. 1–66		-	-	-	-	-	-	-	-	-	√	-	-	-	-	-	-	-	-	-	-	-	-	-	-	-	-	3.5

Family	Specie	Samples	Figure	Notes	1	2	3	4	5	6	7	8	9	10	11	12	13	14	15	16	17	18	19	20	21	22	23	24	25	26	Depth (m)
Thorectidae	*Hyrtios communis* (Carter, 1885)	**MA12**	Fig. 1–67		-	-	-	-	-	-	-	-	-	-	-	-	-	-	-	-	-	-	-	-	-	-	√	-	-	-	1
Thorectidae	*Hyrtios reticulatus* (Thiele, 1899)	**PH36**	Fig. 1–68		-	-	-	-	√	-	-	-	-	-	-	-	-	-	-	-	-	-	-	-	-	-	-	-	-	20
Thorectidae	*Phyllospongia papyracea* (Esper, 1794)	M3, M4, **PH6**, BA3	Fig. 1–69		-	-	-	-	√	-	-	-	-	-	-	-	-	-	-	-	-	-	-	-	-	-	-	-	-	20
Thorectidae	*Carteriospongia foliascens* (Pallas, 1766)	**BU112**, BU343	Fig. 1–70		-	-	-	-	-	-	-	√	-	-	-	-	-	-	-	-	√	-	-	-	-	-	-	-	-	-	5

Histological sections were prepared from fragments of sponges fixed *in situ* in buffered 2.5% glutaraldehyde in artificial sea water, dehydrated in graded ethanol series, desilicified in 4% hydrofluoric acid, decalcified in 4% hydrochloride acid and embedded in Technovit 8100 (Kulzer). Other fragments were routinely paraffin-embedded and sectioned to obtain preparations of the associated sponges.

Comparative type material of *Acanthostrongylophora ingens* (Thiele, 1899) was kindly provided by The Naturhistorisches Museum at Basel (**NMB**) (Switzerland). Type material is deposited at the Museo di Storia Naturale di Genova Giacomo Doria (**MSNG**), Italy.

Results

A total of 94 demosponge species belonging to 33 families is documented and identified; these species are listed in Table 1; seven of these are new records for the area (Table 1). Six new species were discovered and are herein described.

Seven species (*Tethytimea tylota* (Hentschel, 1912), *Rhabdastrella distincta* (Thiele, 1900), *Thoosa letellieri* Topsent, 1891, *Theonella mirabilis* (de Laubenfels, 1954), *Tedania* (*Tedania*) *coralliophila* Thiele, 1903, *Podospongia colini* Sim-Smith and Kelly, 2011 and *Amphimedon* cf. *sulcata* Fromont, 1993) were recorded for the first time since their original description; for those involved in symbiotic relationships (*T. tylota*, *R. distincta*, and *A.* cf. *sulcata*), extensive morphological and ecological remarks are added, while the others are otherwise briefly described in the Suppl. material 2. Additional taxonomic notes and pictures are added for *Acanthostrongylophora ingens* Thiele, 1889, *Spirastrella pachyspira* Lévi, 1958 and *Mycale* (*Mycale*) *vansoesti sensu* Calcinai, Cerrano, Totti, Romagnoli & Bavestrello, 2006. In vivo pictures of the listed species are given in Suppl. material 1.

Taxonomy

Class Demospongiae
Subclass Heteroscleromorpha
Order Suberitida Morrow & Cárdenas, 2015
Family Suberitidae
Genus *Aaptos* Gray, 1867

***Aaptos lobata* Calcinai, Bastari, Bertolino & Pansini, sp. n.**
http://zoobank.org/A771C968-0DB7-406C-A3A8-9B56BE236ABF
Figure 2

Material examined. Holotype: MSNG 60134, PH-1, 13/01/2005, Timur (Bunaken Island), about 20 m depth. Paratype: MSNG 60135, PH-27, 13/01/2005, same locality as holotype, about 20 m depth.

Other material. BU-82, 22/03/2000, Lekuan II (Bunaken Island), 20 m depth. BU-580, 27/06/2004, Alung Banua (Bunaken Island), 16 m depth. INDO-079, 08/05/2005, Tanjung Kopi (Manado Tua), unknown depth, N01°39'07.4"; E124°41'58.8". INDO-278, 11/05/2005, Tansung Pisok (Manado), unknown depth, N01°34'31.2"; N01°34'31.2". INDO-336, 12/05/2005, Bualo (Manado), unknown depth, N01°37'00.7"; E124°41'21.9". INDO-339, 12/05/2005, Bualo (Manado), unknown depth, N01°37'00.7"; E124°41'21.9".

Diagnosis. Cushion-shaped, sub-spherical sponge; yellow, brown or dark orange. Strongyloxeas, styles and subtylostyles not separable in size categories, forming ascending tracts protruding through the sponge surface.

Description. The sponge is massive, sub-spherical or lobate (Fig. 2A, B). The holotype (Fig. 2A) is a fragment about 1.5 cm long and 1 cm thick, sampled from a large globular specimen; the paratype is a small portion, approximately 2.5 cm long and 1 cm thick, of a large cushion-shaped specimen approximately 60 cm across. The paratype (Fig. 2B) shows a sort of lobate organisation, with roundish parts connected by bottleneck narrowings. The colour in life is yellow, varying between orange and brown according to light exposure; it is not uniform, but presents dark red spots or stripes (Fig. 2A, B). The sponge is always yellow inside. Alcohol-preserved specimens are dark green-brown. The sponge surface is smooth, but microscopically hispid. Ostia, grouped in distinct areas on the sponge surface, have such a large diameter that they are visible to the naked eye. Oscula are flush, more or less circular, with a very low rim. Converging exhalant canals are visible in their lumen (Fig. 2A). Consistency is hard when preserved.

Skeleton. The choanosomal skeleton is radiate, regular in the outer part of the sponge and more irregular in the deeper part. Due to high spicule density, spicule tracts are not easily detectable (Fig. 2C, D). In the ectosome, the smallest styles are arranged in palisade and do not form brushes, whereas the spicules of intermediate size are concentrated in the sub-ectosomal layer and protrude through the surface with their tips (Fig. 2C, D). Abundant spheroulous cells, approximately 12 μm in diameter, are detectable in the choanosome.

Spicules. Three size categories of megascleres, partially overlapping at the extremities of their size-frequency distributions. The larger spicules are straight strongyloxeas with acerate or slightly stepped tips (Fig. 2E) and often evident axial canal. Intermediate and small megascleres, straight or slightly curved, vary in shape from strongyloxeas to subtylostyles to thin styles (Fig. 2F). The measurements are given in Table 2.

Etymology. The name refers to the multi-lobate organisation of the sponge.

Remarks. The genus *Aaptos* Gray, 1867, according to van Soest et al. (2016), encompasses in total 24 valid species, 10 of which distributed in the tropical Indo-Pacific and adjacent areas (Table 2). The descriptions are usually based on the very few diagnostic features detectable in the genus, making it difficult to differentiate species (Kelly-Borges and Bergquist 1994). The radial skeleton, the arrangement of the megascleres and the spicule morphology, being quite uniform within the genus, are seldom accurately described (Kelly-Borges and Bergquist 1994). Therefore, the importance of other

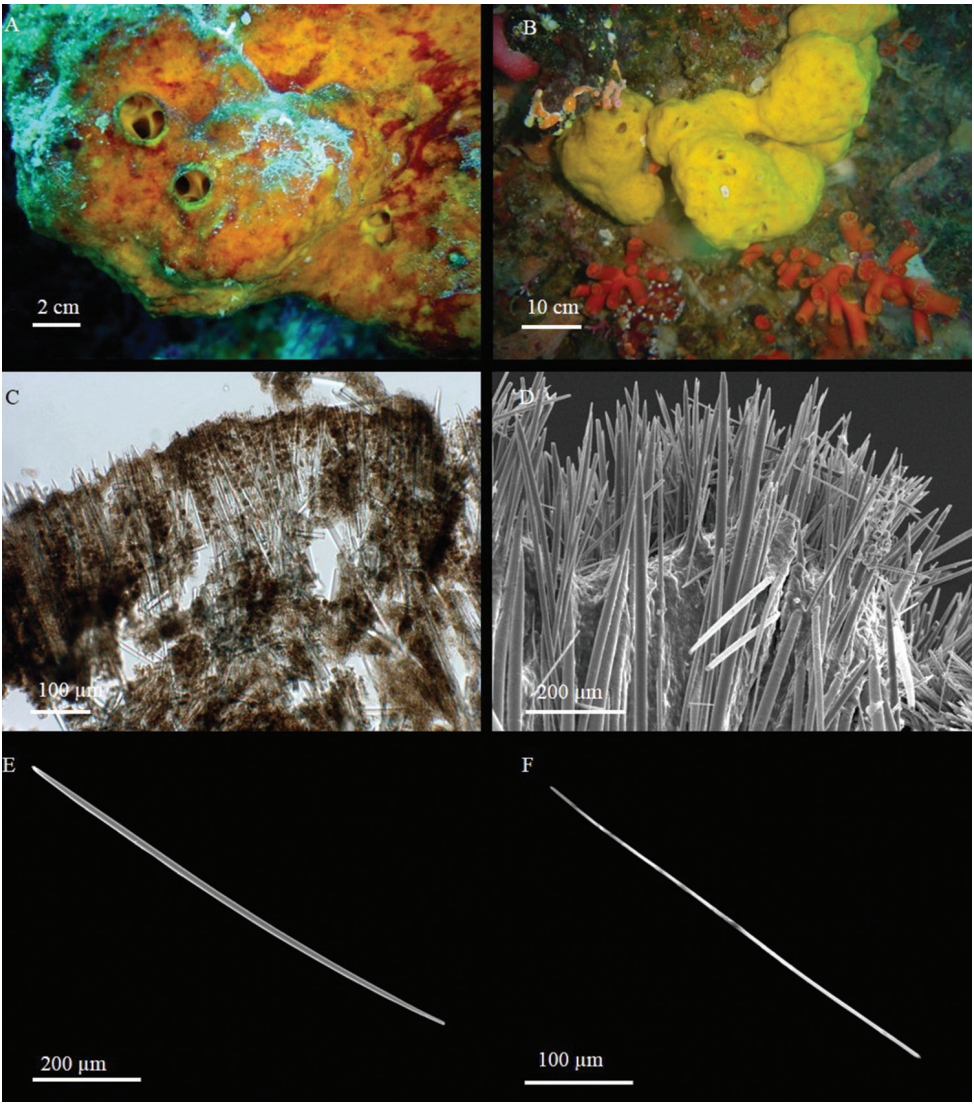

Figure 2. *Aaptos lobata* sp. n. **A, B** specimens *in situ*: **A** holotype **B** paratype **C** skeleton organisation (transverse section) **D** peripherical part of the skeleton **E** large strongyloxea **F** thin style.

morphological characters useful to differentiate species, such as colour, collagen distribution in the cortex, shape and arrangement of megasclere tracts, presence of interstitial spicules, is greatly emphasised (Kelly-Borges and Bergquist 1994). Recently, Carvalho et al. (2013) stressed the importance of other morphological aspects as main characters for the species distinction in the genus, such as external morphology, colour, shape and size of the megascleres, ectosomal spicules arrangement (palisade or bouquets).

The skeletal organisation of *Aaptos lobata* sp. n. is comparable with that of the type species of the genus, the Atlantic-Mediterranean *Aaptos aaptos* (Schmidt, 1864)

Table 2. *Aaptos* species distributed in the tropical Indo-Pacific and adjacent areas.

Species	Shape and surface	Colour	Consistence	Skeleton	Spicules (µm)
A. ciliata (Wilson, 1925)	Massive, lobate; surface conulose and hispid	Whitish brown	-	Collagenous ectosome 0,5 mm thick, with cavities Choanosome dense with ill-defined spicule tracts	Styles 1400–2000 × 20–36 Ectosomal styles 1100–1300 × 4
A. conferta Kelly-Borges & Bergquist, 1994	Thickly encrusting, lobate; surface smooth or micro-hispid	Jet black outside, mustard yellow inside	Just compressible	Stout megasclere tracts with interstitial spicules	Strongyloxeas 662–1813 × 13–29 2 categories of styles Oxeas 156–537 × 3–8
A. globosa Kelly-Borges & Bergquist, 1994	Spherical; surface smooth	Deep red brown outside, mustard yellow inside	Incompressible	Tracts of primary megascleres radiating at the surface; superficial palisade not piercing the sponge surface	Strongyloxeas I 980–2401 × 18–33 Strongyloxeas II 332–1029 × 8–16 Tylostyles 104–198 × 4–5 Subtylostyles 208–458 × 5–8
A. horrida (Carter, 1886)	Massive elongate; surface even and villous	Grey	Very compact	Very compact	2 size categories of fusiform, acerate spicules
A. laxosuberites (Sollas, 1902)	Encrusting; surface slightly hispid	Whitish, in spirit	-	Ascending and diverging tracts of megascleres Ectosomal skeleton of small styles	Strongyloxeas I 750–1120 × 26–40 II 250 × 4 Tylostyles 700 × 20
A. niger Hoshino, 1981	Massive, embedding extraneous material; surface minutely hispid	Black	Incompressible	Ectosome with small styles; radiate architecture and confused spicules in the choanosome	Strongyloxeas I 540–1310 × 18–46 II 170–270 × 5–10
A. nuda (Kirkpatrick, 1903)	Massive; surface finely papillate	Pale brown outside, interior lighter (in spirit)	Rather hard	Ill-defined bundles of oxeas radiating towards the surface	Oxeas 1700 × 45
A. rosacea Kelly-Borges & Bergquist, 1994	Spherical to semi spherical; surface smooth and faintly hispid	Oxide red outside and golden yellow inside	Incompressible	Choanosomal tracts of megascleres branching at the surface and forming tufts Superficial palisade of tylostyles and subtylostyles	Strongyloxeas 735–2009 × 10–23 Styles 367–1102 × 5–12 Tylostyles 94–218 × 3–8 Subtylostyles 198–447 × 4–13
A. suberitoides (Broensted, 1934)	Massive; surface faintly hispid	Black outside, dark red inside	Very firm	Radiate, with loose spicule tracts	Styles 900–1100 × 15–23

Species	Shape and surface	Colour	Consistence	Skeleton	Spicules (µm)
A. tentum Kelly-Borges & Bergquist, 1994	Globular or sub-spherical; surface microscopically hispid	Different shades of brown outside, brown yellow inside	Firm	Large, loose tracts of megascleres in the choanosome, replaced in the outer region by intermediate spicules; superficial palisade of small tylo- and subtylostyles	Strongyloxeas I 980–2572 × 21–42; II 416–1298 × 10–21; Tylostyles 104–198 × 5–8; Styles or subtylostyles 187–441 × 8–13
Aaptos lobata sp. n.	Globular, sub-spherical	Yellow, dark orange, brown	Hard (preserved)	Radiate tracts of larger megascleres protrude towards the surface; intermediate and small spicules, abundant in the outer part, concur to the hispidation	Strongyloxeas: 810–993.91(±119.38)-1320 × 10–19.84(±3.84)-30; Intermediate megascleres: 405–540.91(±107.64)-750 × 7.5–11.53(±4.05)-25; Small megascleres 145–264.87(±65.20)-395 × 2.5–4.91(±1.43)-7.5

(see van Soest 2002). *Aaptos lobata* sp. n. has been compared with all the congeneric species and especially with those recorded from the Indo-Pacific and adjacent areas, whose characteristics are reported in Table 2. *Aaptos ciliata* (Wilson, 1925) has spicules different in size and shape; in particular, the ectosomal styles are longer (1,100–1,300 × 4 μm). The species *A. conferta* Kelly-Borges & Bergquist, 1994, is an encrusting sponge, black outside and yellow inside, that has oxeas as additional spicules, whereas *A. globosa* Kelly-Borges & Bergquist, 1994 differs in colour (dark red outside and yellow inside) and in the skeletal organisation, since choanosomal tracts are thick and ramified under the surface and the intermediate megascleres form tracts. *Aaptos horrida* (Carter, 1886) and *A. nuda* (Kirkpatrck, 1903) have oxeas as megascleres instead of strongyloxeas; *A. laxosuberites* (Sollas, 1902) is encrusting, white in alcohol and has strongyloxeas and long tylostyles as megascleres. *Aaptos niger* Hoshino, 1981 is a black, massive sponge, usually embedding exogenous material; while *A. rosacea* Kelly-Borges & Bergquist, 1994, is red outside and yellow inside and differs from the new species in skeletal arrangement and size of spicules. The species *A. suberitoides* (Brøndsted, 1934), black outside and dark red inside, has a very simple skeleton of styles only, while *A. tenta* Kelly-Borges & Bergquist, 1994, brown in colour, has a peculiar skeletal arrangement and different spicules. Since no species in this vast geographic area matches with the characters of our specimens, we decided to erect a new species.

Order Tethyida Morrow & Cárdenas, 2015
Family Tethyidae Gray, 1848
Genus *Tethytimea* de Laubenfels, 1936

***Tethytimea tylota* (Hentschel, 1912)**
Figure 3

Donatia tylota Hentschel, 1912: 317.

Material examined. BU-98, 23/03/2000, Lekuan II (Bunaken Island), 5 m depth. BU-289, 17/05/2001, Raymond's Point (Bunaken Island), unknown depth. BU-533, 21/06/2004, Bualo (Manado Tua Island), about 8 m depth. BU-545, 23/06/2004, Raymond's Point (Bunaken Island), about 20 m depth. BU-562, 26/06/2004, Bualo (Manado Tua Island), unknown depth.

Description. Encrusting sponge 3–6 mm thick; the largest examined specimen (BU-289) is approximately 10 cm in diameter. The consistence is firm; the body of the sponge lacunose. The surface is irregular, with extended verrucous areas covered by sand and largely colonised by epibiotic ascidians, algae and hydroids (Fig. 3A). In the microscopic observation, the surface appears micro-hispid. The colour of living specimens is orange; when preserved, the sponge becomes yellowish-green.

Skeleton. *Tethytimea tylota* does not have a distinguishable ectosomal skeleton or a proper cortex; the choanosomal skeleton is formed by bundles of big tylostyles of

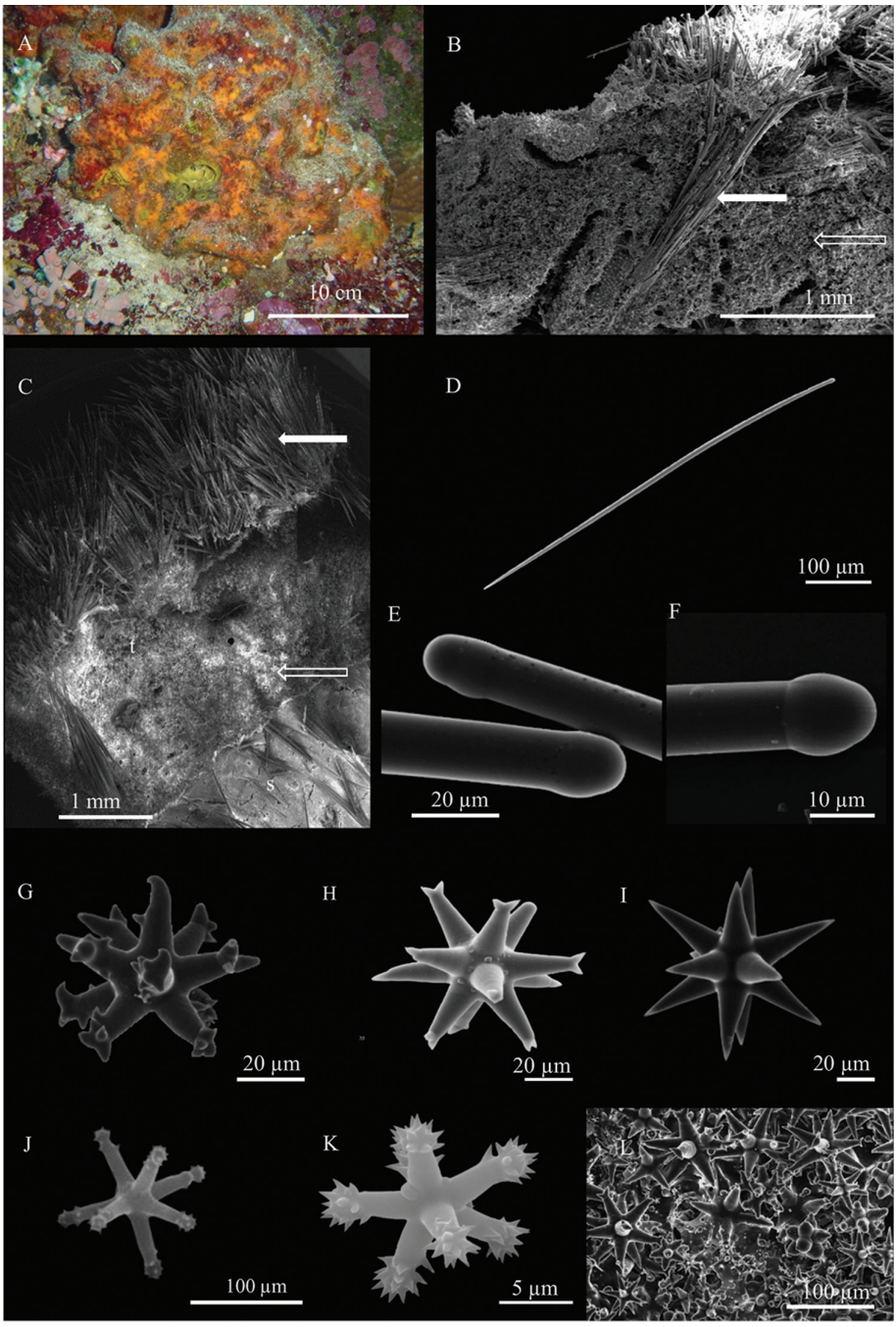

Figure 3. *Tethytimea tylota* (Hentschel, 1912) **A** specimen *in situ* (BU-562) **B** cross section showing bundles of big tylostyles (full arrow) and the microscleres (empty arrow) **C** SEM image showing fans of small tylostyles (full arrow) and microscleres (empty arrow) of *T. tylota* (**t**), below the sponge *Stelletta* sp. n. (**s**) involved in the association **D** small tylostyle **E, F** heads of tylostyles **G–I** oxysphersters **J, K** tylasters **L** groups of microscleres.

100–200 μm directed outwards (Fig. 3B). Close to the surface, these main bundles support fans of small tylostyles hispidating the sponge surface (Fig. 3B, C).

Spicules. Megascleres are straight tylostyles with a slightly developed head (Fig. 3D). They can be distinguished into two size classes (Fig. 3E, F); tylostyles I measure 930 - (1,104.8 ± 146.7) - 1,339 × 12.5 - (17.8 ± 3.4) - 25 μm; tylostyles II (Fig. 3D) measure 490 - (576.6 ± 72.5) - 660 × 5 - (6.6 ± 2.0) - 10 μm and form the superficial fans that protrude out of the surface; microscleres are two kinds of asters (Fig. 3G–K). Oxyspherasters (Fig. 3G–I) with thick ramified or rounded, often bifurcated rays, measuring 65 - (122.5 ± 39.6) - 200 μm. Tylasters with rays variable in length ending with apical groups of spines variable in number (Fig. 3J, K); they measure 7.5 - (11.1 ± 1.9) - 16.3 μm. Microscleres are abundant throughout the sponge, but more concentrated close to the surface (Fig. 3L), where the smallest tylasters form a thin, continuous layer (Fig. 4H, inlet).

Remarks. This sponge was exclusively found as epizoic on *Stelletta tethytimeata* sp. n. (see below). It has been attributed to *T. tylota* for its skeletal organisation, made of bundles of main tylostyles supporting superficial fans of small tylostyles, the superficial layer of tylasters (present also in the holotype), the size and shape of megascleres and microscleres (Sarà 2002). The genus *Tethytimea* is monospecific and *T. tylota* was found at Aru Island (Indonesia). This is the first record of this species since the original description (Hentschel 1912). In the revision of the genus (based on the re-examination of the type material), Sarà (2002) confirmed the presence in the holotype of very rare spheres; these spicules were not detected in the present specimens as in the paratype (Sarà 2002).

It is interesting to note that the holotype of *T. tylota* was encrusting on a stone and in association with another sponge (Sarà 2002).

Remarks on the association. See below.

Order Tetractinellida Marshall, 1876
Family Ancorinidae Schmidt, 1870
Genus *Stelletta* Schmidt, 1862

***Stelletta tethytimeata* Calcinai, Bastari, Bertolino & Pansini, sp. n.**
http://zoobank.org/8C01D0F2-326D-4C50-827F-706CF3D6EAF6
Figure 4

Material examined. Holotype: MSNG 60136, BU-289, 17/05/2001, Raymond's Point (Bunaken Island), unknown depth. Paratype: MSNG 60137, BU-562, 26/06/2004, Bualo (Manado Tua Island), unknown depth.

Other material. BU-533, 21/06/2004, Bualo (Manado Tua Island), about 8 m depth. BU-545, 23/06/2004, Raymond's Point (Bunaken Island), about 20 m depth. BU-98, 23/03/2000, Lekuan II (Bunaken Island), 5 m depth.

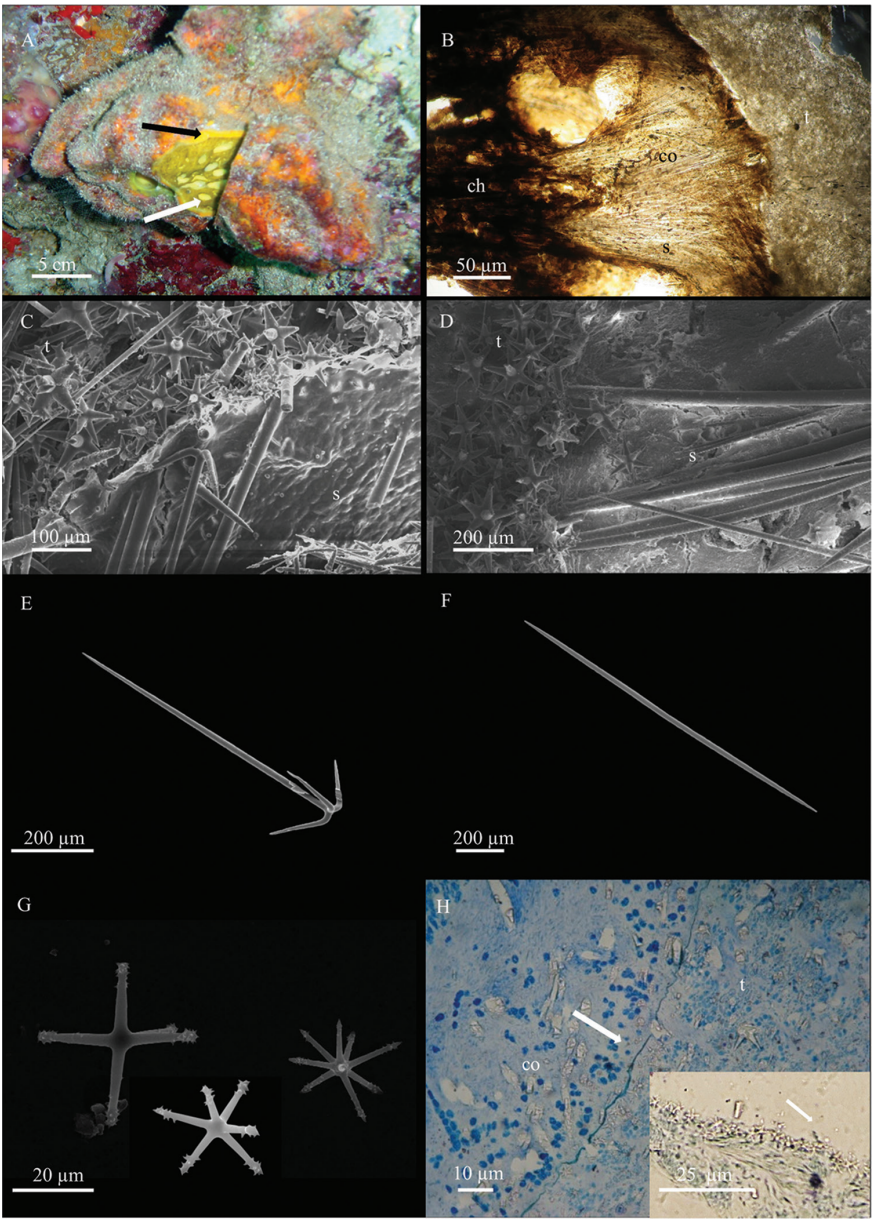

Figure 4. *Stelletta tethytimeata* sp. n. **A** specimen *in situ* (BU-533), partially cut to put in evidence the association with *Tethytimea tylota*. The black arrow indicates the thin layer of the external sponge (*T. tylota*, orange) while the white arrow indicates *S. tethytimeata* sp. n. **B** paraffin-embedded section of *T. tylota* (**t**) and *S. tethytimeata* sp. n. (**s**) **co** and **ch** indicate, respectively, the cortex and the choanosome of *S. tethytimeata* sp. n. **C** cross section showing triaenes close to the boundary between *T. tylota* (**t**) and *S. tethytimeata* sp. n. (**s**) **D** bundles of oxeas reaching the boundary between *T. tylota* (**t**) and *S. tethytimeata* sp. n. (**s**) **E** anatriaene **F** oxea **G** microasters **H** histological preparation showing the cortex (**co**) of *S. tethytimeata* sp. n. The arrow points to the collagenous layer between *S. tethytimeata* sp. n. and *T. tylota* (**t**). The inset shows the layer of tylasters of *T. tylota* (arrow).

Diagnosis. Massively rounded yellow sponge; the colour changes after fixation. Megascleres are anatriaenes with characteristic bending and a single type of oxeas; microscleres are represented by a heterogeneous set of tylasters and oxyasters.

Description. The sponge is light yellow-lemon *in vivo* (Fig. 4A); the colour changes in the preserved specimens, becoming dark-brown to blackish. It is almost totally covered by the associated epibiotic species *T. tylota* (see above), with the exception of the oscula that, protruding from the surface of *T. tylota*, are clearly distinguishable for their different colour (Figs 3A, 4A). Since the external sponge *T. tylota* is thinly encrusting, most of the mass of the associated sponges is due to *S. tethytimeata* sp. n. that can be as large as 10 cm across (Fig. 4A, B).

Skeleton. The cortex is a collagenous layer 400-700 μm thick (Fig. 4B); the triaenes have their clades tangential to the surface and sometimes protrude from it (Fig. 4C), merging in the tissue of the epibiotic *T. tylota*. The choanosomal skeleton is formed by tracts of oxeas without a clear radial arrangement with microscleres scattered in between (Fig. 4D). Towards the sponge surface, the spicule density lowers and oxeas are more or less parallelly arranged (Figs 3C, 4B, D).

Spicules. Megascleres are anatriaenes (Fig. 4E), with straight, sharp-pointed rhabdome of 570 - (708.2 ± 119.3) - 800 × 10 - (15.7 ± 3.8) - 22.5 μm and clads of 80 - (113.4 ± 43.3) - 225 × 7.5 - (9.0 ± 2.6) - 12.5 μm with sharp tips and characteristic bending. Oxeas straight, fusiform, with sharp tips (Fig. 4F), sometimes modified into styles; they measure 1274 - (1514.5 ± 145.3) - 1950 × 20 - (24.5 ± 3.9) - 30 μm. Microscleres encompass a heterogeneous set of tylasters and oxyasters (Fig. 4G), with 4–9 rays, with spines along the rays or grouped at the extremities 20 - (27.2 ± 4.4) - 35 μm.

Etymology. The name refers to the association with *Tethytimea tylota*.

Remarks. *Stelletta tethytimeata* sp. n. is characterised by one type of triaenes and by a single category of oxeas. Out of the 146 species of *Stelletta*, distributed in all the oceans (van Soest et al. 2016), 49 are from the tropical Indo-Pacific area (van Soest 1994). However, they all differ from the new species in colour, skeletal organisation and especially in the spicule features. They show different categories of megascleres (oxeas of different sizes, plagio-, orto- and dico-triaenes) and microscleres. In particular, 10 species of the tropical Indo-Pacific *Stelletta* species present a single type of triaenes: *S. bocki* Rao, 1941, *S. brevioxea* (Pulitzer-Finali, 1993) and *S. cavernosa* (Dendy, 1916) have ortotriaenes; *S. brevis* Hentschel, 1909, *S. centroradiata* Lévi and Lévi, 1983, *S. centrotyla* Lendelfeld, 1907 and *S. herdmani* Dendy, 1905 have plagiotriaenes; *S. herdmani* var. *robusta* Thomas, 1979 has protriaenes, whereas *S. hyperoxea* Lévi and Lévi, 1983, *S. vaceleti* (Lévi and Lévi, 1983), *S. phialimorpha* Lévi, 1993 and *S. digitata* (Pulitzer-Finali, 1993) have dicotriaenes. Actually, *Stelletta tethytimeata* sp. n. is the only species of the genus in this area possessing anatriaenes (peculiar for the characteristic clad bending) and a single category of oxeas. It is therefore justified, based on the five specimens in association with *Tethytimea tylota* encountered in this region, to erect a new species.

Remarks on the association. The associated specimens of *T. tylota* and *S. tethytimeata* are flat or cushion-shaped with big, rounded lobes and wide oscular structures (Figs 3A, 4A).

By superficial analysis, the two associated species could appear as a single large individual sponge. The external species (*T. tylota*) can be detached with difficulty from the internal one (*S. tethytimeata* sp. n.); the contact area may be observed in SEM images (Fig. 3C) and by histological preparations where the presence of a thin collagen layer of separation between the two species is detectable (Fig. 4B, H). Histological preparations clearly show the presence of the cortex of *S. tethytimeata* sp. n. made by a collagen layer up to 700 μm thick (Fig. 4B, H). In the cortex, collencytes are clearly visible and pigmentary cells are numerous (Fig. 4H).

The two associated species are quite common in North Sulawesi, always in association, generally in dim-light conditions, at a maximum depth of 20 m.

Genus *Rhabdastrella* Thiele, 1903

Rhabdastrella distincta (Thiele, 1900)

Figure 5

Coppatias distinctus Thiele, 1900: 56.

Material examined. BU-560, 26/06/2004, Bualo (Bunaken Island), unknown depth. BU-575, 27/06/2004, Alung Bauna (Bunaken Island), 27 m depth.

Description. The sponge has a massive and irregular shape, a large size, up to 50 cm in diameter, and was exclusively found partially covered by *Amphimedon* cf. *sulcata* (see below). In the part not covered by the epibiotic sponge, *R. distincta* is yellow-lemon (Fig. 5A), or dark green (Fig. 5B), turning black when cut or preserved. Wide oscular areas are often evident (Fig. 5A, B).

Skeleton. Spherasters are located in the outer part of the sponge, but do not form a real cortex (Fig. 5C, D). The choanosomal skeleton consists of scattered oxeas which tend to form radial tracts towards the peripheral part (Fig. 5C). Oxyasters and oxyspheraster are dispersed in the choanosome.

Spicules. Megascleres are fusiform oxeas (Fig. 5E) with rather sharp tips, 720 - (832.5 ± 65.7) - 990 × 10 - (13.3 ± 2.9) - 20 μm. Microscleres are spherasters of variable size, 12.5 - (29.5 ± 6.4) - 35 μm in diameter (Fig. 5F), with a large centre and thick rays with sharp or bifurcated tips; oxyasters (Fig. 5G) with small centre and thin rays, 35 - (49 ± 8.1) - 65 μm in diameter; oxyspherasters with well-developed centre (Fig. 5H), 10 - (15.1 ± 2.6) - 20 μm.

Remarks. The Indonesian specimens fit with the description of *R. distincta* in having the same skeletal organisation (characterised by oxeas scattered in the inner part of the sponge and radially arranged close to the surface), absence of triaenes, spherasters in the peripheral part, oxyasters and oxyspheraster scattered in the choanosome. Spicule sizes are comparable to those of the type species that are fusiform oxeas of 850 × 25 μm, spherasters up to 40 μm, oxyasters up to 80 μm and oxyspherasters of 15 μm (see Uriz 2002). The principal difference with Thiele's original description is

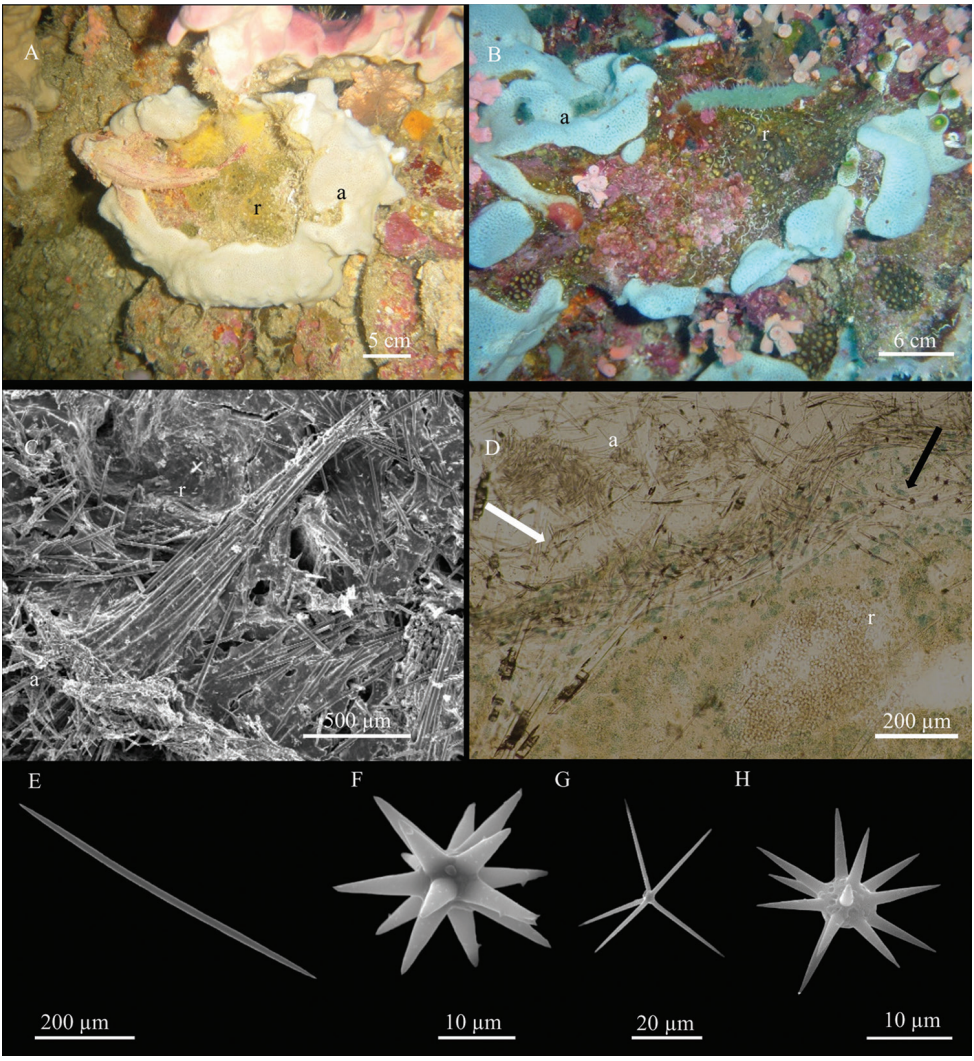

Figure 5. *Rhabdastrella distincta* (Thiele, 1903) **A, B** specimens *in situ* (**r**), partially covered by the epibiotic sponge *Amphimedon* cf. *sulcata* Fromont, 1993 (**a**) specimen of Figure 5A is BU-575, that of Figure 5B is BU-560 **C** SEM image of a cross section of *R. distincta* (**r**) showing the radial tracts of oxeas in proximity of the external part, **a** indicates the epibiotic sponge *A.* cf. *sulcata* **D** histological preparation of *R. distincta* (**r**) and *A.* cf. *sulcata* (**a**) showing spherasters (black arrow) in the peripheral part, and oxeas of *R. distincta* (white arrow) penetrating the tissues of *A.* cf. *sulcata* **E** oxea **F** spheraster **G** oxyaster **H** oxyspheraster.

that smooth microscleres were not observed and a real cortex is not detectable in the studied specimens.

This is the first record of the species since the original description of Thiele (1900) based on two specimens from Ternate, Indonesia.

Remarks on the association. See below.

Order Haplosclerida Topsent, 1928
Family Niphatidae
Genus *Amphimedon* Duchassing & Michelotti, 1864

***Amphimedon* cf. *sulcata* Fromont, 1993**
Figure 6

Material examined. BU-560, 26/06/2004, Bualo (Bunaken Island), unknown depth. BU-575, 27/06/2004, Alung Bauna (Bunaken Island), 27 m depth.

Description. The sponge is flat, with a roundish contour, about 1 cm thick, without visible oscules. It is completely free of epibiotic organisms. Colour *in situ* may be greyish-white (Figs 5A, 6A) or pale cerulean (Figs 5B, 6B), off-white to greyish in the preserved state. The sponge shows ridges and grooves, covered by a very thin membrane, that give a typical convoluted or brain-like aspect to its surface (Fig. 6B).

Skeleton. The ectosomal skeleton is a reticulation of pauci-spicular tracts (3-4 spicules) (Fig. 6C) organised in quite regular triangular meshes with scarce spongin at the nodes. The choanosomal skeleton (Fig. 6D) is formed by a reticulation of multispicular tracts and round meshes of approximately 60 μm in diameter, with abundant scattered spicules. The spicule tract extremities barely protrude from the sponge surface, causing micro-hispidation.

Spicules. Megascleres are straight or slightly curved oxeas with sharp tips; they measure 125 - (188.9 ± 33.5) - 247.5 × 2 - (5.2 ± 3.4) - 12.5 μm (Fig. 6E); numerous thin oxeas are present (Fig. 6F); microscleres are very thin, C-shaped, sigmas 10 - (12.9 ± 1.5) - 15 × ≤ 1μm (Fig. 6G).

Remarks. The sponge here described has a skeleton organisation fitting with the diagnosis of the genus *Amphimedon* that is characterised by an ectosomal skeleton of tangential fibres forming meshes, covered by a thin membrane and by a choanosomal skeleton formed by a plumose, irregular reticulation of multispicular tracts (Desqueyroux-Fáundez and Valentine 2002).

Our specimens are similar to *A. sulcata*, especially for the very characteristic surface: "meandering parallel ridges, interspersed with spaces, give a convolute or brain-like appearance to the surface" (Fromont 1993), for the thin membrane covering the ridges and the absence of abundant spongin.

Among the Indo-Pacific species of *Amphimedon*, only *A. sulcata* has sigmas similar in size (13 - (15.9) - 16.9 μm) to our specimens, but its oxeas (122 - (139) - 153 × 3 - (4.5) - 5.3 μm) are smaller than those we observed. Another difference is in the colour: "mauve alive, cream or fawn in alcohol" in *A. sulcata* (Fromont, 1993).

Remarks on the association. *Amphimedon* cf. *sulcata* is not tightly attached to *Rhabdastrella distincta*, and the two sponges can be separated rather easily. Frequently, wide areas of *R. distincta* are not covered by the outer sponge (Figs 5A, B, 6A, B), and exhalant and probably also inhalant parts of *R. distincta* are in these portions, free from the epibiont.

In the boundary between the two sponges, a thin collagenous layer is present. Both in the histological preparations and in SEM images, the oxeas of *R. distincta* are

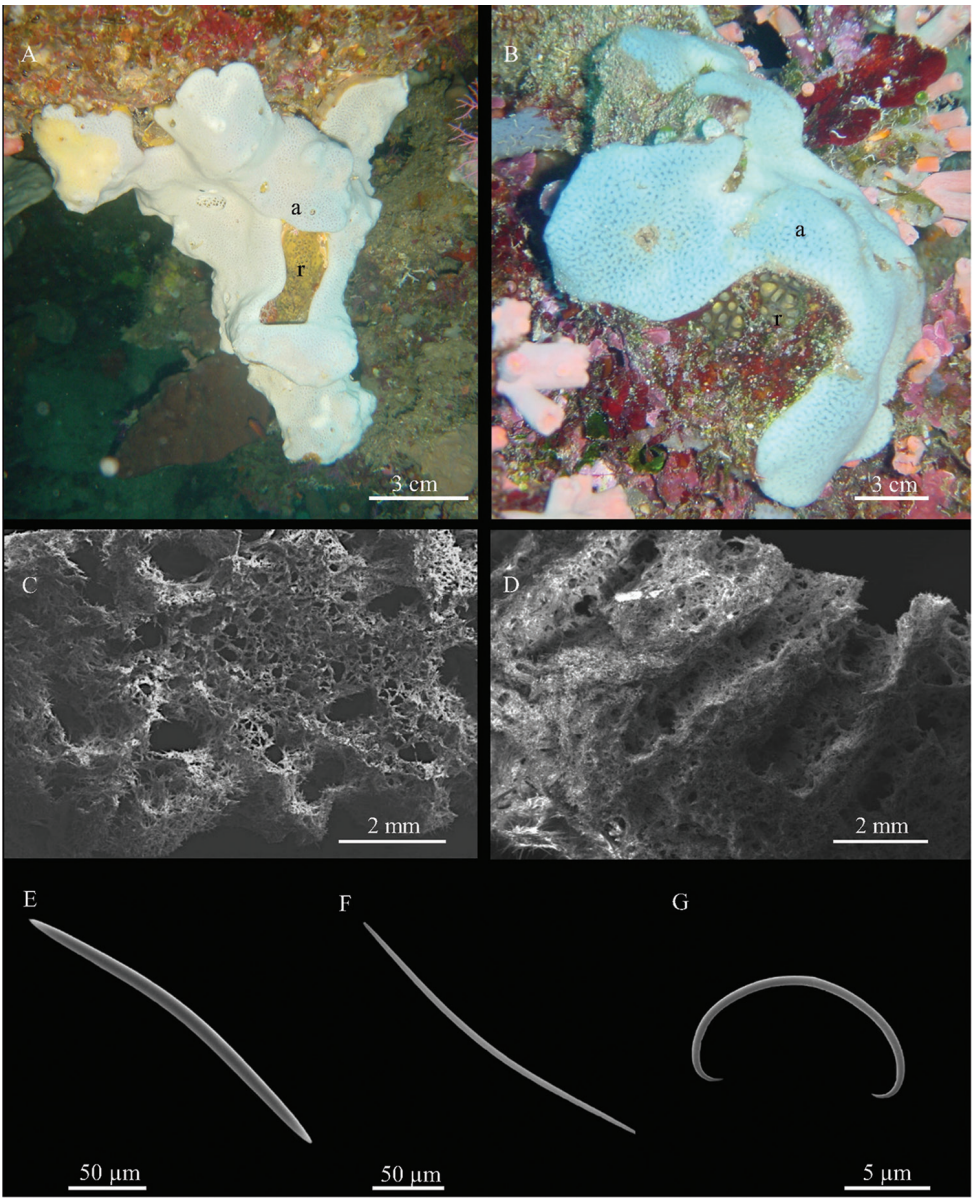

Figure 6. *Amphimedon* cf. *sulcata* Fromont, 1993 **A, B** specimens *in situ* (**a**), partially covering the associated sponge *Rhabdstrella distincta* (**r**), specimen BU-560a1 in Figure 6A, BU-560 in Figure 6B **C** SEM image of the ectosome **D** SEM image of the choanosome **E** oxea **F** thin oxea **G** sigma.

clearly visible, protruding out of the surface and penetrating inside the tissues of the external sponge (Fig. 5C, D), as it is usual in similar associations (Ávila et al. 2007). This association was frequently observed in North Sulawesi, usually below a depth of 30 m.

Amphimedon anastomosa **Calcinai, Bastari, Bertolino & Pansini, sp. n.**
http://zoobank.org/768365CA-8FBA-4660-A3B9-90E76B42A940
Figure 7

Material examined. Holotype: MSNG 60138, PH-58, 17/01/2005, Tiwoho (Bunaken Island), about 20 m depth.

Diagnosis. Dark green, highly branched sponge with an irregular ectosomal skeleton of rectangular, paucispicular meshes and multispicular choanosomal fibres, forming an irregular reticulation. Oxeas are mucronate.

Description. Highly branched sponge (Fig. 7A) with repent habit. Anastomosing branches are flattened, 4–8 mm in diameter, creeping over the substrate. Colour *in situ* is dark green to dark brown, greenish in alcohol or in the dried state. Consistence soft and brittle; the sponge easily crumbles when dried. Surface slightly rough, irregular; when the transparent membrane is preserved, it gives a smooth appearance at the macroscopic observation. Oscula not visible. Numerous barnacles are embedded in the sponge tissue, with only their openings free (Fig. 7B).

Skeleton. The ectosomal skeleton is an irregular reticulation of rectangular meshes 120–150 μm, up to 190–250 μm in diameter, formed by fibres 20–40 μm thick (Fig. 7B, C). Fibres are cored by 4–6 spicules. In the well-preserved parts of the sponge, a thin dermal membrane covers the surface. When the membrane is damaged, the sponge surface is microhispid due to protruding fibres. The choanosomal skeleton (Fig. 7D) is irregular, formed by primary multispicular (approximately 10 spicules) fibres, about 60 μm thick, directed towards the surface; secondary fibres are 20–35 μm in diameter. Secondary and primary fibres create an irregular reticulation of more or less circular meshes 170–300 μm across. Spongin is not abundant.

Spicules. Megascleres are oxeas slightly curved, with sharp tips (Fig. 7E, F), 97 - (111.6 ± 6.7) - 122.4 × 2.6 - (4.5 ± 1.2) - 5.2 μm.

Etymology. The name refers to the habitus of the sponge, characterised by anastomosing branches.

Remarks. The species described here may be attributed to the genus *Amphimedon* due to its skeleton characteristics. Out of the 54 species of *Amphimedon* hitherto described (van Soest et al. 2016), only two (*A. denhartogi* de Voodg, 2003 and *A. elastica* (Kieschnick, 1898) are present in Indonesia, whereas 30 have been recorded in the Indo-Pacific region. *Amphimedon denhartogi* and *A. elastica* differ from *A. anastomosa* sp. n. in their skeletal organisation and general morphological characters. The species *A. denhartogi* is green in life, like *A. anastomosa* sp. n., but it has an erect, flabellate shape and star-shaped oscula; moreover, it has strongyles as spicules. In contrast, *A. elastica* is a single-tube yellow-brownish sponge with a wide apical osculum (11 mm in diameter) and smooth surface; spicules are oxeas of 90–100 μm. Also, the other Indo-Pacific species show significant differences with *A. anastomosa* sp. n.; *A. aculeata* Pulitzer-Finali, 1982 is a vase-shaped sponge with conical projections on the surface and strongyles as spicules, whereas *A. aitsuensis* (Hoshino, 1981), described from Japan, is a massive sponge, grey in colour and with oxeas of two distinct size categories

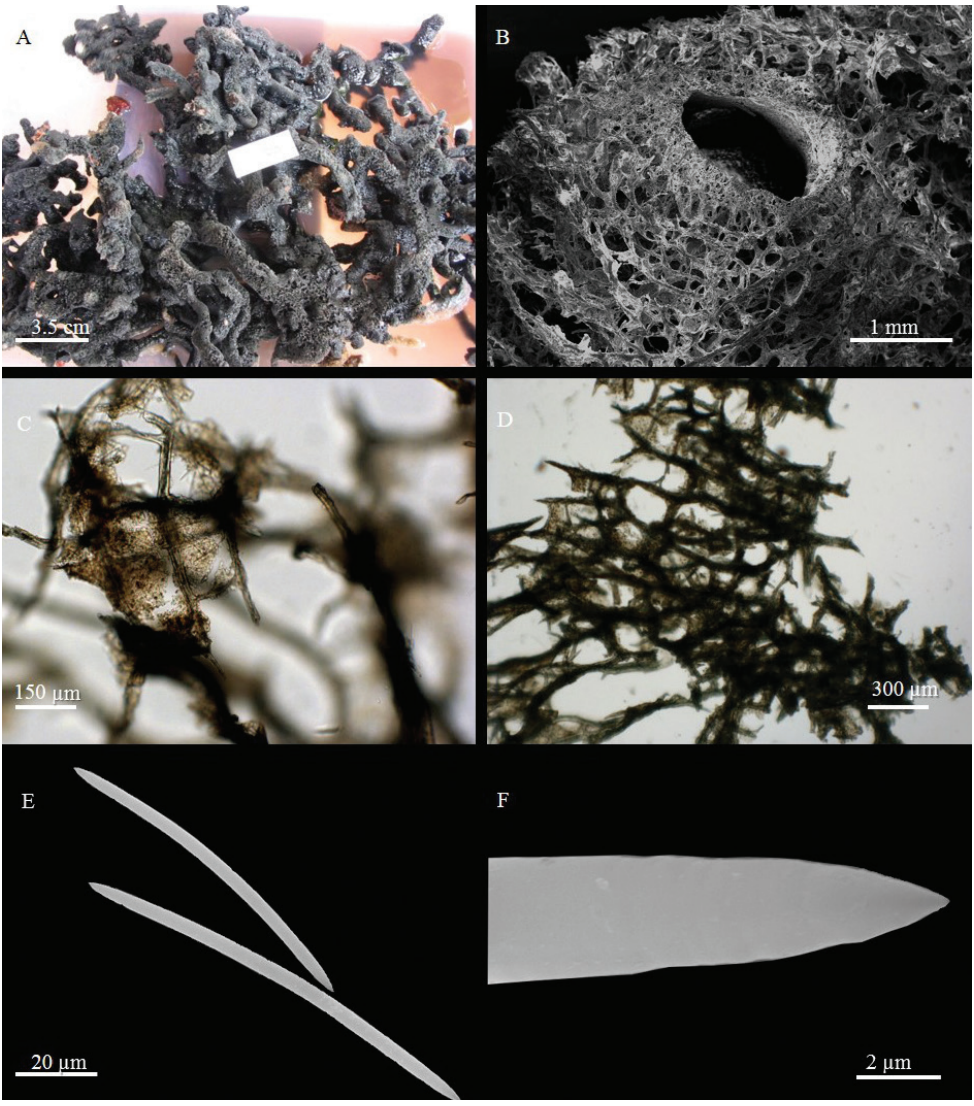

Figure 7. *Amphimedon anastomosa* sp. n. **A** The holotype just after collection **B** Sponge surface with the round opening of a symbiotic barnacle **C** ectosomal skeleton **D** choanosomal skeleton **E** oxeas **F** magnification of an oxea tip.

(thick oxeas of 132–148 × 7–9 µm and thin oxeas of 115–135 × 4–6 µm). *Amphimedon alata* Pulitzer-Finali, 1996 has oxeas of 100–130 × 7–11.5 µm and peculiar, small, wing-shaped toxas (11–50 µm); *A. brevispiculifera* (Dendy, 1905) is an erect sponge light-brown in the dry state; it is digitate or flabellate, with evident large oscula; it differs from *A. anastomosa* sp. n. also for its stout primary fibres 164 µm thick. The two species *A. chinensis* and *A. flexa* have been described by Pulitzer-Finali (1982) from Hong Kong; *A. chinensis* differs from the new species for the orange colour, the pres-

ence of oscula arranged in a single row and the larger oxeas (125–145 × 8–9.5 μm), while *A. flexa* is plurilobate with oscula on top of the lobes; its primary fibres, slightly thicker than those of the new species, create larger meshes from 300 to 900 μm across. The species *A. chloros* Ilan et al., 2004 is green, like *A. anastomosa* sp. n., but cushion-shaped, with oxeas that usually become strongyloxeas. In contrast, *A. conferta* Pulitzer-Finali, 1996 is sub-cylindrical, brown in life, cream in the dry state, with ectosomal tracts 75 μm in diameter; spicules are oxeas longer and thicker (140–160 × 7–9 μm) than those of *A. anastomosa* sp. n., with frequent stylote modifications. *Amphimedon cristata* Pulitzer-Finali, 1996 is sub-cylindrical, violet in colour and rigid, with an apical osculum; it has large oxeas (230–370 × 11–18 μm) with blunt extremities. Other three species of *Amphimedon* have been described by Helmy and van Soest (2005) from the Red Sea: *A. dinae*, *A. jalae*, *A. hamadai*. *Amphimedon dinae* is a brown, massive sponge with oscula 2-4 mm wide and very thin and short oxeas (52–61 × 1–1.5 μm); *A. jalae* is massive, cushion-shaped, with large oxeas (100–170 × 4–6 μm) and choanosomal rounded meshes of 600–800 μm. *Amphimedon hamadai* is brown, irregularly lobated, with very short oxeas (48–60 × 2–3 μm), while *A. delicatula* (Dendy, 1889) is erect, bushy, yellow in colour and with stout fibres 126 μm thick and very slender, slightly curved oxeas (98 by 3.5 μm). *Amphimedon lamellata* Fromont, 1993 is a lamellate, erect sponge, pale pink in colour; with a reticular choanosomal skeleton and two types of oxeas differing in thickness (111–130 × 2.5–4.4 μm and 105–126 × 1.3–2.3 μm); *A. massalis* (Carter, 1886) is massive, yellow in the basal portion, dark brown-red on the surface, with vents "on monticular elevations" and oxeas measuring 155 × 6 μm. *Amphimedon navalis*, *A. rubida*, *A. rubiginosa* and *A. spinosa* have been described by Pulitzer-Finali (1993) from Kenya. *Amphimedon navalis* is a cushion-shaped sponge, dark blue and violet in colour, with blunt oxeas (160–210 × 11–15 μm); *A. rubida* is cylindrical, red brownish, with meshes of 220–360 μm across and oxeas measuring 185–230 × 11.5–18 μm. *Amphimedon rubiginosa* has a massive shape with elevated oscula and a skeletal organisation with ill-defined plurispicular tracts. *Amphimedon spinosa* has a tubular shape and fibres cored by single spicules, while *A. paraviridis* Fromont, 1993 is encrusting or ramose, green-olive in life, with primary fibres of 50–160 μm and secondary of 20–50 μm, thicker than those of the new species. Moreover, abundant oxeas (133–151 × 3.9–8.0 μm) are scattered in between the fibre reticulation (absent in *A. anastomosa* sp. n.). *Amphimedon queenslandica* Hooper & van Soest, 2006 is a blue-grey and green sponge with an encrusting base from which lobate or digitate portions rise. Unlike the new species, it has unispicular fibres. *A. robusta* (Carter, 1885) is a branching-digitate, orange sponge with oscula located on one side; *A. rudis* Pulitzer-Finali, 1996 is violet-brownish, with blunt and very stout oxeas (360–420 × 10–12.5 μm). *Amphimedon strongylata* Pulitzer-Finali, 1996 is sub-cylindrical, grey in colour, with strongyloxeas as megascleres; *A. subcylindrica* (Dendy, 1905) is a cylindrical sponge with reptant habit; it has a smooth surface and oscula with prominent rims; its fibres are cored by a high number of spicules (slightly longer (140 × 8 μm) oxeas), without visible spongin. *Amphimedon sulcata* Fromont, 1993 is a small, globular sponge with oxeas of 122–153 × 3.0–5.3 μm and C-shaped sigmas

as microscleres. Finally, *A. zamboangae* (Lévi, 1961), which is green in colour, has a velvety surface, thick fibres (130 μm) and two types of oxeas (120–150 × 4–6 μm and 120–130 × 3 μm).

"*Amphimedon* differ from other Niphatidae in having an optically smooth, but microscopically microtuberculate fibrous superficial skeleton, usually with abundant spongin, and lacking microscleres" (Hooper and van Soest 2006). Because of the slight differences between *Amphimedon* and *Niphates* (Desqueyroux-Fáundez & Valentine 2002), all the Indo-Pacific species of the latter genus were also checked. All these species of *Niphates* differ from the new species in shape, colour and skeletal organisation. The most similar species, in terms of the branched shape, is *N. aga* (de Laubenfelds, 1954), but it has a confused ectosomal skeleton and longer oxeas (175–180 μm). *Amphimedon anastomosa* sp. n. is well characterised by its growth form and colour. Since no species in this vast geographic area matches with our specimen, we are justified to erect a new species.

Genus *Niphates* Duchassaing & Michelotti, 1864

Niphates laminaris Calcinai, Bastari, Bertolino & Pansini, sp. n.

http://zoobank.org/4E0827B5-02C7-45D4-8456-78E0F8AE1B31
Figure 8

Material examined. Holotype: MSNG 60139, PH-47, 17/01/2005, Tiwoho (Bunaken Island), 20 m depth.

Diagnosis. Lamellate, azure-violet sponge, with differentiated inhalant and oscular faces. Skeleton is a regular reticulum of primary and secondary fibres, with superficial brushes hispidating the surface; megascleres are straight and sinuous oxeas. Microscleres are sigmas.

Description. The sponge is a thin, irregular, folded lamina, attached to the substrate in few points (Fig. 8A); its rim is more or less rounded, not regular (Fig. 8B). The holotype consists in alcohol-preserved fragments, collected from a bigger specimen (Fig. 8A, B). The largest observed specimen is approximately 8 × 4 cm long and 2 mm thick. The colour in life is azure-violet in the part exposed to light and beige on the shadowed side (Fig. 8B). The sponge becomes white-bluish when dried. Consistence soft, slightly elastic. The aspect of the two sides of the laminar sponge is different: roundish vents, 700–1,300 μm in diameter, most probably acting as oscula, are concentrated on the excurrent side (Fig. 8C); on the opposite side, a thin dermal membrane, pierced by numerous pores, covers several smaller apertures, not visible to the naked eye (Fig. 8D). In the dried state, spicule brushes and small ridges (made by tracts of tangential oxeas connecting the brushes) create a microconulose surface, visible also to the naked eye, in both sides of the sponge.

Skeleton. The ectosomal skeleton is a reticulation of multispicular tracts (30–60 μm thick) forming polygonal (mostly quadrangular) meshes 340–900 μm in diameter, with brushes of spicules at the nodes (Fig. 8D). The choanosomal skeleton is a not very

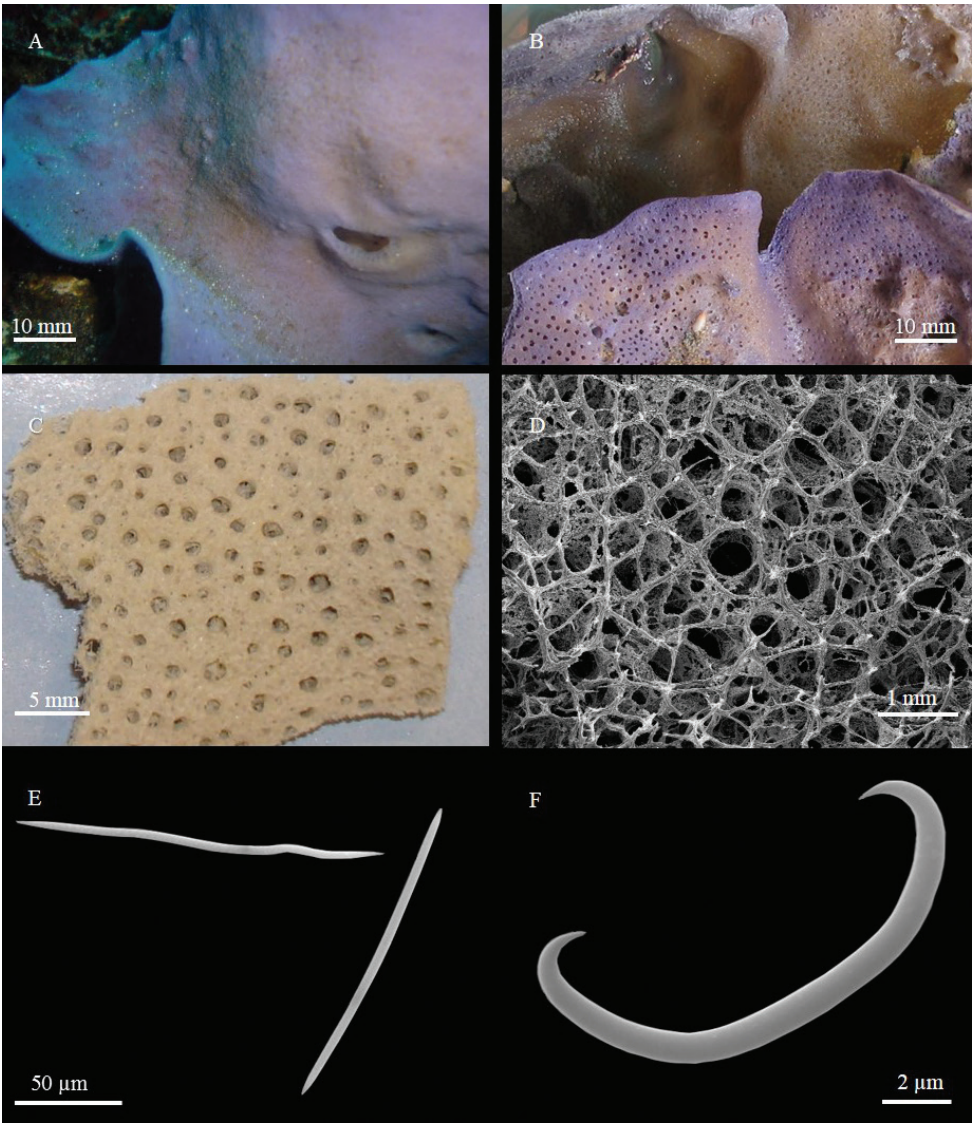

Figure 8. *Niphates laminaris* sp. n. **A** holotype *in situ* **B, C** holotype freshly collected showing the exhalant side of the sponge **D** sponge skeleton on the exhalant side with in evidence the choanosomal ascending tracts protruding through the surface and the vents **E** sinuous and straight oxeas **F** sigma.

regular reticulation, with elongated, almost rectangular meshes 400–800 µm across and empty spaces. The spicule tracts may be divided into ascending primary tracts, 55–100 µm thick, and secondary tracts, 25–35 µm thick, with a more or less transverse arrangement. The extremities of the ascending tracts protrude through the surface, forming brushes (Fig. 8D). Very numerous pigmented (green) cells and abundant spicules, both megascleres and microscleres, are dispersed in the ectosome and choanosome.

Spicules. Oxeas slightly curved or sinuous, rarely straight, with acerate tips (Fig. 8E). They measure 150.8 - (163.37 ± 7.0) - 176.8 × 2.5 - (3.7 ± 1.1) - 5.2 μm. Sigmas C-shaped, sometimes with a part of the shaft almost straight (Fig. 8F). They measure 13 - (17.0 ± 3.18) - 23.4 μm × 1 μm.

Etymology. The name refers to the lamellate shape of the sponge.

Remarks. The new species clearly belongs to the family Niphatidae for the presence of multispicular fibres in the ectosome and to the genus *Niphates* for the skeletal organisation. The genus *Niphates* includes sponges with "Surface conulose to spiny [….] produced by primary longitudinal fibres ending on surface" (Desqueyroux-Faúndez and Valentine 2002). The ectosomal skeleton is a tangential network of secondary fibres, obscured by protruding tufts of primary fibres. Microscleres are rare sigmas (Desqueyroux-Faúndez and Valentine 2002). However, other species of the genus (e.g. *Niphates nitida* Fromont, 1993) have a smooth surface as the new species.

Niphates laminaris sp. n. is characterised by a non-spiny, rather irregular, microconulose surface and by a choanosomal skeleton with a reticulation of primary and secondary tracts. Microscleres are numerous. In the Indo-Pacific area, only *N. nitida* has sigmas. However, *N. nitida* is a sponge with repent habit, with oscula located at the top of small erect lobes; a choanosomal fibrous reticulation with round or triangular meshes (104–146 μm) and oxeas measuring 128 × 5.6 μm. Therefore, it substantially differs from *Niphates* sp. n; all other *Niphates* in the area differ from the new species for the absence of sigmas and for other significant features listed below. *Niphates olemda* (de Laubenfelds, 1954) is a blue, or pink tubular sponge with small oxeas (92–100 × 2–3 μm), while *N. aga* (de Laubenfelds, 1954) is ramose with superficial projections, a confused ectosomal skeleton and straight and large oxeas (175–180 × 5 μm). *Niphates cavernosa* Kelly-Borges & Bergquist, 1988 is a massive, creeping and branching sponge, violet in life, with two categories of oxeas differing in thickness (oxeas I: 5–10 μm thick; oxeas II: 2–4 μm); *N. furcata* (Keller, 1889) is green, erect, branching, with rather short oxeas (100 × 12 μm). *Niphates hispida* Desqueyroux-Fáundez, 1984 is a hard and incompressible sponge with very small oxeas (60-80 × 2-4 μm), consisting of a series of coalescent, cylindrical tubes arising from a massive common base. *Niphates mirabilis* (Bowerbank, 1873) is an ochre-pinkish sponge with a unispicular ectosomal reticulation, while *N. obtusispiculifera* (Dendy, 1905) is a branching, cylindrical sponge with strongyles as megascleres. *Niphates plumosa* (Bowerbank, 1876) is fawn-coloured and has a peculiar, stipitate and fan-shaped growth form with only oxeas as spicules. *Niphates rowi* Ilan et al., 2004 is the species most similar to the new species. Its ectosomal skeleton is a reticulation of fibres creating quadrangular meshes which are smaller than those of *Niphates laminaris* sp. n. (70–115 μm). In addition, the choanosomal reticulation of *N. rowi* has rectangular meshes which are smaller (115–200 μm) than those of *Niphates laminaris* sp. n., whereas the oxea size is similar (115 - (140) - 170 × 5.5 - (6.5) - 7.5 μm). In conclusion *N. rowi*, which is an encrusting sponge, differs from *Nipahtes laminaris* sp. n. in the growth form, the absence of sigmas and sinuous oxeas and in the size of the ectosomal and choanosomal meshes.

Subclass Keratosa
Order Dictyoceratida
Family Irciniidae Gray, 1867
Genus *Psammocinia* Lendenfeld, 1889

***Psammocinia alba* Calcinai, Bastari, Bertolino & Pansini, sp. n.**
http://zoobank.org/2304C2B3-8156-4163-AC33-0AEC55EBADEE
Figure 9

Material examined. Holotype: MSNG 60140, PH-41, 14/01/2005, Timur (Bunaken Island), 22 m depth.

Diagnosis. Lobate, white sponge with oscular cavities at the top of the lobes. Thin armoured surface with sand and foreign spicules. Slightly fasciculated fibres, not very dense.

Description. Massive, lobate sponge with flush, roundish oscular cavities (about 1.5 cm) where the excurrent canals converge, located at the top of the lobes (Fig. 9A). The deposited holotype consists of fragments 3 × 1.5 cm, coming from a larger specimen approximately 15 cm across (Fig. 9A).

The colour in life is white outside (Fig. 9A) and cerulean inside; it becomes light cerulean after collection and beige after preservation in alcohol. Surface characterised by numerous small conules, 0.5–1 mm high and 2 mm apart, united by ridges (Fig. 9A, B). Consistence soft, but elastic, difficult to tear apart.

Skeleton. The surface is covered by a thin reticulation of sand and foreign spicules, forming regular, more or less circular, meshes 100 μm in diameter (Fig. 9C), well visible in the stereo-microscope. The density of the fibres is moderate. The primary fibres of the choanosome are slightly fasciculated (Fig. 9D), about 80 μm thick and cored with foreign debris and a few foreign spicules. The secondary fibres are thinner (20 μm in diameter) and free from inclusions (Fig. 9D). The size of the ovoid meshes ranges from 50 × 80 to 57.5 × 115 μm; a few smaller meshes, 30 × 55 μm, are also present. Filaments, 2.5 μm thick, are numerous and dense.

Etymology. Referring to the white colour in life.

Remarks. Our species is attributed to *Psammocinia* due to the presence of a surface armoured by sand and foreign spicules and to the reticular skeleton of primary and secondary fibres.

According to van Soest et al. (2016), 25 species of *Psammocinia* are known in total. Most of them have been described from New Zealand and South Korea and only one from Brazil.

Psammocinia bulbosa Bergquist, 1995 from New Caledonia and *P. lobatus* Sim & Lim, 2002 from Korea are the most similar species to *Psammocinia alba* sp. n. *Psammocinia bulbosa* is a massive, repent sponge with quite long oscular fistules. Its surface is covered by small conules 0.5–1 mm high and has a sandy crust up to 1 mm thick. The skeleton is formed by primary fibres giving rise to columns up to 700 μm long and secondary fibres 30–50 μm in diameter. The main differences to our species are the presence of fistules, a distinctive characteristic of *P. bulbosa*, and thicker fibres. *Psam-*

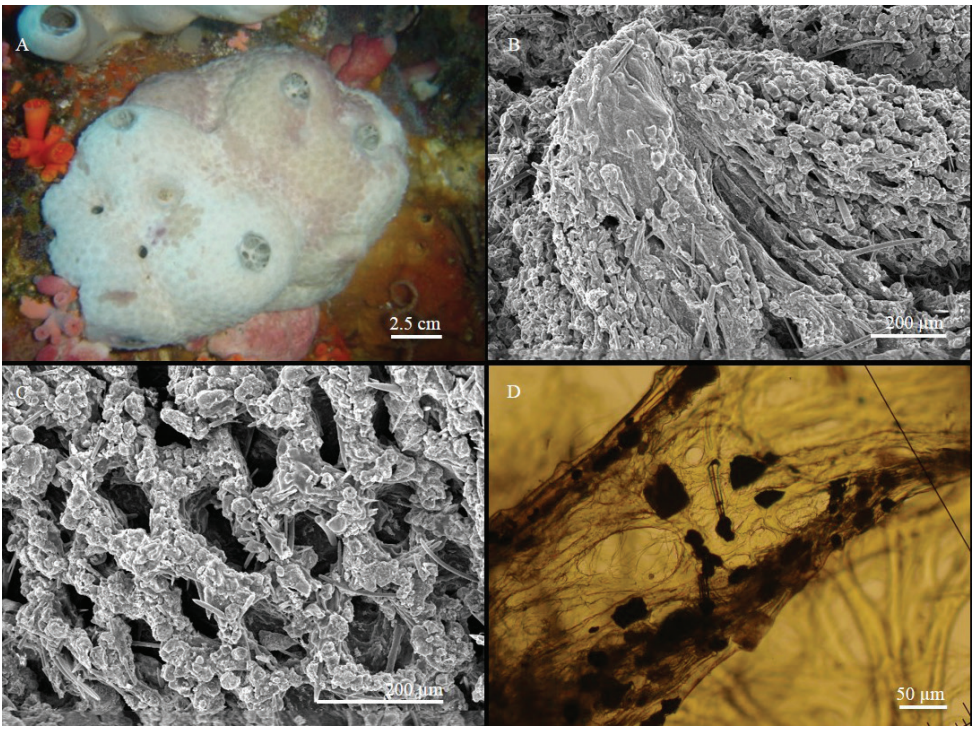

Figure 9. *Psammocinia alba* sp. n. **A** the sponge *in situ* **B** a small conule at SEM **C** reticulation made of sand grains and foreign spicules **D** primary fibres cored with foreign material and, on the right, secondary fibres free from inclusions.

mocinia lobatus, lobate in shape, has a surface covered by conules 1–2 mm high and 2–5 mm apart. Both primary and secondary fibres (60–10 µm thick) are comparable in size with our species. The main differences to *P. alba* sp. n. are the colour (dark brown, black), the presence of sharp conules and the small amount of foreign material present in the fibres. From New Zealand, the following species have been described: *P. beresfordae* Cook & Bergquist, 1996, formed by a compact base with broad-based fistules with an apical osculum 3–7 mm in diameter and primary fibres 120 µm thick; *P. verrucosa* Cook & Bergquist, 1996, a small, massive sponge with a very characteristic surface with rounded lamellae supported by skeletal fibres and a reticulate pattern; *P. hirsuta* Cook & Bergquist, 1998, formed by a coalescent group of digitate structures or lobes, with long, cylindrical fistules and a thick (400 µm) superficial sand layer; *P. charadrodes* Cook & Bergquist, 1998, a massive sponge with very long, rounded conules and very thick (till 1086 µm) primary fibres; *P. papillata* Cook & Bergquist, 1998, a massive, compact sponge with a coarsely conulose surface and both primary and secondary fibres thicker than in *Psammocinia alba* sp. n.; *P. perforodosa* Cook & Bergquist, 1998, a massive, compact sponge without conules, with a folded surface (800 µm thick) armoured by sand, foreign spicules and rocky fragments; *P. maorimotu* Cook & Bergquist, 1998,

a lobate sponge with oscula on top, a surface with grooves and ridges and primary fibres with a thickness of 349 μm. From South Korea and China, the following species have been described: *P. conulosa* Lee & Sim, 2004, a massive sponge with ectosomal membrane covered by sand but devoid of circular meshes, oscula scattered and sharp conules 2–4 mm high; *P. ulleungensis* Lee & Sim, 2004, dark grey in colour, with a smooth surface and thick, slightly fasciculated, primary fibres (100–300 μm); *P. mammiformis* Sim, 1998, a massive, grey or purple coloured sponge, covered with mammiform protuberances and with very thick choanosomal fibres 550–900 μm; *P. mosulpia* Sim, 1998 mainly differs from *P. alba* sp. n. for its crust of sand and foreign spicules not organised in circular meshes; *P. jejuensis* Sim, 1998, characterised by tick fibres (up to 470 μm) and by filaments with large terminal knobs (12–20 μm in diameter); *P. gageoensis* Sim & Lee, 2001, has no detritus in the fasciculated primary fibres. Both *P. samyangensis* Sim & Lee, 1998 and *P. wandoensis* Sim & Lee, 1998 differ from *P. alba* sp. n. mainly in the thickness of the secondary fibres. Finally, *P. rubra* Sim & Lee, 2002 differs from *P. alba* sp. n. for its red colour and the larger size (up to 320 μm) and colour (reddish-brown) of the fibres.

The other species of *Psammocinia* have a particular morphology, very different respect to *Psammocinia alba* sp. n.; *P. arenosa* (Lendenfeld, 1888) and *P. hawere* Cook & Bergquist, 1996 are cup-shaped sponges. *Psammocinia halmiformis* (Lendenfeld, 1888) is irregularly lamellate and *P. vesiculifera* (Poléjaeff, 1884) is a tube sponge. *Psammocinia amodes* Cook & Bergquist, 1998 is a spatulate sponge with a thin, semicylindrical basal portion for anchoring to the substrate, while *P. bergquistae* Sim & Lee, 2001 has a thumb shape and secondary fibres, forming a secondary web.

Due to the difficulties to differentiate, in some cases, species of the genus *Psammocinia* from other taxa of the family Irciniidae, we also examined the species belonging to *Ircinia* and *Sarcotragus* from the Indo-Pacific area. All these species are different from *Psammocinia alba* sp. n. in morphology, fibre thickness, and structure (see below).

The incorporation of foreign material can play several roles in sponge growth. Usually, this behaviour is explained just as strengthening of the sponge tissue, but other roles could be considered, e.g. the enhancement of sponging fibre production (Cerrano et al. 2007).

Genus *Ircinia* Nardo, 1833

Ircinia colossa Calcinai, Bastari, Bertolino & Pansini, sp. n.

http://zoobank.org/3547C559-C615-420B-874F-6782568B7D40
Figure 10

Material examined. Holotype: MSNG 60141, PH-44, 15/01/2005, Timur (Bunaken Island), about 20 m depth. Paratype: MSNG 60142, BKA 25, 12/09/2014, Yellow coco (Bangka Island), about 20–25 m depth.

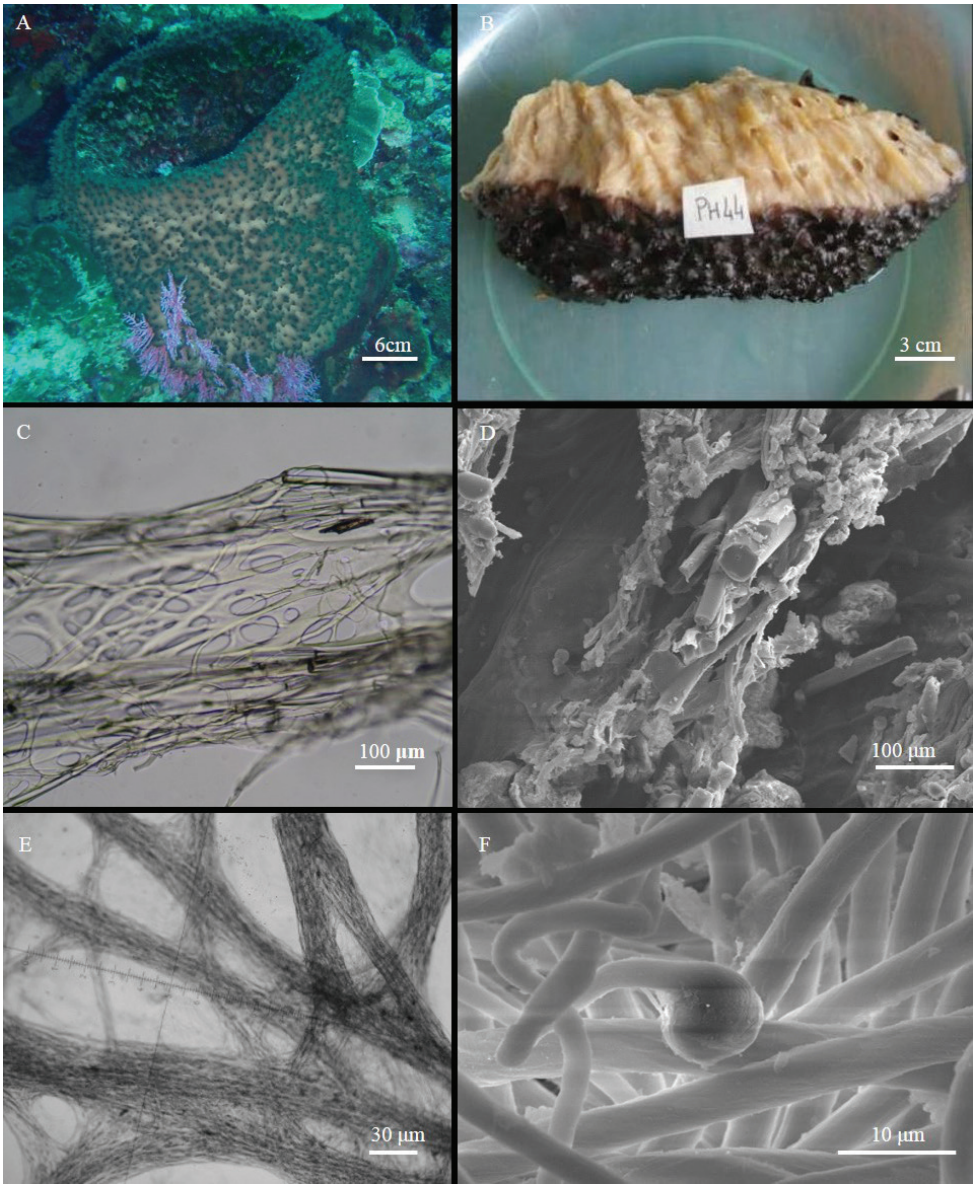

Figure 10. *Ircinia colossa* sp. n. **A** specimen BU-590 *in situ* **B** portion of the holotype **C** fasciculated fibres **D** primary fibres with foreign spicules **E** filaments organised in tracts **F** filaments with a terminal knob in evidence.

Other material. BU-590, 27/07/2004, Timur (Bunaken Island), 25 m depth. INDO-431, 13/05/2005, Jetty (Siladen), depth not stated, N01°37'38.8"; E124°48'00.8".

Diagnosis. Soft and elastic cup-shaped *Ircinia* with a large, central cavity; conulose surface; heavily fasciculated fibres with foreign material.

Description. The sponge is columnar, reminding of a partially hollow cylinder, due to the presence of a wide central cavity (Fig. 10A). It may be as high as 80 cm, with a wall 1–2 cm thick. The holotype is a fragment approximately 4.5 × 2 cm. The external colour is light brown with greenish tinges on the conules and on the rim of the cavity (Fig. 10A). The freshly collected sponge is beige inside (Fig. 10B). Alcohol-preserved specimens remain almost the same in colour. The sponge surface is strongly conulose, with rounded or slightly flattened conules 2–4 mm high (Fig. 10A, B). The oscula (3–5 mm in diameter) are present in the inner part of the central cavity. Consistence is soft and elastic, but the sponge is difficult to tear off.

Skeleton. The choanosomal skeleton is formed by primary fibres cored by foreign spicules (Fig. 10C, D), 180–350 μm in diameter and heavily fasciculated (Fig. 10C). They are connected by secondary fibres 50–80 μm in diameter, sometimes cored by single spicules. The fibres form a reticulation of elongated meshes, 100–150 μm in size, and cribrose plates (Fig. 10C). Very abundant thin filaments are mainly organised in tracts (Fig. 10E), but also dispersed in the mesohyl. They are 3-5 μm thick and present an oval or rounded terminal knob (7.5–10 μm in diameter) (Fig. 10F).

Etymology. The name refers to the sturdy and large size of the sponge.

Remarks. The studied specimens are attributed, according to Cook and Bergquist 2002, to the genus *Ircinia* for the strong fasciculation of fibres, with foreign material inside and the presence of filaments. There are more than 40 species of massive, encrusting, digitate or branching *Ircinia* in the Indo-Pacific area (van Soest et al. 2016), which differ from *Ircinia colossa* sp. n. in morphology, fibre thickness and quantity of external debris in the skeleton.

Only two species of *Ircinia*, living between 10 and 40 m depth in the temperate water of South-East Australia, show a central cavity: *I. caliculata* (Lendenfeld, 1888) and *I. rubra* (Lendenfeld, 1889). *Ircinia caliculata* differs from *I. colossa* sp. n. in the general morphology, colour, and organisation of the fibres. It has the rim of the cup bent outwards; the internal part of the cavity with small conules 2–3 mm high. The external part of the sponge presents digitate processes about 10 mm thick. The colour is dark-red brownish. It has fasciculated fibres full of sand grains. *Ircinia rubra* differs from *I. colossa* sp. n. in the general shape and fibre size. It is a small, conical, pedunculate sponge with a central cavity. All the fibres are full of debris and foreign spicules and the secondary fibres, 100 μm in diameter, are thicker than those of *Ircinia colossa* sp. n.

We also examined species belonging to the genus *Sarcotragus*; none of them fits with the characters of the new species. *Sarcotragus aliger* (Burton, 1928) is clavate, cylindrical with an apical osculum and fibres 80 μm in diameter, while *S. australis* (Lendenfeld, 1888) is a massive red sponge. *Sarcotragus coreanus* (Sim & Lee, 2002) is massive to encrusting, beige in colour; *S. gapaensis* Sim & Lee, 2000 is subspherical, dark brown to black, with big primary fibres 280–530 μm in diameter. *Sarcotragus maraensis* Sim & Lee, 2000 is globular with sharp conules 2–8 mm high and an ivory and purple colour. *Sarcotragus myrobalanus* (Lamarck, 1814) is an ovoid sponge with a long peduncle, brown-reddish in colour; *S. tuberculatus* (Poléjaeff, 1884) has fibres

that often do not ramify and its surface, greyish in colour, is covered by rounded tubercles; filaments are roundish and 55 μm in diameter.

Ircinia colossa sp. n. is frequent in the Bunaken Park and the nearby Bangka Island (North Sulawesi); the paratype was found with other relatively large specimens (50 cm high or more) near a hot vent flowing from a sandy bottom (Bertolino et al. 2017).

This species is probably present also throughout northern Australia and Papua New Guinea (J. Hooper, pers. comm.). Molecular analysis, compared against sequences made by Pöppe et al. (2011) for *Ircinia* and *Psammocinia* species from northern Australia, would be very useful to confirm if *Ircinia colossa* sp. n. and *P. alba* sp. n. are also present in Australia.

Conclusions

The marine diversity in Indonesia is still far from being well known. The present contribution highlights the underexplored diversity of Porifera in this area, suggesting the presence of a very high number of still undescribed species. Thanks to this impressive diversity, the areas here considered are important spots for diving tourism, requiring the urgent development of sustainable tourism practices. In particular, at Bangka Island, mining activities are rapidly damaging reef integrity, even if this process is currently strongly counteracted by the local population. It is worth noting that also there, as in many other strongly populated areas, the conflict between the need to preserve local biodiversity and the economic development can quickly lead to a lose-lose equilibrium.

Generally, the economic value of biodiversity is still far from being adequately understood; in particular, the actual value of sponges in the maintenance of the homeostasis of a reef needs to be studied in more detail.

In temperate regions affected by climatic anomalies, filter feeders are among the most affected functional categories (Coma et al. 2009, Di Camillo and Cerrano 2015), and negative trends of sponge diversity and abundance have been reported from several areas (Wulff 2013).

The area of the present study is very rich in terms of diversity, but the baseline needs urgent implementation and constant update to avoid the possibility of disregarding changes.

We have documented 94 sponge species from three small spots of the northern tip of Sulawesi. Since 1989, van Soest has reported approximately 830 species from Indonesia; the species recorded here represent only a small part of the astonishing sponge diversity of the area.

The coral triangle is known for its high level of biodiversity and continuously, in recent years, new marine organisms have been described. Moreover, many authors (see for example Barber et al. 2000) have demonstrated strong regional genetic differentiation even across short distances and even for reef organisms presumed to be subjected to rapid dispersion even between distant populations. Sponge diversity across Indonesian coral reefs could be extraordinarily underestimated considering the limited capac-

ity of sponge larval dispersal (Maldonado and Bergquist 2002). Unfortunately, for North Sulawesi and the rest of the archipelago, both collecting and taxonomic efforts remain limited.

The listed taxa (Table 1) sometimes include well-known sponge species because reef sponges of Indonesia are also present in the Indo-Pacific area (van Soest 1990); for other poorly known species, specimen photos and short taxonomic notes may assist for further identification, supporting future, desirable monitoring work (Supplementary files 1 and 2).

Acknowledgments

The authors are indebted to the staff of the research outpost Coral Eye (http://coral-eye.net/contact-us.html) for logistic support and to Francesca Azzini and M. Boyer (http://www.kudalaut.com) for field support. This work was partially supported by Italian MIUR and MAE funds.

References

Ávila E, Carballo JL, Cruz-Barraza JA (2007) Symbiotic relationships between sponges and other organisms from the Sea of Cortes (Mexican Pacific coast): same problems, same solutions. Porifera Research: Biodiversity, Innovation and Sustainability, 147–156.

Azzini F, Calcinai B, Pansini M (2008) A new species of *Coelocarteria* (Porifera: Demospongiae) from Sulawesi, Indonesia. Journal of the Marine Biological Association of the United Kingdom 87: 1349–1353.

Bavestrello G, Calcinai B, Boyer M, Cerrano C, Pansini M (2002) The Aquiferous system of two *Oceanapia* species (Porifera, Demospongiae) studied by corrosion casts. Zoomorphology 121: 195–201. https://doi.org/10.1007/s00435-002-0056-x

Becking LE (2013) Revision of the genus *Placospongia* (Porifera, Demospongiae, Hadromerida, Placospongiidae) in the Indo-West Pacific. ZooKeys 298: 39–76. https://doi.org/10.3897/zookeys.298.1913

Bell JJ (2008) The Functional Roles of Marine Sponges. Estaurine, Coastal and Shelf Science 79: 341–353. https://doi.org/10.1016/j.ecss.2008.05.002

Bell JJ, Smith D (2004) Ecology of sponge assemblages (Porifera) in the Wakatobi region, south-east Sulawesi, Indonesia: richness and abundance. Journal of the Marine Biological Association of the United Kingdom 84: 581–591. https://doi.org/10.1017/S0025315404009580h

Bertolino M, Oprandi A, Santini C, Castellano M, Pansini M, Boyer M, Bavestrello G (2017) Hydrothermal waters enriched in silica promote the development of a sponge community in North Sulawesi (Indonesia). The European Zoological Journal 84(1): 128–135. https://doi.org/10.1080/11250003.2016.1278475

Calcinai B, Bavestrello G, Cerrano C (2004) Dispersal and association of two alien species in the Indonesian coral reefs: the octocoral *Carijoa riisei* and the demosponge *Desmapsamma*

anchorata. Journal of the Marine Biological Association of the United Kingdom 84: 937–941. https://doi.org/10.1017/S0025315404010227h

Calcinai B, Bavestrello G, Cerrano C (2005a) Excavating sponges species from the Indo-Pacific Ocean. Zoological Studies 44(1): 5–18.

Calcinai B, Cerrano C, Bavestrello G (2005b) Le spugne come hotspot di biodiversità. Biologia Marina Mediterranea 12: 63–68.

Calcinai B, Cerrano C, Totti C, Romagnoli T, Bavestrello G (2006) Symbiosis of *Mycale* (*Mycale*) *vansoesti* sp. nov. (Porifera, Demospongiae) with a coralline alga from North Sulawesi (Indonesia). Invertebrate Biology 125: 195–204. https://doi.org/10.1111/j.1744-7410.2006.00052.x

Calcinai B, Cerrano C, Bavestrello G (2007) Three new species and one re-description of *Aka*. Journal of the Marine Biological Association of the United Kingdom 87: 1355–1365. https://doi.org/10.1017/S0025315407058377

Calcinai B, Bavestrello G, Bertolino M, Pica D, Wagner D, Cerrano C (2013) Sponges associated with octocorals in the Indo-Pacific, with the description of four new species. Zootaxa 3617: 1–61. https://doi.org/10.11646/zootaxa.3617.1.1

Calcinai B, Bastari A, Makapedua DM, Cerrano C (2016) Mangrove sponges from Bangka Island (North Sulawesi, Indonesia) with the description of a new species. Journal of the Marine Biological Association of the United Kingdom. https://doi.org/10.1017/S0025315416000710

Carvalho MS, da Silva SM, Pinheiro U (2013) Two new species of *Aaptos* (Demospongiae, Hadromerida) from Brazil (western Atlantic). Zootaxa 3750: 357–366. https://doi.org/10.11646/zootaxa.3750.4.4

Cerrano C, Calcinai B, Pinca S, Bavestrello G (2006) Reef sponges as hosts of biodiversity: cases from North Sulawesi. In: Suzuki Y, Nakamori T, Hidaka M, Kayanne H, Casareto BE, Nadao K, Yamano H, Tsuchiya M (Eds) Xth Coral Reef Symposium, Okinawa, 208–213.

Cerrano C, Calcinai B, Di Camillo CG, Valisano L, Bavestrello G (2007) How and why do sponges incorporate foreign material? Strategies in Porifera. In: Custódio MR et al. (Eds) Porifera research: Biodiversity, Innovation & Sustainabilty. Rio de Janeiro, Museu Nacional, 239–246.

Chianese G, Fattorusso E, Scala F, Teta R, Calcinai B, Bavestrello G, Dien HA, Kaiser M, Tasdemirg D, Taglialatela-Scafati O (2012) Manadoperoxides, a new class of potent antitrypanosomal agents of marine origin. Organic & Biomolecular Chemistry 10: 7197–7207. https://doi.org/10.1039/c2ob26124c

Coma R, Ribes M, Serrano E, Jiménez E, Salat J, Pascuals J (2009) Global warming-enhanced stratification and mass mortality events in the Mediterranean. PNAS 106: 6176–6181. https://doi.org/10.1073/pnas.0805801106

Cook SDC, Bergquist PR (2002) Family Irciniidae Gray, 1867. In: Hooper JNA, van Soest RW M (Eds) Systema Porifera. A guide to the classification of sponges. 1. Kluwer Academic/ Plenum Publishers: New York, Boston, Dordrecht, London, Moscow, 1022–1027. https://doi.org/10.1007/978-1-4615-0747-5_95

Desqueyroux-Faúndez R, Valentine C (2002) Family Petrosiidae van Soest, 1980. In: Hooper JNA, van Soest RW M (Eds) Systema Porifera. A guide to the classification of sponges.

1. Kluwer Academic/ Plenum Publishers: New York, Boston, Dordrecht, London, Moscow, 906–917.

Di Camillo CG, Cerrano C (2015) Mass Mortality Events in the NW Adriatic Sea: Phase Shift from Slow- to Fast-Growing Organisms. PLoS ONE 10(5): e0126689. https://doi.org/10.1371/journal.pone.0126689

Fava F, Ponti M, Scinto, A, Calcinai B, Cerrano C (2009) Possible effects of human impacts on epibenthic communities and coral rubble features in the marine Park of Bunaken (Indonesia). Estuarine, Coastal and Shelf Science 85(1): 151–156. https://doi.org/10.1016/j.ecss.2009.02.028

Fromont J (1993) Descriptions of species of the Haplosclerida (Porifera: Demospongiae) occurring in tropical waters of the Great Barrier Reef. The Beagle, Records of the Northern Territory Museum of Arts and Sciences 10(1): 7–40.

de Goeij JM, van Oevelen D, Vermeij MJA, Osinga R, Middelburg JJ, de Goeij AFPM, Admiraal W (2013) Surviving in a marine desert: The sponge loop retains resources within coral reefs. Science (Wash.) 342: 108–110. https://doi.org/10.1126/science.1241981

Hentschel E (1912) Kiesel- und Hornschwämme der Aru- und Kei-Inseln. Abhandlungen herausgegeben von der Senckenbergischen naturforschenden Gesellschaft 34: 293–448. https://doi.org/10.5962/bhl.title.85325

Hofman CC, van Soest RWM (1995) *Lissodendoryx* species of the Indo-Malayan Archipelago (Demospongiae: Poecilosclerida). Beaufortia 45(6): 77–103.

Hogg MM, Tendal OS, Conway KW, Pomponi SA, van Soest RWM, Gutt J, Krautter M, Roberts JM (2010) Deep-sea sponge grounds: reservoirs of biodiversity, Cambridge: World Conservation Monitoring Centre, UNEP regional seas report and studies 189, UNEP-WCMC Biodiversity Series 32.

Hooper JNA (1984) A new genus and two new species of haplosclerid sponges (Porifera: Demospongiae) from the Timor Sea, Northwest Australia. Proceedings of the Royal Society of Victoria (New Series) 96(2): 55–60.

Hooper JNA (2000) Sponguide. Guide to sponge collection and identification. http://www.qm.qld.gov.au/organisation/sections/SessileMarineInvertebrates/spong.pdf [accessed 2011]

Hooper JNA, van Soest RWM (2006) A new species of *Amphimedon* (Porifera, Demospongiae, Haplosclerida, Niphatidae) from the Capricorn-Bunker Group of Islands, Great Barrier Reef, Australia: target species for the 'sponge genome project'. Zootaxa 1314: 31–39.

Kelly-Borges M, Bergquist PR (1994) A redescription of *Aaptos aaptos* with descriptions of new species of *Aaptos* (Hadromerida: Suberitidae) from northern New Zealand. Journal of Zoology 234(2): 301–323. https://doi.org/10.1111/j.1469-7998.1994.tb06077.x

Lévi C (1958) Résultats scientifiques des Campagnes de la 'Calypso'. Campagne 1951–1952 en Mer Rouge (suite). 11. Spongiaires de Mer Rouge recueillis par la 'Calypso' (1951–1952). Annales de l'Institut océanographique 34(3): 3–46.

Maldonado M, Bergquist PR (2002) Phylum Porifera. In: Young CM (Ed.) Atlas of marine invertebrate larvae. Academic, London, 21–50.

Muricy G (2011) Diversity of Indo-Australian *Plakortis* (Demospongiae: Plakinidae), with description of four new species. Journal of the Marine Biological Association of the United Kingdom, 91(2): 303–319. https://doi.org/10.1017/S0025315410000743

Pöppe J, Sutcliffe P, Hooper JNA, Wörheide G, Erpenbeck D (2011) COI barcoding reveals new clades and radiation patterns of Indo-Pacific sponges of the family Irciniidae (Demospongiae: Dictyoceratida). PLoS ONE 5(4): e9950. https://doi.org/10.1371/journal.pone.0009950

Powell A, Smith DJ, Hepburn LH, Jones T, Berman J, Jompa J, Bell JJ (2014) Reduced Diversity and High Sponge Abundance on a Sedimented Indo-Pacific Reef System: Implications for Future Changes in Environmental Quality. PLoS ONE 9(1): e85253. https://doi.org/10.1371/journal.pone.0085253

Rossi G, Montori S, Cerrano C, Calcinai B (2015) The coral killing sponge *Chalinula nematifera* (Porifera: Haplosclerida) along the eastern coast of Sulawesi Island (Indonesia) 82: 143–148.

Rützler K (1974) The Burrowing Sponges of Bermuda. Smithsonian Contributions to Zoology 165: 1–32. http://dx.doi.org/10.5479/si.00810282.165

Sarà M (2002) Family Tethyidae Gray, 1848. In: Hooper JNA, van Soest RW M (Eds) Systema Porifera. A guide to the classification of sponges. 1. Kluwer Academic/ Plenum Publishers: New York, Boston, Dordrecht, London, Moscow, 245–267. https://doi.org/10.1007/978-1-4615-0747-5_26

Scheffers SR, van Soest RWM, Nieuwland G, Bak RPM (2010) Coral reef framework cavities: is functional similarity reflected in composition of the cryptic macrofaunal community? Atoll Research Bulletin 583: 1–24. https://doi.org/10.5479/si.00775630.583.1

Sim-Smith C, Kelly M (2011) Two new genera in the family Podospongiidae (Demospongiae: Poecilosclerida) with eight new Western Pacific species. Zootaxa 2976: 32–54.

van Soest RWM (1989) The Indonesian sponge fauna: a status report. Netherlands Journal of Sea Research 23: 223–230. https://doi.org/10.1016/0077-7579(89)90016-1

van Soest RWM (1990) Shallow-water reef sponges of eastern Indonesia. In: Rützler K (Ed) New Perspectives in Sponge Biology. Washington DC, Smithsonian Institution Press, 302–308.

van Soest RWM (1994) Demosponge distribution patterns. In: van Soest RWM, van Kempen TMG, Braekman JC (Eds) Sponges in Time and Space, Balkema, Rotterdam, 213–223.

van Soest RWM (2002) Family Suberitidae. In: Hooper JNA, van Soest RWM (Eds) Systema Porifera, a guide to the classification of the sponges (in 2 volumes). Kluwer Academic / Plenum Publishers, New York, 1–1708.

van Soest RWM, Boury-Esnault N, Hooper JNA, Rützler K, de Voogd NJ, Alvarez de Glasby B, Hajdu E, Pisera AB, Manconi R, Schoenberg C, Janussen D, Tabachnick KR, Klautau M, Picton B, Kelly M, Vacelet J, Dohrmann M, Díaz MC, Cárdenas P (2016) World Porifera database. http://www.marinespecies.org/porifera [accessed on 14 Nov 2016]

Thiele J (1899) Studien über pazifische Spongien. II. Ueber einige Spongien von Celebes. Zoologica. Original-Abhandlungen aus dem Gesamtgebiete der Zoologie. Stuttgart 24(2): 1–33.

Thiele J (1900) Kieselschwämme von Ternate. I. Abhandlungen herausgegeben von der Senckenbergischen naturforschenden Gesellschaft.Frankfurt 25: 19–80.

Tomascik T, Mah AJ, Nontji A, Moosa MK (1997) The Ecology of the Indonesian Seas. Dalhousie University/Periplus Editions, Singapore, 1388 pp.

Topsent E (1891) Deuxième contribution à l'étude des Clionides. Archives de Zoologie Expérimentale et Générale (2)9: 555–592.

Uriz MJ (2002) Family Ancorinidae Schmidt, 1870. In: Hooper JNA, van Soest RW M (Eds) Systema Porifera. A guide to the classification of sponges. 1. Kluwer Academic/Plenum Publishers, New York, Boston, Dordrecht, London, Moscow, 108–126. https://doi.org/10.1007/978-1-4615-0747-5_12

de Voogd NJ (2003) *Amphimedon denhartogi* spec. nov. (Porifera: Haplosclerida) from deep reef habitats in Indonesia. Zoologische Verhandelingen 345: 413–418.

de Voogd NJ (2004) *Callyspongia* (*Euplacella*) *biru* (Porifera: Demospongiae: Haplosclerida) from Indonesia. Zoologische Mededelingen Leiden 78: 477–483.

de Voogd NJ, Cleary DFR (2008) An analysis of sponge diversity and distribution at three taxonomic levels in the Thousand Islands/Jakarta Bay reef complex, West-Java, Indonesia. Marine ecology-an evolutionary perspective 29: 205–215. https://doi.org/10.1111/j.1439-0485.2008.00238.x

de Voogd NJ, van Soest RWM (2002) Indonesian sponges of the genus *Petrosia* Vosmaer (Demospongiae: Haplosclerida). Zoologische Mededelingen Leiden 76: 193–209.

de Voogd NJ, van Soest RWM (2007) *Acanthotetilla celebensis* sp. nov., a new species from North Sulawesi, Indonesia (Porifera: Demospongiae: Spirophorida: Tetillidae). Zootaxa 1397: 25–28. https://doi.org/10.11646/zootaxa.1397.1.3

de Voogd NJ, Becking LE, Cleary DFR (2009) Sponge community composition in the Derawan Islands, NE Kalimantan, Indonesia. Marine ecology progress series 396: 169–180. https://doi.org/10.3354/meps08349

de Voogd NJ, Parra-Velandia FJ, van Soest RWM (2008) A new *Agelas* (Demospongiae: Agelasida: Agelasidae) from the Thousand Islands, West-Java, Indonesia. Zoologische Mededelingen Leiden 82(22): 235–243.

de Weerdt WH, van Soest RWM (2001) *Haliclona* (*Halichoclona*) *vanderlandi* spec.nov. (Porifera: Demospongiae: Haplosclerida) from Indonesia. Zoologische Verhandelingen Leiden 334: 189–194.

Wulff JL (2006) Ecological interactions of marine sponges. Canadian Journal of Zoology 84: 146–1. https://doi.org/10.1139/z06-019

Wulff JL (2012) Ecological interactions and the distribution, abundance, and diversity of sponges. In: Becerro MA (Ed) Advances in Sponge Science: Phylogeny, Systematics, Ecology. Advances in Marine Biology 61: 273–344. https://doi.org/10.1016/B978-0-12-387787-1.00003-9

Wulff JL (2013) Recovery of sponges after extreme mortality events: morphological and taxonomic patterns in regeneration versus recruitment. Integrative and comparative biology 53(3): 1–12. https://doi.org/10.1093/icb/ict059

Supplementary material 1

Underwater photos of the species.

Authors: Barbara Calcinai, Azzurra Bastari, Giorgio Bavestrello, Marco Bertolino, Santiago Bueno Horcajadas, Maurizio Pansini, Daisy M. Makapedua, Carlo Cerrano

Data type: species data

Link: https://doi.org/10.3897/zookeys.680.12135.suppl1

Supplementary material 2

Additional remarks of the species

Authors: Barbara Calcinai, Azzurra Bastari, Giorgio Bavestrello, Marco Bertolino, Santiago Bueno Horcajadas, Maurizio Pansini, Daisy M. Makapedua, Carlo Cerrano

Data type: species data

Link: https://doi.org/10.3897/zookeys.680.12135.suppl2